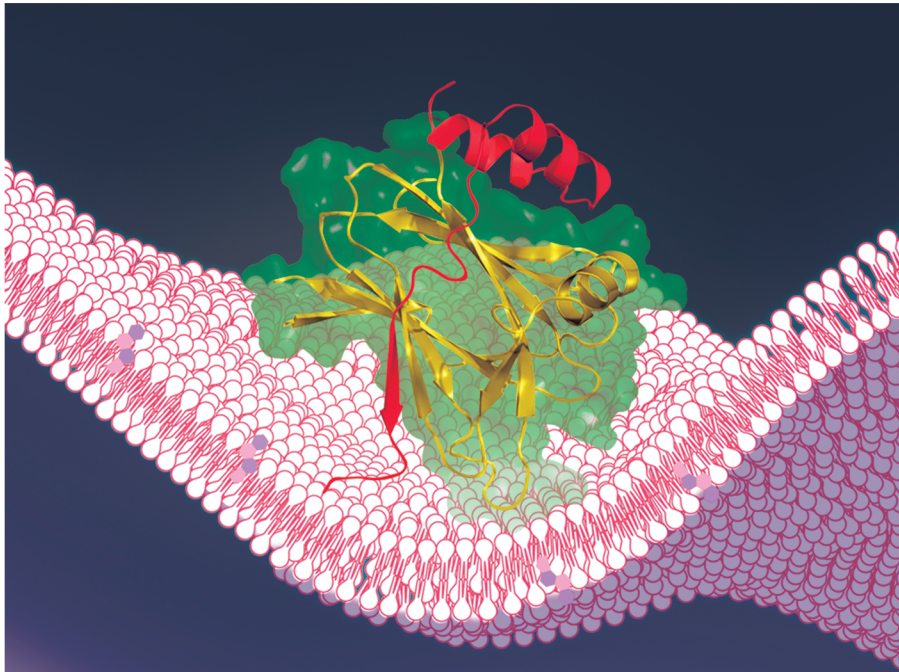

ROLE OF **HOST FACTORS**
REGULATING MEMBRANE HOMEOSTASIS IN
ENTEROVIRUS REPLICATION



HEYRHYOUNG LYOO

Role of Host Factors Regulating Membrane Homeostasis in Enterovirus Replication

Hey Rhyoung Lyoo

ISBN: 978-90-393-7390-3

DOI: <https://doi.org/10.33540/675>

Cover and thesis design: Heyrhyoung Lyoo

Cover illustration: Heyrhyoung Lyoo & Hyunjung Park (IG: coco.1011)

Printed by: Proefschrift-AIO

Printing of this thesis was partly sponsored by Infection and Immunity Utrecht.

The studies in this thesis were financially supported by the European Union (Horizon 2020 Marie Skłodowska-Curie ETN 'ANTIVIRALS', grant agreement number 642434).

Copyright © 2021 Heyrhyoung Lyoo

Role of host factors regulating membrane homeostasis in enterovirus replication

De rol van gastheerfactoren die membraanhomeostase reguleren
tijdens enterovirus replicatie

(met een samenvatting in het Nederlands)

Proefschrift

ter verkrijging van de graad van doctor aan de
Universiteit Utrecht
op gezag van de
rector magnificus, prof.dr. H.R.B.M. Kummeling,
ingevolge het besluit van het college voor promoties
in het openbaar te verdedigen op

donderdag 30 september 2021 des middags te 2.15 uur

door

Hey Rhyoung Lyoo

geboren op 28 februari 1988
te Seoul, Republiek Korea

Promotor:

Prof. dr. F.J.M. van Kuppeveld

Copromotoren:

Dr. J.R.P.M. Strating

Dr. H. M. van der Schaar

Dit proefschrift werd (mede) mogelijk gemaakt met financiële steun van De Europese Unie (Horizon 2020 Marie Skłodowska-Curie ETN 'ANTIVIRALS', grant agreement number 642434)

*“Trust yourself and go your own road
solely, slowly, freely that nobody has taken yet.”*

Charles Handy

TABLE OF CONTENTS

Chapter 1	General introduction	1
Chapter 2	Direct-acting antivirals and host-targeting strategies to combat enterovirus infections	21
Chapter 3	Escaping host factor PI4KB inhibition: enterovirus genomic RNA replication in the absence of replication organelles	35
Chapter 4	Modulation of proteolytic polyprotein processing by coxsackievirus mutants resistant to inhibitors targeting PI4KB or OSBP	65
Chapter 5	ACBD3 is an essential pan-enterovirus host factor that mediates the interaction between viral 3A protein and cellular protein PI4KB	75
Chapter 6	Convergent evolution in the mechanisms of ACBD3 recruitment to picornavirus replication sites	97
Chapter 7	Characterization of the c10orf76-PI4KB complex, and its necessity for Golgi PI4P Levels and enterovirus replication	131
Chapter 8	Summary and general discussion	161
Appendices	I. Nederlandse Samenvatting II. 한글요약 III. Acknowledgments IV. Curriculum vitae V. List of publications	189

CHAPTER 1

GENERAL INTRODUCTION

GENERAL INTRODUCTION

Compartmentalization of intracellular organelles is one of the key features representing eukaryotes. Each organelle has a unique structure composed of different membrane lipids and exerts a distinct function to uphold cellular homeostasis. All known positive-strand (+) RNA viruses exploit intracellular membranes to build their own membrane compartments, so-called replication organelles (ROs) which facilitate viral RNA replication. ROs have been recognized as an essential platform for efficient genome replication and have been implicated as a physical barrier against sensors of the innate immune system during replication. Interactions with host factors are crucial for the virus to induce the endomembrane reorganization and the subsequent RO formation. This thesis uncovers underlying mechanisms of virus-host interactions over the replication process, especially during the formation of ROs by enteroviruses of the family *Picornaviridae*.

Picornaviruses

Picornaviridae is one of the large families of positive-sense, single-stranded (+) RNA viruses. It comprises many human and animal pathogens causing a wide variety of diseases (reviewed in [1]). Currently, the *Picornaviridae* family consists of 158 species in 68 genera (<http://www.picornaviridae.com>). Several representative viruses as well as viruses that are most relevant to this thesis are presented in Figure 1.

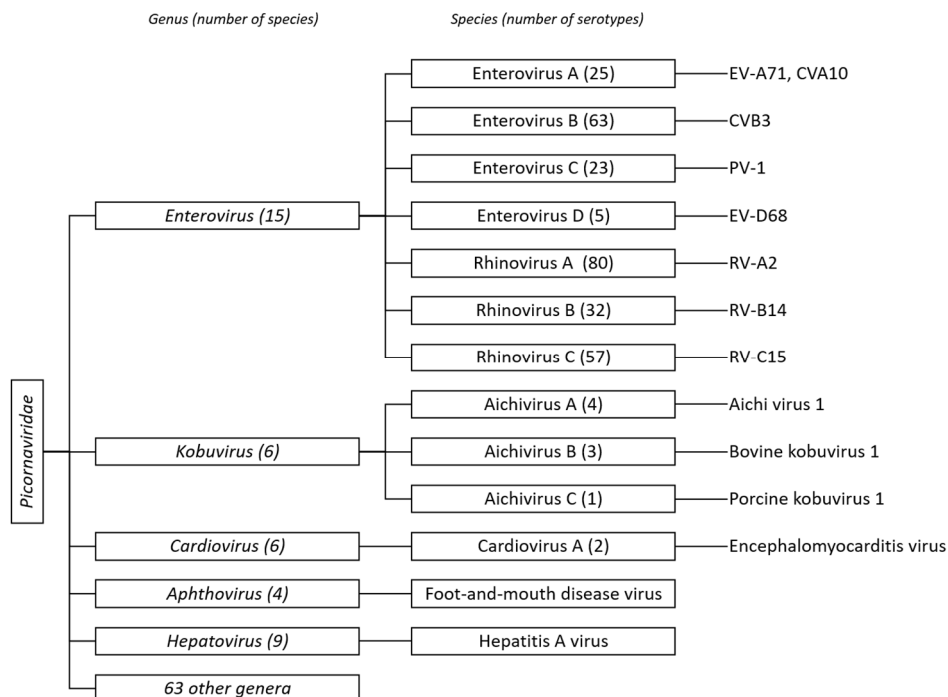


Figure 1. Classification of picornaviruses as of March 2021. Viruses that are most relevant to this thesis are depicted.

Enteroviruses

The genus *Enterovirus* is by far the largest genus among the *Picornaviridae*. Among 15 assigned species, 7 species contain human pathogens (i.e., enterovirus A-D, rhinovirus A-C). The most notorious disease caused by enteroviruses is poliomyelitis caused by poliovirus (PV). The history of poliomyelitis seems to have begun in prehistoric times as evidence has been found from ancient Egyptian relics. Outbreaks and epidemics became more prevalent in the 20th century in Europe and in the United States. The development of poliovirus vaccines greatly contributed to bring the disease under control and eliminated it from most parts of the world. Today, wild type PV circulates in only two countries (Afghanistan and Pakistan) and only one strain (type 1) out of three wild type strains still exists. Yet, an outbreak from circulating vaccine-derived PVs (cVDPVs) is a remaining hurdle that hinders the complete eradication of PV (<http://polioeradication.org>).

Besides PV, there are more than 280 serotypes of non-polio enteroviruses (NPEVs) including coxsackieviruses, echoviruses, numbered enteroviruses and rhinoviruses. NPEVs can cause various mild and more severe diseases, especially in young children and immunocompromised individuals. Coxsackieviruses (CVs), echoviruses, and numbered enteroviruses (EVs) can cause among others viral aseptic meningitis, encephalitis, acute flaccid paralysis, hand-foot-and-mouth disease, herpangina, pleurodynia, acute myocarditis, pancreatitis, and acute hemorrhagic conjunctivitis. Rhinoviruses (RVs) are the most common viral cause of the common cold, but also more severe respiratory diseases including exacerbation of asthma and chronic obstructive pulmonary disease (COPD) are attributed to RV infections.

Apart from vaccines against PV and EV-A71, there are no approved prevention and treatment measures for enterovirus infections. Development of vaccines against all individual serotypes or subgroups of enteroviruses is laborious, given the large number of (sero-)types (i.e., >100 non-polio enteroviruses and >150 rhinoviruses). To target the large variety of enteroviruses as well as to minimize the risk of PV circulation in the post-eradication era, there is a great need for (broad-acting) antivirals against enteroviruses. A detailed summary of antiviral drug development is described in Chapter 2 of this thesis.

Enterovirus life cycle

The genome of enteroviruses is ~7.5 kb and it encodes a single polyprotein that can be divided into 3 regions: P1, P2, and P3 (Figure 2). The P1 region harbors 4 structural proteins (VP4, VP2, VP3, VP1) that together form the capsid coat of the virion, while P2 and P3 encode replication proteins that are only expressed in infected cells. The P2 region contains protease 2A, viroporin 2B, and multifunctional protein 2C that among others has RNA helicase and ATPase activities. The P3 region includes the key membrane reorganizer 3A, RNA primer 3B, viral protease 3C, and RNA-dependent RNA polymerase (RdRp) 3D. Unlike cellular mRNA, the genome of enterovirus is not capped at 5'-end but covalently bound to VPg (viral protein genome-linked; 3B), which acts as a primer during the RNA replication stage [2]. The long 5'-UTR (untranslated region) contains structured RNA regions such as the cloverleaf and IRES (internal ribosome entry site) as functional domains. The short 3'-UTR contains a poly(A) tail [3].

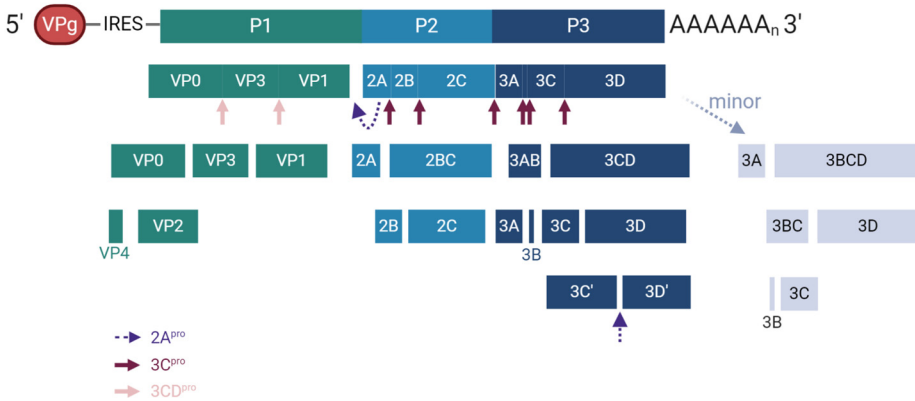


Figure 2. Genome orientation of enterovirus and the processing of viral polyprotein by viral proteases. Translation of enterovirus genome is undertaken by host translation machinery that is recruited to the internal ribosome entry site (IRES) in the 5'-UTR. Translation yields a single polyprotein that undergoes co- and post-translational processing by viral proteases as depicted in the figure. Created with BioRender.com.

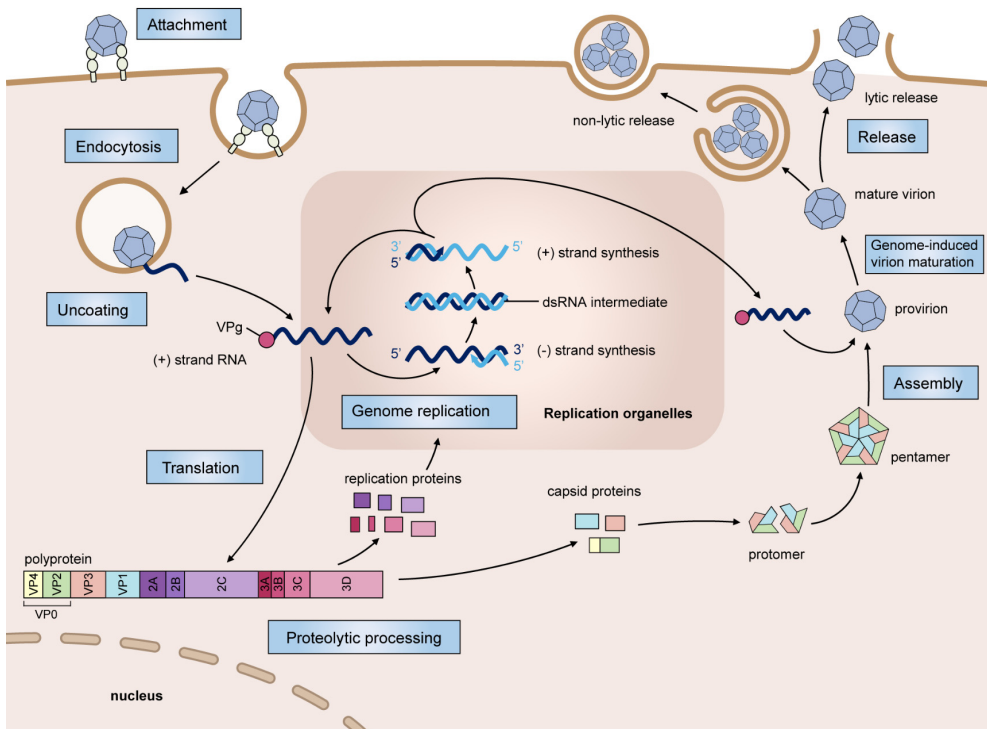


Figure 3. Schematic overview of the enterovirus life cycle. After virion binding to its receptor(s) and endocytic uptake, (+) RNA genome is released into the cytoplasm. Genome translation yields a single polyprotein that is cleaved into replication proteins (2A–2C and 3A–3D) and capsid proteins (VP0, VP1, and VP3). Genome replication by the viral RNA-dependent RNA polymerase (3D^{pol}) synthesizes a (–) RNA that serves as a template for synthesis of new (+) RNA. Replication takes place in conjunction with replication organelles. (+) RNA molecules can either enter a new round of replication or be packaged into progeny virions. Capsid proteins organize into protomers and pentamers by themselves and assemble into provirions containing (+) RNA. Upon the genome-induced cleavage of VP0 into VP4 and VP2, provirions are converted into infectious, mature virions. Mature virions exit the host cell via non-lytic release or via cell lysis. dsRNA, double-stranded RNA. Adapted from [4] with permission.

A schematic illustration of the enterovirus life cycle is presented in Figure 3. Infection of a cell begins with the attachment of a virion to its receptor on the cell surface. For some enteroviruses, binding to its receptor destabilizes the virion to promote uncoating, while other enteroviruses require a low pH present in the endosomes as an uncoating cue (reviewed in [4]). The subsequent process of RNA release is still poorly understood. Recently, the host factor phospholipase A2 group XVI (PLA2G16) was identified as a universal host factor of enteroviruses that facilitates the genome release from endocytic vesicles, possibly by facilitating membrane pore formation [5].

The genome is immediately translated into a single large polyprotein, which is subsequently proteolytically processed by the viral proteinases 2A^{pro} and 3C^{pro}/3CD^{pro} to yield the individual capsid proteins, replication proteins, and some stable and functional precursors such as 2BC, 3AB, and 3CD. Replication of the viral genome by 3D^{pol} starts with the synthesis of complementary negative-strand (-) RNA molecules, which serve as a template for the synthesis of multiple new (+) RNA molecules. Newly synthesized (+) RNA molecules either enter another round of translation and replication or are assembled with capsid proteins into progeny virions. More detailed explanation for genome translation and replication is described in the following section. The new virions are released into the extracellular environment upon host cell lysis, although growing evidence suggests that virions can also be secreted via nonlytic release prior to cell lysis and transmitted in vesicles containing multiple virions [6], similar to the mode observed previously for the other picornaviruses, hepatitis A virus [7] and encephalomyocarditis virus [8].

Genome translation and replication

The genomic RNA of enteroviruses lacks a 5' cap that can be recognized by ribosome. Instead, translation is driven by recruiting translation machinery to the internal ribosome entry site (IRES) in the 5'-UTR [3]. Genome translation yields a single polyprotein that undergoes co- and post-translational processing. This process does not depend on host proteases and is governed by viral proteases that catalyze protein cleavages in *cis* and *trans*. The primary processing occurs at the N'-terminal of 2A to separate capsid proteins (P1) from replication proteins (P2-P3) [9] (Figure 2). The cleavage at the P2/P3 junction is mediated by 3C^{pro}. 3C^{pro} is also responsible for the processing of P2 and P3 precursors to functional intermediates (e.g., 2BC, 3AB, and 3CD) or mature proteins [10, 11]. The processing of P1 capsid precursors is mediated by 3CD^{pro} [12]. 2A^{pro} and 3C^{pro} are also responsible for the cleavage of several host factors. Cellular innate immune sensors such as MDA5 are cleaved by these proteases during infection which limit a type I interferon-mediated response [13]. EIF4G, which is required for cap-dependent mRNA translation, is cleaved by 2A^{pro}, resulting in the shutoff of host protein production [14, 15].

After initial translation of the incoming viral RNA (vRNA), the synthesis of complementary negative-strand (-) RNA molecules is catalyzed by 3D^{pol}. The RNA replication mechanism is well-conserved among picornaviruses [16]. This requires a membrane-associated replication complex (RC) consisting of viral and cellular proteins and a viral RNA template with the *cis*-acting replication elements. A RC is formed around the 5' cloverleaf RNA structure that interacts with the poly(A) binding protein (PABP) bound to the 3' poly(A) tail, resulting in the circularization of the viral genome. Formation of this circular complex is required for initiation of (-) strand RNA synthesis [17], which in turn serves as a template for the synthesis of multiple new (+) RNA molecules. A cloverleaf-like structure located at the very end of 5'-UTR also has a functional role in RNA replication by forming essential ribonucleoprotein (RNP)

complexes with 3CD protein in the presence of either host protein PCBP or viral protein 3AB. Mutations that disrupt the RNP formation abrogate RNA replication but do not affect translation [18]. The CRE, a small hairpin structure at 2C, is used as a template for the uridylation of VPg, which yields mono- and di-uridylylated VPg (VPgpU and VPgpUpU respectively) during the initiation phase of RNA synthesis. 3D^{pol} uses uridylylated VPg as primer for (-) and (+) RNA synthesis, respectively [19]. Newly synthesized (+) RNA molecules can either enter a new round of translation and replication or be assembled with capsid proteins into progeny virions.

Remodeling of host membranes: the formation of replication organelles

Since electron tomography has become widely available over the past decade, the architectures of replication organelles (ROs) have been described for many different (+) RNA viruses (reviewed in [20]). The endomembrane system in cells infected with (+) RNA viruses undergoes drastic changes over the course of virus replication. Cellular organelles can be targeted and rearranged to build complex and unique membranous structures; so called viral replication organelles (ROs). The structure, the composition, and the formation process of ROs can vary greatly among groups of viruses and even between viruses that belong to the same family [21, 22]. Yet, two functions of ROs are generally accepted as common features. ROs can facilitate the genome replication by concentrating viral factors and essential host factors in specific compartment. Additionally, ROs can also be a physical barrier to hide vRNA replication intermediates from cellular sensors [22].

The morphology of ROs can be divided into two types: invagination-type and protrusion-type (reviewed in [22, 23]). Flaviviruses, such as Dengue virus, West Nile virus, Yellow fever virus, and Zika virus, induce the invagination of endoplasmic reticulum (ER). RNA synthesis takes place within the spherules, which are connected to the cytoplasm through a pore-like opening ranging from 4 to 10 nm in diameter. These openings allow the exchange of small molecules such as nucleotides or newly synthesized RNAs but are not sufficiently large for cellular sensors of viral RNA to pass through [24, 25].

Double membrane vesicles (DMVs) are the hallmark of structures that are found in many protrusion-type ROs, but the pathways of DMV biogenesis can be different between virus groups. For enteroviruses, DMVs are gradually derived from single membrane vesicles or tubules and eventually transformed to multilamellar structures [26-28] (Figure 4). A similar pathway seems to take place in norovirus- and hepatitis C virus (HCV)-infected cells [29-31]. In coronavirus (CoV)-infected cells, however, another pathway of DMV biogenesis was observed, where paired ER membranes undergo bending and fission, and finally develop into DMVs [32-34]. DMVs are the most abundant component of CoV ROs, and it appears to be the central hubs for viral RNA synthesis as double-stranded RNA (dsRNA) is found inside DMVs [35, 36]. As CoV-induced DMVs appeared as completely closed compartments, it remained a mystery that how synthesized RNAs would be transported to outside. A recent discovery finally revealed the presence of a molecular pore complex spanning membranes of DMVs in CoV-infected cells which allows RNA to be exported to the cytosol [37].

Unlike DMVs in CoV-infected cells, viral RNA synthesis of enteroviruses is unlikely to occur within the DMVs. DMVs in enterovirus-infected cells are often found as a closed compartment, and more importantly, the majority of RNA synthesis seems to precede the formation of DMVs [26]. RNA replication during early infection is mostly associated with the cytosolic side of single membrane structures [38]. It is unclear whether ROs are indispensable for enterovirus replication.

The origin of enterovirus ROs remains unclear. ER and Golgi, where the early vRNA synthesis was observed, have been suggested as a membrane donor for enteroviral ROs [39]. Not to mention that several Golgi-residing proteins were found on RO membranes, RO formation often coincided with the Golgi disassembly in infected cells, which have pointed transformation of Golgi membranes into ROs [40-53]. In addition to that, the hijacked autophagic pathway could also play a key role in RO formation. The formation of DMVs and the subsequent enwrapping process are reminiscent of autophagosome formation. In accordance with this, many enteroviruses have been found to facilitate the production of autophagosomes, and inhibition of autophagy impeded virus replication [54-65]. Still, sites of early vRNA synthesis may not necessarily correspond to the sites exploited for RO formation and direct connection between cellular organelles and ROs have not been shown.

Several viral and host factors are known to be important for intracellular membrane reorganization and subsequent RO formation in enterovirus-infected cells (Figure 5), which are described in more details below.

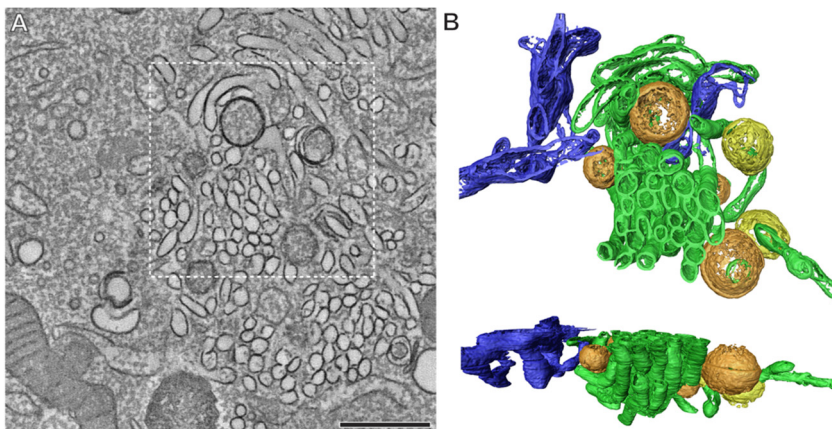


Figure 4. Electron tomography of the early structures of coxsackievirus B3-induced replication organelles. (A) Tomographic slice through the serial tomogram, with clusters of single-membrane structures and sparsely embedded double membrane vesicles (DMVs). The scale bar is 500 nm. (B) Top and side views of a surface-rendered model of the region boxed in panel A showing single-membrane tubules (green), open (orange) and closed (yellow) DMVs, and ER (blue). Adapted from [26] with permission.

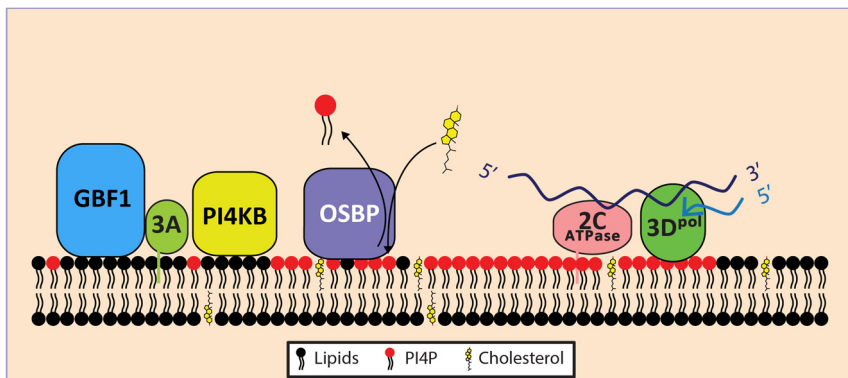


Figure 5. Schematic representation of RO membranes. For a detailed description, see the main text.

Viral proteins

Not all viral proteins are involved in membrane rearrangement. 2B, 2C, and 3A (as well as the stable precursors, 2BC and 3AB) can anchor to cellular membranes and modify membrane properties. Enterovirus 2B targets ER and Golgi membranes where it acts as a viroporin, modulates membrane permeability and disrupts the Ca^{2+} concentration gradient. Expression of 2B in cells blocks protein secretion and induces permeabilization of the plasma membrane and Golgi fragmentation [40, 41, 66-68]. Yet it is not clear whether its function as a viroporin is required for RO formation. The 2C protein of enteroviruses is one of the most versatile viral proteins. Known enzymatic activities of 2C protein include ATPase and RNA helicase [69-72]. Additionally, the 2C protein was suggested to be involved in uncoating of virions [73] and encapsidation of newly formed viral genomes [74-76]. The interaction between 2C and ER proteins called reticulons indicates that 2C could play a role in vesicle formation from ER membranes [77]. Expression of either 2C or 2BC alone is sufficient to induce membrane alteration, but the structures that resembles ROs were only observed when 2BC and 3A are coexpressed [39, 78-80]. Enterovirus 3A proteins vary in size, ranging from 74 to 89 aa, but they all have a hydrophobic domain at the C-terminus that anchors 3A and 3AB to membranes. Expression of 3A protein alone seems to target primarily Golgi membranes and induces Golgi disassembly. 3A is known to interact with multiple host factors including Golgi-resident proteins GBF1 and PI4KB [47] which are described in detail below.

Host factors*PI4KB and PI4P*

Cellular structural lipids are mainly composed of phospholipids (PLs). Among diverse PLs, phosphoinositides (PIs), which make up only a small fraction of PLs, are major determinants of organelle identity and function, and are among others involved in vesicular trafficking and lipid distribution (reviewed in [81]). There are seven PIs, and the interconversion between different PIs are mediated by various PI kinases and PI phosphatases. One of the most abundant PIs in the cell is phosphatidylinositol 4-phosphate (PI4P). Four distinct phosphatidylinositol 4-kinases (PI4Ks) are responsible for the synthesis of PI4P from phosphatidylinositol in mammalian cells: type II alpha (PI4KIIA) and beta (PI4KIIB), type III alpha (PI4KA) and beta (PI4KB). PI4Ks catalyze the ATP-dependent phosphorylation of phosphatidylinositol on the D4 position.

PI4Ks and PI4P are involved in regulating structures and functions of the Golgi complex through various mechanisms. Enrichment of PI4P on the cytosol-facing, outer lipid layer may promote vesicle formation via intrinsically inducing curvature in membranes through the shape of the PI4P molecule [82] or by recruiting lipid-binding proteins such as GOLPH3 [83] or arfaptins [84]. PI4P, usually in concert with the small GTPase Arf1, also mediates recruitment of several different lipid transfer proteins such as oxysterol binding protein (OSBP), a regulator of cholesterol/PI4P exchange at ER-Golgi membrane contact sites, and phosphoinositide 4-phosphate adapter protein 2 (FAPP2) via their PI4P-specific PH domains. Recruitment of OSBP greatly alters the composition of membranes to contain increased levels of cholesterol [85] and sphingomyelin [86], whereas FAPP2, by binding to PI4P, is capable of transforming membrane sheets into tubules [87, 88]. Recruitment of the small GTPase Rab11 by PI4KB followed by recruitment of effector proteins such as FIP3 can facilitate anterograde vesicle transport [89, 90]. Furthermore, PI4P is also suggested as an important signaling molecule. Phospholipase C α

(PLC ϵ) hydrolyzes Golgi PI4P to generate diacylglycerol (DAG), which can activate the ERK/MAPK pathway [91, 92]. Both PI4KB and OSBP have been shown to be regulators of PI4P-dependent ERK and MAPK pathways [93-95].

Among all four PI4Ks that have associated with Golgi functions (reviewed in [96]), the role of PI4KB is best studied and it is widely accepted that PI4KB is especially important for regulating PI4P level at the Golgi. PI4KB takes part in diverse trafficking pathways by regulating the formation of secretory (reviewed in [96]), endosomal [97, 98], and non-canonical autophagic vesicles [47, 48, 99]. Several proteins have been reported to be responsible for the recruitment of PI4KB to the Golgi, which include Arf1 [100], GGA2 [98], NCS-1 [101], and ACBD3 [47, 48, 99]. Among those binding partners, detailed structural evidence strongly supports the key role of ACBD3 in the recruitment of PI4KB to the Golgi membrane (Figure 6) [99]. While it was initially suggested that ACBD3 could mediate the activation of PI4KB, subsequent studies supported the idea that ACBD3 merely brings the enzyme closer to its substrate rather than activating the kinase [99, 102]. Together with the 14-3-3 protein family, Arf1 has been suggested to be a positive regulator of PI4KB activity [103, 104]. Binding of 14-3-3 proteins to PI4KB, however, does not stimulate the catalytic activity of the kinase but protects it from dephosphorylation to stabilize the enzymatic activity [105].

The importance of PI4P has been studied well for several (+) RNA viruses including enteroviruses, cardioviruses, and kobuviruses (*Picornaviridae*), and hepatitis C viruses (HCV; *Flaviviridae*) [48, 53, 106]. Enteroviruses and kobuviruses depend on the Golgi-resident PI4KB to induce PI4P production at ROs, while cardioviruses and HCV require the ER-resident PI4KA. Increased levels of PI4P may drive the bending of the targeted membrane into a positive curvature and provide a docking platform for host factors (e.g., OSBP) that can create membrane contact sites (MCSs) between ROs and ER [107]. As a negatively charged lipid, PI4P, in consort with viral 3B protein, can recruit the viral polymerase 3D [53, 108]. All enteroviruses depend on PI4KB activity for efficient replication and RO formation, which made PI4KB a promising target for a broad-spectrum antiviral drug against enteroviruses. Mutations in 3A proteins of several enteroviruses have been identified to confer resistance to PI4KB inhibitors [109-112]. The 3A protein of Aichi virus (AiV), which belongs to the *Kobuvirus* genus in the *Picornavirus* family, recruits PI4KB to ROs via an 3A-ACBD3-PI4KB interaction [48, 113]. There has not yet been a consensus about whether enterovirus 3A proteins also depend on ACBD3 for the recruitment of PI4KB.

OSBP and cholesterol

Over the past decades, the importance of membrane contact sites (MCSs) has emerged and has been studied to a great extent including the role of tethering proteins (reviewed in [114, 115]). One of these proteins, OSBP, is involved in the MCS formation between ER and the Golgi. It binds to the ER receptor VAP through its central FFAT motif, whereas the PH domain at the other side simultaneously binds Arf1 and PI4P at the Golgi. Once the MCS is formed, OSBP exchanges sterol-PI4P through its lipid transfer domain. In this sterol-PI4P exchange reaction, PI4P follows its concentration gradient while sterols are being pumped against their concentration gradient [85]. A PI4P-generating kinase at the Golgi (e.g., PI4KB) and a PI4P-degrading phosphatase in the ER (e.g., Sac1) play key roles in regulating the directionality of the PI4P-sterol exchange reaction.

In uninfected cells, OSBP transfers cholesterol from ER to *trans*-Golgi in a PI4P-dependent manner [85, 116]. Similar to this canonical function of OSBP, PI4P-OSBP-cholesterol pathway is exploited by enteroviruses [51, 107, 117, 118], AiV [119] and encephalomyocarditis virus (EMCV) [106, 118] to

create a novel MCS between ER and ROs, resulting in increased cholesterol level in RO membranes[120]. Pharmacological inhibition of OSBP activity effectively suppressed enterovirus replication, but the same mutations in 3A proteins that conferred resistance to PI4KB inhibitors, also allowed viruses to be independent of OSBP activity [107]. This suggests that exploitation of PI4KB and OSBP by enteroviruses is mainly mediated by 3A proteins.

Cholesterol levels in infected cells can also be regulated by other viral proteins than 3A. Ectopic expression of 2BC protein alone was sufficient to increase endocytic uptake of cholesterol and induces intracellular cholesterol levels in cells [117, 120], implying another level of complexity behind the hijacking of cholesterol by enteroviruses. Lipid droplets (LDs) have also been suggested as a source of cholesterol. LDs were found near the replication sites and a LD-associated lipase (i.e., hormone-sensitive lipase; HSL) that catalyzes hydrolysis of various cholesteryl esters from LDs to cholesterol was shown to be required for efficient rhinovirus replication [51]. Recently, poliovirus 2B, 2C and their precursor 2BC were found to be targeting LDs via the amphipathic helix domain [121]. In the same study, mainly RO-localizing viral 3A protein was found to interact with the LD-associated lipases ATGL and HSL, which suggests the presence of MCSs between ROs and LDs. Whether 3A directly drives the interaction between ROs and LDs or whether 2B, 2C or 2BC are involved in the formation this MCS requires further investigation.

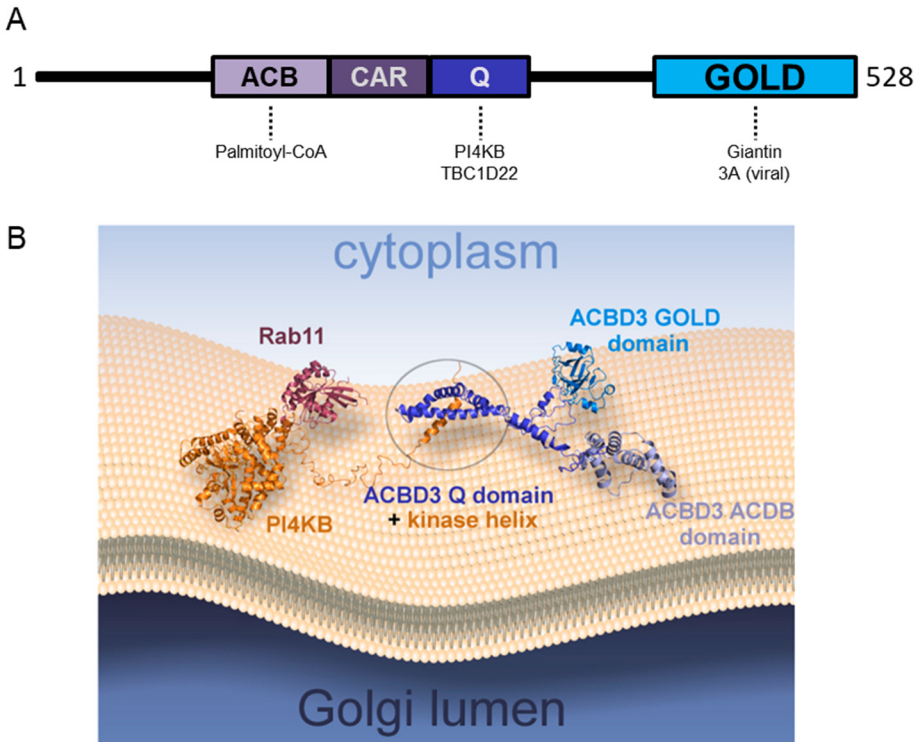


Figure 6. Schematic representation of ACBD3 domains and pseudoatomic model of PI4KB-ACBD3 complex. (A) Domains of ACBD3 and interactors. (B) A pseudoatomic model of ACBD3 based on structures of individual domains. Adapted from [99].

ACBD3

The Golgi-resident protein acyl-CoA binding domain containing 3 (ACBD3) is well known to recruit PI4KB to the Golgi [47, 48, 99]. ACBD3 was first found as a Golgi scaffolding protein that interacts with the Golgi tethering proteins Giantin and Golgin-160, supports the structural integrity and the functioning of the Golgi, and additionally regulates apoptosis [122-124]. To date, more than 15 different interaction partners of ACBD3 have been identified, including several bacterial and viral proteins, pointing out the miscellaneous functions of this protein in both physiology and pathology. In addition to its role in Golgi structure maintenance, ACBD3 is suggested to take part in steroidogenesis, lipid metabolism and transport, and iron uptake (reviewed in [125]).

ACBD3 directly interacts with PI4KB via its Q domain, while the GOLD domain mediates targeting to the Golgi by binding to Giantin, Golgin160, and/or Golgin45 (Figure 6). The GOLD domain also mediates the interaction with 3A proteins of enteroviruses and kobuviruses. The 3A-GOLD interaction and the Giantin-GOLD interaction are mutually exclusive, and the colocalization of ACBD3 and Giantin disappears in virus-infected cells [48]. The ACB domain, which is conserved among all ACB domain containing proteins (ACBD1 – ACBD7), has a cavity that at least in some family members has been shown to accommodate acyl-CoA [126].

ACBD3 has been shown to bind to the 3A proteins of a number of enteroviruses, including those of PV, CVB3, and RV [47, 127], which suggests that ACBD3 is a cofactor required for PI4KB recruitment to the ROs. For AiV (*Kobuvirus*), viral protein 3A was shown to directly interact with ACBD3 and recruit PI4KB to ROs [48, 128]. Enterovirus 3A proteins differ from *Kobuvirus* 3A both in sequence and in structure, implying that enteroviruses may apply different tactics to recruit ACBD3 and PI4KB to ROs. Several studies have investigated whether enteroviruses depend on ACBD3 to recruit PI4KB. While silencing of ACBD3 inhibited PV replication in one study [47], another reported no inhibition of PV replication upon ACBD3-knockdown [50]. Similar to this, neither inhibition of CVB3 or RV replication nor effects on PI4KB recruitment were observed in ACBD3-silenced cells [52, 127]. Thus, the role of ACBD3 for PI4KB recruitment during enterovirus infection remains under discussion. Considering the multifaceted interactions that are mediated by ACBD3, the role of ACBD3 in enterovirus seems complex and needs to be investigated further.

GBF1 and Arf1

Arf1 belongs to the Arf (ADP-ribosylation factor) family of G proteins including six Arfs and more than 20 Arf-like proteins that regulate vesicle trafficking, organelle structure, and cellular signaling (reviewed in [129]). The activity of Arfs is regulated through a cycle of GTP binding and GTP hydrolysis regulated by Arf guanine nucleotide exchange factors (GEFs) and GTPase-activating proteins (GAPs), respectively. GBF1 (Golgi brefeldin A resistant guanine nucleotide exchange factor 1) is a GEF and an activator of Arf1 [130, 131]. Activation of Arf1 by GBF1 among others serves to recruit COPI vesicle coat proteins to the Golgi membrane, which is crucial for Golgi-to-ER trafficking [132, 133]. Besides its role in regulating the secretory pathway, Arf1/COPI machinery also has been suggested to be involved in LD formation and LD-ER MCS formation [134, 135]. GBF1 binds to Arf1 in the GDP-form through its catalytic Sec7 domain, inducing a conformational change of Arf1 and promoting the exchange of GDP for GTP, which eventually leads to the dissociation of Arf1-GTP from GBF1. There are also five non-catalytic domains in GBF1, but the functions of these domains remain mostly obscure.

Many functions of GBF1 have been identified by utilizing inhibitors such as the bacterial metabolite Brefeldin A (BFA) and the small molecule Golgicide A (GCA). Although both molecules work in a similar way by stabilizing the complex between Arf1-GDP and GEF through binding at SEC7 domain, thereby blocking the function of GEFs [136], GCA is a specific GBF1 inhibitor while BFA also targets other GEFs like BIG1 and BIG2 [137]. Inhibition of GBF1 function interferes with the vesicle transport and induces the disassembly of Golgi cisternae.

Application of these drugs has aided the discovery of the importance of GBF1 in the replication of many RNA viruses from different families (reviewed in [138]). The inhibition of GBF1 function by siRNA knockdown or by an inhibitor hindered replication of enteroviruses throughout different species [42, 46, 49, 127, 139-146]. The role of GBF1 in enterovirus replication is still not clearly understood, yet. It is suggested that GBF1 is dispensable for the formation of ROs but is required for recruiting Arf1 to ROs [142], resulting in the depletion of COPI from RO membranes and the inhibition of cellular secretory pathway [43-45, 147]. The recruitment of GBF1 to RO membranes is mediated by the viral 3A protein via interaction of N-terminal parts of GBF1 and 3A [43-45, 142, 147, 148]. Nonetheless, whether the 3A-GBF1 interaction is crucial for enterovirus replication remains ambiguous. Mutations in 3A that abolish the interaction with GBF1 have relatively small effects on genome replication of PV and CVB3 [44, 46, 142, 147]. Furthermore, RV-B14 3A and RV-A2 3A have little to no interaction with GBF1 whilst GBF1 can be recruited to their ROs [45, 52], indicating a minimal role of the 3A-GBF1 interaction in GBF1 recruitment. However, GBF1 mutants that are incapable of interacting with 3A could not restore virus replication in the presence of a GBF1 inhibitor and viruses with mutations in 3A became more sensitive to BFA treatment [46, 142]. All these findings are adding complexity to understanding the mechanism by which enteroviruses exploit GBF1.

It remains elusive whether Arfs are necessary for enterovirus replication and, if so, whether they are activated by GBF1 or other GEFs. The depletion of Arfs by siRNA was shown to reduce the replication of EV-A71, CVB3, and CVB4 [53, 145, 146]. Yet, Arf activation during enterovirus infection could be independent of the catalytic activity of GBF1 since the overexpression of a GBF1 mutant lacking the Sec7 domain still restored enterovirus replication upon BFA treatment to a certain extent [46, 148]. Also, the expression of constitutively activated Arf1 could not rescue PV replication upon depletion of GBF1 function either by siRNA or by BFA, which suggests that an Arf1-independent GBF1 function is required for virus replication [142]. Although there is no evidence for direct interaction between Arf1 and PI4KB, PI4KB is an effector of Arf1 at the Golgi [100]. Hence, it was proposed that GBF1/Arf1 may play a role in PI4KB recruitment by 3A. However, the 3A proteins of CVB3 and rhinovirus were shown to recruit the kinase independently of GBF1/Arf1 [52, 127].

Recent studies suggest the involvement of GBF1 in regulating the lipid flux from LDs to ROs. GBF1 directly interacts with adipose triglyceride lipase (ATGL) and GBF1, Arf1, COPI machinery have been shown to be involved in recruiting ATGL and ADRP (adipophilin) to LDs [149, 150]. ATGL, together with hormone-sensitive lipase (HSL) were recently found to be important for mobilizing neutral lipids from LDs, thereby fueling phospholipid synthesis that drives RO formation [151]. The role of GBF1/Arf1 in enterovirus replication might be different from their canonical functions and requires further evaluation.

c10orf76

c10orf76 has been first identified as a PI4KB interactor by mass spectrometry [152, 153], and is still a poorly characterized protein. *c10orf76* is recently suggested as a novel enterovirus host factor seemingly by regulating the level of PI4P at the Golgi [154]. While the genome replication and RO formation of CV-A10 were abolished in *c10orf76* KO cells, CV-B1 replication remained unaffected. Since two viruses that were tested belong to different enterovirus species, this could indicate a species-specific dependence on *c10orf76*. Yet, the cell type might have affected the outcome, since the Hap1 cells that were used in that study do not support replication of all enteroviruses to the same extent. Further investigation is needed to understand to which extent different enteroviruses require *c10orf76*, and whether *c10orf76* is involved in PI4KB recruitment to ROs.

Aim and outline of this thesis

The formation of ROs is a universal feature that can be found in infected cells by any positive-strand RNA viruses. Both viral proteins and host factors are required for the membrane reorganization process. For enteroviruses, viral protein 3A and the cellular lipid kinase PI4KB, among other viral and cellular factors, have been suggested to be the key factors that drive this process. This thesis aims to provide mechanistic insights on the role of PI4KB and its interactors in enterovirus replication and RO formation.

Chapter 2 provides a comprehensive summary of the status of anti-enteroviral drug development and discusses different drug development strategies as well as the pros and cons of each strategy. To date, there are no approved antivirals that can treat enterovirus infections. Given the large number of (sero-)types, development of vaccines against all enteroviruses is unlikely attainable. Antivirals with broad-acting efficacy are most desired to combat numerous enterovirus infections. One of the classical approaches is to develop direct-acting inhibitors such as capsid inhibitors that block attachment and/or entry or polymerase inhibitors that can terminate genomic RNA synthesis. Alternatively, a function of essential host factors can be a promising target to treat a broad range of enteroviruses. The findings that have been made in the following chapters will contribute to developing host targeting antivirals.

Mutations in viral protein 3A confer resistance to PI4KB and OSBP inhibitors. In **chapter 3** and **4**, we employed a mutant virus that is insensitive to PI4KB inhibition (i.e., CVB3 3A-H57Y) to understand the functions of PI4KB and its product, PI4P, in RO biogenesis and the potential mechanism of enteroviruses to overcome PI4KB inhibition. We explored the role of PI4KB and PI4P in RO genesis and evaluated if ROs play a critical role as a physical barrier towards cellular innate immunity sensors. Additionally, we investigated whether the polyprotein processing of viral proteins is affected by lipid compositions of ROs, and how mutations in viral proteins provide benefit.

The 3A-PI4KB interaction is crucial for enterovirus replication, yet the molecular understanding of this interaction is poorly understood. In **chapter 5**, we studied the role of the Golgi-resident protein ACBD3 as a mediator of the 3A-PI4KB interaction. We generated ACBD3 KO cells by utilizing CRISPR-Cas9 techniques to better understand the importance of ACBD3. A broad range of enteroviruses was tested to determine if the ACBD3 dependency is a generic trait among enteroviruses. By utilizing mutant versions of ACBD3 and PI4KB that cannot bind to each other, we revealed the importance of the ACBD3-PI4KB interaction for replication of all enteroviruses (including rhinoviruses). Furthermore, in **chapter 6**, we determined the crystal structure of the ACBD3 GOLD domain together with 3A proteins from different enteroviruses. The binding interface between 3A and ACBD3 was further characterized by a mutagenesis study.

Protein c10orf76 was poorly characterized in terms of its localization and its function, except for being an interactor of PI4KB. In **chapter 7**, we aimed to identify the canonical role of c10orf76 in cells as well as its possible involvement in enterovirus replication. We utilized hydrogen-deuterium exchange mass spectrometry, biochemical assay, as well as cell-based assays to characterize the c10orf76-PI4KB interaction. Based on this characterization, we generated mutants that prevent the interaction between c10orf76 and PI4KB to define the role of the c10orf76-PI4KB complex in PI4KB activity and enterovirus replication.

Chapter 8 provides a summary of main findings and a general discussion.

REFERENCES

1. Tapparel, C., et al., *Picornavirus and enterovirus diversity with associated human diseases*. Infection, Genetics and Evolution, 2013. 14: p. 282-293.
2. Paul, A.V., et al., *Protein-primed RNA synthesis by purified poliovirus RNA polymerase*. Nature, 1998. 393(6682): p. 280-4.
3. Ehrenfeld, E., E. Domingo, and R.P. Roos, *The Picornaviruses*. 2010: American Society of Microbiology.
4. Baggen, J., et al., *The life cycle of non-polio enteroviruses and how to target it*. Nature Reviews Microbiology, 2018. 16(6): p. 368-381.
5. Staring, J., et al., *PLA2G16 represents a switch between entry and clearance of Picornaviridae*. Nature, 2017. 541(7637): p. 412-416.
6. Mohamud, Y. and H. Luo, *The Intertwined Life Cycles of Enterovirus and Autophagy*. Virulence, 2019. 10(1): p. 470-480.
7. Kirkegaard, K., *Unconventional secretion of hepatitis A virus*. Proceedings of the National Academy of Sciences of the United States of America, 2017. 114(26): p. 6653-6655.
8. van der Grein, S.G., et al., *Picornavirus infection induces temporal release of multiple extracellular vesicle subsets that differ in molecular composition and infectious potential*. PLOS Pathogens, 2019. 15(2): p. e1007594.
9. Skern, T., et al., *Structure and Function of Picornavirus Proteinases*, in *Molecular Biology of Picornavirus*. 2002, American Society of Microbiology. p. 199-212.
10. Korant, B., et al., *Virus-specified protease in poliovirus-infected HeLa cells*. Proc Natl Acad Sci U S A, 1979. 76(6): p. 2992-5.
11. Hanecak, R., et al., *Proteolytic processing of poliovirus polypeptides: antibodies to polypeptide P3-7c inhibit cleavage at glutamine-glycine pairs*. Proc Natl Acad Sci U S A, 1982. 79(13): p. 3973-7.
12. Ypma-Wong, M.F., et al., *Protein 3CD is the major poliovirus proteinase responsible for cleavage of the p1 capsid precursor*. Virology, 1988. 166(1): p. 265-270.
13. Dotzauer, A. and L. Kraemer, *Innate and adaptive immune responses against picornaviruses and their counteractions: An overview*. World J Virol, 2012. 1(3): p. 91-107.
14. Glaser, W. and T. Skern, *Extremely efficient cleavage of eIF4G by picornaviral proteinases L and 2A in vitro*. FEBS Lett, 2000. 480(2-3): p. 151-5.
15. Novoa, I. and L. Carrasco, *Cleavage of eukaryotic translation initiation factor 4G by exogenously added hybrid proteins containing poliovirus 2Apro in HeLa cells: effects on gene expression*. Mol Cell Biol, 1999. 19(4): p. 2445-54.
16. Paul, A.V. and E. Wimmer, *Initiation of protein-primed picornavirus RNA synthesis*. Virus Res, 2015. 206: p. 12-26.
17. Herold, J. and R. Andino, *Poliovirus RNA replication requires genome circularization through a protein-protein bridge*. Molecular cell, 2001. 7(3): p. 581-591.
18. Paul, A.V., et al., *Model of Picornavirus RNA Replication*, in *Viral Genome Replication*, K.D. Raney, M. Gotte, and C.E. Cameron, Editors. 2009, Springer US: Boston, MA. p. 3-23.
19. Murray, K.E. and D.J. Barton, *Poliovirus CRE-dependent VPg uridylylation is required for positive-strand RNA synthesis but not for negative-strand RNA synthesis*. J Virol, 2003. 77(8): p. 4739-50.
20. Sachse, M., et al., *The viral replication organelles within cells studied by electron microscopy*. Adv Virus Res, 2019. 105: p. 1-33.
21. Harak, C. and V. Lohmann, *Ultrastructure of the replication sites of positive-strand RNA viruses*. Virology, 2015. 479-480: p. 418-33.
22. Romero-Brey, I. and R. Bartenschlager, *Membranous replication factories induced by plus-strand RNA viruses*. Viruses, 2014. 6(7): p. 2826-2857.
23. Strating, J.R. and F.J. van Kuppeveld, *Viral rewiring of cellular lipid metabolism to create membranous replication compartments*. Current opinion in cell biology, 2017. 47: p. 24-33.
24. Welsch, S., et al., *Composition and three-dimensional architecture of the dengue virus replication and assembly sites*. Cell host & microbe, 2009. 5(4): p. 365-375.
25. Gillespie, L.K., et al., *The endoplasmic reticulum provides the membrane platform for biogenesis of the flavivirus replication complex*. Journal of virology, 2010. 84(20): p. 10438-10447.
26. Limpens, R.W.A.L., et al., *The transformation of enterovirus replication structures: a three-dimensional study of single- and double-membrane compartments*. mBio, 2011. 2(5): p. e00166-11.
27. Belov, G.A., et al., *Complex dynamic development of poliovirus membranous replication complexes*. Journal of virology, 2012. 86(1): p. 302-312.

28. Romero-Brey, I., et al., *Three-dimensional architecture and biogenesis of membrane structures associated with hepatitis C virus replication*. PLoS Pathog, 2012. 8(12): p. e1003056.
29. Doerflinger, S.Y., et al., *Membrane alterations induced by nonstructural proteins of human norovirus*. PLOS Pathogens, 2017. 13(10): p. e1006705.
30. Ferraris, P., et al., *Sequential biogenesis of host cell membrane rearrangements induced by hepatitis C virus infection*. Cellular and Molecular Life Sciences, 2013. 70(7): p. 1297-1306.
31. Paul, D., et al., *Glycine Zipper Motifs in Hepatitis C Virus Nonstructural Protein 4B Are Required for the Establishment of Viral Replication Organelles*. Journal of Virology, 2018. 92(4): p. e01890-17.
32. Oudshoorn, D., et al., *Expression and Cleavage of Middle East Respiratory Syndrome Coronavirus nsp3-4 Polyprotein Induce the Formation of Double-Membrane Vesicles That Mimic Those Associated with Coronavirus RNA Replication*. mBio, 2017. 8(6).
33. Oudshoorn, D., et al., *Antiviral Innate Immune Response Interferes with the Formation of Replication-Associated Membrane Structures Induced by a Positive-Strand RNA Virus*. mBio, 2016. 7(6).
34. van der Hoeven, B., et al., *Biogenesis and architecture of arterivirus replication organelles*. Virus Res, 2016. 220: p. 70-90.
35. Knoops, K., et al., *SARS-coronavirus replication is supported by a reticulovesicular network of modified endoplasmic reticulum*. PLoS Biol, 2008. 6(9): p. e226.
36. Snijder, E.J., et al., *A unifying structural and functional model of the coronavirus replication organelle: Tracking down RNA synthesis*. PLoS Biol, 2020. 18(6): p. e3000715.
37. Wolff, G., et al., *A molecular pore spans the double membrane of the coronavirus replication organelle*. Science, 2020. 369(6509): p. 1395-1398.
38. Bienz, K., D. Egger, and L. Pasamontes, *Association of polioviral proteins of the P2 genomic region with the viral replication complex and virus-induced membrane synthesis as visualized by electron microscopic immunocytochemistry and autoradiography*. Virology, 1987. 160(1): p. 220-6.
39. Suhay, D.A., T.H. Giddings, Jr., and K. Kirkegaard, *Remodeling the endoplasmic reticulum by poliovirus infection and by individual viral proteins: an autophagy-like origin for virus-induced vesicles*. J Virol, 2000. 74(19): p. 8953-65.
40. Doedens, J.R. and K. Kirkegaard, *Inhibition of cellular protein secretion by poliovirus proteins 2B and 3A*. The EMBO journal, 1995. 14(5): p. 894-907.
41. Sandoval, I.V. and L. Carrasco, *Poliovirus infection and expression of the poliovirus protein 2B provoke the disassembly of the Golgi complex, the organelle target for the antipoliovirus drug Ro-090179*. Journal of Virology, 1997. 71(6): p. 4679-4693.
42. Gazina, E.V., et al., *Differential requirements for COPI coats in formation of replication complexes among three genera of Picornaviridae*. J Virol, 2002. 76(21): p. 11113-22.
43. Wessels, E., et al., *A proline-rich region in the coxsackievirus 3A protein is required for the protein to inhibit endoplasmic reticulum-to-golgi transport*. J Virol, 2005. 79(8): p. 5163-73.
44. Wessels, E., et al., *A viral protein that blocks Arf1-mediated COP-I assembly by inhibiting the guanine nucleotide exchange factor GBF1*. Dev Cell, 2006. 11(2): p. 191-201.
45. Wessels, E., et al., *Effects of picornavirus 3A Proteins on Protein Transport and GBF1-dependent COP-I recruitment*. J Virol, 2006. 80(23): p. 11852-60.
46. Lanke, K.H., et al., *GBF1, a guanine nucleotide exchange factor for Arf, is crucial for coxsackievirus B3 RNA replication*. J Virol, 2009. 83(22): p. 11940-9.
47. Greninger, A.L., et al., *The 3A protein from multiple picornaviruses utilizes the golgi adaptor protein ACBD3 to recruit PI4KIIIbeta*. J Virol, 2012. 86(7): p. 3605-16.
48. Sasaki, J., et al., *ACBD3-mediated recruitment of PI4KB to picornavirus RNA replication sites*. EMBO J, 2012. 31(3): p. 754-66.
49. Wang, J., Z. Wu, and Q. Jin, *COPI is required for enterovirus 71 replication*. PLoS One, 2012. 7(5): p. e38035.
50. Teoule, F., et al., *The Golgi protein ACBD3, an interactor for poliovirus protein 3A, modulates poliovirus replication*. J Virol, 2013. 87(20): p. 11031-46.
51. Roulin, P.S., et al., *Rhinovirus uses a phosphatidylinositol 4-phosphate/cholesterol counter-current for the formation of replication compartments at the ER-Golgi interface*. Cell Host Microbe, 2014. 16(5): p. 677-90.
52. Dorobantu, C.M., et al., *GBF1- and ACBD3-independent recruitment of PI4KIIIbeta to replication sites by rhinovirus 3A proteins*. J Virol, 2015. 89(3): p. 1913-8.
53. Hsu, N.Y., et al., *Viral reorganization of the secretory pathway generates distinct organelles for RNA replication*. Cell, 2010. 141(5): p. 799-811.
54. Alirezaei, M., et al., *Pancreatic acinar cell-specific autophagy disruption reduces coxsackievirus replication and pathogenesis in vivo*. Cell Host Microbe, 2012. 11(3): p. 298-305.

55. Corona, A.K., et al., *Enteroviruses Remodel Autophagic Trafficking through Regulation of Host SNARE Proteins to Promote Virus Replication and Cell Exit*. Cell Rep, 2018. 22(12): p. 3304-3314.
56. Delorme-Axford, E., et al., *BPIFB3 regulates autophagy and coxsackievirus B replication through a noncanonical pathway independent of the core initiation machinery*. mBio, 2014. 5(6): p. e02147.
57. Fu, Y., et al., *Enterovirus 71 induces autophagy by regulating has-miR-30a expression to promote viral replication*. Antiviral Res, 2015. 124: p. 43-53.
58. Huang, S.C., et al., *Enterovirus 71-induced autophagy detected in vitro and in vivo promotes viral replication*. J Med Virol, 2009. 81(7): p. 1241-52.
59. Jackson, W.T., et al., *Subversion of cellular autophagosomal machinery by RNA viruses*. PLoS Biol, 2005. 3(5): p. e156.
60. Kemball, C.C., et al., *Coxsackievirus infection induces autophagy-like vesicles and megaphagosomes in pancreatic acinar cells in vivo*. J Virol, 2010. 84(23): p. 12110-24.
61. Klein, K.A. and W.T. Jackson, *Human rhinovirus 2 induces the autophagic pathway and replicates more efficiently in autophagic cells*. J Virol, 2011. 85(18): p. 9651-4.
62. Shi, Y., et al., *Coxsackievirus A16 elicits incomplete autophagy involving the mTOR and ERK pathways*. PLoS One, 2015. 10(4): p. e0122109.
63. Tabor-Godwin, J.M., et al., *The role of autophagy during coxsackievirus infection of neural progenitor and stem cells*. Autophagy, 2012. 8(6): p. 938-53.
64. Wong, J., et al., *Autophagosome supports coxsackievirus B3 replication in host cells*. J Virol, 2008. 82(18): p. 9143-53.
65. Yoon, S.Y., et al., *Coxsackievirus B4 uses autophagy for replication after calpain activation in rat primary neurons*. J Virol, 2008. 82(23): p. 11976-8.
66. Aldabe, R., A. Barco, and L. Carrasco, *Membrane Permeabilization by Poliovirus Proteins 2B and 2BC*. Journal of Biological Chemistry, 1996. 271(38): p. 23134-23137.
67. Van kuppeveld, F.J., et al., *Structure-function analysis of coxsackie B3 virus protein 2B*. Virology, 1997. 227(1): p. 111-8.
68. van Kuppeveld, F.J.M., et al., *Coxsackievirus protein 2B modifies endoplasmic reticulum membrane and plasma membrane permeability and facilitates virus release*. The EMBO Journal, 1997. 16(12): p. 3519-3532.
69. Guan, H., et al., *Crystal structure of 2C helicase from enterovirus 71*. Sci Adv, 2017. 3(4): p. e1602573.
70. Klein, M., H.J. Eggers, and B. Nelsen-Salz, *Echovirus 9 strain barty non-structural protein 2C has NTPase activity*. Virus Res, 1999. 65(2): p. 155-60.
71. Klein, M., H.J. Eggers, and B. Nelsen-Salz, *Echovirus-9 protein 2C binds single-stranded RNA unspecifically*. J Gen Virol, 2000. 81(Pt 10): p. 2481-2484.
72. Rodriguez, P.L. and L. Carrasco, *Poliovirus protein 2C has ATPase and GTPase activities*. J Biol Chem, 1993. 268(11): p. 8105-10.
73. Li, J.P. and D. Baltimore, *An intragenic revertant of a poliovirus 2C mutant has an uncoating defect*. J Virol, 1990. 64(3): p. 1102-7.
74. Vance, L.M., et al., *Poliovirus 2C region functions during encapsidation of viral RNA*. J Virol, 1997. 71(11): p. 8759-65.
75. Liu, Y., et al., *Direct interaction between two viral proteins, the nonstructural protein 2C and the capsid protein VP3, is required for enterovirus morphogenesis*. PLoS Pathog, 2010. 6(8): p. e1001066.
76. Wang, C., et al., *A C-terminal, cysteine-rich site in poliovirus 2C(ATPase) is required for morphogenesis*. J Gen Virol, 2014. 95(Pt 6): p. 1255-1265.
77. Tang, W.F., et al., *Reticulon 3 binds the 2C protein of enterovirus 71 and is required for viral replication*. J Biol Chem, 2007. 282(8): p. 5888-98.
78. Aldabe, R. and L. Carrasco, *Induction of membrane proliferation by poliovirus proteins 2C and 2BC*. Biochem Biophys Res Commun, 1995. 206(1): p. 64-76.
79. Bienz, K., et al., *Intracellular distribution of poliovirus proteins and the induction of virus-specific cytoplasmic structures*. Virology, 1983. 131(1): p. 39-48.
80. Cho, M.W., et al., *Membrane Rearrangement and Vesicle Induction by Recombinant Poliovirus 2C and 2BC in Human Cells*. Virology, 1994. 202(1): p. 129-145.
81. Balla, T., *Phosphoinositides: tiny lipids with giant impact on cell regulation*. Physiol Rev, 2013. 93(3): p. 1019-137.
82. Furse, S., et al., *Lipid membrane curvature induced by distearoyl phosphatidylinositol 4-phosphate*. Soft Matter, 2012. 8(11): p. 3090-3093.
83. Rahajeng, J., et al., *Efficient Golgi Forward Trafficking Requires GOLPH3-Driven, PI4P-Dependent Membrane Curvature*. Developmental Cell, 2019. 50(5): p. 573-585.e5.

84. Cruz-Garcia, D., et al., *Recruitment of arfaptins to the trans-Golgi network by PI(4)P and their involvement in cargo export*. The EMBO Journal, 2013. 32(12): p. 1717-1729.
85. Mesmin, B., et al., *A four-step cycle driven by PI(4)P hydrolysis directs sterol/PI(4)P exchange by the ER-Golgi tether OSBP*. Cell, 2013. 155(4): p. 830-43.
86. Banerji, S., et al., *Oxysterol binding protein-dependent activation of sphingomyelin synthesis in the golgi apparatus requires phosphatidylinositol 4-kinase IIa*. Mol Biol Cell, 2010. 21(23): p. 4141-50.
87. Cao, X., et al., *Golgi protein FAPP2 tubulates membranes*. Proc Natl Acad Sci U S A, 2009. 106(50): p. 21121-5.
88. Lenoir, M., et al., *Structural basis of wedging the Golgi membrane by FAPP pleckstrin homology domains*. EMBO Rep, 2010. 11(4): p. 279-84.
89. de Graaf, P., et al., *Phosphatidylinositol 4-kinase beta is critical for functional association of rab11 with the Golgi complex*. Mol Biol Cell, 2004. 15(4): p. 2038-47.
90. Burke, J.E., et al., *Structures of PI4KIIIβ complexes show simultaneous recruitment of Rab11 and its effectors*. Science, 2014. 344(6187): p. 1035-8.
91. de Rubio, R.G., et al., *Phosphatidylinositol 4-phosphate is a major source of GPCR-stimulated phosphoinositide production*. Sci Signal, 2018. 11(547).
92. Zhang, L., et al., *Phospholipase Cε hydrolyzes perinuclear phosphatidylinositol 4-phosphate to regulate cardiac hypertrophy*. Cell, 2013. 153(1): p. 216-27.
93. Wortzel, I., et al., *Mitotic Golgi translocation of ERK1c is mediated by a PI4KIIIβ-14-3-3γ shuttling complex*. J Cell Sci, 2015. 128(22): p. 4083-95.
94. Blagoveshchenskaya, A., et al., *Integration of Golgi trafficking and growth factor signaling by the lipid phosphatase SAC1*. J Cell Biol, 2008. 180(4): p. 803-12.
95. Wang, P.Y., J. Weng, and R.G. Anderson, *OSBP is a cholesterol-regulated scaffolding protein in control of ERK 1/2 activation*. Science, 2005. 307(5714): p. 1472-6.
96. Waugh, M.G., *The Great Escape: how phosphatidylinositol 4-kinases and PI4P promote vesicle exit from the Golgi (and drive cancer)*. Biochem J, 2019. 476(16): p. 2321-2346.
97. Daboussi, L., G. Costaguta, and G.S. Payne, *Phosphoinositide-mediated clathrin adaptor progression at the trans-Golgi network*. Nat Cell Biol, 2012. 14(3): p. 239-48.
98. Daboussi, L., et al., *Conserved role for Gga proteins in phosphatidylinositol 4-kinase localization to the*. Proc Natl Acad Sci U S A, 2017. 114(13): p. 3433-3438.
99. Klima, M., et al., *Structural insights and in vitro reconstitution of membrane targeting and activation of human PI4KB by the ACBD3 protein*. Sci Rep, 2016. 6: p. 23641.
100. Godi, A., et al., *ARF mediates recruitment of PtdIns-4-OH kinase-beta and stimulates synthesis of PtdIns(4,5)P2 on the Golgi complex*. Nat Cell Biol, 1999. 1(5): p. 280-7.
101. Zhao, X., et al., *Interaction of neuronal calcium sensor-1 (NCS-1) with phosphatidylinositol 4-kinase beta stimulates lipid kinase activity and affects membrane trafficking in COS-7 cells*. J Biol Chem, 2001. 276(43): p. 40183-9.
102. McPhail, J.A., et al., *The Molecular Basis of Aichi Virus 3A Protein Activation of Phosphatidylinositol 4 Kinase IIIbeta, PI4KB, through ACBD3*. Structure, 2017. 25(1): p. 121-131.
103. Hausser, A., et al., *Protein kinase D regulates vesicular transport by phosphorylating and activating phosphatidylinositol-4 kinase IIIbeta at the Golgi complex*. Nat Cell Biol, 2005. 7(9): p. 880-6.
104. Hausser, A., et al., *Phospho-specific binding of 14-3-3 proteins to phosphatidylinositol 4-kinase III beta protects from dephosphorylation and stabilizes lipid kinase activity*. J Cell Sci, 2006. 119(Pt 17): p. 3613-21.
105. Chalupska, D., et al., *Structural analysis of phosphatidylinositol 4-kinase IIIβ (PI4KB) - 14-3-3 protein complex reveals internal flexibility and explains 14-3-3 mediated protection from degradation in vitro*. J Struct Biol, 2017. 200(1): p. 36-44.
106. Dorobantu, C.M., et al., *Modulation of the Host Lipid Landscape to Promote RNA Virus Replication: The Picornavirus Encephalomyocarditis Virus Converges on the Pathway Used by Hepatitis C Virus*. PLoS Pathog, 2015. 11(9): p. e1005185.
107. Strating, J.R., et al., *Itraconazole inhibits enterovirus replication by targeting the oxysterol-binding protein*. Cell Rep, 2015. 10(4): p. 600-15.
108. Dubankova, A., et al., *Negative charge and membrane-tethered viral 3B cooperate to recruit viral RNA dependent RNA polymerase 3D*. Sci Rep, 2017. 7(1): p. 17309.
109. Heinz, B.A. and L.M. Vance, *The antiviral compound enviroxime targets the 3A coding region of rhinovirus and poliovirus*. J Virol, 1995. 69(7): p. 4189-97.
110. Heinz, B.A. and L.M. Vance, *Sequence determinants of 3A-mediated resistance to enviroxime in rhinoviruses and enteroviruses*. J Virol, 1996. 70(7): p. 4854-7.

111. Arita, M., T. Wakita, and H. Shimizu, *Cellular kinase inhibitors that suppress enterovirus replication have a conserved target in viral protein 3A similar to that of enviroxime*. J Gen Virol, 2009. 90(Pt 8): p. 1869-1879.
112. van der Schaar, H.M., et al., *Coxsackievirus mutants that can bypass host factor PI4KIIIbeta and the need for high levels of PI4P lipids for replication*. Cell Res, 2012. 22(11): p. 1576-92.
113. Ishikawa-Sasaki, K., J. Sasaki, and K. Taniguchi, *A complex comprising phosphatidylinositol 4-kinase IIIbeta, ACBD3, and Aichi virus proteins enhances phosphatidylinositol 4-phosphate synthesis and is critical for formation of the viral replication complex*. J Virol, 2014. 88(12): p. 6586-98.
114. Bohnert, M., *Tether Me, Tether Me Not-Dynamic Organelle Contact Sites in Metabolic Rewiring*. Dev Cell, 2020. 54(2): p. 212-225.
115. Prinz, W.A., A. Toulmay, and T. Balla, *The functional universe of membrane contact sites*. Nat Rev Mol Cell Biol, 2020. 21(1): p. 7-24.
116. Ridgway, N.D., *Oxysterol-binding proteins*. Subcell Biochem, 2010. 51: p. 159-82.
117. Arita, M., *Phosphatidylinositol-4 kinase III beta and oxysterol-binding protein accumulate unesterified cholesterol on poliovirus-induced membrane structure*. Microbiol Immunol, 2014. 58(4): p. 239-56.
118. Albulescu, L., et al., *Cholesterol shuttling is important for RNA replication of coxsackievirus B3 and encephalomyocarditis virus*. Cellular Microbiology, 2015. 17(8): p. 1144-1156.
119. Ishikawa-Sasaki, K., et al., *Model of OSBP-Mediated Cholesterol Supply to Aichi Virus RNA Replication Sites Involving Protein-Protein Interactions among Viral Proteins, ACBD3, OSBP, VAP-A/B, and SAC1*. J Virol, 2018. 92(8).
120. Illytska, O., et al., *Enteroviruses harness the cellular endocytic machinery to remodel the host cell cholesterol landscape for effective viral replication*. Cell Host Microbe, 2013. 14(3): p. 281-93.
121. Laufman, O., J. Perrino, and R. Andino, *Viral Generated Inter-Organelle Contacts Redirect Lipid Flux for Genome Replication*. Cell, 2019. 178(2): p. 275-289.e16.
122. Sbdio, J.I., et al., *GCP60 preferentially interacts with a caspase-generated golgin-160 fragment*. J Biol Chem, 2006. 281(38): p. 27924-31.
123. Sbdio, J.I. and C.E. Machamer, *Identification of a redox-sensitive cysteine in GCP60 that regulates its interaction with golgin-160*. J Biol Chem, 2007. 282(41): p. 29874-81.
124. Sohda, M., et al., *Identification and characterization of a novel Golgi protein, GCP60, that interacts with the integral membrane protein giantin*. J Biol Chem, 2001. 276(48): p. 45298-306.
125. Yue, X., et al., *Acyl-CoA-Binding Domain-Containing 3 (ACBD3; PAP7; GCP60): A Multi-Functional Membrane Domain Organizer*. Int J Mol Sci, 2019. 20(8).
126. Fan, J., et al., *Acyl-coenzyme A binding domain containing 3 (ACBD3; PAP7; GCP60): an emerging signaling molecule*. Prog Lipid Res, 2010. 49(3): p. 218-34.
127. Dorobantu, C.M., et al., *Recruitment of PI4KIIIbeta to coxsackievirus B3 replication organelles is independent of ACBD3, GBF1, and Arf1*. J Virol, 2014. 88(5): p. 2725-36.
128. Ishikawa-Sasaki, K., J. Sasaki, and K. Taniguchi, *A Complex Comprising Phosphatidylinositol 4-Kinase IIIβ, ACBD3, and Aichi Virus Proteins Enhances Phosphatidylinositol 4-Phosphate Synthesis and Is Critical for Formation of the Viral Replication Complex*. J Virol, 2014. 88(12): p. 6586-6598.
129. Donaldson, J.G. and C.L. Jackson, *ARF family G proteins and their regulators: roles in membrane transport, development and disease*. Nature Reviews Molecular Cell Biology, 2011. 12(6): p. 362-375.
130. Mansour, S.J., et al., *Human GBF1 is a ubiquitously expressed gene of the sec7 domain family mapping to 10q24*. Genomics, 1998. 54(2): p. 323-7.
131. Claude, A., et al., *GBF1: A novel Golgi-associated BFA-resistant guanine nucleotide exchange factor that displays specificity for ADP-ribosylation factor 5*. J Cell Biol, 1999. 146(1): p. 71-84.
132. Zhao, X., T.K. Lasell, and P. Melançon, *Localization of large ADP-ribosylation factor-guanine nucleotide exchange factors to different Golgi compartments: evidence for distinct functions in protein traffic*. Mol Biol Cell, 2002. 13(1): p. 119-33.
133. Beck, R., et al., *The COPI system: molecular mechanisms and function*. FEBS Lett, 2009. 583(17): p. 2701-9.
134. Guo, Y., et al., *Functional genomic screen reveals genes involved in lipid-droplet formation and utilization*. Nature, 2008. 453(7195): p. 657-661.
135. Wilfling, F., et al., *Arf1/COPI machinery acts directly on lipid droplets and enables their connection to the ER for protein targeting*. eLife, 2014. 3: p. e01607.
136. Mossessova, E., R.A. Corpina, and J. Goldberg, *Crystal structure of ARF1*Sec7 complexed with Brefeldin A and its implications for the guanine nucleotide exchange mechanism*. Mol Cell, 2003. 12(6): p. 1403-11.
137. Sáenz, J.B., et al., *Golginicide A reveals essential roles for GBF1 in Golgi assembly and function*. Nature Chemical Biology, 2009. 5(3): p. 157-165.

138. Martínez, J.L. and C.F. Arias, *Role of the Guanine Nucleotide Exchange Factor GBF1 in the Replication of RNA Viruses*. *Viruses*, 2020. 12(6).
139. Maynell, L.A., K. Kirkegaard, and M.W. Klymkowsky, *Inhibition of poliovirus RNA synthesis by brefeldin A*. *J Virol*, 1992. 66(4): p. 1985-94.
140. Cuconati, A., A. Molla, and E. Wimmer, *Brefeldin A inhibits cell-free, de novo synthesis of poliovirus*. *J Virol*, 1998. 72(8): p. 6456-64.
141. Belov, G.A., et al., *Hijacking components of the cellular secretory pathway for replication of poliovirus RNA*. *J Virol*, 2007. 81(2): p. 558-67.
142. Belov, G.A., et al., *A critical role of a cellular membrane traffic protein in poliovirus RNA replication*. *PLoS Pathog*, 2008. 4(11): p. e1000216.
143. van der Linden, L., et al., *Differential effects of the putative GBF1 inhibitors Golgicide A and AG1478 on enterovirus replication*. *J Virol*, 2010. 84(15): p. 7535-42.
144. Qin, Y., et al., *Curcumin inhibits the replication of enterovirus 71 in vitro*. *Acta Pharm Sin B*, 2014. 4(4): p. 284-94.
145. Wang, J., J. Du, and Q. Jin, *Class I ADP-ribosylation factors are involved in enterovirus 71 replication*. *PLoS One*, 2014. 9(6): p. e99768.
146. Ferlin, J., et al., *Investigation of the role of GBF1 in the replication of positive-sense single-stranded RNA viruses*. *J Gen Virol*, 2018. 99(8): p. 1086-1096.
147. Wessels, E., et al., *Molecular determinants of the interaction between coxsackievirus protein 3A and guanine nucleotide exchange factor GBF1*. *J Virol*, 2007. 81(10): p. 5238-45.
148. Belov, G.A., et al., *Poliovirus replication requires the N-terminus but not the catalytic Sec7 domain of ArfGEF GBF1*. *Cell Microbiol*, 2010. 12(10): p. 1463-79.
149. Ellong, E.N., et al., *Interaction between the triglyceride lipase ATGL and the Arf1 activator GBF1*. *PLoS One*, 2011. 6(7): p. e21889.
150. Soni, K.G., et al., *Coatomer-dependent protein delivery to lipid droplets*. *J Cell Sci*, 2009. 122(Pt 11): p. 1834-41.
151. Viktorova, E.G., et al., *Phospholipid synthesis fueled by lipid droplets drives the structural development of poliovirus replication organelles*. *PLoS Pathog*, 2018. 14(8): p. e1007280.
152. Greninger, A.L., et al., *ACBD3 interaction with TBC1 domain 22 protein is differentially affected by enteroviral and kobuviral 3A protein binding*. *MBio*, 2013. 4(2): p. e00098-13.
153. Jovic, M., et al., *Two phosphatidylinositol 4-kinases control lysosomal delivery of the Gaucher disease enzyme, beta-glucocerebrosidase*. *Mol Biol Cell*, 2012. 23(8): p. 1533-45.
154. Blomen, V.A., et al., *Gene essentiality and synthetic lethality in haploid human cells*. *Science*, 2015. 350(6264): p. 1092-6.

CHAPTER 2

DIRECT-ACTING ANTIVIRALS AND HOST-TARGETING STRATEGIES TO COMBAT ENTEROVIRUS INFECTIONS

*Lisa Bauer**, *Heyrhyoung Lyoo**, *Hilde M van der Schaar*, *Jeroen RPM Strating*,
Frank JM van Kuppeveld[#]

Department of Biomolecular Health Sciences, Virology Division, Faculty of Veterinary
Medicine, Utrecht University, Utrecht, The Netherlands

*These authors contributed equally.

[#]Corresponding author

ABSTRACT

Enteroviruses (e.g., poliovirus, enterovirus-A71, coxsackievirus, enterovirus-D68, rhinovirus) include many human pathogens causative of various mild and more severe diseases, especially in young children. Unfortunately, antiviral drugs to treat enterovirus infections have not been approved yet. Over the past decades, several direct-acting inhibitors have been developed, including capsid binders, which block virus entry, and inhibitors of viral enzymes required for genome replication. Capsid binders and protease inhibitors have been clinically evaluated, but failed due to limited efficacy or toxicity issues. As an alternative approach, host-targeting inhibitors with potential broad-spectrum activity have been identified. Furthermore, drug repurposing screens have recently uncovered promising new inhibitors with disparate viral and host targets. Together, these findings raise hope for the development of (broad-range) anti-enteroviral drugs.

HIGHLIGHTS

- Enteroviruses cause many human diseases, yet no antiviral drugs are available
- Capsids and viral enzymes are promising targets for direct-acting antiviral therapy
- Fundamental research has unveiled host factors for broad-spectrum drug development
- Drug repurposing screens have yielded new promising enterovirus inhibitors

INTRODUCTION

The Picornaviridae constitutes a large family of non-enveloped, positive-stranded RNA (+RNA) viruses, currently consisting of 31 genera. The genus Enterovirus, which is by far the largest genus, comprises many human pathogens, including poliovirus, coxsackie A and B viruses, echoviruses, numbered enteroviruses (e.g., EV-A71 and EV-D68), and the rhinoviruses. Infections with non-polio enteroviruses can result in a wide variety of symptoms, including hand-foot-and-mouth disease, conjunctivitis, aseptic meningitis, severe neonatal sepsis-like disease and acute flaccid paralysis, whereas infections with rhinoviruses cause the common cold as well as exacerbations of asthma and chronic obstructive pulmonary disease (COPD) (reviewed in [1]). Vaccines are only available against poliovirus and EV-A71. Development of vaccines against all enteroviruses seems unfeasible, given the large number of (sero)types (i.e., >100 non-polio enteroviruses and >150 rhinoviruses). Hence, there is a great need for (broad-acting) antivirals against enteroviruses. Here, we will review recent efforts to develop direct-acting antivirals as well as host factor-targeting inhibitors to treat enterovirus infections.

DIRECT-ACTING ANTIVIRALS

Entry inhibitors

Enterovirus capsids are icosahedral (pseudo T=3) structures composed of 60 copies of each of the four capsid proteins (VP1 to VP4). The enterovirus replication cycle (Figure 1B) is initiated by binding of a virion to its receptor. Most enterovirus receptors are protein receptors that belong to the Ig superfamily or the integrin receptor family (reviewed in [2]). The receptors usually bind in the “canyon”, a depression in the virion surface around the five-fold axes of symmetry [2]. Receptor-binding induces virion destabilization and release of the “pocket factor”, a fatty acid located in a hydrophobic pocket beneath the canyon, to initiate virion uncoating [2].

So-called “capsid binders” are the most extensively studied class of anti-enteroviral compounds [3,4]. These compounds replace the pocket factor in the canyon and thereby block virion uncoating. Clinical trials for the capsid binders pleconaril, vapendavir (a.k.a. BTA798), and pocapavir (a.k.a. V-073) are currently in progress or have recently been completed, the status of which has been described last year [5]. Since then, another trial with pleconaril was conducted for the treatment of neonates with enterovirus sepsis, which showed greater survival among pleconaril recipients [6]. A major drawback of capsid binders is the rapid emergence of resistance. Indeed, in a clinical trial for the treatment of rhinovirus infections with pleconaril, compound-resistant viruses were isolated [7]. In addition, naturally occurring pleconaril-resistant viruses (e.g., an echovirus 11 strain) have been reported [8]. These resistance issues may complicate the application of capsid binders in the clinic.

Many capsid binders are active against rhinovirus A and B species members [3], but not against members of the rhinovirus C species [9,10]. The recent elucidation of the atomic virion structure of rhinovirus-C15 by cryo-EM revealed a unique “spiky” structure, vastly different from other enterovirus species. Furthermore, the hydrophobic pocket is filled with bulky hydrophobic residues, thereby not providing sufficient space for a pocket factor or a capsid binder. These features likely explain why rhinovirus C species are not responsive to pocket-binding compounds [11**].

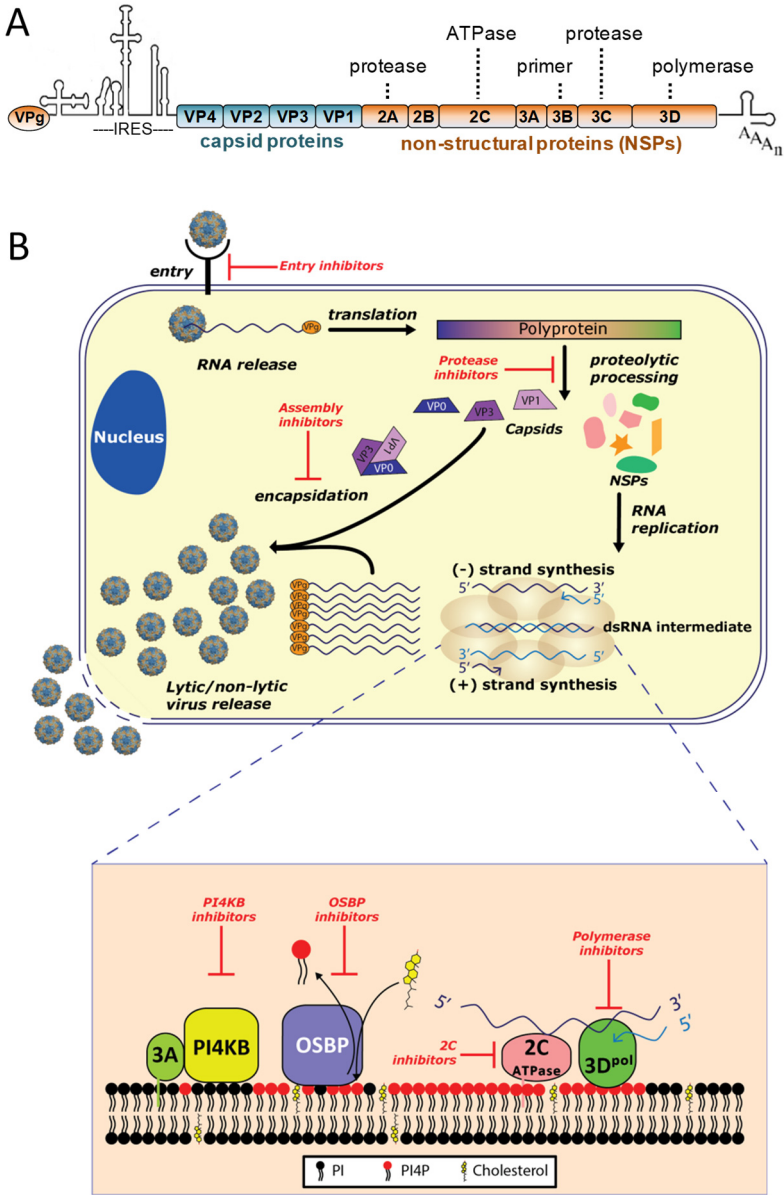


Figure 1. Enterovirus genome, replication cycle, and antiviral targets. (A) The enterovirus genome encodes four structural proteins (VP1-VP4) and seven non-structural proteins (2A, 2B, 2C, 3A, 3B, 3C, and 3D). IRES: internal ribosome entry site. (B) The enterovirus life cycle begins with the attachment of the virus particle to a cellular receptor followed by the internalization of the particle into the host cell. The genome is released and directly translated into a polyprotein, which is processed by virally encoded proteases into the individual viral proteins. Non-structural proteins rewire host cell membranes and generate replication organelles (ROs) for viral RNA replication. Several host proteins, such as PI4KB (phosphatidylinositol 4-kinase III beta) and OSBP (oxysterol-binding protein), are recruited to ROs by viral 3A protein, which results in ROs with a unique lipid composition. Genome replication starts with synthesis of complementary negative-stranded RNA, which is used as template for the synthesis of a large number of +RNA molecules. Newly synthesized +RNAs either enter a new round of genome replication or are packaged into capsid proteins to build infectious particles. Viruses are released by a non-lytic mechanism as well as upon cell lysis. Inhibitors of the different stages in the replication cycle are depicted in red.

The atomic structure of rhinovirus-C also revealed a potential binding site for sialic acids in a sequence-conserved surface depression [11**]. Sialic acids were recently shown to also facilitate entry of EV-D68 [12,13]. Targeting sialic acid (reviewed in [14]), which has also been applied for influenza virus, could be an approach to inhibit rhinovirus-C and EV-D68 infections. One of the best-described compounds targeting sialic acids is DAS181, a bacterial sialidase that cleaves α 2,3- and α 2,6-sialic acid linkages, and that has been tested in a phase II clinical trial for (para)influenza infection [15,16]. DAS181 also inhibits EV-D68 replication in vitro [17], but it remains to be tested in vivo.

Protease inhibitors

The 7.5 kb +RNA genome of enteroviruses encodes a single polyprotein harboring the structural P1 proteins and the non-structural P2 and P3 proteins (Fig 1A). This polyprotein is proteolytically processed into individual proteins by viral proteases 2Apro, 3Cpro, and 3CDpro.

The development of protease inhibitors has focused particularly on 3Cpro, since it is more conserved than 2Apro. One of the most potent 3Cpro inhibitors developed over the years is rupintrivir (a.k.a. AG7088). Rupintrivir is a peptidomimetic compound that irreversibly binds to the catalytic site of 3Cpro [18]. Because it is very active against a broad panel of enteroviruses [3,19-21], this compound was selected for clinical trials, despite its poor oral bioavailability [22,23]. Although the results of rhinovirus challenge trials were promising [24], rupintrivir did not reduce disease severity in naturally infected patients [25], hence the clinical development was halted. However, many rupintrivir derivatives are currently under development [26-28]. Furthermore, non-peptidomimetic small molecule inhibitors are developed to circumvent difficulties with bioavailability [29], but they have yet to be evaluated in clinical trials.

3Dpol inhibitors

The viral RNA-dependent RNA polymerase 3Dpol catalyzes viral RNA synthesis in replication complexes that are associated with so-called replication organelles (ROs, see below). Inhibitors of 3Dpol can be divided into two classes based on their structure, being nucleoside/nucleotide inhibitors (NIs) and non-nucleoside/nucleotide inhibitors (NNIs).

NIs.

Antiviral NIs can act in two ways. They can be incorporated into the viral genome by mimicking nucleotides to induce lethal mutagenesis or terminate elongation of the nascent chain, or inhibit viral replication in an indirect manner by affecting the cellular nucleotide pools (reviewed in [30]). Until now, few NIs against enteroviruses have been developed, but compounds developed against other viruses offer promising results, such as ribavirin [31], which is clinically used for the treatment of hepatitis C virus (HCV) infections [32,33]. Another example is NITD008, which failed in preclinical studies for the treatment of dengue virus infection due to toxicity. However, a 10-fold lower concentration of NITD008 protected mice from a lethal challenge with EV-A71 without showing any cytotoxicity [34]. Drug repurposing – i.e., the concept of using compounds developed for a certain disease to treat a different condition – offers an attractive alternative to de novo drug development, as profound pharmacological and toxicological profiles are already available allowing a bypass of expensive (pre-)clinical studies. For example, the NI gemcitabine, an anticancer drug, was recently found to exert broad-spectrum anti-

enteroviral activity [35,36]. Besides incorporation into nascent viral RNA, gemcitabine has been suggested to block access of nucleotides into the active side of the polymerase. Furthermore, gemcitabine blocks viral genome replication by inhibiting ribonucleotide reductase, the cellular enzyme that catalyzes the conversion of deoxyribonucleotides to ribonucleotides [35]. The dose of gemcitabine needed for antiviral activity is significantly lower than the dose for the anticancer activity, which raises hope for an application without toxic effects that are inherent to many anticancer drugs.

NNIs.

Several NNIs of 3Dpol have been identified (e.g., gliotoxin, DTrip-22, aurincarboxylic acid, BPR-3P0128, and GPC-N114), but their mechanism of action is poorly understood, except for amiloride, which decreases the polymerase fidelity (reviewed in [5]). GPC-N114 was identified as a novel broad-range enterovirus inhibitor that targets the RNA template-primer site in the core of 3Dpol, making it the first anti-enteroviral compound with this mechanism of action [37**]. Unfortunately, the efficacy of GPC-N114 in animal models remains to be tested due to problems with formulating the compound for in vivo use. Alternative strategies for 3Dpol inhibition, although thus far unexplored, may be to interfere with posttranslational modifications of 3Dpol like sumoylation and ubiquitination, both of which are important for 3Dpol activity [38].

2CATPase inhibitors

The highly conserved viral protein 2C, an ATPase, is an attractive target for broad-spectrum enterovirus inhibitors. 2CATPase has several functions in genome replication (reviewed in [5]). Several structurally disparate 2CATPase inhibitors have been identified, such as guanidine hydrochloride, HBB, MRL-1237 and TBZE-029 [3]. In addition, drug repurposing screens have recently uncovered a number of FDA-approved drugs (fluoxetine, pirlindole, dibucaine, zuclopenthixol) that inhibit replication of enterovirus species B and D members [39-41]. Since mutations in 2CATPase provide resistance to these compounds, they are considered to target 2CATPase. Indeed, fluoxetine (i.e., Prozac) was shown to interfere with the ATPase activity of 2CATPase, but the mechanism of inhibition of the other drugs has to be unraveled [40]. Recent in vitro experiments have confirmed the long-presumed ATP-dependent RNA helicase activity and ATPase-independent RNA chaperone functions of 2CATPase [42**], paving the way for studies to elucidate the mechanism of action of 2CATPase inhibitors in more detail. So far, 2CATPase inhibitors have not been tested in clinical trials. However, fluoxetine was effective in an immunocompromised child with chronic enterovirus encephalitis [43*], implying that 2CATPase inhibitors have potential for clinical use.

Assembly inhibitors

Virion morphogenesis is a poorly understood, step-wise process [44]. The first step is the liberation of P1 from the polyprotein. Assisted by the chaperone Hsp90 [44,45], P1 is processed into VP0 (i.e., the precursor of VP4 and VP2), VP1, and VP3, which spontaneously form a protomer. Five protomers subsequently assemble into a pentamer, twelve of which in turn form an empty capsid (a.k.a. procapsid). Assembly of pentamers and procapsids is supported by glutathione by an as yet unidentified mechanism [46*,47*]. Governed by interactions between VP1/VP3 and 2CATPase [44,48-50], actively

replicating viral RNA is included in the procapsid to form a provirion. The final step in virion morphogenesis is the cleavage of VP0 into VP4 and VP2 to form a stable icosahedral particle.

Only a few assembly inhibitors have been identified so far. Geldanamycin and its analog 17-AAG target Hsp90 to inhibit the processing of P1 [51]. Buthionine sulfoximine, an inhibitor of glutathione synthesis, and TP219, a small molecule that covalently binds to glutathione, both impede the role of glutathione in morphogenesis [46*,47*]. Yet, not all enteroviruses rely on glutathione [47*], thereby precluding glutathione as an important target for broad-spectrum inhibitors.

INHIBITORS OF HOST FACTORS

Viruses critically depend on specific host factors. In recent years, several host factors required for enterovirus replication have been discovered, spurring host-directed drug development. Since some host factors appear to be used by many – or even all – enteroviruses, inhibitors of these cellular factors may have broad-spectrum activity.

PI4KB

Enteroviruses, like all +RNA viruses, induce specific alterations in intracellular membranes and lipid homeostasis to form replication organelles (ROs). The formation of enterovirus ROs is mediated by the concerted actions of viral proteins 2B, 2C, and 3A, as well as a selected set of hijacked host factors (recently reviewed in [52]). One of these pivotal host factors is phosphatidylinositol 4-kinase type III β (PI4KB) [52-54]. It is recruited to membranes by the viral protein 3A and enriches ROs in phosphatidylinositol 4-phosphate (PI4P) lipids, which is essential for genomic RNA replication [53**]. As PI4KB is essential for all enteroviruses, inhibitors of this enzyme (e.g., PIK93, GW5074, T-00127-HEV1 and BF738735 (reviewed in [5]) have broad-spectrum activity [53**-56]. However, some PI4KB inhibitors showed lethal toxicity in mice and affected lymphocyte function in vitro, which has stalled the development of PI4KB inhibitors [57]. Besides the fact that PI4KB inhibitors may be toxic, their activity may also be overcome by some mutations in the viral 3A, as recently published [58,59].

OSBP

Itraconazole, a clinically used antifungal drug that also has anti-cancer properties, was identified in drug repurposing screens as a broad-spectrum enterovirus inhibitor [36,60**,61]. We identified the oxysterol-binding protein (OSBP) as a novel target of itraconazole responsible for the antiviral effects [60**]. OSBP is a PI4P-binding protein that shuttles cholesterol and PI4P at ER-Golgi membrane contact sites [62]. OSBP is recruited to ROs through the PI4KB-mediated increase in PI4P and its lipid shuttling activity is essential for viral genome replication. Other OSBP inhibitors (e.g., 25-hydroxycholesterol, AN-12-H5, T-00127-HEV2, TTP-8307, and the natural compound OSW-1) also impaired enterovirus replication [56,63-65]. In a rhinovirus mouse model, prophylactic intranasal treatment with itraconazole reduced viral titers and pathology, raising expectations for topically applied itraconazole to prevent or treat common colds [66].

Cyclophilins

Cyclophilin A plays a role during the uncoating process of EV-A71 [67*]. In line with this, cyclophilin A inhibitors HL05100P2 and cyclosporine A block EV-A71 replication [67*]. Cyclophilins facilitate protein folding by catalyzing peptide bond isomerization and also play a role in the replication of other +RNA viruses, including HCV and coronaviruses (reviewed in [68]). Because cyclophilin inhibitors like cyclosporine A have an immunosuppressive effect, non-immunosuppressive inhibitors (e.g., NIM-811 [69]) were developed and are currently in clinical trials for antiviral activity (e.g., alisporivir, a.k.a. Debio025, for HCV treatment). It remains to be established whether uncoating of other enteroviruses also relies on cyclophilins. Hence, the spectrum of anti-enteroviral activity of cyclophilin inhibitors remains to be explored.

Table 1. Overview of directing-acting or host-targeting inhibitors discussed in this review.

Type of inhibitor		Compounds
Capsid binder		Pirodavisir ^[5] , Pleconaril ^{**[5]} , Pocapavir(V-073) ^{**[5]} , Vapendavir (BTA798) ^{**[5]}
3C^{pro} inhibitor	peptidic mimetic	Rupintrivir (AG7088) ^{**[18]} and its analogs (eg Compound 1*) ^[26-28]
	non-peptidic mimetic	DC07090 ^[29]
3D^{pol} inhibitor	nucleoside analog	Gemcitabine ^[35] , NITD008 ^[34] , Ribavirin ^[71]
	non-nucleoside analog	Amiloride ^[5] , Aurintricarboxylic acid ^[5] , BPR-3P0128 ^[5] , DTrip-22 ^[5] , Gliotoxin ^[5] , GPC-N114 ^[37**]
2C^{ATPase} inhibitor		Dibucaine ^[72] , Fluoxetine ^[41] , Guanidine hydrochloride ^[5] , HBB ^[5] , MRL-1237 ^[5] , Pirlindole ^[72] , TBZE-029 ^[5] , Zuclopenthixol ^[72]
Host factor inhibitor	HSP90	Geldanamycin (analog 17-AAG) ^[51]
	PI4KB	BF738735 ^[5] , Enviroxime ^{**[5]} , GW5074 ^[5] , PIK93 ^[5] , T-00127-HEV1 ^[5]
	OSBP	25-hydroxycholesterol ^[5] , AN-12-H5 ^[64] , Itraconazole ^[61] , OSW-1 ^[63] , T-00127-HEV2 ^[64] , TTP-8307 ^[65]
	Cyclophilins	Cyclosporin A ^[67*] , HL05100P2 ^[67*] , NIM-811 ^[69]
	Glutathione	Buthionine Sulfoximine (BSO) ^[46*] , TP219 ^[47*]

* Phase 1 clinical trial; ** Phase 2 clinical trial or completed. HSP90, heat shock protein 90; PI4KB, phosphatidylinositol 4 kinase III beta; OSBP, oxysterol-binding protein.

OUTLOOK

Currently, there are no antiviral drugs available for the treatment of enterovirus infections, while several potent antivirals are available against HCV, a +RNA virus with a similar replication strategy. Possibly, the small market for anti-enteroviral drugs impedes extensive (industrial) efforts to develop enterovirus inhibitors. Yet, antiviral drugs are urgently needed as enterovirus infections can be life-threatening especially in young children. Furthermore, antiviral drugs are expected to play a crucial role in poliovirus eradication and the post-eradication era.

Capsid binders are currently most advanced in clinical trials, but the inherent problem of rapid resistance development raises concerns. The development of protease inhibitors requires the synthesis of relatively complex peptidomimetic molecules. 2CATPase and 3Dpol may be more promising targets for direct-acting antiviral drugs as they can be inhibited by small molecules, and several inhibitors of

these factors were found to have broad-range anti-enteroviral activity. Other targets for broad-spectrum antiviral drugs are host factors, as many host factors are shared by enteroviruses, but a possible downside is the chance of adverse effects and toxicity, as exemplified by PI4KB inhibitors. Lately, several enterovirus inhibitors have been discovered in drug repurposing screens. These compounds are already available or at least quite advanced in (pre-)clinical development for their respective conditions, thus shortening the development process. Importantly, several of those inhibitors have broad-range, sometimes even pan-enterovirus activity.

Besides targeting individual viral or cellular proteins, an emerging concept in drug design is to interfere with essential protein-protein interactions. In the case of enterovirus infections, one may pharmaceutically disrupt essential interactions between viral proteins and host factors, which likely hampers virus replication without causing the overt toxicity issues that may be associated with inhibition of host proteins. Unfortunately, most protein-protein interactions cannot be addressed by current drug formats, including small molecules. The recent development of small cell-permeating, synthetic protein scaffolds (e.g., Alphabodies) may potentially lead to a novel approach to target protein-protein interactions in (entero)virus-infected cells [70].

Since targeted drug discovery depends heavily on basic knowledge of virus replication, fundamental research on the role of viral enzymes as well as essential host factors for enterovirus replication remains needed for the development of broad-range antiviral drugs against these important pathogens.

ACKNOWLEDGEMENT

We apologize to our colleagues whose work we could not cite due to space limitations. This work was supported by research grants from the Netherlands Organisation for Scientific Research (NWO-VENI-863.12.005 to HMvdS, NWO-VENI-722.012.066 to JRPMS, NWO-VICI-91812628 to FJMvK, ERASysApp project 'SysVirDrug' ALW project number 832.14.003 to FJMvK) and from the European Union (Horizon 2020 Marie Skłodowska-Curie ETN 'ANTIVIRALS', grant agreement number 642434 to FJMvK).

REFERENCES

* of interest

** of outstanding interest

1. Tapparel C, Siegrist F, Petty TJ, Kaiser L: Picornavirus and enterovirus diversity with associated human diseases. *Infection, Genetics and Evolution* 2013, 14:282-293.
2. Bergelson JM, Coyne CB: Picornavirus entry. *Adv Exp Med Biol* 2013, 790:24-41.
3. De Palma AM, Vlieghe I, De Clercq E, Neyts J: Selective inhibitors of picornavirus replication. *Med Res Rev* 2008, 28:823-884.
4. Thibaut HJ, De Palma AM, Neyts J: Combating enterovirus replication: state-of-the-art on antiviral research. *Biochem Pharmacol* 2012, 83:185-192.
5. van der Linden L, Wolthers KC, van Kuppeveld FJ: Replication and Inhibitors of Enteroviruses and Parechoviruses. *Viruses* 2015, 7:4529-4562.
6. Abzug MJ, Michaels MG, Wald E, Jacobs RF, Romero JR, Sanchez PJ, Wilson G, Krogstad P, Storch GA, Lawrence R, et al.: A Randomized, Double-Blind, Placebo-Controlled Trial of Pleconaril for the Treatment of Neonates With Enterovirus Sepsis. *J Pediatric Infect Dis Soc* 2016, 5:53-62.
7. Pevear DC, Hayden FG, Demenczuk TM, Barone LR, McKinlay MA, Collett MS: Relationship of pleconaril susceptibility and clinical outcomes in treatment of common colds caused by rhinoviruses. *Antimicrob Agents Chemother* 2005, 49:4492-4499.
8. Benschop KS, Wildenbeest JG, Koen G, Minnaar RP, van Hemert FJ, Westerhuis BM, Pajkrt D, van den Broek PJ, Vossen AC, Wolthers KC: Genetic and antigenic structural characterization for resistance of echovirus 11 to pleconaril in an immunocompromised patient. *J Gen Virol* 2015, 96:571-579.
9. Basta HA, Ashraf S, Sgro JY, Bochkov YA, Gern JE, Palmenberg AC: Modeling of the human rhinovirus C capsid suggests possible causes for antiviral drug resistance. *Virology* 2014, 448:82-90.
10. Hao W, Bernard K, Patel N, Ulbrandt N, Feng H, Svabek C, Wilson S, Stracener C, Wang K, Suzich J, et al.: Infection and propagation of human rhinovirus C in human airway epithelial cells. *J Virol* 2012, 86:13524-13532.
- **11. Liu Y, Hill MG, Klose T, Chen Z, Watters K, Bochkov YA, Jiang W, Palmenberg AC, Rossmann MG: Atomic structure of a rhinovirus C, a virus species linked to severe childhood asthma. *Proc Natl Acad Sci U S A* 2016, 113:8997-9002.
Describes the crystal structure of rhinovirus C virion and reveals the mechanism of resistance to capsid binders.
12. Baggen J, Thibaut HJ, Staring J, Jae LT, Liu Y, Guo H, Slager JJ, de Bruin JW, van Vliet AL, Blomen VA, et al.: Enterovirus D68 receptor requirements unveiled by haploid genetics. *Proc Natl Acad Sci U S A* 2016, 113:1399-1404.
13. Liu Y, Sheng J, Baggen J, Meng G, Xiao C, Thibaut HJ, van Kuppeveld FJ, Rossmann MG: Sialic acid-dependent cell entry of human enterovirus D68. *Nat Commun* 2015, 6:8865.
14. Stencel-Baerenwald JE, Reiss K, Reiter DM, Stehle T, Dermody TS: The sweet spot: defining virus-sialic acid interactions. *Nat Rev Micro* 2014, 12:739-749.
15. Moss RB, Hansen C, Sanders RL, Hawley S, Li T, Steigbigel RT: A phase II study of DAS181, a novel host directed antiviral for the treatment of influenza infection. *J Infect Dis* 2012, 206:1844-1851.
16. Nicholls JM, Moss RB, Haslam SM: The use of sialidase therapy for respiratory viral infections. *Antiviral Res* 2013, 98:401-409.
17. Rhoden E, Zhang M, Nix WA, Oberste MS: In Vitro Efficacy of Antiviral Compounds against Enterovirus D68. *Antimicrob Agents Chemother* 2015, 59:7779-7781.
18. Matthews DA, Dragovich PS, Webber SE, Fuhrman SA, Patick AK, Zalman LS, Hendrickson TF, Love RA, Prins TJ, Marakovits JT, et al.: Structure-assisted design of mechanism-based irreversible inhibitors of human rhinovirus 3C protease with potent antiviral activity against multiple rhinovirus serotypes. *Proc Natl Acad Sci U S A* 1999, 96:11000-11007.
19. Binford SL, Maldonado F, Brothers MA, Weady PT, Zalman LS, Meador JW, 3rd, Matthews DA, Patick AK: Conservation of amino acids in human rhinovirus 3C protease correlates with broad-spectrum antiviral activity of rupintrivir, a novel human rhinovirus 3C protease inhibitor. *Antimicrob Agents Chemother* 2005, 49:619-626.

20. Kaiser L, Crump CE, Hayden FG: In vitro activity of pleconaril and AG7088 against selected serotypes and clinical isolates of human rhinoviruses. *Antiviral Res* 2000, 47:215-220.
21. Patick AK, Binford SL, Brothers MA, Jackson RL, Ford CE, Diem MD, Maldonado F, Dragovich PS, Zhou R, Prins TJ, et al.: In vitro antiviral activity of AG7088, a potent inhibitor of human rhinovirus 3C protease. *Antimicrob Agents Chemother* 1999, 43:2444-2450.
22. Hsyu PH, Pithavala YK, Gersten M, Penning CA, Kerr BM: Pharmacokinetics and safety of an antirhinoviral agent, ruprintrivir, in healthy volunteers. *Antimicrob Agents Chemother* 2002, 46:392-397.
23. Zhang KE, Hee B, Lee CA, Liang B, Potts BC: Liquid chromatography-mass spectrometry and liquid chromatography-NMR characterization of in vitro metabolites of a potent and irreversible peptidomimetic inhibitor of rhinovirus 3C protease. *Drug Metab Dispos* 2001, 29:729-734.
24. Hayden FG, Turner RB, Gwaltney JM, Chi-Burris K, Gersten M, Hsyu P, Patick AK, Smith GJ, 3rd, Zalman LS: Phase II, randomized, double-blind, placebo-controlled studies of ruprintrivir nasal spray 2-percent suspension for prevention and treatment of experimentally induced rhinovirus colds in healthy volunteers. *Antimicrob Agents Chemother* 2003, 47:3907-3916.
25. Patick AK, Brothers MA, Maldonado F, Binford S, Maldonado O, Fuhrman S, Petersen A, Smith GJ, 3rd, Zalman LS, Burns-Naas LA, et al.: In vitro antiviral activity and single-dose pharmacokinetics in humans of a novel, orally bioavailable inhibitor of human rhinovirus 3C protease. *Antimicrob Agents Chemother* 2005, 49:2267-2275.
26. Tan J, George S, Kusov Y, Perbandt M, Anemuller S, Mesters JR, Norder H, Coutard B, Lacroix C, Leyssen P, et al.: 3C protease of enterovirus 68: structure-based design of Michael acceptor inhibitors and their broad-spectrum antiviral effects against picornaviruses. *J Virol* 2013, 87:4339-4351.
27. Tan YW, Ang MJ, Lau QY, Poulsen A, Ng FM, Then SW, Peng J, Hill J, Hong WJ, Chia CS, et al.: Antiviral activities of peptide-based covalent inhibitors of the Enterovirus 71 3C protease. *Sci Rep* 2016, 6:33663.
28. Wu C, Zhang L, Li P, Cai Q, Peng X, Yin K, Chen X, Ren H, Zhong S, Weng Y, et al.: Fragment-wise design of inhibitors to 3C proteinase from enterovirus 71. *Biochim Biophys Acta* 2016, 1860:1299-1307.
29. Ma GH, Ye Y, Zhang D, Xu X, Si P, Peng JL, Xiao YL, Cao RY, Yin YL, Chen J, et al.: Identification and biochemical characterization of DC07090 as a novel potent small molecule inhibitor against human enterovirus 71 3C protease by structure-based virtual screening. *Eur J Med Chem* 2016, 124:981-991.
30. Jordheim LP, Durantel D, Zoulim F, Dumontet C: Advances in the development of nucleoside and nucleotide analogues for cancer and viral diseases. *Nat Rev Drug Discov* 2013, 12:447-464.
31. Pfeiffer JK, Kirkegaard K: A single mutation in poliovirus RNA-dependent RNA polymerase confers resistance to mutagenic nucleotide analogs via increased fidelity. *Proceedings of the National Academy of Sciences of the United States of America* 2003, 100:7289-7294.
32. Manns MP, McHutchison JG, Gordon SC, Rustgi VK, Shiffman M, Reindollar R, Goodman ZD, Koury K, Ling M, Albrecht JK: Peginterferon alfa-2b plus ribavirin compared with interferon alfa-2b plus ribavirin for initial treatment of chronic hepatitis C: a randomised trial. *Lancet* 2001, 358:958-965.
33. Fried MW, Shiffman ML, Reddy KR, Smith C, Marinos G, Goncalves FL, Jr., Haussinger D, Diago M, Carosi G, Dhumeaux D, et al.: Peginterferon alfa-2a plus ribavirin for chronic hepatitis C virus infection. *N Engl J Med* 2002, 347:975-982.
34. Deng CL, Yeo H, Ye HQ, Liu SQ, Shang BD, Gong P, Alonso S, Shi PY, Zhang B: Inhibition of enterovirus 71 by adenosine analog NITD008. *J Virol* 2014, 88:11915-11923.
35. Kang H, Kim C, Kim DE, Song JH, Choi M, Choi K, Kang M, Lee K, Kim HS, Shin JS, et al.: Synergistic antiviral activity of gemcitabine and ribavirin against enteroviruses. *Antiviral Res* 2015, 124:1-10.
36. Zhang Z, Yang E, Hu C, Cheng H, Chen CY, Huang D, Wang R, Zhao Y, Rong L, Vignuzzi M, et al.: Cell-based high-throughput screening assay identifies 2', 2'-difluoro-2'-deoxycytidine Gemcitabine as potential anti-poliovirus agent. *ACS Infect Dis* 2016.
- **37. van der Linden L, Vives-Adrian L, Selisko B, Ferrer-Orta C, Liu X, Lanke K, Ulferts R, De Palma AM, Tanchis F, Goris N, et al.: The RNA template channel of the RNA-dependent RNA polymerase as a target for development of antiviral therapy of multiple genera within a virus family. *PLoS Pathog* 2015, 11:e1004733.
- This paper identifies the novel non-nucleoside analog GPC-N114 and identifies the RNA template channel of 3Dpol as novel target for broad-spectrum antiviral therapy.
38. Liu Y, Zheng Z, Shu B, Meng J, Zhang Y, Zheng C, Ke X, Gong P, Hu Q, Wang H: SUMO Modification Stabilizes Enterovirus 71 Polymerase 3D to Facilitate Viral Replication. *J Virol* 2016.

39. Ulferts R, de Boer SM, van der Linden L, Bauer L, Lyoo HR, Mate MJ, Lichiere J, Canard B, Lelieveld D, Omta W, et al.: Screening of a Library of FDA-Approved Drugs Identifies Several Enterovirus Replication Inhibitors That Target Viral Protein 2C. *Antimicrob Agents Chemother* 2016, 60:2627-2638.
40. Ulferts R, van der Linden L, Thibaut HJ, Lanke KH, Leyssen P, Coutard B, De Palma AM, Canard B, Neyts J, van Kuppeveld FJ: Selective serotonin reuptake inhibitor fluoxetine inhibits replication of human enteroviruses B and D by targeting viral protein 2C. *Antimicrob Agents Chemother* 2013, 57:1952-1956.
41. Zuo J, Quinn KK, Kye S, Cooper P, Damoiseaux R, Krogstad P: Fluoxetine is a potent inhibitor of coxsackievirus replication. *Antimicrob Agents Chemother* 2012, 56:4838-4844.
- **42. Xia H, Wang P, Wang GC, Yang J, Sun X, Wu W, Qiu Y, Shu T, Zhao X, Yin L, et al.: Human Enterovirus Nonstructural Protein 2CATPase Functions as Both an RNA Helicase and ATP-Independent RNA Chaperone. *PLoS Pathog* 2015, 11:e1005067.

Paper showing that 2CATPase possesses the long-sought ATP-dependent RNA helicase activity, allowing studies to elucidate the mode of action of 2C inhibitors with a yet unknown mechanism.

- *43. Gofshiteyn J, Cardenas AM, Bearden D: Treatment of Chronic Enterovirus Encephalitis With Fluoxetine in a Patient With X-Linked Agammaglobulinemia. *Pediatr Neurol* 2016.

This is the first report showing that the repurposed drugs fluoxetine could be used as potential therapy in the clinic for chronic enterovirus infection.

44. Jiang P, Liu Y, Ma HC, Paul AV, Wimmer E: Picornavirus morphogenesis. *Microbiol Mol Biol Rev* 2014, 78:418-437.
45. Geller R, Vignuzzi M, Andino R, Frydman J: Evolutionary constraints on chaperone-mediated folding provide an antiviral approach refractory to development of drug resistance. *Genes Dev* 2007, 21:195-205.
- *46. Ma HC, Liu Y, Wang C, Strauss M, Rehage N, Chen YH, Altan-Bonnet N, Hogle J, Wimmer E, Mueller S, et al.: An interaction between glutathione and the capsid is required for the morphogenesis of C-cluster enteroviruses. *PLoS Pathog* 2014, 10:e1004052.

First description of the importance of glutathione in enterovirus morphogenesis.

- *47. Thibaut HJ, van der Linden L, Jiang P, Thys B, Canela MD, Aguado L, Rombaut B, Wimmer E, Paul A, Perez-Perez MJ, et al.: Binding of glutathione to enterovirus capsids is essential for virion morphogenesis. *PLoS Pathog* 2014, 10:e1004039.

First description of the importance of glutathione in enterovirus morphogenesis.

48. Asare E, Mugavero J, Jiang P, Wimmer E, Paul AV: A Single Amino Acid Substitution in Poliovirus Nonstructural Protein 2CATPase Causes Conditional Defects in Encapsidation and Uncoating. *J Virol* 2016, 90:6174-6186.
49. Liu Y, Wang C, Mueller S, Paul AV, Wimmer E, Jiang P: Direct interaction between two viral proteins, the nonstructural protein 2C and the capsid protein VP3, is required for enterovirus morphogenesis. *PLoS Pathog* 2010, 6:e1001066.
50. Wang C, Jiang P, Sand C, Paul AV, Wimmer E: Alanine scanning of poliovirus 2CATPase reveals new genetic evidence that capsid protein/2CATPase interactions are essential for morphogenesis. *J Virol* 2012, 86:9964-9975.
51. Tsou YL, Lin YW, Chang HW, Lin HY, Shao HY, Yu SL, Liu CC, Chitra E, Sia C, Chow YH: Heat shock protein 90: role in enterovirus 71 entry and assembly and potential target for therapy. *PLoS One* 2013, 8:e77133.
52. van der Schaar HM, Dorobantu CM, Albuлесcu L, Strating JR, van Kuppeveld FJ: Fat(al) attraction: Picornaviruses Usurp Lipid Transfer at Membrane Contact Sites to Create Replication Organelles. *Trends Microbiol* 2016, 24:535-546.
- **53. Hsu NY, Ilnytska O, Belov G, Santiana M, Chen YH, Takvorian PM, Pau C, van der Schaar H, Kaushik-Basu N, Balla T, et al.: Viral reorganization of the secretory pathway generates distinct organelles for RNA replication. *Cell* 2010, 141:799-811.

Identification of PI4KB as an important host factor for enterovirus replication. This information spurred the development of PI4KB inhibitors as broad-range enterovirus replication inhibitors.

54. van der Schaar HM, Leyssen P, Thibaut HJ, de Palma A, van der Linden L, Lanke KH, Lacroix C, Verbeke E, Conrath K, Macleod AM, et al.: A novel, broad-spectrum inhibitor of enterovirus replication that targets host cell factor phosphatidylinositol 4-kinase IIbeta. *Antimicrob Agents Chemother* 2013, 57:4971-4981.

55. Arita M, Kojima H, Nagano T, Okabe T, Wakita T, Shimizu H: Phosphatidylinositol 4-kinase III beta is a target of enviroxime-like compounds for antipoliovirus activity. *J Virol* 2011, 85:2364-2372.
56. Roulin PS, Lotzcher M, Torta F, Tanner LB, van Kuppeveld FJ, Wenk MR, Greber UF: Rhinovirus uses a phosphatidylinositol 4-phosphate/cholesterol counter-current for the formation of replication compartments at the ER-Golgi interface. *Cell Host Microbe* 2014, 16:677-690.
57. Lamarche MJ, Borawski J, Bose A, Capacci-Daniel C, Colvin R, Dennehy M, Ding J, Dobler M, Drumm J, Gaitner LA, et al.: Anti-hepatitis C virus activity and toxicity of type III phosphatidylinositol-4-kinase beta inhibitors. *Antimicrob Agents Chemother* 2012, 56:5149-5156.
58. Arita M: Mechanism of Poliovirus Resistance to Host Phosphatidylinositol-4 Kinase III beta Inhibitor. *ACS Infect Dis* 2016, 2:140-148.
59. van der Schaar HM, van der Linden L, Lanke KH, Strating JR, Purstinger G, de Vries E, de Haan CA, Neyts J, van Kuppeveld FJ: Coxsackievirus mutants that can bypass host factor PI4KIIIbeta and the need for high levels of PI4P lipids for replication. *Cell Res* 2012, 22:1576-1592.
- *60. Strating JR, van der Linden L, Albulescu L, Bigay J, Arita M, Delang L, Leyssen P, van der Schaar HM, Lanke KH, Thibaut HJ, et al.: Itraconazole inhibits enterovirus replication by targeting the oxysterol-binding protein. *Cell Rep* 2015, 10:600-615.

Itraconazole, an FDA-approved drug to target fungal infections, is identified as a broad-spectrum enterovirus inhibitor and shown to target the lipid shuttling activity of oxysterol-binding protein that is essential for viral replication organell formation and/or function.

61. Gao Q, Yuan S, Zhang C, Wang Y, Wang Y, He G, Zhang S, Altmeyer R, Zou G: Discovery of itraconazole with broad-spectrum in vitro antienterovirus activity that targets nonstructural protein 3A. *Antimicrob Agents Chemother* 2015, 59:2654-2665.
62. Mesmin B, Bigay J, Moser von Filseck J, Lacas-Gervais S, Drin G, Antony B: A four-step cycle driven by PI(4)P hydrolysis directs sterol/PI(4)P exchange by the ER-Golgi tether OSBP. *Cell* 2013, 155:830-843.
63. Albulescu L, Strating JR, Thibaut HJ, van der Linden L, Shair MD, Neyts J, van Kuppeveld FJ: Broad-range inhibition of enterovirus replication by OSW-1, a natural compound targeting OSBP. *Antiviral Res* 2015, 117:110-114.
64. Arita M, Kojima H, Nagano T, Okabe T, Wakita T, Shimizu H: Oxysterol-binding protein family I is the target of minor enviroxime-like compounds. *J Virol* 2013, 87:4252-4260.
65. Albulescu L, Bigay J, Biswas B, Weber-Boyvat M, Dorobantu CM, Delang L, van der Schaar HM, Jung YS, Neyts J, Olkkonen VM, et al.: Uncovering oxysterol-binding protein (OSBP) as a target of the anti-enteroviral compound TTP-8307. *Antiviral Res* 2017, 140:37-44.
66. Shim A, Song JH, Kwon BE, Lee JJ, Ahn JH, Kim YJ, Rhee KJ, Chang SY, Cha Y, Lee YS, et al.: Therapeutic and prophylactic activity of itraconazole against human rhinovirus infection in a murine model. *Sci Rep* 2016, 6:23110.
- *67. Qing J, Wang Y, Sun Y, Huang J, Yan W, Wang J, Su D, Ni C, Li J, Rao Z, et al.: Cyclophilin A associates with enterovirus-71 virus capsid and plays an essential role in viral infection as an uncoating regulator. *PLoS Pathog* 2014, 10:e1004422.

First description of the role of cyclophilin in the uncoating process of an enterovirus and the potential of cyclophilin inhibitors to interfere with enterovirus infection.

68. Frausto SD, Lee E, Tang H: Cyclophilins as modulators of viral replication. *Viruses* 2013, 5:1684-1701.
69. Seizer P, Klingel K, Sauter M, Westermann D, Ochmann C, Schonberger T, Schleicher R, Stellos K, Schmidt EM, Borst O, et al.: Cyclophilin A affects inflammation, virus elimination and myocardial fibrosis in coxsackievirus B3-induced myocarditis. *J Mol Cell Cardiol* 2012, 53:6-14.
70. Desmet J, Verstraete K, Bloch Y, Lorent E, Wen Y, Devreese B, Vandenbroucke K, Loverix S, Hettmann T, Deroo S, et al.: Structural basis of IL-23 antagonism by an Alphabody protein scaffold. *Nat Commun* 2014, 5:5237.
71. Crotty S, Maag D, Arnold JJ, Zhong WD, Lau JYN, Hong Z, Andino R, Cameron C: The broad-spectrum antiviral ribonucleoside ribavirin is an RNA virus mutagen. *Nature Medicine* 2001, 7:255-255.
72. Ulferts R, de Boer M, van der Linden L, Bauer L, Lyoo HR, Mate MJ, Lichiere J, Canard B, Lelieveld D, Omta W, et al.: Screening of a library of FDA-approved drugs identifies several enterovirus replicaton inhibitors that target viral protein 2C. *Antimicrob Agents Chemother* 2016.

CHAPTER 3

ESCAPING HOST FACTOR PI4KB INHIBITION: ENTEROVIRUS GENOMIC RNA REPLICATION IN THE ABSENCE OF REPLICATION ORGANELLES

Charlotte E Melia^{1,}, Hilde M van der Schaar^{2,*}, Heyrhyoung Lyoo², Ronald WAL Limpens¹, Qian Feng², Maryam Wahedi², Gijs J Overheul³, Ronald P van Rij³, Eric J Snijder⁴, Abraham J Koster¹, Montserrat Bárcena^{1,#}, Frank JM van Kuppeveld^{2,#}*

1 Department of Molecular Cell Biology, Section Electron Microscopy, Leiden University Medical Center, Leiden, The Netherlands

2 Department of Infectious Diseases & Immunology, Virology Division, Faculty of Veterinary Medicine, Utrecht University, Utrecht, The Netherlands

3 Department of Medical Microbiology, Radboud University Medical Center, Radboud Institute for Molecular Life Sciences, Nijmegen, The Netherlands

4 Department of Medical Microbiology, Molecular Virology Laboratory, Center of Infectious Diseases, Leiden University Medical Center, Leiden, The Netherlands

* These authors contributed equally.

Corresponding author

SUMMARY

Enteroviruses reorganize cellular endomembranes into replication organelles (ROs) for genome replication. Although enterovirus replication depends on phosphatidylinositol 4-kinase type III β (PI4KB), its role, and that of its product PI4P, is only partially understood. Exploiting a mutant coxsackievirus resistant to PI4KB inhibition, we uncover that PI4KB activity has distinct functions in proteolytic processing of the viral polyprotein and in RO biogenesis. The escape mutation rectified a proteolytic processing defect imposed by PI4KB inhibition, pointing to a possible escape mechanism. Remarkably, under PI4KB inhibition the mutant virus could replicate its genome in the absence of ROs, using instead the Golgi apparatus. This impaired RO biogenesis provided an opportunity to investigate the proposed role of ROs in shielding enteroviral RNA from cellular sensors. Neither accelerated sensing of viral RNA nor enhanced innate immune responses were observed. Together, our findings challenge the notion that ROs are indispensable for enterovirus genome replication and immune evasion.

HIGHLIGHTS

- PI4KB activity expedites the formation of coxsackievirus replication organelles (ROs)
- PI4KB inhibition impairs polyprotein processing, which is rescued by a 3A mutation
- Upon PI4KB inhibition, this mutant replicates at the Golgi in the absence of ROs
- Innate immune responses are not enhanced when RO biogenesis is delayed

INTRODUCTION

The group of positive-strand RNA (+RNA) viruses comprises many human pathogens, such as hepatitis C virus, Zika virus, dengue virus, SARS- and MERS-coronavirus, and enteroviruses. Despite substantial genetic divergence across virus families, some features of replication are common to all +RNA viruses infecting eukaryotes. One of the most striking is the remodelling of host cell endomembranes into novel membranous compartments in the cytoplasm of the infected cell. These compartments serve as compositionally unique platforms upon which the components of the viral RNA synthesis machinery assemble, and whose micro-environments may facilitate efficient genome replication (reviewed in [1] and [2]). In addition, they have been postulated to play a role in the evasion of the innate antiviral host responses by shielding viral RNA products from cytosolic sensors such as MDA5 and RIG-I, which signal to activate the type I interferon (IFN- α/β) pathway, and protein kinase R (PKR), which activates an integral stress response [3, 4].

Members of the Enterovirus genus, belonging to the Picornaviridae family, include poliovirus, coxsackie A and B viruses, several numbered enteroviruses (e.g. EV-D68, EV-A71), and rhinoviruses, which are causative agents of various human diseases. Enteroviruses, like other positive-sense RNA viruses, modify host-cell membranes to form structures with novel morphologies. These modified membranes serve as platforms for viral replication, which we will refer to as replication organelles (ROs). At earlier stages of coxsackievirus B3 (CVB3) or poliovirus (PV) infection, ROs emerge as single-membrane tubules that appear to form at the expense of the Golgi apparatus. These tubules are interspersed with double-membrane vesicles (DMVs), which are believed to arise as tubules deform and enwrap small volumes of cytosol. In this way, most tubules transform into DMVs over the course of infection, and DMVs may be further enwrapped to form multilamellar vesicles [5, 6]. Each stage of virus replication, including the transformation of cellular membranes into ROs, is dependent upon the interplay between viral proteins and host factors. The small, membrane-anchored enterovirus 3A protein has a key role in generating ROs [7], and is known to recruit host factors that are essential for genome replication. One of these factors is phosphatidylinositol 4-kinase type III β (PI4KB) [8, 9]. In uninfected cells PI4KB is a Golgi-resident enzyme that generates phosphatidylinositol 4-phosphate (PI4P), while during enterovirus infection the viral 3A protein recruits PI4KB to ROs, enriching them in PI4P [8, 10].

The importance of PI4P in viral infections has been the subject of several recent investigations, both for the Picornaviridae, such as Aichivirus (genus Kobuviruses) and encephalomyocarditis virus (EMCV) (genus Cardiovirus) and for other +RNA viruses, such as hepatitis C virus (HCV) (reviewed in [11] and [12]). In uninfected cells, PI4P is involved in a multitude of functions, including signalling, membrane trafficking, regulation of Golgi apparatus organisation, and lipid homeostasis (reviewed in [13] and [14]). Of particular relevance for viruses that utilise PI4P is the counterflux of PI4P and cholesterol between Golgi apparatus and ER, which is mediated by the oxysterol-binding protein (OSBP). OSBP acts as a bridge between these two membrane compartments to generate a membrane contact site, using PI4P as a Golgi-based anchor and vesicle-associated membrane protein-associated protein A (VAP-A) as an ER anchor [15]. During enterovirus infection, OSBP is diverted to create a novel type of membrane contact site between ROs and the ER. These sites mediate the exchange of PI4P for cholesterol, which is another essential lipid for enterovirus genome replication [16-18].

Recruitment of PI4KB by the viral 3A protein is critical for enterovirus genome replication [8, 9], but its exact role is unclear. The stage of genome replication in the enterovirus life cycle encompasses different processes, including proteolytic processing of the polyprotein, RO biogenesis, and RNA

synthesis by the viral replication machinery. In this study, we used a CVB3 mutant resistant to PI4KB inhibition, i.e. CVB3 3A-H57Y [19], to further dissect the role of PI4KB and the PI4P-rich environment it generates during genome replication. We show that PI4KB activity facilitates efficient proteolytic processing of the CVB3 polyprotein. The 3A-H57Y substitution compensates for the impairment of polyprotein processing caused by PI4KB inhibition, which may represent the escape mechanism of this mutant virus. Distinct from its effect on polyprotein processing, we found that PI4KB inhibition also delayed RO formation. Remarkably, CVB3 3A-H57Y could replicate its genome in the absence of detectable ROs when PI4KB was inhibited. Under these conditions, viral RNA synthesis was observed instead at a cellular organelle, the Golgi apparatus, which challenges the notion that ROs are essential for the exponential phase of genome replication. Golgi disintegration and RO formation did eventually occur under PI4KB inhibition, which suggests that PI4KB activity is not fundamentally required for RO biogenesis, but expedites the process. The delay in RO formation under PI4KB inhibition was exploited to experimentally test the hypothesis that ROs shield viral RNA from cytoplasmic sensors of the innate immune system. Our results suggest that, in addition to being dispensable for viral RNA synthesis, enterovirus ROs do not play a pivotal role in suppression of the innate antiviral response pathways.

RESULTS

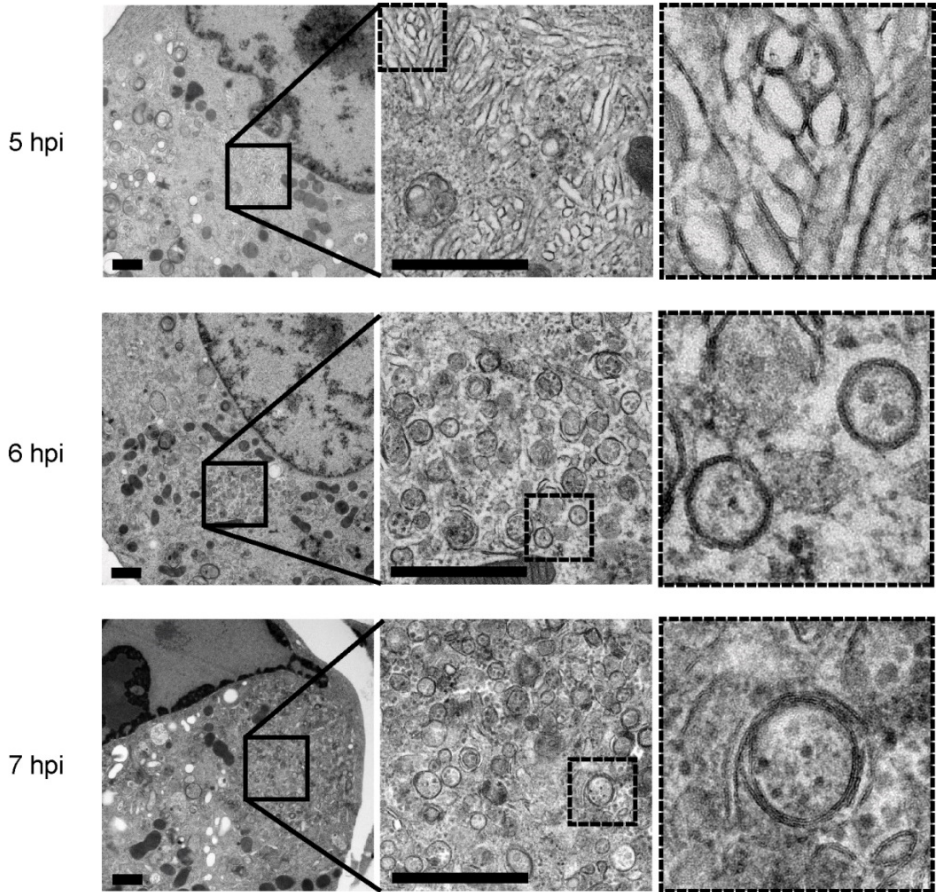
CVB3 3A-H57Y RO formation is impaired under PI4KB inhibition

First, we set out to study the morphology of the ROs induced by CVB3 3A-H57Y under conditions where PI4KB is not inhibited. Infected BGM cells were prepared for electron microscopy (EM) by high-pressure freezing and freeze-substitution at different times post-infection and analysed for the presence of membrane modifications. The first ROs induced by CVB3 3A-H57Y were detected at 5 hours post infection (hpi). At this stage single-membrane tubules were predominant, interspersed with double-membrane vesicles (DMVs) (Fig. 1A). The emergence of ROs coincides with disintegration of the Golgi apparatus in wt infection [5] and, concordantly, the Golgi apparatus was not observed in cell sections that contained ROs at any time point in this analysis. Later in infection tubules had largely transformed into DMVs (Fig. 1A, 6 hpi) and into multilamellar structures (Fig. 1A, 7 hpi). This progression closely reflects observations of wt CVB3 RO development with regard to both the specific morphologies induced and the time frame over which they develop [5], (Fig. S1A). Together, these results indicate that the 3A-H57Y substitution does not affect RO development or their general architecture.

Next, we investigated the effect of PI4KB inhibition on RO development during CVB3 3A-H57Y infection. To determine suitable time points for EM analysis of cells infected in the presence of a PI4KB inhibitor, we first measured viral replication in the presence of BF738735, a potent and specific PI4KB inhibitor without overt cytotoxicity (a.k.a. Compound 1; [9, 20]). Unlike CVB3 wt (Fig. S2A), CVB3 3A-H57Y was resistant to BF738735 (Fig. S2B), although its replication was nevertheless delayed and impaired in the presence of BF738735 with regard to both viral RNA (vRNA) and infectious progeny virus. This is in agreement with observations using other PI4KB inhibitors (e.g. PIK93; [19]). To examine whether the impairment of replication upon PI4KB inhibition was the consequence of a decrease in the number of infected cells and/or a reduced level of vRNA replication, we collected cells infected with EGFP-CVB3 3A-H57Y at different time points post infection and analysed them with flow cytometry. PI4KB inhibition reduced the number of CVB3 3A-H57Y-infected cells (by ~3-fold), delayed replication (by ~1-2 h), and limited viral protein production, as reflected by reduced EGFP levels (Fig. S2C). These results indicate

that the PI4KB inhibitor imposes a critical barrier to CVB3 3A-H57Y replication in a subpopulation of cells, and reduces the efficiency of replication in those cells where infection is established.

A



B

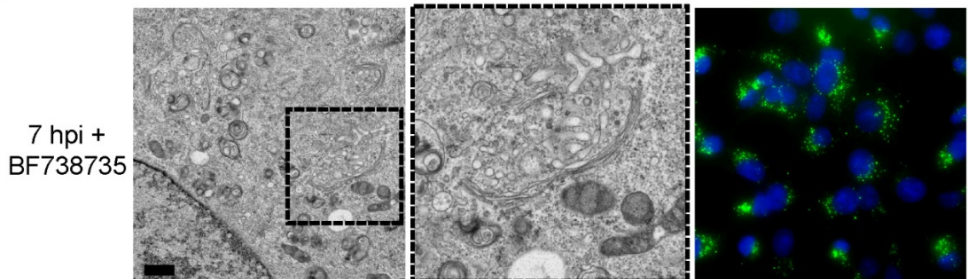


Figure 1. CVB3 3A-H57Y RO formation is impaired under PI4KB inhibition. A, B) BGM cells infected with CVB3 3A-H57Y (MOI 50). A) Cells fixed for EM analysis at early (5 hpi), intermediate (6 hpi) or late (7 hpi) stages of infection show the progression in RO development. B) ROs were not observed in EM cell sections (up to 8 hpi, n = 153) from cells treated with BF738735. (Left) An example of the Golgi apparatus in cells fixed at 7 hpi. (Right) Parallel immunofluorescence data (dsRNA (green) and nuclear stain (blue)). Scale bars, 1 μ m. See also Figs. S1 and S2.

3

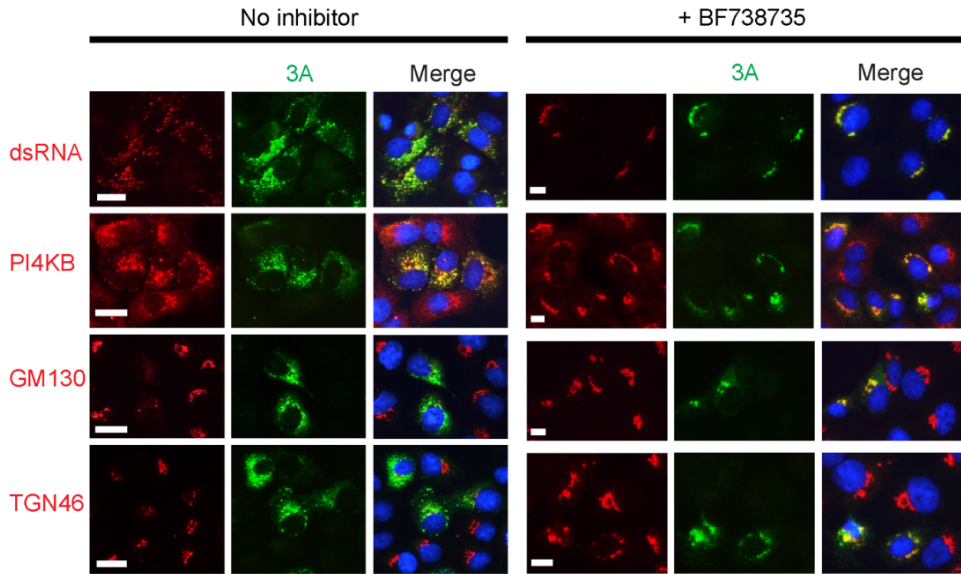
Based on the growth curve analysis, cells were fixed and processed for EM between 5 and 8 hpi, as this period encompasses the exponential phase of vRNA replication for CVB3 3A-H57Y under PI4KB inhibition. Remarkably, while ROs were detected at a frequency of ~50% in EM cell-sections from infections in the absence of PI4KB inhibitor ($n = 43$ cell-sections assessed at 6 hpi), neither archetypal enterovirus ROs (i.e. clusters of single-membrane tubules and/or DMVs) nor cellular membranes with atypical morphologies were detected in cells infected under PI4KB inhibition ($n = 153$ cell-sections), even at late time points (7-8 hpi, $n = 47$ cell-sections, example shown in Fig. 1B). Seemingly intact Golgi cisternae were apparent in these cells and were detected at a frequency similar to that of mock-infected or BF738735-treated cells (Fig. S1B and C respectively). Corresponding immunofluorescence microscopy data showed a high percentage of cells positive for dsRNA labelling, confirming that the lack of membrane modifications in the EM analysis was not simply due to a low number of infected cells (Fig. 1B, right). These data show that RO development is impaired by PI4KB inhibition, and suggest that replication may be taking place instead at a cellular organelle.

CVB3 3A-H57Y replicates its genome at the Golgi apparatus under PI4KB inhibition

As an initial indicator of the replication site under PI4KB inhibition, we performed immunofluorescence microscopy on infected cells (Fig. 2A). Cells were fixed at 5 hpi in the absence of inhibitor, and at 6 hpi in the presence of inhibitor given the delay in replication. Similar to findings for wt virus [8, 19], both 3A and dsRNA were detected throughout the cytoplasm in cells infected with CVB3 3A-H57Y in the absence of PI4KB inhibition (Fig. 2A, left panels). Golgi disassembly could be readily visualized through the signal reduction and dispersion of the cis-Golgi marker GM130 and the trans-Golgi network marker TGN46, whereas the PI4KB signal overlapped with the 3A labelling. Upon PI4KB inhibitor treatment however, 3A and dsRNA were primarily confined to the perinuclear region (Fig. 2A, right panels). In wide-field images, the strength and distribution of GM130 and TGN46 signals were largely maintained and overlapped with the viral 3A signal. These results suggested that both the 3A-H57Y protein and dsRNA reside at the Golgi apparatus in the presence of inhibitor. To confirm that these observations were due to specific inhibition of PI4KB, the localisation of 3A-GFP was assessed using different PI4KB inhibitors. Similar to BF738735, enviroxime, GW5074 or PIK93 treatment resulted the accumulation of 3A specifically at the Golgi region, although confocal imaging revealed that 3A did not directly co-localise with the cis-Golgi marker GM130 (Fig. 2B).

To unambiguously determine the subcellular location of the 3A-H57Y protein under PI4KB inhibitor treatment, correlative light and electron microscopy (CLEM) was performed. For this we employed the split-GFP system [21] to label the 3A-H57Y protein, in a similar approach to that previously reported for wt CVB3 [22]. To produce a split-GFP CVB3 3A-H57Y mutant, the final beta sheet of GFP, i.e. strand 11, further referred to as GFP(S11), was introduced into the 3A-H57Y protein to produce CVB3 3A-H57Y(S11). Upon CVB3 3A-H57Y(S11) infection of BGM cells stably expressing the remaining portion of GFP (GFPS1-10), the two fragments of GFP self-assemble to produce GFP-tagged 3A-H57Y. GFP-tagged 3A-H57Y was then visualized by confocal microscopy before chemical fixation and processing for EM. Overlays of 3A-H57Y-GFP signal with the corresponding EM cell-sections fixed at 6 hpi revealed that the 3A protein localised specifically to the Golgi apparatus (Fig. 3A).

A



3

B

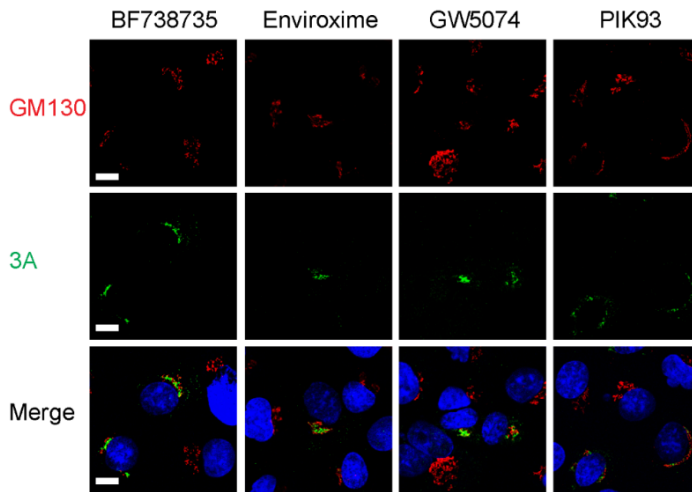
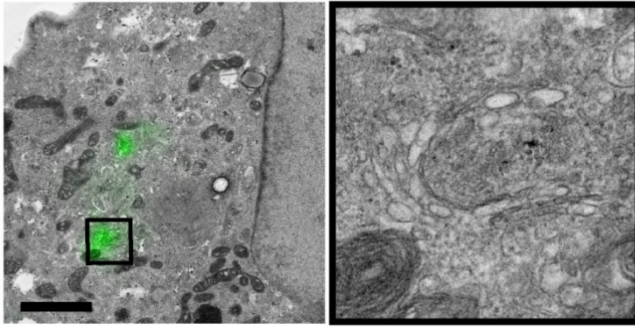
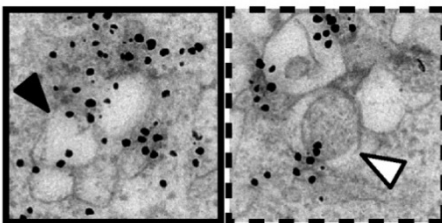
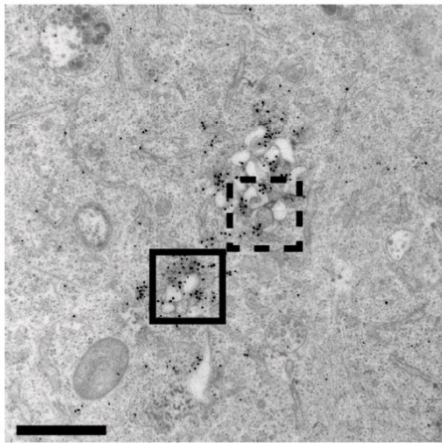


Figure 2. The 3A protein localises to the Golgi apparatus under PI4KB inhibition. (A, B) BGM cells infected with CVB3 3A-H57Y (MOI 10). Untreated cells were fixed at 5 hpi ((A) left panels) and drug treated cells were fixed at 6 hpi ((A) right panels, and (B)). Fixed cells were labelled with the indicated antibodies and a nuclear stain (blue). Scale bars, 10 μ m.

A



B



C

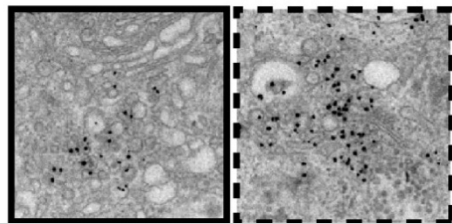
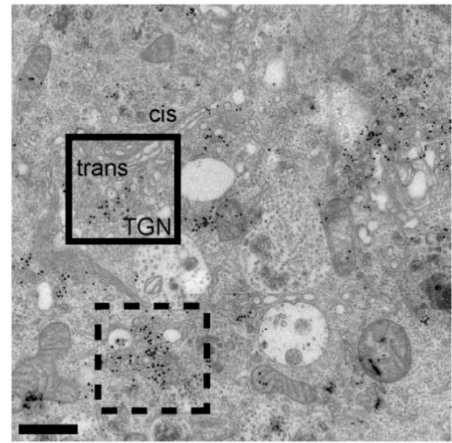


Figure 3. Replication under PI4KB inhibition occurs at the Golgi apparatus. (A) BGM(GFPS1-10) cells infected with CVB3 3A-H57Y(S11) (MOI 7) monitored by live-cell LM, fixed at 6 hpi, and processed for CLEM. Overlay of the 3A-GFP signal at the time of fixation with the corresponding EM image (left). Inset highlights one of two 3A-GFP foci present in the image shown, both of which correspond to Golgi membranes. (B, C) BGM cells infected with CVB3 3A-H57Y (MOI 50), metabolically labelled, fixed at 6 hpi (B) or 7 hpi (C), and processed for EM autoradiography to detect newly-synthesized vRNA (ARG). ARG signal is apparent as electron-dense grains. (B) ROs positive for ARG signal were readily observed in the absence of BF738735. (C) In cells treated with BF738735 ROs were not observed, and clusters of ARG signal were found exclusively at the Golgi apparatus. cis = Golgi apparatus cis face, trans = Golgi apparatus trans face, TGN = trans Golgi network. Scale bars, 2 μ m (A) or 1 μ m (B, C).

The presence of the 3A-H57Y protein at the Golgi apparatus suggested that vRNA replication occurs at this compartment under PI4KB inhibition. To further investigate this, metabolic labelling was performed to detect newly synthesized vRNA in situ. Infected cells were pre-treated with 10 μ g/ml dactinomycin to inhibit cellular transcription, and incubated with tritiated uridine for 45 minutes prior to fixation to label newly-synthesised vRNA. As a control, mock-infected cells underwent the same treatment. After

processing for EM, radiolabelled uridine was detected by autoradiography (ARG). In cells infected with CVB3 3A-H57Y without PI4KB inhibition, abundant ARG signal was found in regions containing typical ROs (Fig. 3B). Although RO membranes in chemically fixed samples appeared somewhat distended in comparison to high-pressure frozen material (see Fig. 1), they were recognisable as clusters of single-membrane compartments (Fig. 3B, black arrowhead) interspersed with DMVs (Fig. 3B, white arrowhead) that closely resemble the ROs observed in chemically fixed PV-infected [6, 23] or wt CVB3-infected cells [22]. In CVB3 3A-H57Y-infected cells treated with PI4KB inhibitor and fixed at 7 hpi ROs were not observed ($n = 148$ cell sections), and abundant ARG signal was found at the Golgi apparatus (Fig. 3C), with the vast majority of signal localising to the trans-side of the Golgi apparatus and trans-Golgi network rather than the Golgi cisternae. This demonstrates that, under PI4KB inhibition, CVB3 3A-H57Y can replicate its genome in the absence of ROs on a seemingly intact Golgi apparatus.

Under PI4KB inhibition, ROs form late in CVB3 3A-H57Y-infected cells

Our results thus far show that, under PI4KB inhibition, CVB3 3A-H57Y replication is possible in association with an apparently intact cellular organelle. We next set out to establish whether PI4KB inhibition precludes Golgi disintegration and RO development entirely, or simply delays the process. Confocal microscopy of live cells expressing mCherry-GM130 was performed to monitor the Golgi apparatus across the course of CVB3 3A-H57Y(S11) infection, either with or without BF738735 treatment (Fig. 4A-C). In the absence of inhibitor, the process of Golgi fragmentation following CVB3 3A-H57Y(S11) infection was similar to that of wt split-GFP CVB3 infections [22]. The onset of Golgi fragmentation occurred in conjunction with or even preceded 3A protein accumulation in the Golgi area, and Golgi disintegration was typically complete within 25 min ($n = 23$ cells) (Fig. 4A and C, upper graph). While in the absence of PI4KB inhibition early 3A signal was often located at peripheral foci (Fig. 4A arrowheads), under PI4KB inhibition the first 3A signal was often found in the Golgi region (Fig. 4B, arrowheads). Remarkably, the Golgi apparatus of most CVB3 3A-H57Y(S11) infected cells did disassemble during infections under PI4KB inhibition, but with markedly different dynamics. The onset of disintegration under these conditions did not coincide with 3A protein accumulation at the Golgi, but suffered a relative average delay of 30 minutes ($n = 48$ cells). Additionally, the time needed for Golgi disintegration was highly variable under PI4KB inhibition. In a minority of infected cells treated with BF738735 Golgi disassembly was as rapid as in untreated cells. However, in most cells the Golgi disintegration process was substantially prolonged (by up to 10 hours) under PI4KB inhibition (Fig. 4B and C, lower graph).

To determine whether Golgi disassembly under PI4KB inhibition was associated with the development of ROs, CLEM was performed on cells infected with split-GFP 3A-H57Y(S11) virus under BF738735 treatment and fixed at 9 hpi. While some cells retained seemingly intact Golgi membranes at this late stage in infection, in those cells lacking recognisable Golgi membranes the 3A-GFP signal was found at structures resembling typical early ROs (Fig. 4D, see Fig. 3A for comparison). As verified by immunofluorescence microscopy, PI4P did not accumulate in cells infected under PI4KB inhibition (Fig. S3), suggesting that the ROs that develop during CVB3 3A-H57Y infection under PI4KB inhibition do so independently of high PI4P levels.

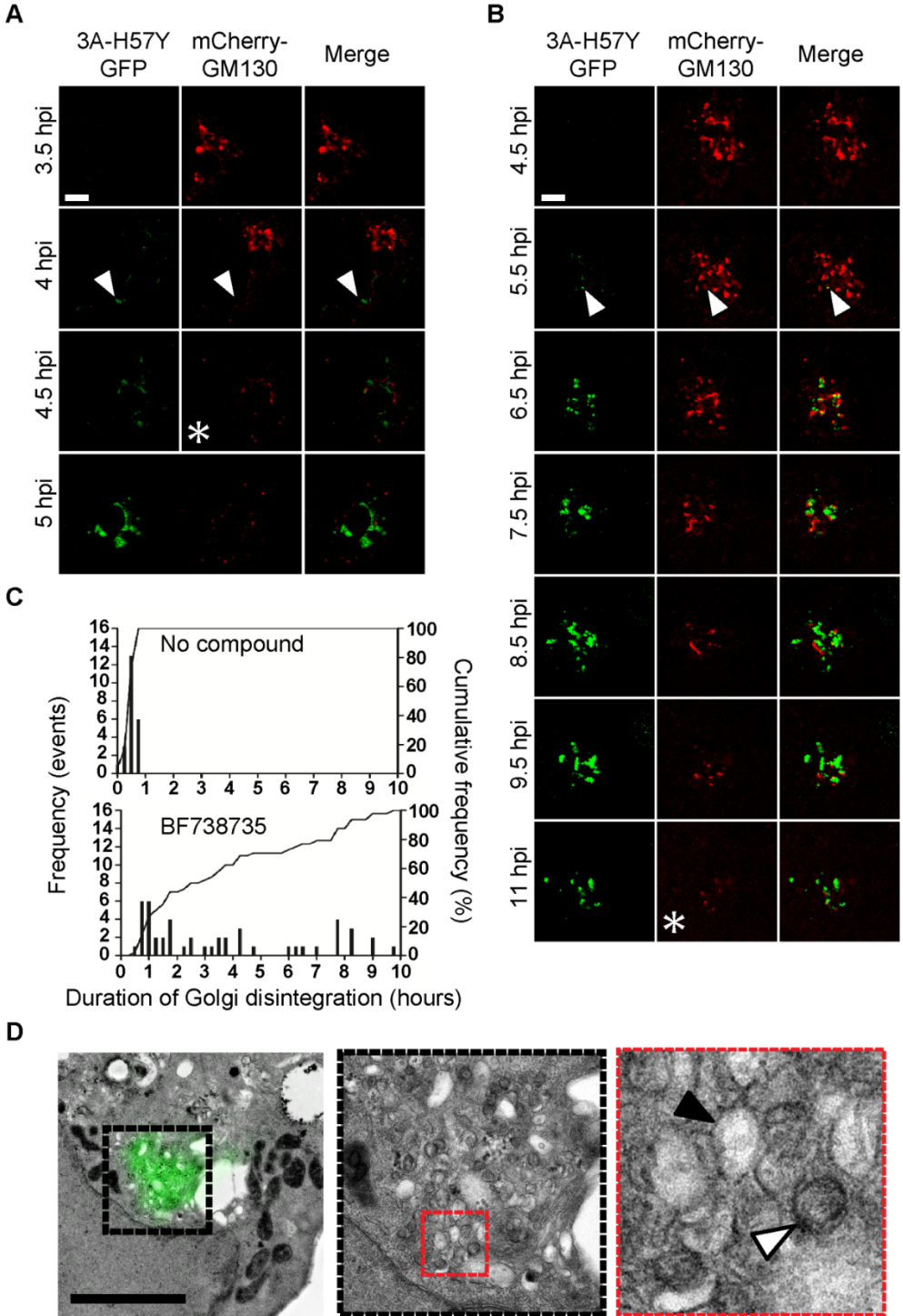


Figure 4. Golgi disintegration during CVB3 3A-H57Y infection is prolonged under PI4KB inhibition, and ultimately results in RO formation. BGM(GFPS1-10) cells transduced with MLV mCherry-GM130, infected with CVB3 3A-H57Y(S11) (MOI 7) and imaged by live-cell confocal microscopy in the absence (A) or presence (B, D) of BF738735. Asterisks (A, B) denote completion of Golgi disintegration, evidenced by an entirely punctate mCherry-GM130 signal. A) Initial 3A-GFP signal was detected primarily at peripheral locations (arrowhead) and Golgi disintegration was typically complete within 25 minutes of its onset (C, upper graph n = 23 cells). B) In cells treated with BF738735, initial 3A-GFP signal was detected primarily at the Golgi apparatus (arrowhead). The Golgi disintegration duration was typically prolonged but highly variable (C, lower graph n = 48 cells). D) Cells were fixed for EM analysis at 9 hpi. The LM-EM overlay reveals single-membrane (black arrowhead) and double-membrane (white arrowhead) structures positive for 3A-GFP signal. Scale bars, 5 μ m (D). See also Fig. S3.

PI4KB activity drives rapid Golgi disassembly and RO formation

RO formation is likely associated with the amount of viral protein produced in the cell, which in turn depends upon vRNA replication levels. Therefore, rather than the absence of high PI4P levels, the delay in CVB3 3A-H57Y vRNA replication under PI4KB inhibition could be solely responsible for impeding RO formation. Previously it was shown that replication-independent expression of PV non-structural proteins results in membranous structures reminiscent of ROs produced upon infection [24]. Here, we engineered a replication-independent CVB3 expression system, which produces high amounts of viral proteins in the absence of vRNA replication. Hence, the inhibition of vRNA replication caused by PI4KB inhibition will not result in a delay in viral protein production in this setup. The system utilizes a CVB3 cDNA placed under the control of the bacteriophage T7 RNA polymerase, and is rendered replication-incompetent through modifications to the cloverleaf structure in the 5' untranslated region (UTR) of the viral genome that prevent replication via the CVB3 polymerase [25]. The 3A-H57Y substitution was introduced into this replication-incompetent CVB3 cDNA. Transfection of the CVB3 3A-H57Y cDNA plasmid in HuH-7/T7 cells, which stably express the T7 RNA polymerase, resulted in the expression of individual viral proteins whose amounts were not affected by the addition of PI4KB inhibitor (Fig. S4). Immunofluorescence analysis of transfected cells showed that the first 3A signal could be detected as early as 3 h post transfection (hpt), but without significant effects on the Golgi apparatus. In the absence of PI4KB inhibitor, Golgi disintegration was observed from 4 hpt onwards, as evidenced by the change in GM130 signal in transfected cells (Fig. 5A, upper panels). Under PI4KB inhibition Golgi disintegration was delayed by \sim 1 h (Fig. 5A middle and lower panels). While Golgi disintegration in the replication-independent system is more rapid than during infection (see Fig. 4), most likely because of the high protein expression levels generated with this system, these data nevertheless demonstrate that in cells with equal levels of viral proteins, PI4KB inhibition delays enterovirus-induced Golgi apparatus disassembly.

To determine the contribution of the 3A-H57Y substitution to (delayed) Golgi disassembly, we examined whether the wt CVB3 cDNA could also induce Golgi disassembly under PI4KB inhibition in the replication-independent system. The results closely resembled those obtained for CVB3 3A-H57Y cDNA both with and without PI4KB inhibition (Fig. 5B). This demonstrates that the 3A-H57Y substitution does not affect Golgi disintegration.

Altogether, these findings strongly suggest that enterovirus RO biogenesis is driven by PI4KB activity.

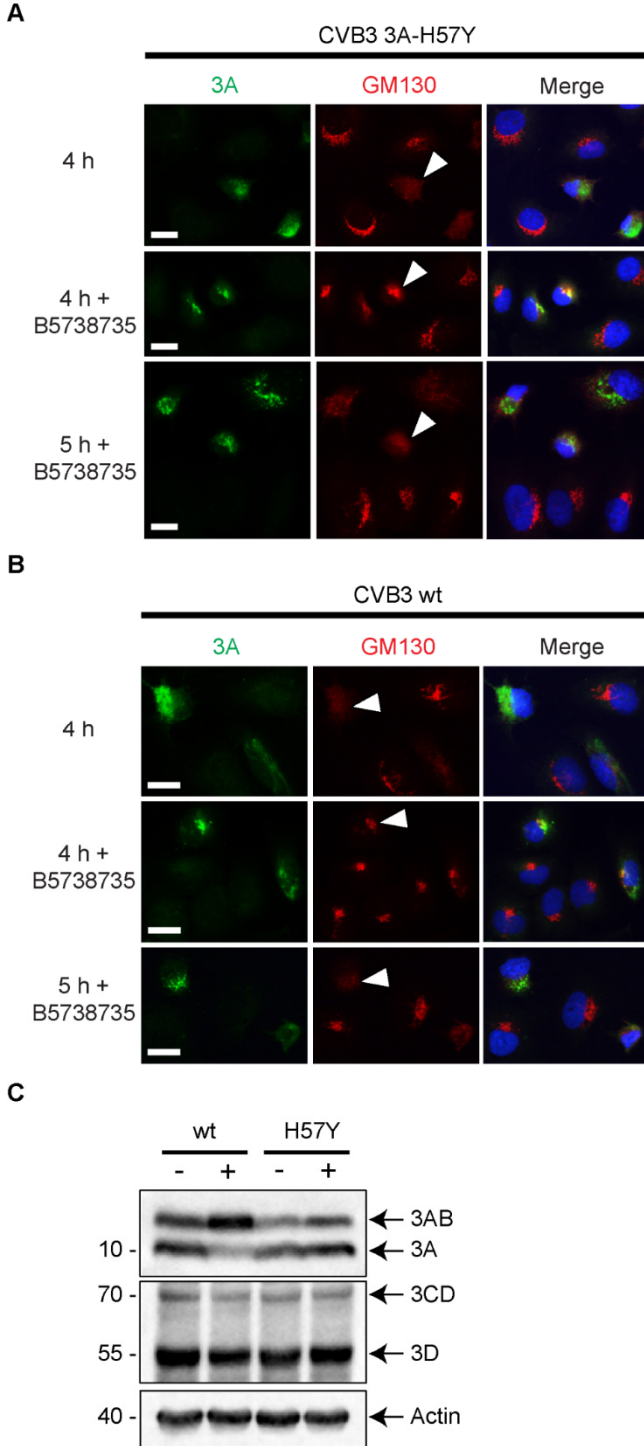


Figure 5. Effect of PI4KB inhibition on enterovirus-induced Golgi disintegration and proteolytic polyprotein processing in a replication-independent CVB3 system. HuH-7/T7 cells transfected with CVB3 3A-H57Y or wt CVB3 cDNA under the control of a T7 promoter, both rendered replication-incompetent by altering the 5'UTR of the genome. Where indicated, cells were treated with BF738735. A, B) Cells fixed at 4 h or 5 h post-transfection and labelled for 3A (green) and GM130 (red) alongside a nuclear stain (blue). Representative 3A-positive cells are indicated (arrowheads). Scale bars, 20 μ m. C) Western blot analysis of lysates from cells at 16 h post-transfection using antibodies against 3A or 3D. Actin was used as a loading control. See also Fig. S4.

The 3A-H57Y substitution rectifies a proteolytic polyprotein processing impairment induced by PI4KB inhibition

Another important step in the enterovirus replication cycle that relies on membranes is the proteolytic processing of the polyprotein by the viral proteases [26]. Proteolytic polyprotein processing is a co- and post-translational event mediated by the viral proteinases 2Apro, 3Cpro, and 3CDpro. These proteinases catalyse a cascade of cleavages in cis and in trans that liberate individual capsid proteins, as well as replication proteins and their precursors (e.g. 2BC, 3AB and 3CD). Recent studies indicate that alterations to the lipid composition of membranes during PV infection impact polyprotein processing efficiency [27-29]. Given that wt virus replication is abolished under PI4KB inhibition, we used the replication-independent CVB3 expression system to study the effects of PI4KB inhibition on polyprotein processing. Cells were lysed at 16 hours post transfection (hpt) and processed for Western blot analysis. PI4KB inhibition led to a relative accumulation of 3AB and a reduction in 3A for the wt polyprotein (Fig 5C, left). Remarkably, the 3A-H57Y substitution rectified this impaired polyprotein processing, as the relative levels of 3AB and 3A were not affected by PI4KB inhibition (Fig. 5C, right). PI4KB inhibition did not affect levels of 3CD or 3D. Together, these results demonstrate that PI4KB activity is important for proteolytic processing at the 3A-3B junction, but not at the 3C-3D junction (nor at the 2C-3A and 3B-3C junctions). The 3A-H57Y substitution restores processing to the level detected in the absence of inhibitor, which may point to a potential strategy of the mutant virus to escape PI4KB inhibition.

The delay in RO formation under PI4KB inhibition does not elicit a strong antiviral response

One of the proposed advantages of ROs is that they may shield vRNA products against viral RNA sensors present in the cytoplasm, such as MDA5, RIG-I, and PKR. Given that CVB3 3A-H57Y is able to replicate its genome at the Golgi apparatus under PI4KB inhibition, vRNA products may be more accessible and better detected in this situation, thereby triggering an antiviral response that might limit or delay replication. To investigate whether viral dsRNA is better sensed under PI4KB inhibition, we studied the activation status of the cytoplasmic RNA sensor PKR. Western blot analyses were performed on infected cell lysates to assess viral protein levels in parallel with dsRNA-activated, phosphorylated PKR (p-PKR). The first appearance and the final levels of viral proteins were delayed and reduced respectively under PI4KB inhibition, which is in agreement with the observed reduction in the proportion of infected cells and the decrease in viral protein per cell (see Fig. S2C). Nevertheless, p-PKR emerged concomitantly with the accumulation of viral proteins both in the presence and absence of PI4KB inhibitor (Fig. 6A), suggesting that delayed RO formation under PI4KB inhibition does not lead to premature activation of PKR.

Another innate antiviral response that is activated upon sensing of vRNA products is the type I interferon (IFN- α/β) pathway. Enteroviruses counteract the transcription of IFN- α/β genes by cleaving components in the signalling pathways that control their activation, such as MDA5 [30] and its downstream adaptor MAVS [30, 31]. The altered location of genome replication under PI4KB inhibition may influence the ability of the viral proteinases to cleave these components. However, we found that the appearance of MAVS degradation products in infected cell lysates coincided with the accumulation of viral proteins irrespective of the presence of PI4KB inhibitor (Fig. 6A). Furthermore, qPCR analysis showed that no substantial IFN- β response was triggered in infected cells in both conditions (Fig. 6B).

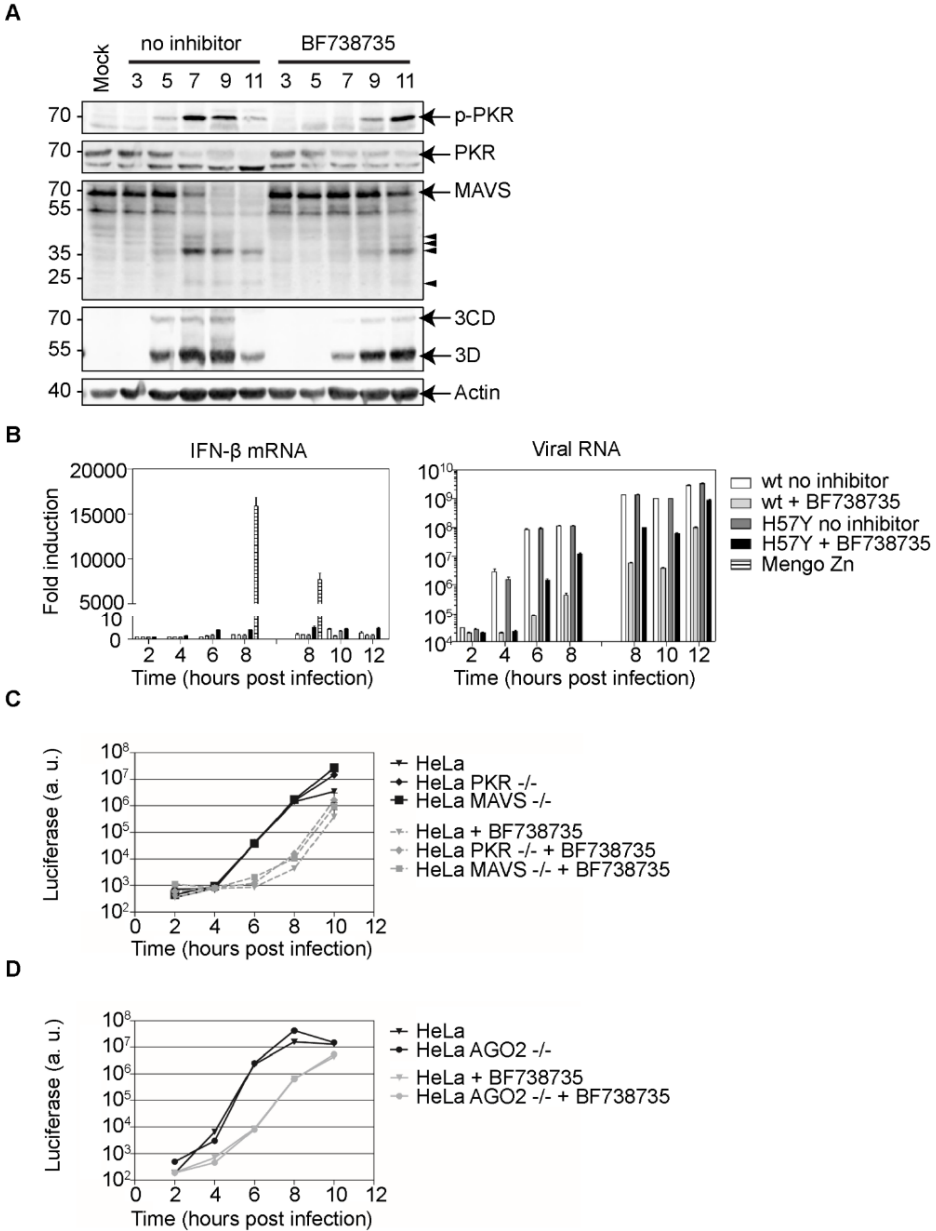


Figure 6. Innate antiviral responses during CVB3 3A-H57Y infection. Cells infected and treated with BF738735 where indicated. A) HeLa cells infected with CVB3 3A-H57Y (MOI 50) were lysed for Western blot analysis at the indicated time points. Band sizes (in kDa), full-length proteins (arrows), and putative cleavage products (arrowheads) are indicated. B) HeLa cells infected with CVB3 wt or CVB3 3A-H57Y (MOI 10). Total RNA was isolated from cells and subjected to reverse transcription-quantitative PCR for interferon- β (IFN- β). Mengo Zn, whose L protein contains substitutions that render it unable to suppress IFN- β induction, was included as a positive control (left graph). Viral RNA levels were determined by quantitative RT-PCR (right graph). Data were normalized to actin mRNA levels. Results are expressed as fold induction relative to quantities in mock-infected cells. Two independent experiments are shown, ranging from 2-8 hpi and 8-12 hpi. C, D) Cells were infected with CVB3-Rluc 3A-H57Y (MOI 0.01) and lysed to determine the intracellular luciferase levels. Values represent mean values of triplicates \pm standard error of the means. See also Figs. S5 and S6.

Together, these results indicate that the delayed formation of ROs during infection does not accelerate cellular sensing of viral dsRNA, nor does it affect the ability of the viral proteinases to cleave MAVS.

As a complementary approach to investigate whether the delay in replication in the presence of PI4KB inhibitor is related to activation of innate antiviral responses, the level of CVB3 3A-H57Y replication was determined in cells lacking sensors of these pathways. Knock-out cells for PKR or MAVS, generated with CRISPR-Cas9 technology, were infected with CVB3 wt or 3A-H57Y that also encode Renilla luciferase as a sensitive measure to quantify the level of viral replication. In the absence of inhibitor, CVB3 3A-H57Y replicated to a similar extent in HeLa, HeLa PKR *-/-*, or HeLa MAVS *-/-* cells (Fig. 6C and S6). In the presence of PI4KB inhibitor, CVB3 3A-H57Y replication was delayed not only in HeLa cells, but also in PKR *-/-* or MAVS *-/-* cells. Thus, replication under PI4KB inhibition was not significantly increased in PKR *-/-* or MAVS *-/-* cells compared to parental HeLa cells. Similar results were obtained in U2OS cells, another human cell line (Fig. S5A and S6).

An alternative strategy employed by some eukaryotes, such as plants, worms, and insects, in response to viral infections is RNA interference (RNAi), although whether RNAi is an antiviral mechanism in mammalian cells remains controversial [32]. In the RNAi pathway, the cytoplasmic sensor Dicer cleaves viral dsRNA into viral siRNAs, which are loaded by Argonaute-2 (AGO2) into the RNA-induced silencing complex (RISC) in order to degrade vRNA [33]. Recently, it was reported that replication of the picornavirus EMCV was enhanced in mammalian somatic cells that lacked AGO2 [34]. To investigate whether the delay in CVB3 3A-H57Y replication in the presence of PI4KB inhibitor is due to triggering of antiviral RNAi, we studied its replication kinetics in HeLa and HEK293T cells that lacked AGO2. Similar to our findings in MAVS and PKR knockout cell lines, the delay in replication under PI4KB inhibition was not alleviated in cells lacking AGO2 (Fig. 6D, S5B).

Altogether, these data suggest that the delay in CVB3 3A-H57Y replication under PI4KB inhibition is not caused by premature triggering of innate antiviral responses as result of impaired RO biogenesis.

DISCUSSION

Like all other +RNA viruses infecting eukaryotes, enteroviruses modify host cell endomembranes to form structures with novel morphologies, termed “replication organelles” (ROs), dedicated to amplification of the viral genome. Enteroviruses hijack host factors and modulate lipid synthesis and homeostasis pathways to build ROs with a unique protein and lipid signature (reviewed in [35, 36]). One of the lipid-modifying host factors previously shown to be essential for enterovirus genome replication is PI4KB [8, 9]. In this study we clarify the role of PI4KB and the PI4P-enriched environment it generates in CVB3-infected cells, by establishing its importance for proteolytic processing of the polyprotein and RO biogenesis. To do so, we exploited the CVB3 3A-H57Y mutant [19], which is able to establish replication under PI4KB inhibition, albeit with a delay. CVB3 3A-H57Y generated ROs in an identical manner to wt CVB3 in the absence of the PI4KB inhibitor. Strikingly, under PI4KB inhibition, ROs were not observed during the peak hours of vRNA synthesis. Instead, vRNA synthesis was detected at the Golgi apparatus. Utilising a replication-independent expression system, we ascertained that the impairment in RO formation was a consequence of PI4KB inhibition, and not merely the result of delayed replication. Together, these findings demonstrate that PI4KB activity drives rapid RO formation. In the absence of ROs, seemingly intact Golgi membranes are sufficient to facilitate vRNA replication of the mutant virus. Thus, the Golgi apparatus might also support initial genome replication during wt

virus infection, prior to RO formation. The detection of CVB3 vRNA at the Golgi apparatus by fluorescence in situ hybridisation early in infection [8], while not directly proving RNA synthesis, would support this possibility. Yet, the Golgi apparatus is rapidly disassembled to form ROs during uninhibited wt CVB3 infections [8, 22], while during 3A-H57Y mutant infections under PI4KB inhibition this phase of replication at the Golgi apparatus was markedly prolonged, encompassing the exponential phase of genome replication. This illustrates a remarkable flexibility in the use of membranes as a platform for genome replication, and contributes to the idea that +RNA virus-induced membrane modification may be an adaptable process. Previous studies have reported that for some +RNA viruses, like tombusviruses and nodaviruses, replication can even be shifted to a different cellular organelle (reviewed in [37]). It is unknown whether these adoptive membranes are still remodelled to form ROs in all cases. Our findings also align with studies that show a relationship between RO formation and PI4P for viruses that depend on the activity of PI4KA (phosphatidylinositol 4-kinase type III α). When PI4KA is depleted or inhibited, HCV and EMCV were found to exhibit atypical RO development, evident as clustering of ROs [38, 39] or altered RO morphology [40], pointing to a central role for PI4P-producing kinases in RO biogenesis for these viruses as well.

PI4KB inhibition did not ultimately prevent the development of enterovirus ROs, which were readily detected at late stages of CVB3 3A-H57Y infection. Immunofluorescence microscopy revealed that these late stages of infection were not associated with an accumulation of PI4P. Thus, despite the role of active PI4KB in facilitating rapid RO biogenesis in uninhibited infections, PI4P is not a strict requirement for their formation. What then is the role of PI4P in RO biogenesis? One possibility is that PI4P serves to recruit cholesterol, a lipid that significantly affects membrane structure and function. Cholesterol has been shown to accumulate at ROs [16-18, 27] and may be involved in their formation. Recent evidence suggests that during wt enterovirus infection cholesterol is trafficked to ROs via two PI4KB-dependent mechanisms. One of these is the PI4P-dependent exchange of cholesterol via OSBP [17, 41]. The second relies on the physical interaction between PI4KB and Rab11 on recycling endosomes, which can divert endosomal cholesterol to ROs [27, 42]. PI4KB inhibitors limit PI4P accumulation and will thus limit OSBP-mediated cholesterol transfer. However, enzymatically inactive PI4KB may retain its ability to interact with Rab11 [43] and CVB3 3A-H57Y could in this way recruit sufficient cholesterol for (delayed) RO formation under PI4KB inhibition.

How can the acquisition of a single point mutation in the 3A protein allow enteroviruses to overcome their dependence on a critical host factor like PI4KB? Recent studies have indicated that the lipid composition of membranes is an important determinant for efficient proteolytic processing of the PV polyprotein, and that PI4KB inhibition can perturb cleavage at specific junctions [27-29]. For wt CVB3 cDNA we observed that 3AB accumulated and 3A levels were reduced under PI4KB inhibition, while levels of other viral proteins were unaffected. This suggests that PI4P facilitates processing specifically at the 3A-3B junction. Importantly, the 3A-H57Y substitution rendered polyprotein processing independent of high levels of PI4P lipids, as normal levels of precursor and products were detected under PI4KB inhibition. Restoring polyprotein processing efficiency may be a general resistance mechanism of enteroviruses to overcome PI4KB inhibition. The PV 3A-A70T substitution, which confers resistance to PI4KB inhibitors, in PV also restored a cleavage defect at the 3A-3B junction in the presence of PI4KB inhibitors [29]. Notably, the H57Y substitution in CVB3 3A and A70T in PV 3A are respectively close to or present in the C-terminal hydrophobic domain. Possibly, these substitutions near or in the membrane anchor of 3A impose an altered conformation to 3AB that increases the accessibility of the 3AB cleavage site in the absence of high PI4P levels.

Why is the replication efficiency of CVB3 3A-H57Y lower under PI4KB inhibition? It may be that impaired RO biogenesis in the absence of PI4KB activity directly limits replication, if enterovirus ROs enhance viral replication by expanding the membrane surface available for vRNA synthesis. The formation of ROs might also contribute to host immune response evasion, leading to a higher replication efficiency. The disassembly of the secretory pathway, which occurs in conjunction with RO formation, has been suggested to limit cytokine secretion and downregulate MHC-I surface expression [44, 45], thereby curtailing activation of the adaptive immune system. ROs may serve as a barrier to activation of the innate immune system by physically segregating viral products and cellular sensors, such as RIG-I, MDA5, and PKR. This strategy is employed by HCV, which limits access of RIG-I and MDA5 to their ROs by diverting components of the nuclear transport machinery [46]. Some +RNA viruses, such as DENV [47] or Zika virus [48], induce negative membrane curvature to form invaginations in the boundary membranes of organelles, in which genome replication takes place. These invagination-type compartments have small pores towards the cytoplasm for selective import/export of material, which is proposed to restrict access of cellular RNA sensors. Enteroviruses, however, induce positive membrane curvature to generate ROs that protrude into the cytosol. Given that genome replication takes place on the cytosolic surface of membranes, enterovirus vRNA products may be more exposed and thus more vulnerable to cellular sensors. Early work with PV showed that “rosettes of virus-induced vesicles” isolated from infected cells provided protection against RNase-treatment *in vitro* [49], but whether ROs in infected cells also protect vRNA from RNase treatment is unknown. In our study, we found no signs of premature sensing of viral dsRNA by PKR under PI4KB inhibition, a condition where RO formation was found to be delayed and replication occurred at a seemingly intact Golgi apparatus. Consistently, the delay in CVB3 3A-H57Y replication under PI4KB inhibition was not alleviated in PKR^{-/-} cells. Furthermore, replication of CVB3 3A-H57Y was not enhanced in MAVS^{-/-} cells, which are defective in signalling induced by MDA5 and RIG-I, nor in AGO2^{-/-} cells in which the Dicer-dependent RNAi pathway is rendered non-functional. Together, these findings challenge the idea that enterovirus ROs have a critical function in shielding viral dsRNA from cellular RNA sensors. Enteroviruses have acquired other mechanisms to suppress innate immune responses, that rely on the cleavage of essential signalling pathway components - such as MDA5, MAVS, and the integral stress response protein G3BP1 - by their proteinases (reviewed in [50]). Yet, the possibility remains that ROs serve as a redundant protective measure against innate immune sensors, perhaps with a more prominent role in other cell types than those used here.

The pervasiveness of virus-induced membrane modifications across the Picornaviridae and other viral families suggests that they provide an inherent benefit to +RNA virus replication, perhaps by facilitating efficient vRNA synthesis or by co-ordinating different events in the viral life cycle. Through further investigations using drug-resistant viruses, replication-independent viral systems or other novel approaches, the intrinsic benefits of these morphologically diverse replication compartments will be unveiled.

EXPERIMENTAL PROCEDURES

Replication-independent system. HuH-7/T7 cells were seeded in 24-well plates containing glass coverslips. The next day, the cells were lipofectamine transfected with CVB3 cDNA rendered replication-deficient through modifications to the cloverleaf structure in the 5' untranslated region (UTR) of the viral genome [25]. One hour later, the medium was replaced with fresh medium. At indicated hours post-transfection, cells were washed and either fixed for immunofluorescence or lysed for Western Blot analysis.

Live cell imaging. BGM(GFPS1-10) cells were grown in glass-bottom 4-chamber 35-mm dishes (CELLview™) to ~35% confluency and transduced with MLV mCherry-GM130 particles described before (see [22]). Infection with CVB3 3A-H57Y(S11) was carried out 18-24 hours later. Prior to imaging cells were washed with Fluorobrite medium (Thermo Fisher Scientific) supplemented with 8% fetal calf serum (FCS) and 25 mM HEPES. Cells were maintained in a live-cell imaging chamber at 37°C and 5% CO₂. Imaging was carried out from ~2.5 (hpi) using a Leica SP5 confocal microscope. Positions of interest (xyz) were marked and imaged sequentially at 5 minute intervals.

High-pressure freezing and freeze substitution. BGM cells were grown on sapphire discs and infected with CVB3 or CVB3 3A-H57Y and refreshed at 1 hpi with medium supplemented with 25 mM HEPES buffer with or without 1 μM BF738735. Cells were high-pressure frozen using a Leica EM PACT2 at different time points post infection. The instruments and procedures used for freeze-substitution, epoxy resin infiltration and polymerisation were identical to those described in [5]. Sections of 70 nm were then prepared for electron microscopy and post-stained with uranyl acetate and lead citrate.

Correlative light and electron microscopy (CLEM) preparation. BGM (GFPS1-10) cells were cultured in gridded 8-well chamber μ-slides (Ibidi) ahead of infection with CVB3 3A-H57Y(S11). Just prior to imaging cells were treated with 100 nM Mitotracker® Deep Red FM for 30 minutes. Live-cell imaging was carried out to monitor the levels of 3A-H57Y-GFP. High resolution (1024x1024) z-stacks were collected of cells of interest just prior to fixation. To aid in the relocation of these cells for CLEM, tile scan overviews were taken and the positions of cells relative to nearby grid co-ordinates were recorded. Following imaging by live-cell light microscopy (LM), cells were prepared for electron microscopy as described previously (see [22]). EM images were collected of cells previously identified by LM. The EM and LM data for each cell were overlaid using the Mitotracker® Deep Red FM signal (LM images) and corresponding mitochondria (EM images) as a guide for image transformation.

Metabolic labelling and autoradiography. A subconfluent layer of BGM cells was grown in 35 mm dishes (Corning) and infected with CVB3 or CVB3 3A-H57Y at MOI 5. Cells were incubated with dactinomycin for 1 hour prior to a 45-minute labelling with tritiated uridine ([5-³H], 1 mCi/ml) (Perkin Elmer). Cells were processed for EM as described in [22]. Sections of 50 nm were collected and post stained with lead citrate and uranyl acetate, then prepared for autoradiography (as described in [51]).

Electron microscopy. Images were collected on an FEI Tecnai12 BioTWIN or TWIN electron microscope at 120 kV using an Eagle 4k slow-scan CCD camera (FEI) or OneView 4k high frame-rate camera (Gatan) respectively. For the collection of larger EM datasets, meshes of overlapping areas across the grid were taken that were later stitched into a single composite image (as described in [52]).

AUTHOR CONTRIBUTIONS

Conceptualization: CEM, HMvdS, MB, FJMvK; Investigation: CEM, HMvdS, HRL, RWALL, QF, MW, GJO, MB; Writing: CEM, HMS, MB, FJMvK; Reviewing and editing of the manuscript: CEM, HMS, RPvR, AJK, EJS, MB, FJMvK; Visualization: CEM, HMS; Supervision: HMS, EJS, AJK, RPvR, MB, FJMvK; Funding Acquisition: HMvdS, EJS, RPvR, AJK, MB, FJMvK.

ACKNOWLEDGMENTS

The authors would like to thank Huib Rabouw for excellent assistance with flow cytometry, and the LUMC light microscopy facility. This work was supported by grants from the Netherlands Organisation for Scientific Research (NWO-VENI-863.12.005 to HMvdS, NWO-VICI-91812628 to FJMvK, ERASysApp project ‘SysVirDrug’ ALW project 832.14.003 to FJMvK, NWO-MEERVOUD 863.10.003 to MB, NWO-CW TOP 700.57.301 to EJS), and the European Union (7th Framework: EUVIRNA Marie Curie Initial Training Network grant agreement 264286 to FJMvK.; European Research Council Consolidator Grant CoG 615680 to RPvR, Horizon 2020: Marie Skłodowska-Curie ETN ‘ANTIVIRALS’ grant agreement 642434 to FJMvK). The funders had no role in study design, data collection and interpretation, or the decision to submit the work for publication.

REFERENCES

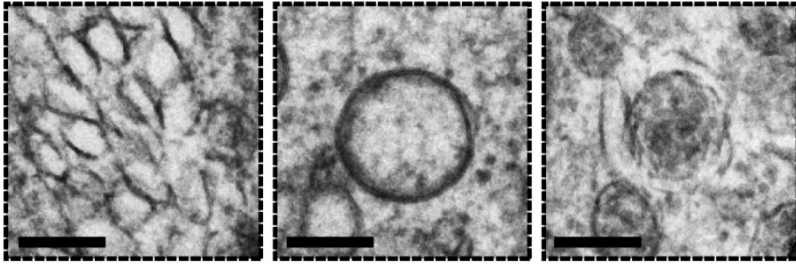
1. Romero-Brey I, Bartschlagler R. 2014. Membranous Replication Factories Induced by Plus-Strand RNA Viruses. *Viruses-Basel* 6:2826-2857.
2. Paul D, Bartschlagler R. 2013. Architecture and biogenesis of plus-strand RNA virus replication factories. *World J Virol* 2:32-48.
3. Schulz KS, Mossman KL. 2016. Viral Evasion Strategies in Type I IFN Signaling - A Summary of Recent Developments. *Front Immunol* 7:498.
4. White JP, Lloyd RE. 2012. Regulation of stress granules in virus systems. *Trends in Microbiology* 20:175-183.
5. Limpens RWAL, van der Schaar HM, Kumar D, Koster AJ, Snijder EJ, van Kuppeveld FJM, Barcena M. 2011. The Transformation of Enterovirus Replication Structures: a Three-Dimensional Study of Single- and Double-Membrane Compartments. *mBio* 2.
6. Belov GA, Nair V, Hansen BT, Hoyt FH, Fischer ER, Ehrenfeld E. 2012. Complex Dynamic Development of Poliovirus Membranous Replication Complexes. *Journal of Virology* 86:302-312.
7. Suhay DA, Giddings TH, Jr., Kirkegaard K. 2000. Remodeling the endoplasmic reticulum by poliovirus infection and by individual viral proteins: an autophagy-like origin for virus-induced vesicles. *J Virol* 74:8953-65.
8. Hsu NY, Ilnytska O, Belov G, Santiana M, Chen YH, Takvorian PM, Pau C, van der Schaar H, Kaushik-Basu N, Balla T, Cameron CE, Ehrenfeld E, van Kuppeveld FJM, Altan-Bonnet N. 2010. Viral Reorganization of the Secretory Pathway Generates Distinct Organelles for RNA Replication. *Cell* 141:799-811.
9. van der Schaar HM, Leyssen P, Thibaut HJ, de Palma A, van der Linden L, Lanke KH, Lacroix C, Verbeke E, Conrath K, Macleod AM, Mitchell DR, Palmer NJ, van de Poel H, Andrews M, Neyts J, van Kuppeveld FJ. 2013. A novel, broad-spectrum inhibitor of enterovirus replication that targets host cell factor phosphatidylinositol 4-kinase IIIbeta. *Antimicrob Agents Chemother* 57:4971-81.
10. Greninger AL, Knudsen GM, Betegon M, Burlingame AL, Derisi JL. 2012. The 3A protein from multiple picornaviruses utilizes the golgi adaptor protein ACBD3 to recruit PI4KIIIbeta. *J Virol* 86:3605-16.
11. Altan-Bonnet N, Balla T. 2012. Phosphatidylinositol 4-kinases: hostages harnessed to build panviral replication platforms. *Trends Biochem Sci* 37:293-302.
12. Dorobantu CM, Albuлесcu L, Harak C, Feng Q, van Kampen M, Strating JRPM, Gorbalenya AE, Lohmann V, van der Schaar HM, van Kuppeveld FJM. 2015. Modulation of the Host Lipid Landscape to Promote RNA Virus Replication: The Picornavirus Encephalomyocarditis Virus Converges on the Pathway Used by Hepatitis C Virus. *Plos Pathogens* 11.
13. Clayton EL, Minogue S, Waugh MG. 2013. Mammalian phosphatidylinositol 4-kinases as modulators of membrane trafficking and lipid signaling networks. *Progress in Lipid Research* 52:294-304.
14. De Matteis MA, Wilson C, D'Angelo G. 2013. Phosphatidylinositol-4-phosphate: the Golgi and beyond. *Bioessays* 35:612-22.
15. Mesmin B, Bigay J, Moser von Filseck J, Lacas-Gervais S, Drin G, Antonny B. 2013. A four-step cycle driven by PI(4)P hydrolysis directs sterol/PI(4)P exchange by the ER-Golgi tether OSBP. *Cell* 155:830-43.
16. Arita M. 2014. Phosphatidylinositol-4 kinase III beta and oxysterol-binding protein accumulate unesterified cholesterol on poliovirus-induced membrane structure. *Microbiology and Immunology* 58:239-256.
17. Strating JRPM, van der Linden L, Albuлесcu L, Bigay J, Arita M, Delang L, Leyssen P, van der Schaar HM, Lanke KH, Thibaut HJ, Ulferts R, Drin G, Schlinck N, Wubbolts RW, Sever N, Head SA, Liu JO, Beachy PA, De Matteis MA, Shair MD, Olkkonen VM, Neyts J, van Kuppeveld FJM. 2015. Itraconazole Inhibits Enterovirus Replication by Targeting the Oxysterol-Binding Protein. *Cell Reports* 10:600-615.
18. Roulin PS, Lotzerich M, Torta F, Tanner LB, van Kuppeveld FJ, Wenk MR, Greber UF. 2014. Rhinovirus uses a phosphatidylinositol 4-phosphate/cholesterol counter-current for the formation of replication compartments at the ER-Golgi interface. *Cell Host Microbe* 16:677-90.
19. van der Schaar HM, van der Linden L, Lanke KH, Strating JR, Purstinger G, de Vries E, de Haan CA, Neyts J, van Kuppeveld FJ. 2012. Coxsackievirus mutants that can bypass host factor PI4KIIIbeta and the need for high levels of PI4P lipids for replication. *Cell Res* 22:1576-92.
20. MacLeod AM, Mitchell DR, Palmer NJ, Van de Poel H, Conrath K, Andrews M, Leyssen P, Neyts J. 2013. Identification of a series of compounds with potent antiviral activity for the treatment of enterovirus infections. *ACS Med Chem Lett* 4:585-9.
21. Cabantous S, Terwilliger TC, Waldo GS. 2005. Protein tagging and detection with engineered self-assembling fragments of green fluorescent protein. *Nature Biotechnology* 23:102-107.
22. van der Schaar HM, Melia CE, van Bruggen JA, Strating JR, van Geenen ME, Koster AJ, Barcena M, van Kuppeveld FJ. 2016. Illuminating the Sites of Enterovirus Replication in Living Cells by Using a Split-GFP-Tagged Viral Protein. *mSphere* 1.

23. Dales S, Eggers HJ, Tamm I, Palade GE. 1965. Electron Microscopic Study of the Formation of Poliovirus. *Virology* 26:379-89.
24. Belov GA, Feng Q, Nikovics K, Jackson CL, Ehrenfeld E. 2008. A Critical Role of a Cellular Membrane Traffic Protein in Poliovirus RNA Replication. *Plos Pathogens* 4.
25. Langereis MA, Feng Q, Nelissen FH, Virgen-Slane R, van der Heden van Noort GJ, Maciejewski S, Filippov DV, Semler BL, van Delft FL, van Kuppeveld FJ. 2014. Modification of picornavirus genomic RNA using 'click' chemistry shows that unlinking of the VPg peptide is dispensable for translation and replication of the incoming viral RNA. *Nucleic Acids Res* 42:2473-82.
26. Molla A, Hellen CU, Wimmer E. 1993. Inhibition of proteolytic activity of poliovirus and rhinovirus 2A proteinases by elastase-specific inhibitors. *J Virol* 67:4688-95.
27. Ilnytska O, Santiana M, Hsu NY, Du WL, Chen YH, Viktorova EG, Belov G, Brinker A, Storch J, Moore C, Dixon JL, Altan-Bonnet N. 2013. Enteroviruses harness the cellular endocytic machinery to remodel the host cell cholesterol landscape for effective viral replication. *Cell Host Microbe* 14:281-93.
28. Ford Siltz LA, Viktorova EG, Zhang B, Kouliavskaja D, Dragunsky E, Chumakov K, Isaacs L, Belov GA. 2014. New small-molecule inhibitors effectively blocking picornavirus replication. *J Virol* 88:11091-107.
29. Arita M. 2016. Mechanism of Poliovirus Resistance to Host Phosphatidylinositol-4 Kinase III beta Inhibitor. *Acs Infectious Diseases* 2:140-148.
30. Feng Q, Langereis MA, Lork M, Nguyen M, Hato SV, Lanke K, Emdad L, Bhoopathi P, Fisher PB, Lloyd RE, van Kuppeveld FJ. 2014. Enterovirus 2Apro targets MDA5 and MAVS in infected cells. *J Virol* 88:3369-78.
31. Mukherjee A, Morosky SA, Delorme-Axford E, Dybdahl-Sissoko N, Oberste MS, Wang T, Coyne CB. 2011. The coxsackievirus B 3C protease cleaves MAVS and TRIF to attenuate host type I interferon and apoptotic signaling. *PLoS Pathog* 7:e1001311.
32. Luna JM, Wu X, Rice CM. 2016. Present and not reporting for duty: dsRNAi in mammalian cells. *EMBO J* 35:2499-2501.
33. tenOever BR. 2016. The Evolution of Antiviral Defense Systems. *Cell Host Microbe* 19:142-9.
34. Li Y, Basavappa M, Lu J, Dong S, Cronkite DA, Prior JT, Reinecker HC, Hertzog P, Han Y, Li WX, Cheloufi S, Karginov FV, Ding SW, Jeffrey KL. 2016. Induction and suppression of antiviral RNA interference by influenza A virus in mammalian cells. *Nat Microbiol* 2:16250.
35. van der Schaar HM, Dorobantu CM, Albuлесcu L, Strating JR, van Kuppeveld FJ. 2016. Fat(al) attraction: Picornaviruses Usurp Lipid Transfer at Membrane Contact Sites to Create Replication Organelles. *Trends Microbiol* 24:535-46.
36. Strating JR, van Kuppeveld FJ. 2017. Viral rewiring of cellular lipid metabolism to create membranous replication compartments. *Curr Opin Cell Biol* 47:24-33.
37. Xu K, Nagy PD. 2014. Expanding use of multi-origin subcellular membranes by positive-strand RNA viruses during replication. *Curr Opin Virol* 9:119-26.
38. Reghellin V, Donnici L, Fenu S, Berno V, Calabrese V, Pagani M, Abrignani S, Peri F, De Francesco R, Neddermann P. 2014. NSSA Inhibitors Impair NSSA-Phosphatidylinositol 4-Kinase III alpha Complex Formation and Cause a Decrease of Phosphatidylinositol 4-Phosphate and Cholesterol Levels in Hepatitis C Virus-Associated Membranes. *Antimicrobial Agents and Chemotherapy* 58:7128-7140.
39. Dorobantu CM, Albuлесcu L, Lyoo H, van Kampen M, De Francesco R, Lohmann V, Harak C, van der Schaar HM, Strating JR, Gorbalenya AE, van Kuppeveld FJ. 2016. Mutations in Encephalomyocarditis Virus 3A Protein Uncouple the Dependency of Genome Replication on Host Factors Phosphatidylinositol 4-Kinase IIIalpha and Oxysterol-Binding Protein. *mSphere* 1.
40. Reiss S, Rebhan I, Backes P, Romero-Brey I, Erfle H, Matula P, Kaderali L, Poenisch M, Blankenburg H, Hiet MS, Longerich T, Diehl S, Ramirez F, Balla T, Rohr K, Kaul A, Buhler S, Pepperkok R, Lengauer T, Albrecht M, Eils R, Schirmacher P, Lohmann V, Bartenschlager R. 2011. Recruitment and Activation of a Lipid Kinase by Hepatitis C Virus NSSA Is Essential for Integrity of the Membranous Replication Compartment. *Cell Host & Microbe* 9:32-45.
41. Albuлесcu L, Wubbolts R, van Kuppeveld FJ, Strating JR. 2015. Cholesterol shuttling is important for RNA replication of coxsackievirus B3 and encephalomyocarditis virus. *Cell Microbiol* 17:1144-56.
42. Burke JE, Inglis AJ, Perisic O, Masson GR, McLaughlin SH, Rutaganira F, Shokat KM, Williams RL. 2014. Structures of PI4KIIIbeta complexes show simultaneous recruitment of Rab11 and its effectors. *Science* 344:1035-8.
43. de Graaf P, Zwart WT, van Dijken RA, Deneka M, Schulz TK, Geijsen N, Coffey PJ, Gadella BM, Verkleij AJ, van der Sluijs P, van Bergen en Henegouwen PM. 2004. Phosphatidylinositol 4-kinasebeta is critical for functional association of rab11 with the Golgi complex. *Mol Biol Cell* 15:2038-47.

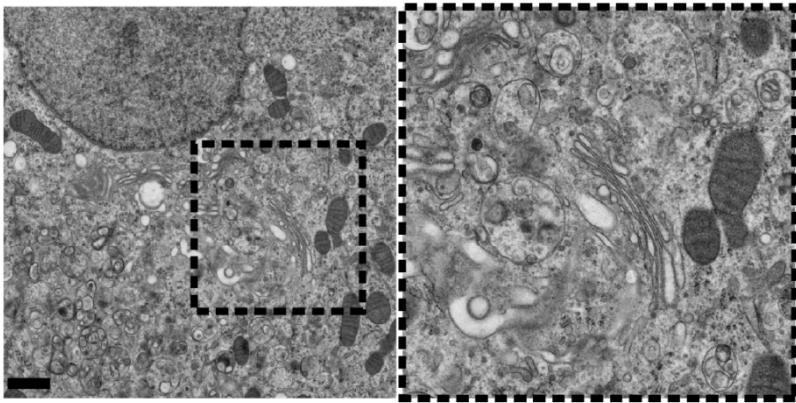
44. Dodd DA, Giddings TH, Jr., Kirkegaard K. 2001. Poliovirus 3A protein limits interleukin-6 (IL-6), IL-8, and beta interferon secretion during viral infection. *J Virol* 75:8158-65.
45. Cornell CT, Kiosses WB, Harkins S, Whitton JL. 2007. Coxsackievirus B3 proteins directionally complement each other to downregulate surface major histocompatibility complex class I. *J Virol* 81:6785-97.
46. Neufeldt CJ, Joyce MA, Van Buuren N, Levin A, Kirkegaard K, Gale M, Jr., Tyrrell DL, Wozniak RW. 2016. The Hepatitis C Virus-Induced Membranous Web and Associated Nuclear Transport Machinery Limit Access of Pattern Recognition Receptors to Viral Replication Sites. *PLoS Pathog* 12:e1005428.
47. Welsch S, Miller S, Romero-Brey I, Merz A, Bleck CK, Walther P, Fuller SD, Antony C, Krijnse-Locker J, Bartenschlager R. 2009. Composition and three-dimensional architecture of the dengue virus replication and assembly sites. *Cell Host Microbe* 5:365-75.
48. Cortese M, Goellner S, Acosta EG, Neufeldt CJ, Oleksiuk O, Lampe M, Haselmann U, Funaya C, Schieber N, Ronchi P, Schorb M, Pruunsild P, Schwab Y, Chatel-Chaix L, Ruggieri A, Bartenschlager R. 2017. Ultrastructural Characterization of Zika Virus Replication Factories. *Cell Rep* 18:2113-2123.
49. Bienz K, Egger D, Pfister T, Troxler M. 1992. Structural and functional characterization of the poliovirus replication complex. *J Virol* 66:2740-7.
50. Lei X, Xiao X, Wang J. 2016. Innate Immunity Evasion by Enteroviruses: Insights into Virus-Host Interaction. *Viruses* 8.
51. Ginsel LA, Onderwater JJ, Daems WT. 1979. Resolution of a gold latensification-elon ascorbic acid developer for Ilford L4 emulsion. *Histochemistry* 61:343-6.
52. Faas FG, Avramut MC, van den Berg BM, Mommaas AM, Koster AJ, Ravelli RB. 2012. Virtual nanoscopy: generation of ultra-large high resolution electron microscopy maps. *J Cell Biol* 198:457-69.

SUPPLEMENTAL FIGURES

A



B



C

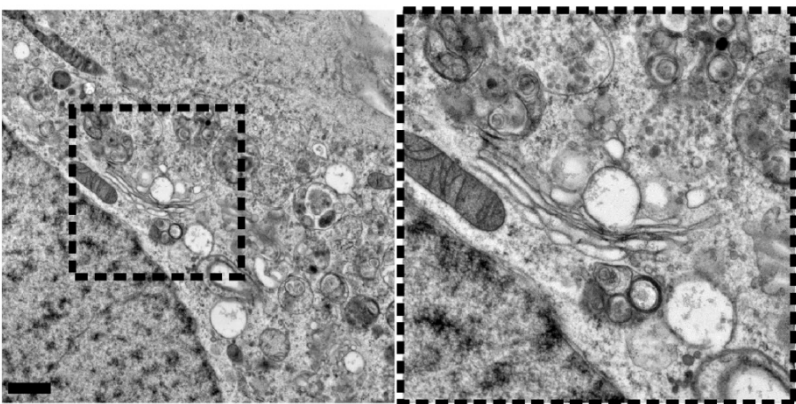


Figure S1. Related to Fig. 1. The morphologies of WT CVB3 and CVB3 3A-H57Y ROs in BGM cells are indistinguishable. BF738735 treatment does not affect Golgi apparatus architecture. (A) BGM cells infected with WT CVB3 and prepared for EM by HPF-FS reveal typical enterovirus ROs, including single-membrane tubules, DMVs and multilamellar vesicles (left to right). (B, C). BGM cells either untreated (B) or treated with BF738735 for 7 hours (C) were fixed for EM analysis. Representative images are shown illustrating that the morphology of the Golgi apparatus was unaffected by treatment. Scale bars, 200 nm (A) or 1 μ m (B, C).

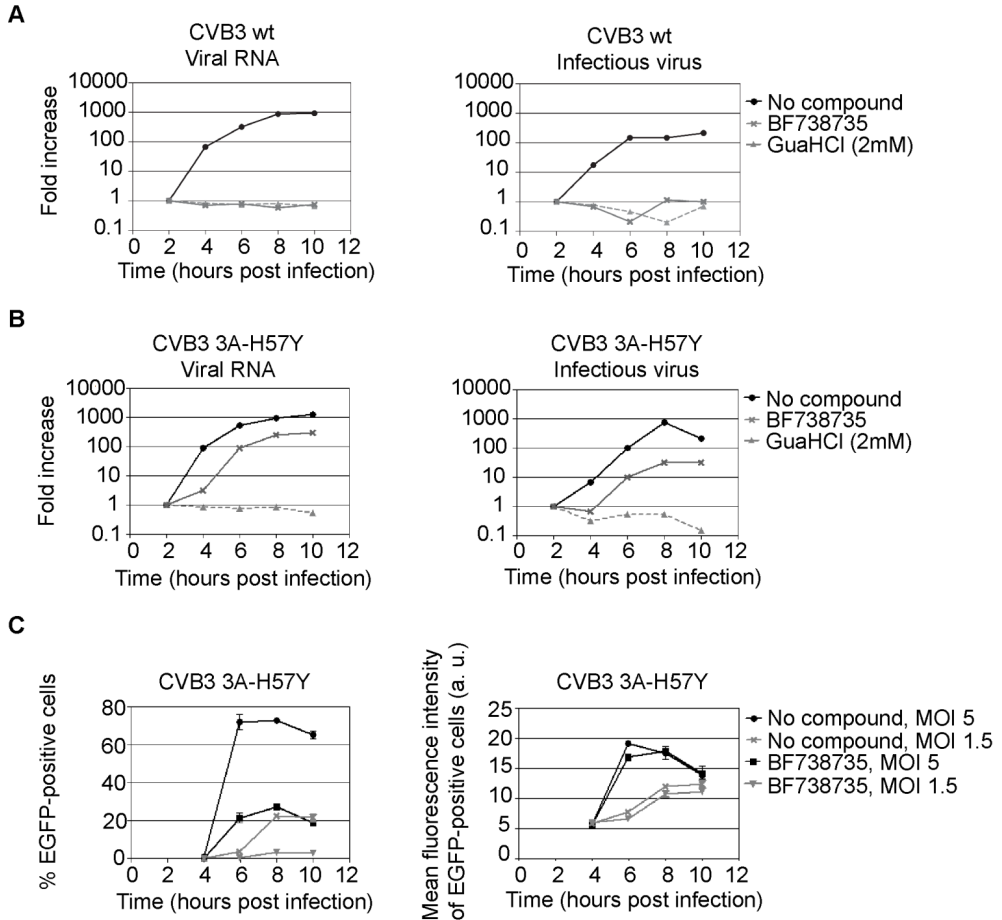


Figure S2. Related to Fig. 1. Replication kinetics of CVB3 3A-H57Y differ in the presence or absence of PI4KB inhibitor. (A, B) Growth curve analysis. BGM cells were infected with CVB3 WT (A) or CVB3 3A-H57Y (B) and treated with compounds where specified. At the indicated time points, cells were either lysed to determine the intracellular level of viral RNA with quantitative RT-PCR (left graphs), or frozen to titrate the total amount of infectious virus produced (right graphs). Results are expressed as fold increase relative to the quantities at 2 hpi. (C) Flow cytometry analysis. BGM cells were infected with EGFP-CVB3 3A-H57Y at different MOIs in the presence or absence of BF738735. At the indicated time points, cells were collected and fixed for flow cytometry analysis to determine the percentage of EGFP-positive cells (left graph) and the mean fluorescence intensity of the EGFP-positive cells (right graph) as an indicator of the level of viral proteins produced. Values represent mean values of triplicates \pm standard error of the means.

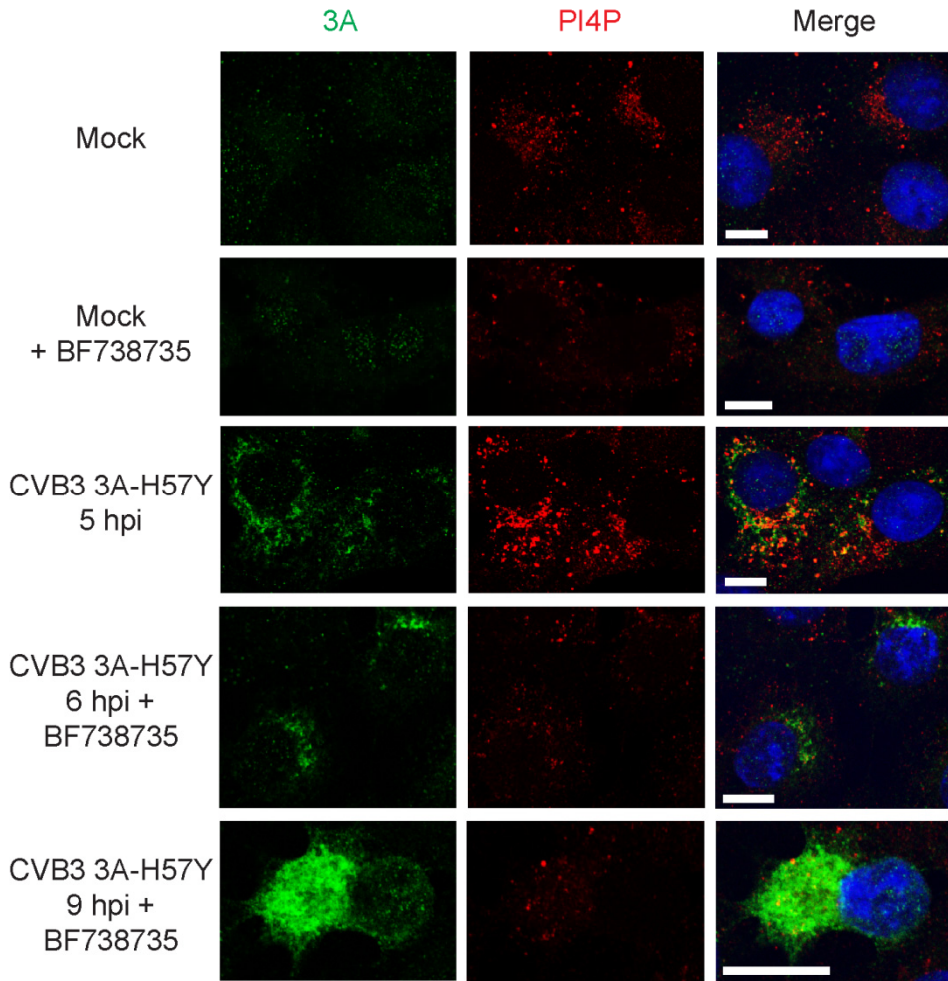


Figure S3. Related to Fig. 4. PI4P accumulation is not detected in cells infected with CVB3 3A-H57Y in the presence of PI4KB inhibitor. BGM cells were infected with CVB3 3A-H57Y at MOI 10 and treated with BF738735 where indicated. At the specified time points, cells were fixed and labelled with antibodies against 3A (green) or PI4P (red) alongside a nuclear stain (blue). Confocal images were acquired with a Leica Spell confocal microscope. Without inhibitor, the level of PI4P signal was considerably elevated (saturated relative to background) in infected cells. In the presence of inhibitor no increase in PI4P was detected in infected cells, even at late time points (9 hpi). Scale bars, 10 μ m.

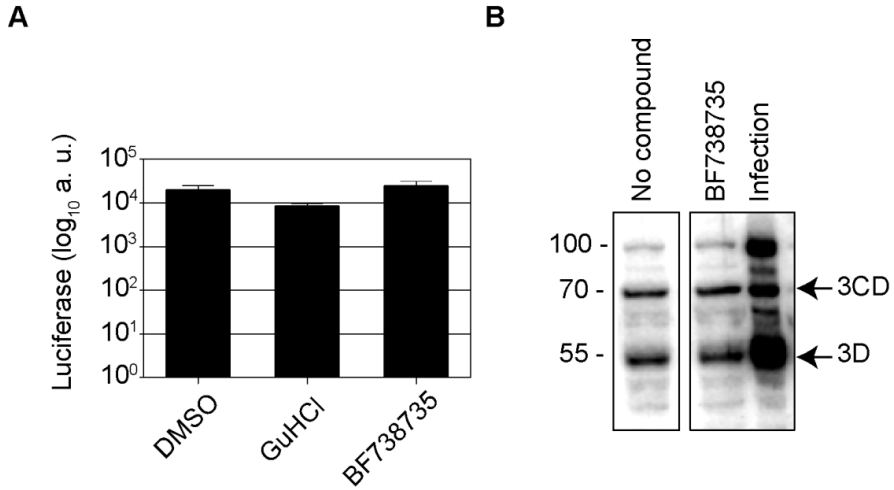


Figure S4. Related to Fig. 5. Viral protein production by the replication-independent expression system is not affected by PI4KB inhibition. HuH-7/T7 cells were mock-transfected or transfected with CVB3 3A-H57Y cDNA, which is under the control of a T7 promoter sequence and rendered replication-incompetent by altering the 5'UTR of the genome. cDNA used in **(A)** additionally encoded *Renilla* luciferase upstream of the P1 region as a sensitive measure for viral protein production. Cells were treated with BF738735 where indicated. **A**) At 6 h post transfection, cells were lysed to determine the intracellular luciferase amount. Guanidine Hydrochloride (GuHCl) (2 mM) was used as a positive control for protein production independent of viral RNA synthesis. Values represent mean values of triplicates \pm standard error of the means. **B**) At 7 h post-transfection, cells were lysed and subjected to Western Blot analysis using an antibody against 3D. A lysate of CVB3-infected cells was used as a positive control. Marker bands of the indicated size (in kDa) are indicated.

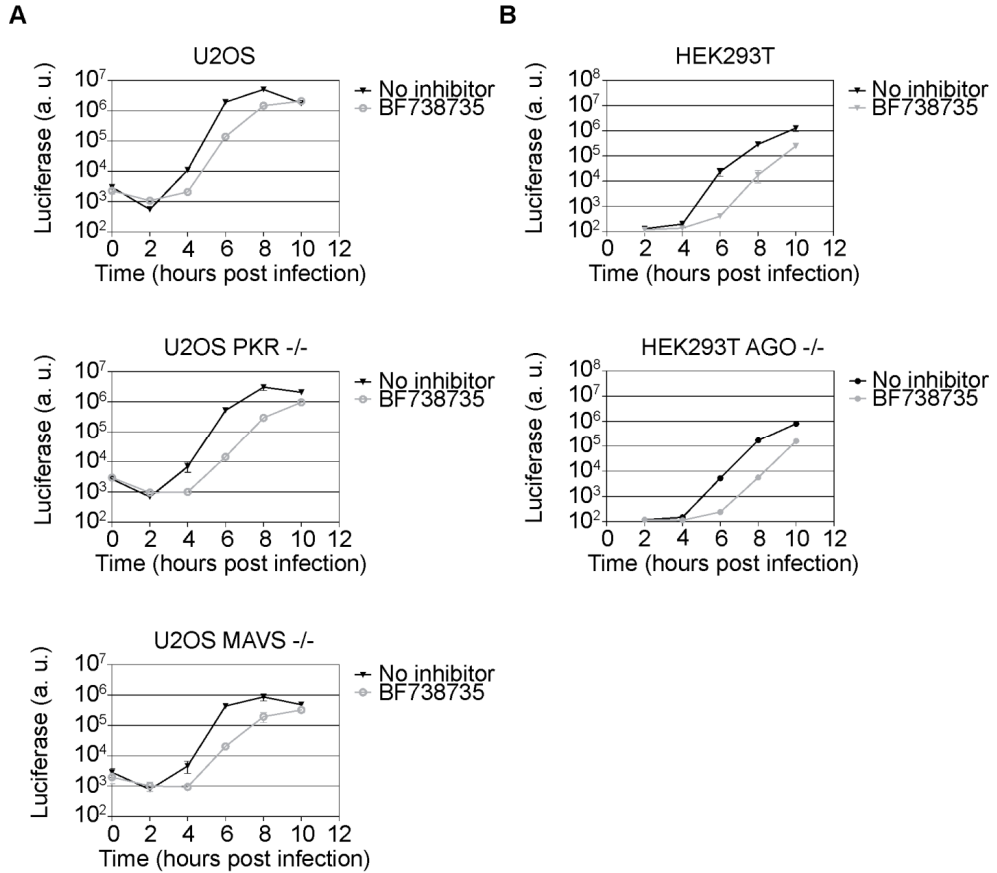
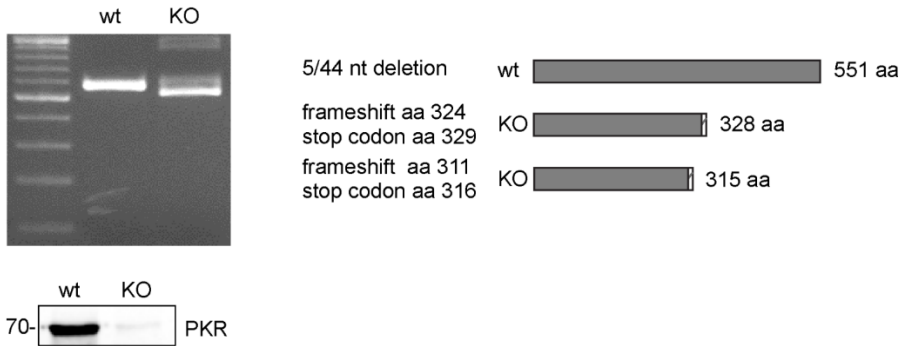
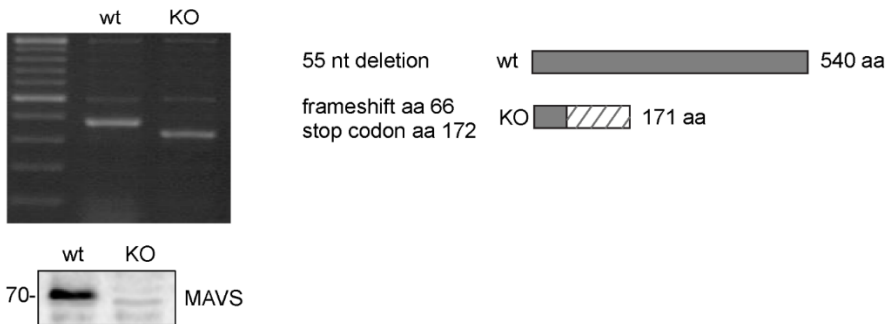


Figure S5. Related to Fig. 6. Innate antiviral responses during CVB3 3A-H57Y infection. U2OS or HEK293T cells (KO for PKR, MAVS and AGO where indicated) were infected with CVB3-Rluc 3A-H57Y at MOI 0.01. Following infection, the inoculum was removed and fresh medium with or without BF738735 inhibitor was added to the cells. Cells were lysed to determine the intracellular amounts of luciferase as a measure of genome replication. Values represent mean values of triplicates \pm standard error of the means.

U2OS PKR^{-/-} cells



HeLa MAVS^{-/-} cells



U2OS MAVS^{-/-} cells

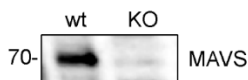


Figure S6. Related to Figs. 6 and S5. Generation of MAVS^{-/-} and PKR^{-/-} cells using the CRISPR-Cas9 system. Single-cell clones of HeLa or U2OS cells were characterized by isolation of genomic DNA and PCR with gene-specific primers for PKR or MAVS, followed by sequence analysis (upper panels). All alleles contain a deletion resulting in a frame-shift event and a premature stop codon. The knock-out was confirmed by Western blot analysis of cell lysates (lower panels; marker bands of the indicated size in kDa are indicated on the left). U2OS MAVS^{-/-} cells were only analysed by Western blot.

SUPPLEMENTAL EXPERIMENTAL PROCEDURES

Cells. BGM, BGM(GFPS1-10) stably expressing GFP(S1-10) (described in [1]), HeLa R19, HEK293T, U2OS, and HuH-7-Lunet T7-BLR (HuH-7/T7) cells, and a cell pool stably expressing T7 RNA polymerase and blasticidin S-deaminase generously provided by R. Bartenschlager (University of Heidelberg, Heidelberg, Germany) ([2]), were maintained in Dulbecco's modified Eagle's medium (Gibco) supplemented with 10% fetal calf serum, penicillin, and streptomycin, and grown at 37°C in 5% CO₂. The culture medium for HuH-7/T7 cells contained 10 µg/ml blasticidine, while that of BGM(GFPS1-10) cells contained 30 µg/ml puromycin.

Knock-out cells. HeLa PKR^{-/-} cells have been described before (see [3]). U2OS PKR^{-/-} were generated using the pCRISPR-hCas9-2xgRNA-Puro plasmid ([4]) with the same gRNAs as used for the HeLa PKR^{-/-} cells, which target the kinase domain of PKR. To target human Ago2, gRNA encoding oligonucleotides cassettes (gRNA1: 5'-ACCGACCGCTCTGCAATGTGACC-3' and 5'-AACGGTCACATTGCAGACGCGGTC-3', gRNA2: 5'-

ACCGCCCATGTTTACAAGTCGGAC-3' and 5'-AACGTCGGACTTGTAACATGGGC-3') were cloned into the Sapl restriction sites of the pCRISPR-hCas9-2xgRNA-Puro plasmid. HEK293T Ago2^{-/-} cells were kindly provided by K.W. Mulder (Radboud University Nijmegen Medical Center, Nijmegen, The Netherlands) and have been described previously (see [5]). To generate HeLa MAVS^{-/-} and U2OS MAVS^{-/-} cells were co-transfected with two plasmids containing gRNA1 5'-GAATACCTTCAGCGCGGCC-3' and gRNA2 5'-GCTGTGAGCTAGTTGATCTCG-3'. Single-cell clones were generated using end-point dilutions. The knock-out was verified by sequence analysis of the genomic DNA and by Western Blot analysis (Fig. S7; HeLa Ago2^{-/-} will be shown elsewhere by RPvR).

Viruses. Coxsackievirus B3 (CVB3) WT was obtained by transfecting *in vitro*-transcribed RNA derived from the p53CB3/T7 plasmid, which contains the cDNA of CVB3 strain Nancy driven by a T7 RNA polymerase promoter. The 3A-H57Y substitution was introduced in the cDNA clones of CVB3, Rluc-CVB3 and EGFP-CVB3 encoding *Renilla luciferase* or *EGFP* upstream of P1 ([6]), or the split-GFP-tagged CVB3 ([1]) using standard DNA cloning techniques. Virus titers were determined by end-point titration analysis and expressed as 50% cell culture infectious dose (CCID₅₀). A Mengovirus which lost its IFN-suppressing activities due to substitutions in the Zn-finger domain of the leader protein (Mengo Zn) has been described previously (see [7]). Virus titers were determined by end-point titration analysis and expressed as 50% cell culture infectious dose (CCID₅₀).

Reagents. BF738735 (2-fluoro-4-(2-methyl-8-(3-(methylsulfonyl)benzylamino)imidazo[1,2-a]pyrazin-3-yl)phenol) ([8], [9]) was provided by Galapagos NV, used at a working concentration of 1 μM and added in all the experiments 1 hour after infection or mock-infection. Guanidine Hydrochloride (GuHCl) and GW5074 were purchased from Sigma and used at a working concentration of 30 μM and 2 mM respectively. Enviroxime has been previously described ([10]) and used at a concentration of 0.5 μg/ml (1.4 μM). PIK93 was provided by Dr K Shokat (University of California San Francisco, San Francisco, California, USA) and used at a concentration of 1 μM.

Antibodies. The rabbit antiserum and the mouse monoclonal antibody directed against the non-structural protein 3A were described previously (see [11], [12]). Rabbit antiserum against CVB3 3D was generously provided by C.E. Cameron (Pennsylvania State University, USA). Primary mouse monoclonal antibodies included anti-β-actin (Sigma Aldrich), anti-GM130 (BD Biosciences), anti-dsRNA J2 (English & Scientific Consulting), and anti-PKR (Santa-Cruz). Primary rabbit polyclonal antibodies included anti-PI4KB (Millipore), anti-TGN46 (Novus Biologicals), anti-phospho-PKR (Abcam), and anti-MAVS (Cardif, Enzo Life Sciences). Alexa Fluor 594-conjugated goat-anti-rabbit IgG and Alexa Fluor 488-conjugated goat-anti-mouse IgG (Molecular Probes) were used as secondary antibodies for immunofluorescence microscopy. For Western Blot analysis, secondary antibody detection included IRDye goat anti-mouse or goat anti-rabbit (LI-COR).

Quantitative PCR. RNA was isolated from infected cells using a Nucleospin RNA kit (Machery-Nagel). cDNA was synthesized using random hexamers as primers with a TaqMan reverse transcription reagents kit (Roche). The cDNA was used for quantitative PCR with the forward primer 5'-CGTGGGGCTACAATCAAGTT-3', the reverse primer 5'-TAACAGGAGCTTTGGGCATC-3', and the LightCycler 480 SYBR Green I master kit (Roche) for 45 cycles (5 s at 95°C, 10 s at 60°C, and 20 s at 72°C) on a LightCycler 480 (Roche). Obtained Ct values were expressed as fold increase with the value at t = 2 h set as 1.

Flow cytometry. BGM cells were seeded in 24-well plates and infected with EGFP-CVB3 3A-H57Y the next day at different MOIs. Cells were released using trypsin, washed once in phosphate buffered saline (PBS), and fixed with 1% paraformaldehyde (PFA) in PBS. Cells were analyzed on FACS Canto (BD) using BD FACS Diva software.

Western Blot analysis. Virus-infected cells were collected in lysis buffer (50 mM TrisHCl pH 7.4, 150 mM NaCl, 1 mM EDTA, 1% Nonidet P-40, 0.05% SDS) and heated for 5 min at 95°C after addition of Laemmli sample buffer. Samples were run on polyacrylamide gels and transferred to a nitrocellulose membrane (Bio-Rad), which following blocking was incubated with primary antibodies overnight at 4°C and secondary antibodies for 1 h at room temperature. Images of blots were acquired with Odyssey Imaging System (LI-COR).

Immunofluorescence microscopy. BGM cells grown on coverslips were infected with CVB3 WT or CVB3 3A-H57Y for 30-60 minutes, after which the inoculum was removed and fresh medium was added. At indicated time points post-infection, cells were fixed with paraformaldehyde and permeabilized with PBS containing 0.1% Triton X-100. Cells were then stained with primary and secondary antibodies and a nuclear stain (DAPI or Hoechst 33342). Wide-field imaging was performed using either an Olympus BX60 or Leica DM5500 fluorescent microscope, and confocal imaging was performed with a Leica Spell confocal microscope.

Replication-independent system. HuH-7/T7 cells were seeded in 24-well plates containing glass coverslips. The next day, the cells were transfected with cDNA of CVB3 rendered replication-deficient through modifications to the cloverleaf structure in the 5' untranslated region (UTR) of the viral genome ([4]) using Lipofectamine 2000 (Thermo Fisher Scientific) according to the manufacturer's protocol. One hour later, the medium was replaced with fresh

medium. At indicated hours post-transfection, cells were washed and either fixed for immunofluorescence or lysed for Western Blot analysis.

Live cell imaging. BGM(GFPS1-10) cells were grown in glass-bottom 4-chamber 35-mm dishes (CELLview™) to ~35% confluency and transduced with MLV mCherry-GM130 particles described before ([1]). Infection with CVB3 3A-H57Y(S11) was carried out 18-24 hours later. In samples to be studied under PI4KB inhibition, infections were maintained in medium containing 1 μ m BF735738 from 1 hpi and for the duration of imaging. Prior to imaging cells were washed with Fluorobrite medium (Thermo Fisher Scientific) supplemented with 8% fetal calf serum (FCS) and 25 mM HEPES. Imaging was carried out from ~2.5 (hpi) using a Leica SP5 confocal microscope equipped with a HyD detector and a 63x (1.4 NA) oil immersion objective, with the confocal pinhole adjusted to 1 airy unit for GFP emission (95.56 μ m pinhole). Cells were maintained in a live-cell imaging chamber at 37°C and 5% CO₂. Positions of interest (xyz) were marked and imaged sequentially at 5 minute intervals. Live-cell imaging data were processed in ImageJ and aligned using the StackReg plugin.

High-pressure freezing and freeze substitution. BGM cells were grown on sapphire discs and infected with CVB3 or CVB3 3A-H57Y and refreshed at 1 hpi with medium supplemented with 25 mM HEPES buffer. Cells were high-pressure frozen using a Leica EM PACT2 at different time points post infection. The instruments and procedures used for freeze-substitution, epoxy resin infiltration and polymerisation were identical to those described in [13]. Briefly, samples were maintained in a Leica AFS2 at -90°C for 44h in a freeze substitution medium containing 10% H₂O, 2% osmium tetroxide and 1% anhydrous glutaraldehyde. The temperature was then raised to 0°C over a period of 22 hours through a series of controlled warming phases. Samples were washed with acetone, infiltrated with epoxy resin LX-112 (Ladd Research) and polymerised at 60°C. Sections of 70 nm were then prepared for electron microscopy and post-stained with uranyl acetate and lead citrate.

Correlative light and electron microscopy (CLEM). BGM(GFPS1-10) cells were cultured in gridded 8-well chamber μ -slides (Ibidi) ahead of infection with CVB3 3A-H57Y(S11). Cells were maintained in 1 μ m BF735738 from 1 hpi in all incubation steps and for the duration of imaging. Just prior to imaging cells were treated with 100 nM Mitotracker® Deep Red FM for 30 minutes, then washed several times in Fluorobrite medium supplemented with 8% FCS and 25 mM HEPES. Images were collected using a Leica SP8 confocal microscope equipped with a HyD detector and using a 63x (1.4 NA) oil immersion objective, while cells were maintained in a live-cell chamber at 37°C and 5% CO₂. High resolution (1024x1024) z-stacks were collected of cells of interest. To aid in the relocation of these cells for CLEM, tile scan ([14]) overviews were taken and the positions of cells relative to nearby grid co-ordinates were recorded. Following imaging by live-cell light microscopy (LM), cells were prepared for electron microscopy as described in [1]. EM images were collected of cells previously identified by LM. To assess the correlation the EM and LM data for each cell were overlaid (Adobe Photoshop CS6) using the Mitotracker® Deep Red FM signal (LM images) and corresponding mitochondria (EM images) as a guide for image transformation.

Metabolic labelling and autoradiography. Subconfluent layers of BGM cells were grown in 35 mm dishes (Corning) and infected with CVB3 3A-H57Y at MOI 5 for 1 hour, after which time the incubation medium was replaced with fresh culture medium. Cells were incubated with 10 μ g/ml dactinomycin for 1 hour prior to a 45-minute labelling with tritiated uridine ([³H], 1 mCi/ml) (Perkin Elmer), after which cells were washed several times to remove unincorporated label and fixed for 1 hour in 1.5% glutaraldehyde in 0.1M cacodylate buffer. Control samples consisting of uninfected BGM cells pre-treated with dactinomycin and incubated with tritiated uridine were also prepared. Cells were then post-fixed with 1% osmium tetroxide for 1 hour in 0.1M cacodylate buffer followed by a 30 minute incubation with 1% tannic acid in 0.1M cacodylate buffer, after which they were dehydrated in ethanol and infiltrated and embedded in LX 112 resin (Ladd Research Industries) before polymerisation at 60°C. Sections of 50 nm were collected on formvar-coated EM grids and post stained with lead citrate and uranyl acetate, then prepared for autoradiography. For the addition of the layer of photographic emulsion (ILFORD L4), grids were first attached to microscope slides by gently pressing the grid edge against a line of double sided sticky tape applied down the length of the slide, taking care to avoid contact between the tape and the formvar layer. A layer of carbon (~12 nm thick) was then evaporated onto the grids to prevent any direct interaction between the stained epon sections and photographic emulsion, which was subsequently placed on the grids with the help of a wire loop. Samples were developed for autoradiography as described in [15].

SUPPLEMENTAL REFERENCES

1. van der Schaar, H.M., et al., Illuminating the Sites of Enterovirus Replication in Living Cells by Using a Split-GFP-Tagged Viral Protein. *mSphere*, 2016. 1(4).
2. Backes, P., et al., Role of annexin A2 in the production of infectious hepatitis C virus particles. *J Virol*, 2010. 84(11): p. 5775-89.
3. Rabouw, H.H., et al., Middle East Respiratory Coronavirus Accessory Protein 4a Inhibits PKR-Mediated Antiviral Stress Responses. *PLoS Pathog*, 2016. 12(10): p. e1005982.
4. Langereis, M.A., et al., Modification of picornavirus genomic RNA using 'click' chemistry shows that unlinking of the VPg peptide is dispensable for translation and replication of the incoming viral RNA. *Nucleic Acids Res*, 2014. 42(4): p. 2473-82.
5. van Eijl, R., et al., Reactivity of human AGO2 monoclonal antibody 11A9 with the SWI/SNF complex: A case study for rigorously defining antibody selectivity. *Sci Rep*, 2017. 7(1): p. 7278.
6. Lanke, K.H., et al., GBF1, a guanine nucleotide exchange factor for Arf, is crucial for coxsackievirus B3 RNA replication. *J Virol*, 2009. 83(22): p. 11940-9.
7. Hato, S.V., et al., The mengovirus leader protein blocks interferon-alpha/beta gene transcription and inhibits activation of interferon regulatory factor 3. *Cell Microbiol*, 2007. 9(12): p. 2921-30.
8. van der Schaar, H.M., et al., A novel, broad-spectrum inhibitor of enterovirus replication that targets host cell factor phosphatidylinositol 4-kinase IIIbeta. *Antimicrob Agents Chemother*, 2013. 57(10): p. 4971-81.
9. MacLeod, A.M., et al., Identification of a series of compounds with potent antiviral activity for the treatment of enterovirus infections. *ACS Med Chem Lett*, 2013. 4(7): p. 585-9.
10. van der Schaar, H.M., et al., Coxsackievirus mutants that can bypass host factor PI4KIIIbeta and the need for high levels of PI4P lipids for replication. *Cell Res*, 2012. 22(11): p. 1576-92.
11. Wessels, E., et al., A viral protein that blocks Arf1-mediated COP-I assembly by inhibiting the guanine nucleotide exchange factor GBF1. *Developmental Cell*, 2006. 11(2): p. 191-201.
12. Dorobantu, C.M., et al., Recruitment of PI4KIII beta to Coxsackievirus B3 Replication Organelles Is Independent of ACBD3, GBF1, and Arf1. *Journal of Virology*, 2014. 88(5): p. 2725-2736.
13. Limpens, R.W.A.L., et al., The Transformation of Enterovirus Replication Structures: a Three-Dimensional Study of Single- and Double-Membrane Compartments. *mBio*, 2011. 2(5).
14. Faas, F.G., et al., Virtual nanoscopy: generation of ultra-large high resolution electron microscopy maps. *J Cell Biol*, 2012. 198(3): p. 457-69.
15. Ginsel, L.A., J.J. Onderwater, and W.T. Daems, Resolution of a gold latensification-elon ascorbic acid developer for Ilford L4 emulsion. *Histochemistry*, 1979. 61(3): p. 343-6.

CHAPTER 4

MODULATION OF PROTEOLYTIC POLYPROTEIN PROCESSING BY COXSACKIEVIRUS MUTANTS RESISTANT TO INHIBITORS TARGETING PHOSPHATIDYLINOSITOL-4-KINASE IIIB OR OXYSTEROL BINDING PROTEIN

*Heyrhyoung Lyoo, Cristina M Dorobantu, Hilde M van der Schaar, Frank JM van Kuppeveld**

Department of Biomolecular Health Sciences, Virology Division, Faculty of Veterinary Medicine, Utrecht University, Utrecht, The Netherlands

*Corresponding author

ABSTRACT

Enteroviruses (e.g. poliovirus, coxsackievirus, and rhinovirus) require several host factors for genome replication. Among these host factors are phosphatidylinositol-4-kinase III β (PI4KB) and oxysterol binding protein (OSBP). Enterovirus mutants resistant to inhibitors of PI4KB and OSBP were previously isolated, which demonstrated a role of single substitutions in the non-structural 3A protein in conferring resistance. Besides the 3A substitutions (i.e., 3A-I54F and 3A-H57Y) in coxsackievirus B3 (CVB3), substitution N2D in 2C was identified in each of the PI4KB-inhibitor resistant CVB3 pools, but its possible benefit has not been investigated yet. In this study, we set out to investigate the possible role of 2C-N2D in the resistance to PI4KB and OSBP inhibition. We show that 2C-N2D by itself did not confer any resistance to inhibitors of PI4KB and OSBP. However, the double mutant (i.e., 2C-N2D/3A-H57Y) showed better replication than the 3A-H57Y single mutant in the presence of inhibitors. Growing evidence suggests that alterations in lipid homeostasis affect the proteolytic processing of the poliovirus polyprotein. Therefore, we studied the effect of PI4KB or OSBP inhibition on proteolytic processing of the CVB3 polyprotein during infection as well as in a replication-independent system. We show that both PI4KB and OSBP inhibitors specifically affected the cleavage at the 3A-3B junction, and that mutation 3A-H57Y recovered impaired proteolytic processing at this junction. Although 2C-N2D enhanced replication of the 3A-H57Y single mutant, we did not detect additional effects of this substitution on polyprotein processing, which leaves the mechanism of how 2C-N2D contributes to the resistance to be revealed.

KEYWORDS

Enterovirus; PI4KB; OSBP; polyprotein processing; resistance mutation

Enteroviruses belong to Picornaviridae family, which is a large group of viruses with a single-stranded, positive-sense RNA genome. Members of the Enterovirus genus, such as poliovirus (PV), coxsackievirus (CV), enterovirus A71 (EV-A71), EV-D68, and rhinovirus, are causative agents of important human diseases (e.g., poliomyelitis, meningitis, hand-foot-and-mouth disease, and respiratory illness) [1]. The genome of enteroviruses encodes a single polyprotein harboring 4 structural proteins (VP4, VP2, VP3, VP1 in the P1 region) and 7 non-structural proteins (P2 region: 2A, 2B, 2C; P3 region: 3A, 3B, 3C, 3D). This polyprotein is proteolytically processed into individual proteins by viral proteases 2Apro, 3Cpro, and 3CDpro. Except for the junction between P1 and P2, which is cleaved by 2Apro, the majority of cleavage events within the viral polyprotein is mediated by 3Cpro [2]. Processing of P2-P3 does not only generate individual viral proteins, but also various cleavage intermediates such as 2BC, 3AB, and 3CD. Together, the non-structural proteins mediate replication of the viral genome.

Enteroviruses depend on several host factors such as phosphatidylinositol-4-kinase III β (PI4KB) [3] and oxysterol binding protein (OSBP) [4, 5] for genome replication. PI4KB is recruited to the replication sites by viral 3A protein, and generates phosphatidylinositol-4 phosphate (PI4P)-enriched membranes. PI4P likely plays a role in recruiting and concentrating cellular proteins, and possibly also viral proteins, on specific membrane sites in order to facilitate viral genome replication. Among the cellular proteins that interact with PI4P are the lipid-transfer proteins, such as OSBP [6]. In uninfected cells, OSBP creates membrane contact sites between endoplasmic reticulum and PI4P-enriched trans-Golgi membranes, and shuttles cholesterol in exchange for PI4P between these organelles [7]. In a similar manner, OSBP is recruited to enterovirus replication organelle (RO) membranes that are enriched in PI4P by PI4KB, and causes an influx of cholesterol to ROs [4]. Disruptions of cholesterol homeostasis by specific inhibitors inhibited PV [8] and CVB3 [9] infection, which revealed the importance of cholesterol for enterovirus replication.

Since all enteroviruses rely on PI4KB and OSBP for efficient viral replication, several PI4KB inhibitors [3, 10-15], including BF738735 [16], and OSBP inhibitors [4, 17], including OSW-1 [18], have been found to exert broad-spectrum antiviral activity. PV and CVB3 mutants that are resistant to PI4KB inhibitors were found to possess single amino acid substitutions in the viral 3A protein [11-13, 19]. Previously, we showed that CVB3 3A mutations confer resistance by bypassing the need for PI4KB activity and PI4P accumulation [14], but the exact resistance mechanism remains to be revealed. The same mutations were also shown to confer resistance to OSBP inhibitors, consistent with the proposed role of PI4P in recruiting OSBP [4, 18, 20].

Previously, three independent CVB3 cultures were generated which were resistant to the PI4KB inhibitor BF738735 [16]. Genome analysis of these isolates revealed two single amino acid substitutions in the 3A protein (H57Y from two isolates and I54F from one isolate). In addition, another substitution (N2D) in the 2C protein appeared in all three isolates, which indicates that it may play an important role in resistance development. However, since the 3A mutants alone were sufficient to provide resistance [16], the importance of this substitution in 2C has not been investigated yet. In this study, we set out to investigate the role of the 2C-N2D substitution in the resistance mechanism to PI4KB and OSBP inhibition. Possibly, this substitution provides resistance to PI4KB inhibition by itself, or it may support the resistance mechanism of the 3A substitution. To test this, we employed a previously established recombinant CVB3 that encodes Renilla luciferase (Rluc). Rluc is located upstream of the P1 region in the viral genome and can be used as a sensitive measure for genome replication. CVB3-Rluc [21] and CVB3-Rluc 3A-H57Y viruses [14] are derived from the full length infectious clones pRluc-53CB3/T7(3A-

H57Y). CVB3-Rluc carrying 2C-N2D alone or a combination of 2C-N2D and 3A-H57Y were obtained in a similar manner as described elsewhere [14]. Cells were infected with these different viruses for 30 min, after which the inoculum was removed and fresh medium lacking or containing PI4KB or OSBP inhibitors was added. At 8 h post-infection, the cells were lysed to determine the intracellular luciferase activity. In agreement with our previous observations, CVB3 3A-H57Y was resistant to both PI4KB inhibitor BF738735 [16] and OSBP inhibitor OSW-1 [18] (Figure 1). Compared to wild-type virus, replication of the 3A-H57Y mutant was enhanced by ~100-fold under PI4KB or OSBP inhibition. The substitution in 2C alone did not provide resistance to either PI4KB or OSBP inhibitors (Figure 1). The 2C-N2D/3A-H57Y double mutant rescued virus replication in the presence of BF738735 to an even greater extent. At all the concentrations of BF738735 tested, the level of replication of 2C-N2D/3A-H57Y was ~3-fold higher than that of 3A-H57Y (Figure 1A). The synergistic effect of 2C-N2D and 3A-H57Y was also observed upon treatment with OSW-1 (Figure 1B). These results show that 2C-N2D provided small additive benefits to CVB3 replication only when accompanied by the substitution in 3A.

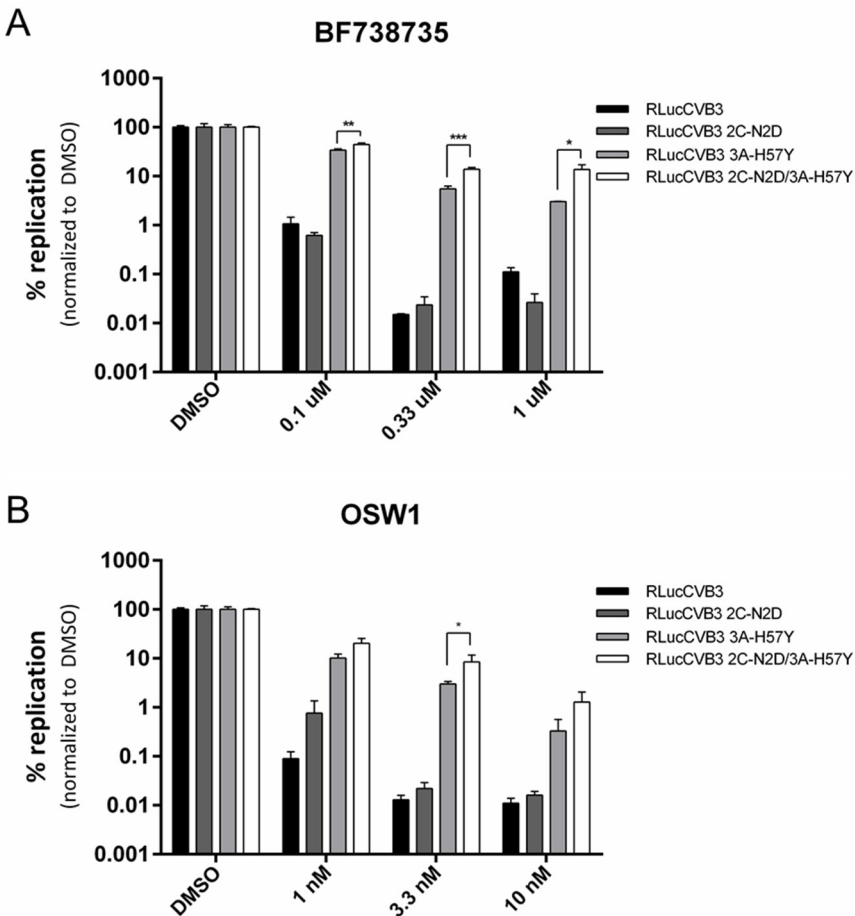


Figure 1. The 2C-N2D substitution enhances the resistance of 3A-H57Y mutant to PI4KB or OSBP inhibitors. HeLa R19 cells were infected with CVB3-Rluc wild-type, 3A-H57Y, 2C-N2D, or 2C-N2D/3A-H57Y at an MOI of 1 for 30 min. After removal of the inoculum, Dimethyl sulfoxide (DMSO), BF738735 (A), or OSW-1 (B) was added to the cells. After 8 h, cells were lysed to determine Renilla luciferase activity. Bars represent the mean of triplicate values \pm SEM. Significant differences were calculated by paired *t* test. *, = $P < 0.05$; **, = $P < 0.01$; ***, = $P < 0.001$

Alterations in lipid homeostasis have been shown to affect the proteolytic processing of the PV polyprotein [8, 22, 23]. Depletion of free cholesterol or disruption of cholesterol within membranes stimulated processing at the 3C-3D junction in PV-infected cells [8]. Upon PI4KB inhibition, accumulation of P2P3 and 3D as well as decrease of 2C and 3CD were observed in an in vitro translation setting [23]. In another study, 3AB accumulation was found in PV-infected cells in the presence of a PI4KB inhibitor, while the level of other proteins was unaffected [5]. Hence, no clear and consistent picture of the role of lipids in polyprotein processing has emerged yet.

In this study, we first investigated the effects of PI4KB inhibition on proteolytic processing of the CVB3 polyprotein in virus-infected cells. HeLa R19 cells were infected with wild-type, 3A-H57Y, or 2C-N2D/3A-H57Y viruses for 30 min, after which the inoculum was removed and fresh medium lacking or containing PI4KB inhibitor BF738735 was added. At 8 h post-infection, the cells were lysed and subjected to Western blot analysis using antibodies against CVB3 2C, 3A, and 3D proteins (Figure 2). In the absence of inhibitor (i.e., DMSO treatment), both 3A-H57Y and 2C-N2D/3A-H57Y virus already showed a better cleavage efficiency at the 3A-3B junction compared to wild-type. The levels of 3CD, 3D, 2BC, and 2C remained comparable between the wild-type and the mutants. Unfortunately, viral protein production of the wild-type virus was impaired already at a very low concentration of PI4KB inhibitor (i.e., 20 nM, which is below the IC50). This impairment in viral protein production is likely due to the inhibitory effect of BF738735 on viral RNA replication. It is well known that the rate of polyprotein processing changes over time during replication. Therefore, it was not possible to achieve a fair comparison between the wild-type virus and the mutant viruses in the presence of inhibitor in infected cells.

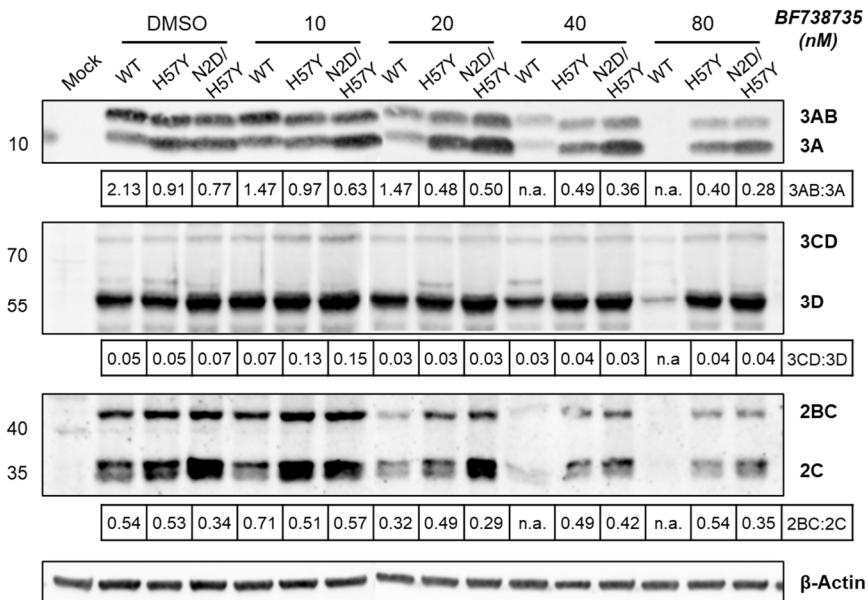


Figure 2. The CVB3 mutants exhibit better cleavage efficiency at the 3A-3B junction compared to the wild-type. HeLa R19 cells were infected with CVB3 wild-type, 3A-H57Y, or 2C-N2D/3A-H57Y at an MOI of 10 for 30 min. After removal of the inoculum, DMSO or BF738735 was added to the cells. After 7 h, cells were lysed and the lysates were subjected to Western blot analysis to examine effects on viral polyprotein processing. Antibodies against 3A, 3D, and 2C were used to detect viral proteins. Actin was used as a loading control. Densitometry of bands was done with LI-COR® Image Studio™ software.

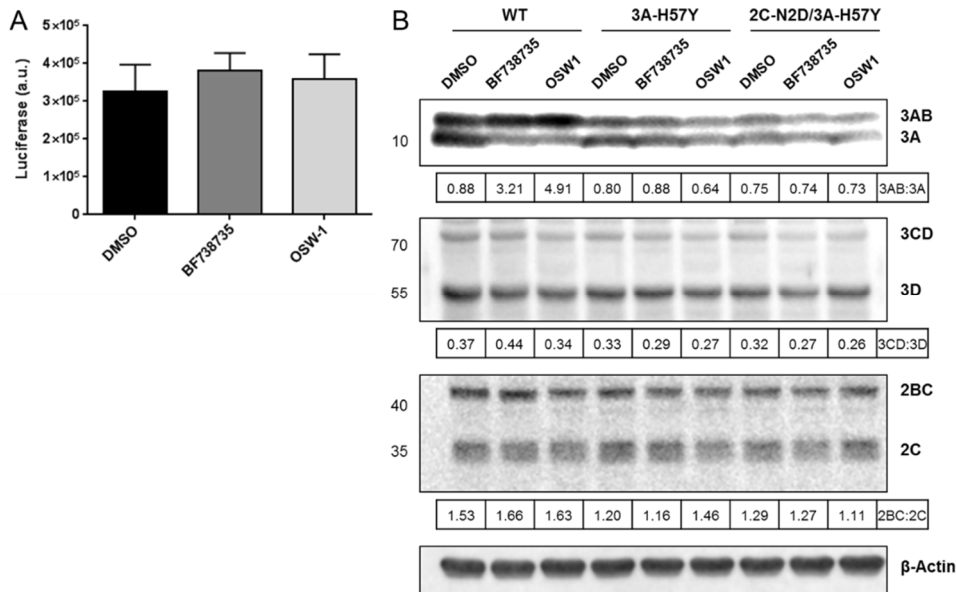


Figure 3. The 3A-H57Y substitution rectifies the impaired polyprotein processing upon PI4KB or OSBP inhibition. (A) Luciferase levels produced upon transfection of RLuc-CVB3- Δ 1-6+5 cDNA were determined to test whether the presence of inhibitors interferes with polyprotein production. Huh7-Lunet/T7 cells were transfected with linearized plasmid in the presence of DMSO, 1 μ M BF738735, or 10 nM OSW-1. Inhibitors were added prior to transfection. After 7 h, cells were lysed to measure *Renilla* luciferase activity. (B) Huh7-Lunet/T7 cells were transfected with p53-CVB3- Δ 1-6+5 wild-type, p53-CVB3- Δ 1-6+5 3A-H57Y, or p53-CVB3- Δ 1-6+5 2C-N2D/3A-H57Y cDNA in the presence of DMSO, 1 μ M BF738735, or 10 nM OSW-1. After 7 h, cells were lysed and the lysates were subjected to Western blot analysis to examine effects on viral polyprotein processing. Antibodies against 3A, 3D, and 2C were used to detect viral proteins. Actin was used as a loading control. Densitometry of bands was done with LI-COR® Image Studio™ software.

To overcome this problem, we set up a replication-independent system, which allows the production of equal amounts of viral protein independent of genome replication. This system exploits a previously established CVB3-(Rluc) cDNA that is rendered replication-deficient through modifications in the cloverleaf (p53CB3/T7-CL-6+5 or pRluc-53CB3/T7-CL-6+5) [24]. Since RNA synthesis is under the control of T7 polymerase, which is stably expressed in the cell line Huh7-Lunet/T7 [25], it is unlikely that the viral protein production is affected by the presence of inhibitors. To verify this, Huh7-Lunet/T7 cells were transfected with pRluc-53CB3/T7-CL-6+5 cDNA in the presence or absence of inhibitors, and were lysed 7 h later to quantify the luciferase activity. Figure 3A shows that the luciferase levels were affected neither by PI4KB inhibition nor by OSBP inhibition. These results corroborate that inhibition of PI4KB or OSBP did not affect the CVB3 polyprotein production.

Next, we analyzed whether the PI4KB and OSBP inhibitors influence the proteolytic processing of the CVB3 polyprotein in this system. Huh7-Lunet/T7 cells were transfected with wild-type, 3A-H57Y, or 2C-N2D/3A-H57Y replication-deficient cDNAs and viral protein levels were assessed by Western blot analysis after 7 h (Figure 3B). The ratio of 3AB:3A for wild-type was prominently perturbed under both PI4KB inhibition and OSBP inhibition, indicating a defect in proteolytic processing at the 3A-3B junction. While the ratio of 3AB:3A was close to 1 in DMSO-treated cells, it increased 4- to 5-fold in the presence of PI4KB and OSBP inhibitors due to a decrease in the 3A level. Both the 3A-H57Y single mutant and the 2C-N2D/3A-H57Y double mutant rescued the impaired proteolytic processing at the 3A-3B junction upon PI4KB and OSBP inhibition. Similar as in infected cells, no effects of the BF738735 or OSW-1 on

3CD:3D or 2BC:2C ratios were observed in this replication-independent system. The observation that levels of 2BC, 2C, 3CD, and 3D did not change upon PI4KB or OSBP inhibition implies that proteolytic processing at the 2A-2B, 2B-2C, 2C-3A, 3B-3C, and 3C-3D cleavage junctions was unaffected. Together, the data demonstrate that inhibition of either PI4KB or OSBP specifically hinders proteolytic processing at the 3A-3B junction and that the substitution in 3A recovers impaired proteolytic processing at this junction.

In summary, we studied the role of 2C-N2D and 3A-H57Y substitutions in the resistance mechanism of CVB3 to PI4KB and OSBP inhibitors. We showed that the CVB3 3A-H57Y mutant can overcome the absence of essential lipids (i.e., PI4P and cholesterol) in membranes by rescuing the impaired proteolytic processing at the 3A-3B junction. A recent study on PV showed that PI4KB inhibition also resulted in the accumulation of 3AB during infection with low concentrations of a PI4KB inhibitor [22]. The PV 3A-A70T mutant, which is resistant to PI4KB inhibition, also compensated for this processing impairment by restoring the ratio of 3AB:3A. Notably, this mutant already showed enhanced 3A production in the absence of inhibitor, as also observed in our CVB3 mutant infected cells (Figure 2). Yet, in the replication-independent system, this enhanced processing at the 3A-3B junction was only noticeable upon PI4KB or OSBP inhibition (Figure 3B). The reasons for these discrepant results are unknown. Clearly, the infection system best represents the natural condition. However, it is known that the rate of proteolytic processing of viral proteins changes over time during replication. Therefore, it cannot be excluded that subtle differences in growth kinetics exist between wild-type and mutants, and that these may (partly) account for the differences in proteolytic processing that we observed. This potential drawback was circumvented by the replication-independent system, yet in this system some subtle effects from genome replication on polyprotein processing may be lacking. Notwithstanding the differences found between the two systems, both showed that PI4KB and OSBP inhibitors specifically impair proteolytic processing at the 3A-3B junction and that a single point mutation can rectify this defect.

It is not clear how the single amino acid substitutions A70T in PV 3A and H57Y in CVB3 3A can rescue the inefficient cleavage at the 3A-3B junction. One possible explanation is that they impose an altered conformation of 3A in PI4P/cholesterol depleted membranes, resulting in a better exposure and accessibility of the 3A-3B cleavage site to 3C(D)pro. Our observation that 3A-3B cleavage is impaired by OSW-1, which inhibits OSBP but has no effect on PI4KB activity [18], points to an important role of cholesterol in determining the 3A conformation and 3A-3B cleavage efficiency.

What then is the role of 2C-N2D in the resistance mechanism? By itself, the 2C-N2D mutant did not confer resistance, but in combination with the 3A mutation it provided better resistance to PI4KB and OSBP inhibition, albeit to a marginal extent. This result suggests that the substitution in 2C plays a synergistic role with 3A in the resistance mechanisms rather than a distinctive resistance mechanism. Since the N2D substitution is near the 2B-2C junction, it may alter the cleavage efficiency at this junction. Although no such effect was observed, this possibility cannot be excluded as subtle effects may be difficult to detect by Western blot analysis. Another possible scenario is that the substitution in 2C provides additive resistance through a mechanism other than polyprotein processing. Biochemical as well as genetic data point to a functional interaction between viral proteins 2C and 3A [26-28]. For example, poliovirus acquired resistance to brefeldin A with substitutions in both 2C and 3A [29, 30]. Hence, 2C-N2D may increase virus fitness by modulating functional interactions between viral proteins

CHAPTER 4

2C and 3A-H57Y. The exact mechanism of how the 2C-N2D mutation increases viral replication upon PI4KB or OSBP inhibition remains to be elucidated.

ACKNOWLEDGEMENTS

We are very grateful to Dr. C.E. Cameron (The Pennsylvania State University, USA) and Dr. J.L. Whitton (The Scripps Research Institute, USA) for providing polyclonal rabbit antibodies against 3D and 2C, respectively, and Dr. R. Bartenschlager (University of Heidelberg, Germany) for providing Huh7-Lunet/T7 cells.

This work was supported by research grants from the Netherlands Organisation for Scientific Research (NWO-VENI-863.12.005 to HMvdS, NWO-VICI-91812628 to FJMvK, ERASysApp project 'SysVirDrug' ALW project number 832.14.003 to FJMvK) and from the European Union (Horizon 2020 Marie Skłodowska-Curie ETN 'ANTIVIRALS', grant agreement number 642434 to FJMvK).

REFERENCES

1. Tapparel, C., et al., Picornavirus and enterovirus diversity with associated human diseases. *Infect Genet Evol*, 2013. 14: p. 282-93.
2. Ypma-Wong, M.F. and B.L. Semler, In vitro molecular genetics as a tool for determining the differential cleavage specificities of the poliovirus 3C proteinase. *Nucleic Acids Res*, 1987. 15(5): p. 2069-88.
3. Hsu, N.Y., et al., Viral reorganization of the secretory pathway generates distinct organelles for RNA replication. *Cell*, 2010. 141(5): p. 799-811.
4. Strating, J.R., et al., Itraconazole inhibits enterovirus replication by targeting the oxysterol-binding protein. *Cell Rep*, 2015. 10(4): p. 600-15.
5. Arita, M., Phosphatidylinositol-4 kinase III beta and oxysterol-binding protein accumulate unesterified cholesterol on poliovirus-induced membrane structure. *Microbiol Immunol*, 2014. 58(4): p. 239-56.
6. Levine, T.P. and S. Munro, Targeting of Golgi-specific pleckstrin homology domains involves both PtdIns 4-kinase-dependent and -independent components. *Curr Biol*, 2002. 12(9): p. 695-704.
7. Mesmin, B., et al., A four-step cycle driven by PI(4)P hydrolysis directs sterol/PI(4)P exchange by the ER-Golgi tether OSBP. *Cell*, 2013. 155(4): p. 830-43.
8. Ilnytska, O., et al., Enteroviruses harness the cellular endocytic machinery to remodel the host cell cholesterol landscape for effective viral replication. *Cell Host Microbe*, 2013. 14(3): p. 281-93.
9. Albulescu, L., et al., Cholesterol shuttling is important for RNA replication of coxsackievirus B3 and encephalomyocarditis virus. *Cell Microbiol*, 2015. 17(8): p. 1144-56.
10. Arita, M., et al., Phosphatidylinositol 4-kinase III beta is a target of enviroxime-like compounds for antipoliovirus activity. *J Virol*, 2011. 85(5): p. 2364-72.
11. Arita, M., T. Wakita, and H. Shimizu, Cellular kinase inhibitors that suppress enterovirus replication have a conserved target in viral protein 3A similar to that of enviroxime. *J Gen Virol*, 2009. 90(Pt 8): p. 1869-79.
12. Heinz, B.A. and L.M. Vance, The antiviral compound enviroxime targets the 3A coding region of rhinovirus and poliovirus. *J Virol*, 1995. 69(7): p. 4189-97.
13. Heinz, B.A. and L.M. Vance, Sequence determinants of 3A-mediated resistance to enviroxime in rhinoviruses and enteroviruses. *J Virol*, 1996. 70(7): p. 4854-7.
14. van der Schaar, H.M., et al., Coxsackievirus mutants that can bypass host factor PI4KIIIbeta and the need for high levels of PI4P lipids for replication. *Cell Res*, 2012. 22(11): p. 1576-92.
15. Wikel, J.H., et al., Synthesis of syn and anti isomers of 6-[[[(hydroxyimino)phenyl]methyl]-1-[(1-methylethyl)sulfonyl]-1H-benzimidazol-2-amine. Inhibitors of rhinovirus multiplication. *J Med Chem*, 1980. 23(4): p. 368-72.
16. van der Schaar, H.M., et al., A novel, broad-spectrum inhibitor of enterovirus replication that targets host cell factor phosphatidylinositol 4-kinase IIIbeta. *Antimicrob Agents Chemother*, 2013. 57(10): p. 4971-81.
17. Arita, M., et al., Oxysterol-binding protein family I is the target of minor enviroxime-like compounds. *J Virol*, 2013. 87(8): p. 4252-60.
18. Albulescu, L., et al., Broad-range inhibition of enterovirus replication by OSW-1, a natural compound targeting OSBP. *Antiviral Res*, 2015. 117: p. 110-4.
19. De Palma, A.M., et al., Mutations in the nonstructural protein 3A confer resistance to the novel enterovirus replication inhibitor TTP-8307. *Antimicrob Agents Chemother*, 2009. 53(5): p. 1850-7.
20. Albulescu, L., et al., Uncovering oxysterol-binding protein (OSBP) as a target of the anti-enteroviral compound TTP-8307. *Antiviral Res*, 2017. 140: p. 37-44.
21. Lanke, K.H., et al., GBF1, a guanine nucleotide exchange factor for Arf, is crucial for coxsackievirus B3 RNA replication. *J Virol*, 2009. 83(22): p. 11940-9.
22. Arita, M., Mechanism of Poliovirus Resistance to Host Phosphatidylinositol-4 Kinase III β Inhibitor. *ACS Infectious Diseases*, 2016. 2(2): p. 140-148.
23. Ford Siltz, L.A., et al., New small-molecule inhibitors effectively blocking picornavirus replication. *J Virol*, 2014. 88(19): p. 11091-107.
24. Langereis, M.A., et al., Modification of picornavirus genomic RNA using 'click' chemistry shows that unlinking of the VPg peptide is dispensable for translation and replication of the incoming viral RNA. *Nucleic Acids Res*, 2014. 42(4): p. 2473-82.
25. Backes, P., et al., Role of annexin A2 in the production of infectious hepatitis C virus particles. *J Virol*, 2010. 84(11): p. 5775-89.
26. Teterina, N.L., et al., Evidence for functional protein interactions required for poliovirus RNA replication. *J Virol*, 2006. 80(11): p. 5327-37.

CHAPTER 4

27. Teterina, N.L., et al., Analysis of poliovirus protein 3A interactions with viral and cellular proteins in infected cells. *J Virol*, 2011. 85(9): p. 4284-96.
28. Yin, J., et al., Complete protein linkage map between the P2 and P3 non-structural proteins of poliovirus. *J Gen Virol*, 2007. 88(Pt 8): p. 2259-67.
29. Crotty, S., et al., The poliovirus replication machinery can escape inhibition by an antiviral drug that targets a host cell protein. *J Virol*, 2004. 78(7): p. 3378-86.
30. Viktorova, E.G., et al., Cell-specific establishment of poliovirus resistance to an inhibitor targeting a cellular protein. *J Virol*, 2015. 89(8): p. 4372-86.

CHAPTER 5

ACBD3 IS AN ESSENTIAL PAN-ENTEROVIRUS HOST FACTOR THAT MEDIATES THE INTERACTION BETWEEN VIRAL 3A PROTEIN AND CELLULAR PROTEIN PI4KB

*Heyrhyoung Lyoo, Hilde M van der Schaar, Cristina M Dorobantu, Huib H Rabouw, Jeroen RPM Strating, Frank JM van Kuppeveld**

Department of Infectious Diseases & Immunology, Virology Division, Faculty of Veterinary Medicine, Utrecht University, Utrecht, The Netherlands

*Corresponding author

ABSTRACT

The enterovirus genus of the picornavirus family includes a large number of important human pathogens such as poliovirus, coxsackievirus, enterovirus-A71, and rhinoviruses. Like all other positive-strand RNA viruses, genome replication of enteroviruses occurs on rearranged membranous structures called replication organelles (ROs). Phosphatidylinositol 4-kinase III β (PI4KB) is required by all enteroviruses for RO formation. The enteroviral 3A protein recruits PI4KB to ROs, but the exact mechanism remains elusive. Here, we investigated the role of Acyl-coenzyme A binding domain containing 3 (ACBD3) in PI4KB recruitment upon enterovirus replication using ACBD3-knockout (ACBD3^{KO}) cells. ACBD3 knockout impaired replication of representative viruses from four enterovirus and two rhinovirus species. PI4KB recruitment was not observed in the absence of ACBD3. The lack of ACBD3 also affected the localization of individually expressed 3A, causing 3A to localize to the endoplasmic reticulum instead of the Golgi. Reconstitution of wt ACBD3 restored PI4KB recruitment and 3A localization, while an ACBD3 mutant that cannot bind to PI4KB restored 3A localization, but not virus replication. Consistently, reconstitution of a PI4KB mutant that cannot bind ACBD3 failed to restore virus replication in PI4KB^{KO} cells. Finally, by reconstituting ACBD3 mutants lacking specific domains in ACBD3^{KO} cells, we show that Acyl-coenzyme A binding (ACB) and charged amino acids region (CAR) domains are dispensable for 3A-mediated PI4KB recruitment and efficient enterovirus replication. Altogether, our data provide new insight into the central role of ACBD3 in recruiting PI4KB by enterovirus 3A and reveal the minimal domains of ACBD3 involved in recruiting PI4KB and supporting enterovirus replication.

IMPORTANCE

As all other positive-strand RNA viruses, enteroviruses reorganize host cellular membranes for efficient genome replication. A host lipid kinase, PI4KB, plays an important role in this membrane rearrangement. The exact mechanism of how enteroviruses recruit PI4KB was unclear. Here, we revealed a role of a Golgi-residing protein, ACBD3, as a mediator of PI4KB recruitment upon enterovirus replication. ACBD3 is responsible for proper localization of enteroviral 3A proteins in host cells, which is important for 3A to recruit PI4KB. By testing ACBD3 and PI4KB mutants that abrogate the ACBD3-PI4KB interaction, we showed that this interaction is crucial for enterovirus replication. The importance of specific domains of ACBD3 was evaluated for the first time, and the domains that are essential for enterovirus replication were identified. Our findings open up a possibility for targeting ACBD3 or its interaction with enteroviruses as a novel strategy for the development of broad-spectrum anti-enteroviral drugs.

INTRODUCTION

The Picornaviridae family is a large group of viruses with a single-stranded, positive-sense RNA genome. Members of the Enterovirus genus, which includes poliovirus (PV), coxsackievirus (CV), enterovirus A71 (EV-A71), EV-D68, and rhinovirus (RV), can cause diverse human diseases such as poliomyelitis, meningitis, hand-foot-and-mouth disease, respiratory illness [1]. Even though enteroviruses are associated with a variety of clinical manifestations, there are currently no approved vaccines against most enteroviruses except for PV and EV-A71, and antiviral drugs are not available.

All positive-strand RNA viruses, including picornaviruses, induce reorganization of host cellular membranes [2-4] into so called replication organelles (ROs). ROs are enriched with viral replication factors and co-opted host factors, and serve several important purposes in virus replication [5] including facilitating genome replication. Among picornaviruses, enteroviruses and kobuviruses exploit a similar mechanism for RO formation. The host factor phosphatidylinositol 4-kinase type III beta (PI4KB) is recruited to the replication sites by viral 3A protein [6-8]. PI4KB is a cytosolic lipid kinase that must be recruited to membranes to exert its function and to generate a phosphatidylinositol 4-phosphate (PI4P)-enriched environment [7, 9]. PI4P recruits and concentrates cellular proteins, and possibly also viral proteins, to facilitate viral genome replication [10, 11]. Among the cellular proteins that interact with PI4P are lipid-transfer proteins, such as oxysterol binding protein (OSBP) [12]. In normal condition, OSBP creates membrane contact sites between endoplasmic reticulum (ER) and PI4P-enriched trans-Golgi membranes and shuttles cholesterol in exchange for PI4P [13]. In a similar manner, OSBP is recruited to RO membranes and mediates a PI4P-dependent flux of cholesterol from ER to ROs [14].

In uninfected cells, PI4KB is recruited to Golgi membranes among others by the small GTPase ADP-ribosylation factor 1 (Arf1) [15] or by acyl-CoA binding domain containing 3 (ACBD3) [7, 8, 16]. Kobuviruses recruit PI4KB through ACBD3, which directly interacts with the viral protein 3A [7, 11]. Recently, the crystal structure of the kobuvirus 3A-ACBD3 complex became available, which revealed the binding sites that are important for the 3A-ACBD3 interaction [6]. Point mutations in 3A and ACBD3 at the binding interface inhibited the activation of PI4KB [17], suggesting that PI4KB recruitment to membranes via 3A-ACBD3-PI4KB interaction is necessary for kobuviruses to exploit PI4KB activity.

Enteroviruses also express a viral protein called 3A, but this differs from Kobuvirus 3A both in sequence and in structure. The 3A proteins of several enteroviruses (e.g., PV and coxsackievirus B3 [CVB3]) bind to brefeldin A resistance guanine nucleotide exchange factor 1 (GBF1), a guanine exchange factor that activates the small GTPase Arf1. Arf1 interacts with PI4KB in non-infected cells. However, PI4KB recruitment by CVB3 and RV 3A likely occurs independently of GBF1 and Arf1 [18, 19]. A number of enterovirus 3A proteins have been shown to bind to ACBD3 [8, 18]. Therefore, several studies have investigated whether enteroviruses depend on ACBD3 to recruit PI4KB. While in one study knockdown of ACBD3 in HeLa cells inhibited poliovirus (PV) replication [8], another reported no inhibition of PV replication in ACBD3-knockdown HEK-293T, IMR5, and HeLa cells [20]. In our previous work, we did not observe inhibition of CVB3 or RV replication and no effects on PI4KB recruitment upon ACBD3 knockdown [18, 19].

Here, we re-evaluated the importance of ACBD3 for enterovirus replication using ACBD3 knockout (ACBD3^{KO}) cells. We observed that ACBD3 supports replication of representative viruses of different human enterovirus species (EV-A/B/C/D, RV-A/B) by mediating PI4KB recruitment by 3A. For the first time, we showed that the interaction between ACBD3 and PI4KB is crucial for enterovirus replication. In addition, we dissected the different domains of ACBD3 and uncovered that the glutamine-rich region

(Q) and Golgi dynamics domain (GOLD) together suffice to support enterovirus replication. Furthermore, our data suggest that ACBD3 is important for proper 3A localization. Overall, our findings implicate that ACBD3 is not just an intermediate through which 3A recruits PI4KB, but may play a central role in RO formation by scaffolding viral proteins and host proteins.

RESULTS

ACBD3 knockout inhibits replication of enterovirus A-D and rhinovirus A-B species.

Previously, we observed no effects on CVB3 and RV replication in HeLa cells, in which ACBD3 was knocked down for more than 90% [18, 19]. Here, we set out to study enterovirus replication in ACBD3^{KO} HeLa cells. HeLa cells lacking ACBD3 were generated with CRISPR-Cas9 technology, and the knockout was confirmed by Western blot analysis (Fig. S1A). Next, we evaluated enterovirus replication kinetics in ACBD3^{KO} cells using representative viruses of four different human enterovirus species (EV-A71 [EV-A], CVB3 [EV-B], PV-1 [EV-C], EV-D68 [EV-D]) and two rhinovirus species (RV-A2 [RV-A] and RV-B14 [RV-B]). RV-C was not tested, as HeLa R19 cells are not susceptible to RV-C because they lack the receptor, cadherin-related family member 3 (CDHR-3) [21]. All of the viruses clearly showed deficient replication in ACBD3^{KO} HeLa cells (Fig. 1A). Replication of enteroviruses was also impaired in another human cell line, haploid human cell line HAP1, in which ACBD3 was knocked out (Fig. S2).

To exclude the role of ACBD3 in virus entry, we assessed viral RNA replication of subgenomic replicons, which are widely used tools to study genome replication specifically and independently of virus entry. Replication of CVB3 and EV-A71 replicons transfected in HeLa ACBD3^{KO} cells was reduced, which indicates a role for ACBD3 in the genome replication step (Fig. 1B). Next, to test whether ACBD3 functions in the same pathway as PI4KB in enterovirus replication, we employed a mutant virus that is less sensitive to PI4KB inhibition, CVB3 3A-H57Y [22]. While the replication of wt CVB3 (RlucCVB3) was impaired in ACBD3^{KO} cells, the replication of RlucCVB3 3A-H57Y was significantly increased (Fig. 1C). Encephalomyelitis virus (EMCV), which belongs to the genus of Cardiovirus within Picornaviridae family, depends on PI4KA but not on PI4KB for generating ROs [23]. The replication of EMCV was not affected in ACBD3^{KO} cells (Fig. S3) suggesting that the inhibition of CVB3 and EV-A71 replication in ACBD3^{KO} cells is connected to the PI4KB pathway. Overall, these results indicate that ACBD3 is an important host factor for enterovirus replication.

ACBD3 is indispensable for PI4KB recruitment.

To determine the importance of ACBD3 for PI4KB recruitment during enterovirus replication, we investigated PI4KB localization in CVB3-infected ACBD3^{KO} cells. Since we observed delayed virus replication in ACBD3^{KO} cells (Fig. 1A), different time points were chosen for HeLa^{wt} cells and ACBD3^{KO} cells to mitigate possible effects of different replication levels on PI4KB recruitment. As previously shown, the CVB3 3A protein colocalized with ACBD3 (Fig. 2A) and PI4KB (Fig. 2B) throughout infection in infected HeLa^{wt} cells, which implies that both ACBD3 and PI4KB localize to CVB3 ROs. PI4KB was more concentrated in 3A-positive cells compared to 3A-negative cells, which suggests that it is actively recruited to virus replication sites. Notwithstanding the similar level of 3A expression compared to HeLa^{wt} cells (Fig. 2A-B), no recruitment of PI4KB was observed in infected ACBD3^{KO} cells at any time point (Fig. 2D). These results indicate that ACBD3 mediates recruitment of PI4KB during enterovirus replication.

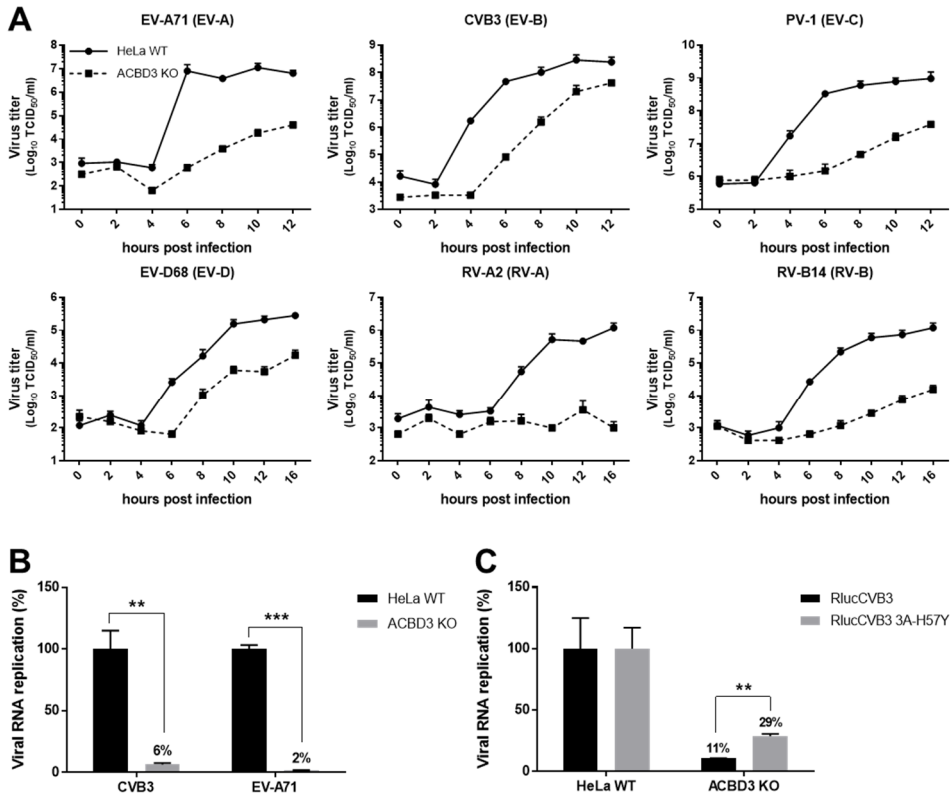


Figure 1. ACBD3 is crucial for enterovirus replication. (A) Growth curves of enteroviruses in HeLa^{wt} and ACBD3^{KO} cells. After infection for 30min at an MOI 5, cells were incubated for the indicated times. Then, cells were freeze-thawed three times to harvest infectious virus particles. Total virus titers were determined by endpoint dilution. (B) RNA replication of CVB3 and EV-A71 virus in HeLa ACBD3^{KO} cells. HeLa^{wt} and ACBD3^{KO} cells were transfected with *in vitro* transcribed RNA of CVB3 or EV-A71 subgenomic replicons encoding firefly luciferase in place of the capsid region. After 7 h, cells were lysed to determine the intracellular luciferase activity. (C) Replication of the CVB3 3A-H57Y mutant in ACBD3^{KO} cells. HeLa^{wt} and ACBD3^{KO} cells were infected with wt or 3A-H57Y mutant CVB3 reporter viruses encoding *Renilla* luciferase (RlucCVB3) at an MOI 0.1. After 8 h, cells were lysed to determine luciferase activity. Bars represent the mean of triplicate values \pm SEM. Values were statistically evaluated using a two-tailed paired t-test. **, $p < 0.01$; ***, $p < 0.001$.

Enterovirus 3A expression alone is sufficient to recruit PI4KB to membranes [9, 18, 19]. To further investigate whether PI4KB recruitment by 3A is mediated by ACBD3, we transiently expressed the 3A proteins from representative human enteroviruses from seven different species (EV-A/B/C/D, RV-A/B/C) with either a C-terminal myc tag or an N-terminal GFP tag and examined the localization of ACBD3 and PI4KB (Fig. 3 and S4). In HeLa^{wt} cells, all 3A proteins colocalized with ACBD3 (Fig. 3A). PI4KB was more concentrated in cells expressing 3A compared to cells that did not express 3A, and colocalized with 3A (Fig. 3B), which indicates that PI4KB is actively recruited by enterovirus 3A proteins. In contrast, no PI4KB recruitment was observed in ACBD3^{KO} cells expressing any of the enterovirus 3A proteins (Fig. 3C). These results imply that all enteroviruses utilize a shared mechanism to recruit PI4KB to replication sites, which is via a 3A-ACBD3-PI4KB interaction. Interestingly, we noticed that the localization of 3A differs from HeLa^{wt} cells to ACBD3^{KO} cells (Fig. 3 and S5). Unlike the punctate localization in HeLa^{wt} cells (Fig. 3A), 3A proteins were dispersed throughout the cytoplasm in ACBD3^{KO} cells into a more reticular pattern (Fig. 3B and S5), suggesting that ACBD3 is important for proper localization of 3A.

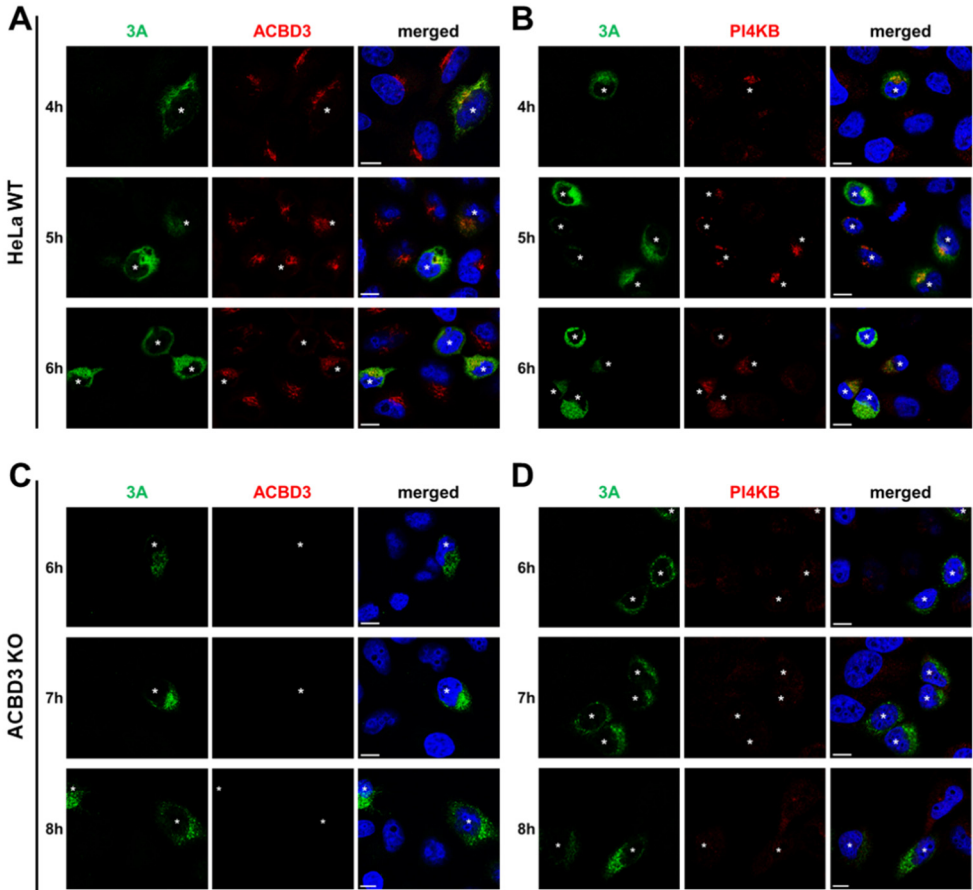


Figure 2. PI4KB recruitment to virus replication sites depends on ACBD3. (A and B) HeLa^{WT} and (C and D) ACBD3^{KO} cells were infected with CVB3 wt at an MOI of 5. At indicated time points, cells were fixed and stained with antibodies against CVB3 3A and ACBD3 (A and C) or CVB3 3A and PI4KB (B and D). Nuclei were stained with DAPI (blue). Asterisks indicate infected cells. Scale bars represent 10 μm.

ACBD3 is crucial for 3A localization to the Golgi.

Because the typical punctate localization of 3A on Golgi-derived membranes is lost in ACBD3^{KO} cells, we assessed the overall structure of the Golgi and ER as well as the colocalization between 3A and markers for the Golgi (GM130 and TGN46) and ER (Calreticulin). In mock-transfected cells, no gross differences in localization of any of the above markers were observed between HeLa^{WT} cells and ACBD3^{KO} cells, although in some ACBD3^{KO} cells the Golgi appeared to be slightly more scattered than in HeLa^{WT} cells (Fig. 4). Importantly, this slight Golgi scattering clearly differs from the massive Golgi scattering that can be observed upon knockout of structural Golgi proteins GRASP55 and GRASP65 [24]. Nevertheless, smaller disruptions of Golgi structure that cannot be readily visualized at the light microscopy level cannot be excluded. Indeed, others have reported fragmentation of Golgi cisterna when they studied ACBD3-knockdown cells by electron microscopy [25]. As previously described, the disintegration of the Golgi in enterovirus-infected cells and in 3A-expressing cells is likely a consequence of the blockage of ER-to-Golgi transport that depends on the interaction between 3A and GBF1/Arf1

[26, 27]. In agreement with this, overexpression of 3A caused disassembly of the Golgi apparatus in both wt and ACBD3^{KO} HeLa cells (Fig. 4B-C), pointing out that the disruption of the Golgi by 3A occurs independently of ACBD3. 3A partially colocalized with the Golgi markers but not the ER marker in HeLa^{wt} cells, whereas 3A was localized to the ER, as labeled by calreticulin, in ACBD3^{KO} cells (Fig. 4B-D). This suggests that 3A cannot localize to the Golgi without ACBD3, which may contribute to the lack of PI4KB recruitment. Collectively, our results suggest that ACBD3 is not merely a mediator between 3A and PI4KB, but plays a central role in recruiting 3A and PI4KB to facilitate virus replication.

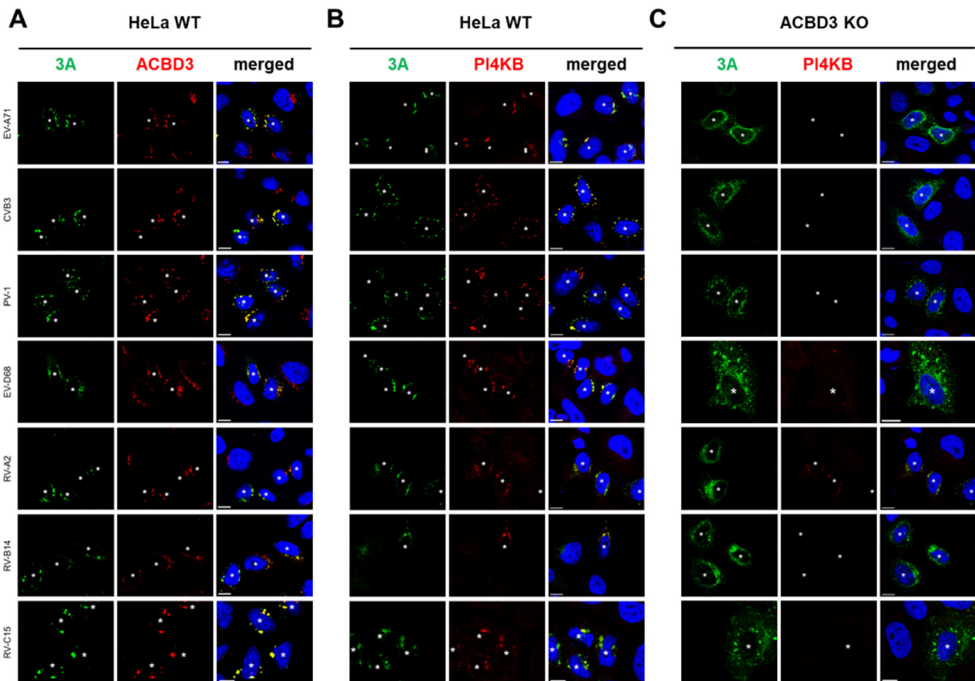


Figure 3. Effects of ACBD3 knockout on the localization of enterovirus 3A proteins and the recruitment of PI4KB. (A) HeLa^{wt} and (B) ACBD3^{KO} cells were transfected with plasmids encoding myc-tagged EV-A71 3A, CVB3 3A, PV-1 3A, or EGFP-tagged EV-D68 3A, RV-2 3A, RV-14 3A. The next day, cells were fixed and stained with antibodies against the myc tag to detect 3A (in the case of myc-3A), ACBD3, or PI4KB. Asterisks indicate 3A expressing cells. Nuclei were stained with DAPI (blue). Scale bars represent 10 μ m.

Exogenous expression of wt ACBD3 in ACBD3^{KO} cells restores 3A localization, PI4KB recruitment, and enterovirus replication.

To confirm that ACBD3 recruits 3A to the Golgi and mediates the interaction between 3A and PI4KB, we tested whether reconstitution of GFP-tagged ACBD3 in ACBD3^{KO} cells can restore 3A localization and PI4KB recruitment. As a negative control, we used a Golgi localized GFP (i.e., GFP coupled to the amino acids 1-60 of galactosyltransferase [GalT]), which failed to restore 3A localization (Fig. 5A; top panel) and PI4KB recruitment (Fig. 5B; top panel). When wt ACBD3 was reconstituted, 3A regained its punctate localization (Fig. 5A; middle panel) and PI4KB was recruited to the same sites (Fig. 5B; middle panel). ACBD3 expressed without 3A was found in the Golgi, where it colocalized with giantin, but no concentrated PI4KB was observed (Fig. S6). These results indicate that proper 3A localization and PI4KB recruitment by 3A depend on ACBD3.

ACBD3 forms a tight complex with PI4KB [16]. Recently, it was reported that one or two amino substitution(s) in the Q domain of ACBD3 (F258A or F258A/Q259A) can abrogate binding between purified recombinant ACBD3 and PI4KB in pull-down experiments [16, 17]. We confirmed that the F258A/Q259A mutant (hereafter called “FQ” mutant) lost its interaction with PI4KB by co-immunoprecipitation (Fig. S7) and employed this mutant to test whether the ACBD3-PI4KB interaction is required for PI4KB recruitment and efficient enterovirus replication. Expression of the ACBD3-FQ mutant restored the punctate localization of 3A (Fig. 5A; bottom panel) but did not support PI4KB recruitment (Fig. 5B; bottom panel). Furthermore, exogenous expression of wt ACBD3 in ACBD3^{KO} cells restored replication of CVB3 to a level comparable to HeLa^{wt} cells, while the negative control (GalT) and ACBD3-FQ mutant could not restore virus replication in ACBD3^{KO} cells (Fig. 5C). Taken together, we showed that 3A localization to the Golgi-derived membranes occurs in an ACBD3-dependent manner and that the interaction between ACBD3-PI4KB is crucial for PI4KB recruitment and efficient virus replication.

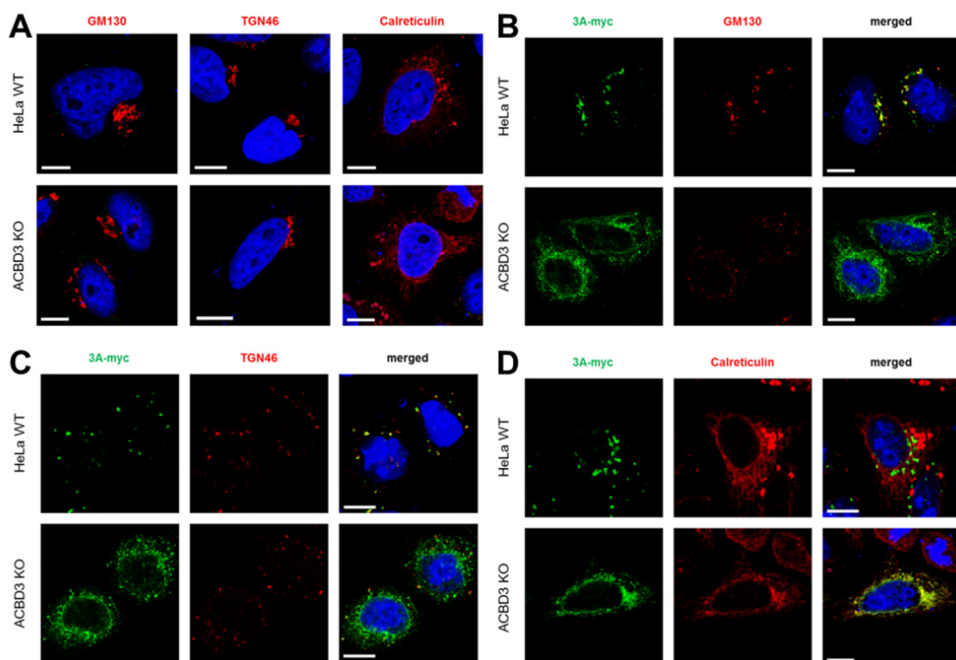


Figure 4. The localization of 3A differs between HeLa^{WT} cells and ACBD3^{KO} cells. (A) Golgi and ER integrity in ACBD3^{KO} cells. HeLa^{WT} and ACBD3^{KO} cells were fixed and stained with antibodies against the Golgi markers GM130 and TGN46 or the ER marker calreticulin. (B-D) HeLa^{WT} and ACBD3^{KO} cells were transfected with plasmid encoding myc-tagged CVB3 3A. The next day, cells were fixed and stained with an antibody against the myc tag to detect 3A and with antibodies against GM130 (B), TGN46 (C), or calreticulin (D). Nuclei were stained with DAPI (blue). Scale bars represent 10 μm.

Reconstituted wt PI4KB in PI4KB^{KO} cells can be recruited to membranes through the 3A-ACBD3-PI4KB interaction, thereby restoring enterovirus replication.

PI4KB is recruited by 3A to ROs during enterovirus replication [8, 9], and depletion of PI4KB by RNAi [9] or pharmacologic inhibition (reviewed in [28]) have been shown to suppress virus replication. Enterovirus mutants resistant to inhibitors of PI4KB contain single amino acid substitutions in the 3A protein (e.g., H57Y for CVB3). CVB3 replication is severely impaired in PI4KB^{KO} cells that we generated

by CRISPR/Cas9 technology (Fig. S1B), while the resistant mutant virus (3A-H57Y) replicated well in PI4KB^{KO} cells (Fig. 6A).

Two PI4KB mutants (I43A and D44A) were previously shown to reduce binding between recombinant PI4KB and ACBD3 in vitro [16, 17]. In agreement with this, the I43A mutant failed to co-immunoprecipitate ACBD3 from cells (Fig. S7). While wt PI4KB reconstituted in PI4KB^{KO} cells colocalized with 3A and ACBD3 (Fig. 6B-C; top panel), the PI4KB-I43A mutant did not colocalize with 3A and ACBD3, and instead mostly localized to the nucleus (middle panel). Unexpectedly, the D44A mutant did colocalize with 3A and ACBD3 (bottom panel). In line with this, wt PI4KB and the D44A mutant could restore enterovirus replication in PI4KB^{KO} cells, while the I43A mutant and the negative controls, EGFP and a PI4KB kinase-dead mutant that lacks catalytic activity (PI4KB-KD) could not (Fig. 6D). Why the D44A mutant behaves differently from the I43A mutant is presently unclear. Possibly, the D44A mutant has residual interaction with ACBD3 that could not be detected in vitro. Nevertheless, these results imply that the interaction between ACBD3 and PI4KB is important for enterovirus replication.

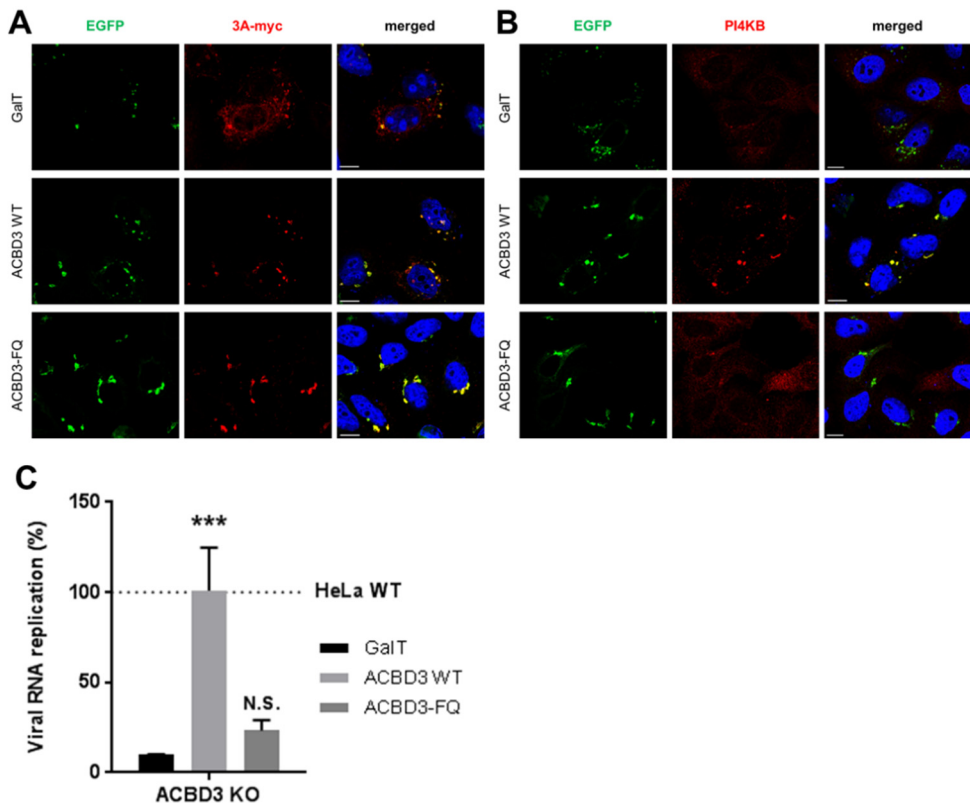


Figure 5. Reconstitution of wt ACBD3 but not ACBD3-FQ mutant rescues PI4KB recruitment and CVB3 replication. (A and B) HeLa ACBD3^{KO} cells were co-transfected with plasmids encoding myc-tagged CVB3 3A and EGFP-tagged GalT, ACBD3 wt, or ACBD3-FQ mutant. The next day, cells were fixed and stained with antibodies against the myc tag to detect 3A (A) or against PI4KB (B). Nuclei were stained with DAPI (blue). Scale bars represent 10 μ m. (C) HeLa^{wt} and ACBD3^{KO} cells were transfected with plasmids encoding EGFP-tagged GalT, ACBD3 wt, or ACBD3-FQ mutant. At 24 h post transfection (p.t.), cells were infected with RlucCVB3 at an MOI of 0.1. After 8 h, cells were lysed to determine luciferase activity. Bars represent the mean of triplicate values \pm SEM. Values were statistically evaluated compared to the EGFP-GalT control using a one-way ANOVA. ***, $p < 0.001$; N.S., not significant.

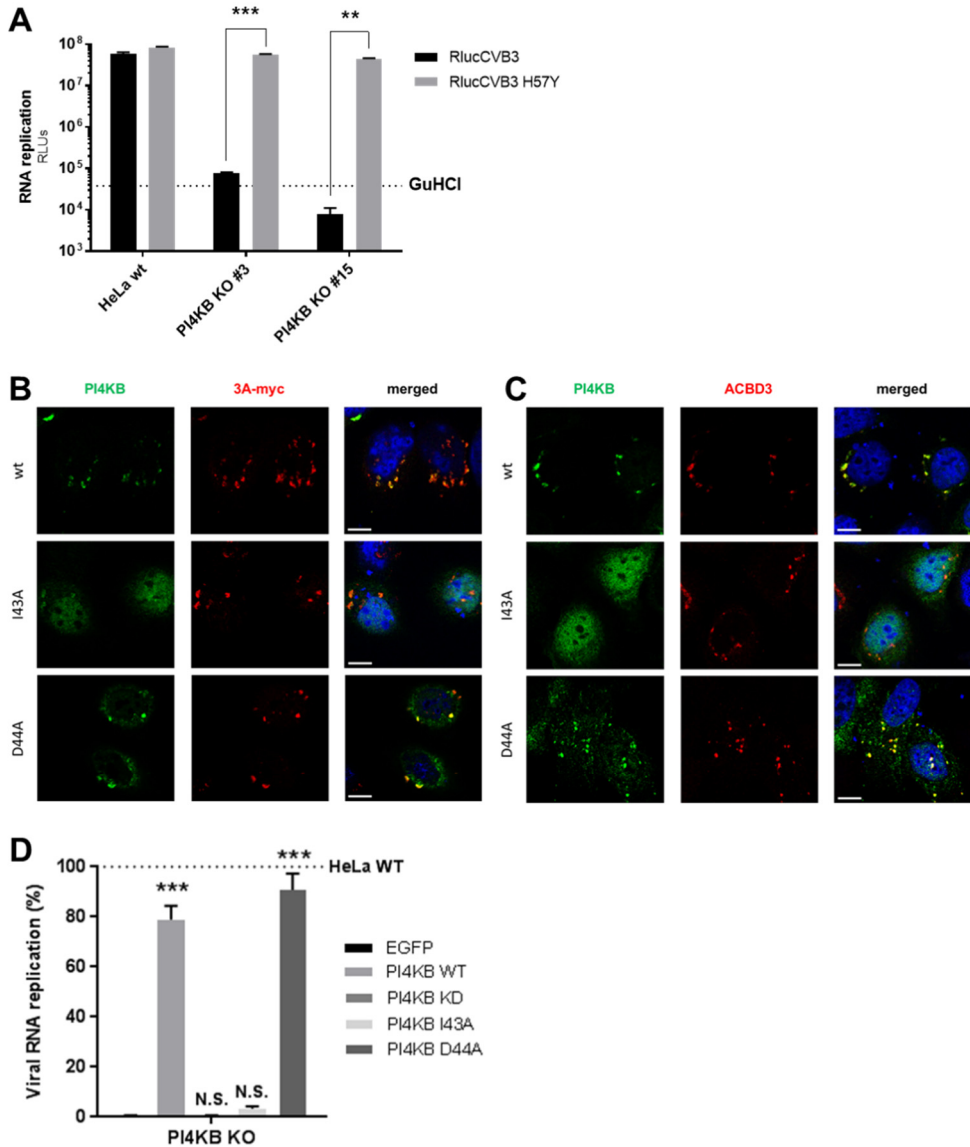


Figure 6. A PI4KB mutant, which does not interact with ACBD3, cannot be recruited by 3A and cannot restore virus replication in PI4KB^{KO} cells. (A) RNA replication of CVB3 mutant in PI4KB^{KO} cells. HeLa^{wt} cells and two PI4KB^{KO} cell clones were infected with wt or 3A-H57Y mutant CVB3 reporter viruses carrying a Renilla luciferase (RlucCVB3) at an MOI 0.1. Guanidine hydrochloride (GuHCl), a replication inhibitor, was included as a control. After 8 h, cells were lysed to determine luciferase activity. Bars represent the mean of triplicate values \pm SEM. Values were statistically evaluated using a two-tailed paired t-test. **, $p < 0.01$; ***, $p < 0.001$. (B, C) HeLa PI4KB^{KO} cells were co-transfected with plasmids encoding myc-tagged CVB3 3A and FLAG-tagged PI4KB wt, PI4KB-I43A or D44A mutants. The next day, cells were fixed and stained with antibodies against the FLAG tag to detect PI4KB and against the myc tag to detect 3A (B) or against ACBD3 (C). Nuclei were stained with DAPI (blue). Scale bars represent 10 μ m. (D) HeLa^{wt} and PI4KB^{KO} cells were transfected with plasmids encoding EGFP-tagged GalT, FLAG-tagged PI4KB wt, PI4KB-I43A or D44A mutants. At 24 h p.t., cells were infected with RlucCVB3 at an MOI of 0.1. After 8 h, cells were lysed to determine luciferase activity. Bars represent the mean of triplicate values \pm SEM. Values were statistically evaluated compared to the EGFP-GalT control using a one-way ANOVA. ***, $p < 0.001$; N.S., not significant.

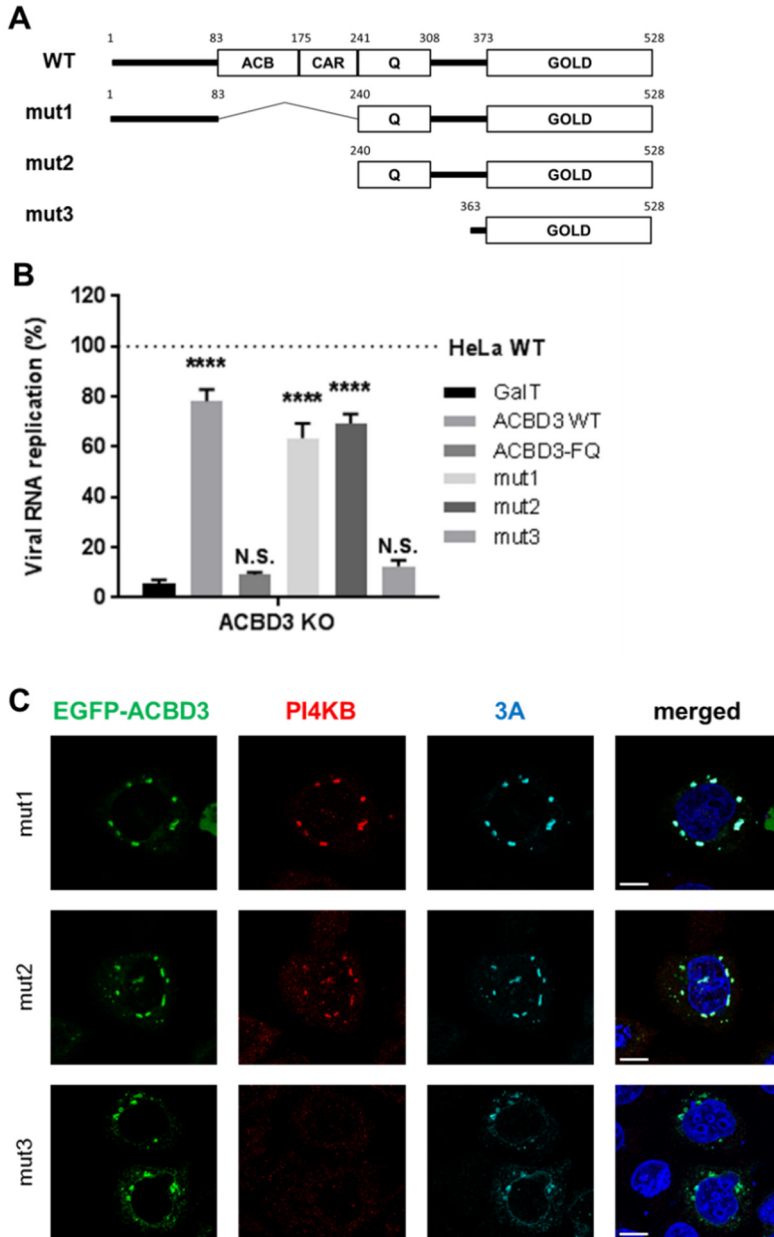


Figure 7. The Q and GOLD domains of ACBD3 are sufficient to support proper 3A localization, PI4KB recruitment, and enterovirus replication. (A) Schematic representation of full-length ACBD3 and its N-terminal deletion mutants (mut1-3). ACBD3 contains the acyl-CoA binding (ACB) domain, the charged amino acids region (CAR), the glutamine rich (Q) domain, and the Golgi dynamics domain (GOLD). Numbers indicate amino-acid positions. (B) HeLa^{wt} and ACBD3^{KO} cells were transfected with plasmids encoding EGFP-tagged GalT, ACBD3 wt, ACBD3-FQ mutant, or ACBD3 N-terminal deletion mutants (mut1-3). At 24 h p.t., cells were infected with RLucCVB3 at an MOI of 0.1. After 8 h, cells were lysed to determine luciferase activity. Bars represent the mean of triplicate values \pm SEM. Values were statistically evaluated compared to the EGFP control using a one-way ANOVA. ****, $p < 0.0001$; N.S., not significant. (C) HeLa ACBD3^{KO} cells were co-transfected with plasmids encoding myc-tagged CVB3 3A and EGFP-tagged ACBD3 wt, or ACBD3 N-terminal deletion mutants (mut1-3). The next day, cells were fixed and stained with the antibodies against PI4KB (red) and the myc tag to detect 3A (light blue) or. Nuclei were stained with DAPI (blue). Scale bars represent 10 μ m.

Enterovirus replication does not require the ACB and CAR domains of ACBD3.

Four domains are recognized in ACBD3; the acyl-CoA binding (ACB) domain, the charged amino acids region (CAR), the glutamine-rich region (Q), and the Golgi dynamics domain (GOLD) (Fig. 7A). The ACB domain, which is relatively conserved among all known ACBD proteins (ACBD1-7), has been suggested to be important for binding to long-chain acyl-CoA [29], and for binding to sterol regulatory element binding protein 1 (SREBP1) causing reduction of de novo palmitate synthesis [30]. The CAR domain contains a nuclear localization signal [31], yet the function of the CAR domain is unknown. The Q domain interacts with the N-terminal helix of PI4KB (12, 18). The GOLD domain interacts with giantin, and by doing so, tethers ACBD3 to the Golgi membrane [31]. Enterovirus and Kobuvirus 3A proteins bind to the GOLD domain, most probably at the same site as giantin [7, 18]. To investigate the importance of the ACB and CAR domains for enterovirus replication we tested whether N-terminal deletion mutants of ACBD3 could restore enterovirus replication in ACBD3^{KO} cells. Mut1 and mut2, which contain intact Q and GOLD domains, could restore virus replication to a level comparable to cells reconstituted with wt ACBD3 (Fig. 7B). This is in alignment with our observation that these mutants colocalize with 3A and PI4KB in ACBD3^{KO} cells (Fig. 7C). In contrast, mut3, which contains only the GOLD domain, could not rescue virus replication (Fig. 7B) or PI4KB recruitment (Fig. 7C), like the negative controls (GalT and the FQ mutant) (Fig. 7B), even though all mutants colocalized with 3A (Fig. 7C). Of note, although mut3 and 3A colocalized in punctate structures, they also partly co-localized to reticular and nuclear envelope-like structures, which may indicate that PI4KB also plays a role in firmly localizing 3A and ACBD3 to Golgi-derived membranes. These results indicate that enterovirus replication requires the Q and GOLD domains of ACBD3 for localization of viral protein 3A to the Golgi and for hijacking PI4KB.

DISCUSSION

Both enteroviruses and kobuviruses of the Picornaviridae family co-opt PI4KB to build up ROs. Viral protein 3A is responsible for PI4KB recruitment to enterovirus replication sites, yet the underlying mechanism has remained elusive. Despite the direct interaction between ACBD3 and enterovirus 3A proteins [8, 18], there has not yet been a consensus about the importance of ACBD3 for enterovirus replication and PI4KB recruitment. Previously, we observed no inhibition of CVB3 and RV replication and no effects on PI4KB recruitment, even though more than 90% of ACBD3-knockdown was achieved by siRNA [18, 19]. In the present study in which we use ACBD3^{KO} cells, we showed that ACBD3 is an important host factor for replication of four different human enterovirus species (EV-A/B/C/D) and two rhinovirus species (RV-A/B). All viruses showed impaired growth in ACBD3^{KO} cells (Fig. 1 and S2). In addition, neither virus infection (Fig. 2) nor the expression of enterovirus 3A proteins alone (Fig. 3) elicited PI4KB recruitment in the absence of ACBD3. In agreement with our data, the inhibition of EV-A71 and CVB3 was recently reported in ACBD3^{KO} cells [32-34]. The discrepancy in the role of ACBD3 from KD to KO condition could result from insufficient suppression of ACBD3 function by RNA interference. In fact, this implicates that the small amounts (~10%) of ACBD3 that remained after knockdown is sufficient to support enterovirus replication and PI4KB recruitment. Similar issues on the differences between knockdown and knockout have been raised by others [35]. For instance, the importance of cyclophilin A (CypA) in nidovirus replication was only prominent in CypA knockout cells but not in knockdown condition, even though CypA protein was undetectable after knockdown [36].

We observed that the lack of ACBD3 has a profound effect on enterovirus 3A protein localization. 3A proteins were found almost exclusively at the ER in ACBD3^{KO} cells (Fig. 4D), whereas in HeLa^{wt} cells they showed a punctate localization mostly on Golgi-derived membranes (Fig. 4B-C). Upon reconstitution of wt ACBD3 in ACBD3^{KO} cells, the localization of 3A was restored to a punctate pattern (Fig. 5A). These findings hint at a new role of ACBD3 for enterovirus replication, which is more than merely being a connector between 3A proteins and PI4KB.

Considering that ACBD3 is involved in several different protein complexes, enteroviruses may take advantage of ACBD3 in several ways, more than just for PI4KB recruitment. ACBD3 may be a scaffold responsible for positioning 3A near cellular factors, including other ACBD3-interacting proteins, required for RO formation. For example, ACBD3 and PV1 3A were found in a protein complex together with the putative Rab33 GTPase-activating proteins TBC1D22A/B [37]. In addition, several Golgi stacking proteins such as Golgin45 and Golgi reassembly stacking protein 2 (GORASP2) were recently identified as novel interaction partners of ACBD3, and ACBD3 was proposed as a scaffold tethering Golgin45, GRASP55, and TBC1D22 for the formation of a Golgi cisternal adhesion complex at the medial Golgi [38]. It is largely unknown which domains of ACBD3 are responsible for the interaction with the above-mentioned interacting partners, and whether these proteins are recruited to enterovirus ROs also remains to be investigated.

The GOLD domain of ACBD3 is responsible for the interaction with enterovirus 3A protein [18, 37], while the Q domain interacts with PI4KB [16, 17]. By utilizing mutants of ACBD3 or PI4KB which disturb the interaction with each other (Fig. 5 and 7), we show for the first time that the interaction between ACBD3 and PI4KB is crucial for enterovirus replication. Aside from the Q and GOLD domains, other domains (i.e., ACB and CAR) of ACBD3 seem to be not involved in enterovirus replication (Fig. 7). This indicates that the functions of the ACB and CAR domains, as well as the cellular proteins and/or lipids that interact with these domains, are unlikely required for enterovirus replication. Although we cannot exclude that additional or unidentified proteins that bind to the Q or GOLD domains of ACBD3 might also be important for enterovirus replication, our findings suggest that ACBD3 mainly serves to coordinate 3A and PI4KB recruitment at RO membranes, involving the Q and GOLD domains.

How exactly enterovirus 3A protein interacts with ACBD3 needs to be further investigated. The GOLD domain of ACBD3 interacts with enterovirus 3A proteins [18]. Similarly, kobuvirus 3A interacts with the ACBD3 GOLD domain and the crystal structure of kobuvirus 3A in complex with the ACBD3 GOLD domain was revealed recently [6]. According to this structure, kobuvirus 3A wraps ACBD3 and stabilizes ACBD3 on membranes through the membrane-binding features at the myristoylated N-terminal and hydrophobic C-terminal ends of 3A. However, enterovirus 3A proteins can bind to membranes only through the hydrophobic C-terminus, and the 3A proteins of enteroviruses differ greatly in sequence from kobuvirus 3A. Therefore, the way by which enterovirus 3A interacts with ACBD3 could be different from kobuvirus. Thus, structural insight into the enterovirus 3A - ACBD3 GOLD complex is urgently required to understand how enterovirus 3A interacts with ACBD3.

In conclusion, our study reveals that enteroviruses employ a conserved mechanism to recruit PI4KB, which depends on the Golgi-residing protein ACBD3. Furthermore, we suggest that ACBD3 tethers viral and host proteins to form ROs. Considering the pan-enteroviral dependency on ACBD3, targeting ACBD3 or the 3A-ACBD3 interaction presents as a novel strategy for broad-spectrum antiviral drug development.

MATERIALS AND METHODS

Cells and culture conditions. HAP1^{wt} cells and HAP1 ACBD3^{KO} cells were obtained from Horizon Discovery. HeLa R19 cells were obtained from G. Belov (University of Maryland and Virginia-Maryland College of Veterinary Medicine, US). HAP1 cells were cultured in IMDM (Thermo Fisher Scientific) supplemented with 10% fetal calf serum (FCS) and penicillin–streptomycin. HeLa cells and HEK 293T cells (ATCC CRL-3216) were cultured in DMEM (Lonza) supplemented with 10% FCS and penicillin–streptomycin. All cells were grown at 37°C in 5% CO₂.

Generation of CRISPR-Cas9 knockout cell line. HeLa ACBD3^{KO} and PI4KB^{KO} cells were generated with CRISPR/Cas9 technology as described previously [39]. In brief, gRNA encoding oligonucleotides cassettes (gRNA1: 5'-GCTGAACGCAGAGCGACTCG-3', gRNA2: 5'-TCGCCACTGGATCCGGTGC-3' for ACBD3; gRNA1: 5'-GTGTGGGTACACGGACCACG-3', gRNA2: 5'-GAGACTCGGGCAGGGAGCTTA-3' for PI4KB) were cloned into the SapI restriction sites of the pCRISPR-hCas9-2xgRNA-Puro plasmid. HeLa R19 cells were transfected with the resulting plasmid. Single-cell clones were generated using end-point dilutions. Knock-out was verified by sequence analysis of the genomic DNA and by Western Blot analysis (Figs. S1A, S1B).

Viruses. The following enteroviruses were used: EV-A71 (strain BrCr, obtained from the National Institute for Public Health and Environment; RIVM, The Netherlands), CVB3 (strain Nancy, obtained by transfection of the infectious clone p53CB3/T7 as described previously [40]), RlucCVB3, RlucCVB3 3A-H57Y (obtained by transfection of infectious clones pRluc-53CB3/T7 as described previously [22]), RlucEMCV (strain Mengovirus, obtained by transfection of the infectious clone pRluc-QG-M16.1 as described previously [41]), PV1 (strain Sabin, ATCC), EV-D68 (strain Fermon, obtained from RIVM, The Netherlands), RV-2 and RV-14 (obtained from Joachim Seipelt, Medical University of Vienna, Austria). Virus titers were determined by end-point titration analysis and expressed as 50% tissue culture infectious dose (TCID₅₀).

Virus infection. Virus infections were carried out by incubating subconfluent HAP1 or HeLa cells for 30 min with virus. Following virus removal, fresh medium or medium containing the control inhibitors guanidine hydrochloride (2 mM) or dipyrindamole (100 μM) was added to the cells. To determine one-step growth kinetics for each virus, infected cells were frozen from 2 to 16 h post infection (p.i.). Virus titers were determined by end-point titration analysis and expressed as 50% tissue culture infectious dose (TCID₅₀). To check for the recruitment of PI4KB upon virus replication, cells were fixed for immunofluorescence staining as described in below section separately. To check genome replication by measuring intracellular Renilla luciferase activity, cells were lysed at 8 h p.i. and followed the manufacturer's protocol (Renilla luciferase assay system; Promega).

RNA transfection. The subgenomic replicons of CVB3 [10] and EV-A71 [42] were described previously. HeLa cells were transfected with RNA transcripts of replicon constructs. After 7 h, cells were lysed to determine intracellular firefly luciferase activity.

Plasmids. p3A(CVB3)-myc [27], pEGFP-3A(RV-2), and pEGFP-3A(RV-14) were described previously [19]. p3A(EV-A71)-myc, p3A(PV1)-myc, pEGFP-3A(EV-D68), and pEGFP-3A(RV-C15) were prepared by cloning cDNA encoding EV-A71 and PV1 3A into p3A(CVB3)-myc vectors from which CVB3 3A was excised using restriction enzyme sites Sall and BamHI, and EV-D68 and RV-C15 3A into pEGFP vectors using restriction enzyme sites BglII and BamHI. pEGFP-GalT was a gift from Jennifer Lippincott-Schwartz (Addgene plasmid #11929). pEGFP-ACBD3 was a gift from Carolyn E. Machamer (Johns Hopkins University, USA). pEGFP-ACBD3-FQ and pEGFP-ACBD3-mut1/mut2/mut3 were generated by using Q5 Site-Directed Mutagenesis kit (New England BioLabs). pCDNA3-FLAG-PI4KB(wt) was a gift from Tamas Balla (NIH, USA). pCDNA3-FLAG-PI4KB(D671A) (KD: kinase activity dead mutant), pCDNA3-FLAG-PI4KB(I43A), and pCDNA3-FLAG-PI4KB(D44A) were generated by using Q5 Site-Directed Mutagenesis kit (New England BioLabs).

Replication rescue assay. HeLa cells were transfected with plasmids carrying wt or mutant ACBD3 (FQ, mut1, mut2, mut3), wt or mutant PI4KB (I43A, D44A), Golgi-targeting EGFP (pEGFP-GalT) or kinase-dead PI4KB (PI4KB-KD) as a negative control. At 24 h post transfection, the cells were infected with RlucCVB3. At 8 h p.i., the intracellular Renilla luciferase activity was determined by using the Renilla luciferase assay system (Promega).

Antibodies. The rabbit antiserum and the mouse monoclonal antibody against CVB3 3A were described previously [18, 26]. Mouse monoclonal antibodies included anti-ACBD3 (Sigma), anti-myc (Sigma), anti-GM130 (BD Biosciences), anti-Giantin (Enzo Life Science). Rabbit polyclonal antibodies included anti-PI4KB (Millipore), anti-myc (Thermo Fisher Scientific), anti-TGN46 (Novus Biologicals), anti-Calreticulin (Sigma), anti-FLAG (Sigma), anti-EGFP (a gift from J. Fransen, NCMLS, Nijmegen, The Netherlands). Conjugated goat anti-rabbit and goat anti-mouse Alexa Fluor 488, 596, or 647 (Molecular Probes) were used as secondary antibodies for immunofluorescence analysis. For Western Blot analysis, IRDye goat anti-mouse or anti-rabbit (LI-COR) were used.

Immunofluorescence microscopy. HeLa cells were grown on coverslips in 24-well plates. Subconfluent cells were transfected with 200 ng of plasmids using Lipofectamine 2000 (Thermo Fisher Scientific) according to the manufacturer's protocol or infected with CVB3 at an MOI of 5. At 16 h post transfection (p.t.) or 5-9 h p.i., cells were fixed with 4% paraformaldehyde for 15 min at room temperature. After permeabilization with 0.1% Triton X-100 in PBS for 5 min, cells were incubated with primary and secondary antibodies diluted in 2% normal goat serum in PBS. Nuclei were stained with DAPI. Coverslips were mounted with FluorSave (Calbiochem), and confocal imaging was performed with a Leica Spell confocal microscope.

Western blot analysis. HAP1 and HeLa cells were harvested and lysed by TEN-lysis buffer (50 mM TrisHCl pH 7.4, 150 mM NaCl, 1 mM EDTA, 1% NP-40, 0.05% SDS). After 30 min incubation on ice, lysates were centrifuged for 20 min at 10,000 xg. Supernatants were boiled in Laemmli sample buffer for 5 min at 95°C. Samples were run on polyacrylamide gels and transferred to a PVDF membrane (Bio-Rad). Membranes were sequentially incubated with primary antibody against ACBD3 or PI4KB at 4°C overnight and secondary antibodies against mouse IgG or rabbit IgG for 1h at room temperature. Images were acquired with an Odyssey imaging system (LI-COR).

ACKNOWLEDGMENTS

We thank the Center for Cell Imaging (Faculty of Veterinary Medicine, Utrecht University) for support with microscopy experiments. This work was supported by research grants from the Netherlands Organisation for Scientific Research (NWO-VENI-863.12.005 to HMvdS, NWO-VENI-722.012.066 to JRPMS, NWO-VICI-91812628, NWO-ECHO-711.017.002 and ERASysApp project 'SysVirDrug' ALW project number 832.14.003 to FJMvK) and from the European Union (Horizon 2020 Marie Skłodowska-Curie ETN 'EU VIRNA', grant agreement number 264286 and 'ANTIVIRALS', grant agreement number 642434 to FJMvK).

CONFLICTS OF INTEREST

The authors declare no conflict of interest. The sponsors had no role in the design of the study; in the collection, analyses, or interpretation of data; in the writing of the manuscript, and in the decision to publish the results.

REFERENCES

1. Tapparel, C., et al., Picornavirus and enterovirus diversity with associated human diseases. *Infect Genet Evol*, 2013. 14: p. 282-93.
2. Belov, G.A. and F.J.M. van Kuppeveld, (+) RNA viruses rewire cellular pathways to build replication organelles. *Curr Opin Virol*, 2012. 2(6): p. 740-747.
3. Miller, S. and J. Krijnse-Locker, Modification of intracellular membrane structures for virus replication. *Nat Rev Microbiol*, 2008. 6: p. 363.
4. Nagy, P.D. and J. Pogany, The dependence of viral RNA replication on co-opted host factors. *Nat Rev Microbiol*, 2011. 10: p. 137.
5. Paul, D. and R. Bartenschlager, Architecture and biogenesis of plus-strand RNA virus replication factories. *World J Virol*, 2013. 2(2): p. 32-48.
6. Klima, M., et al., Kobuviral Non-structural 3A Proteins Act as Molecular Harnesses to Hijack the Host ACBD3 Protein. *Structure*, 2017. 25(2): p. 219-230.
7. Sasaki, J., et al., ACBD3-mediated recruitment of PI4KB to picornavirus RNA replication sites. *EMBO J*, 2012. 31(3): p. 754-66.
8. Greninger, A.L., et al., The 3A protein from multiple picornaviruses utilizes the golgi adaptor protein ACBD3 to recruit PI4KIIIbeta. *J Virol*, 2012. 86(7): p. 3605-16.
9. Hsu, N.Y., et al., Viral reorganization of the secretory pathway generates distinct organelles for RNA replication. *Cell*, 2010. 141(5): p. 799-811.
10. Lanke, K.H., et al., GBF1, a guanine nucleotide exchange factor for Arf, is crucial for coxsackievirus B3 RNA replication. *J Virol*, 2009. 83(22): p. 11940-9.
11. Ishikawa-Sasaki, K., J. Sasaki, and K. Taniguchi, A Complex Comprising Phosphatidylinositol 4-Kinase III β , ACBD3, and Aichi Virus Proteins Enhances Phosphatidylinositol 4-Phosphate Synthesis and Is Critical for Formation of the Viral Replication Complex. *J Virol*, 2014. 88(12): p. 6586-6598.
12. Levine, T.P. and S. Munro, Targeting of Golgi-specific pleckstrin homology domains involves both PtdIns 4-kinase-dependent and -independent components. *Curr Biol*, 2002. 12(9): p. 695-704.
13. Mesmin, B., et al., A four-step cycle driven by PI(4)P hydrolysis directs sterol/PI(4)P exchange by the ER-Golgi tether OSBP. *Cell*, 2013. 155(4): p. 830-43.
14. Strating, J.R., et al., Itraconazole inhibits enterovirus replication by targeting the oxysterol-binding protein. *Cell Rep*, 2015. 10(4): p. 600-15.
15. Godi, A., et al., ARF mediates recruitment of PtdIns-4-OH kinase-beta and stimulates synthesis of PtdIns(4,5)P₂ on the Golgi complex. *Nat Cell Biol*, 1999. 1(5): p. 280-7.
16. Klima, M., et al., Structural insights and in vitro reconstitution of membrane targeting and activation of human PI4KB by the ACBD3 protein. *Sci Rep*, 2016. 6: p. 23641.
17. McPhail, J.A., et al., The Molecular Basis of Aichi Virus 3A Protein Activation of Phosphatidylinositol 4 Kinase IIIbeta, PI4KB, through ACBD3. *Structure*, 2017. 25(1): p. 121-131.
18. Dorobantu, C.M., et al., Recruitment of PI4KIIIbeta to coxsackievirus B3 replication organelles is independent of ACBD3, GBF1, and Arf1. *J Virol*, 2014. 88(5): p. 2725-36.
19. Dorobantu, C.M., et al., GBF1- and ACBD3-independent recruitment of PI4KIIIbeta to replication sites by rhinovirus 3A proteins. *J Virol*, 2015. 89(3): p. 1913-8.
20. Teoule, F., et al., The Golgi protein ACBD3, an interactor for poliovirus protein 3A, modulates poliovirus replication. *J Virol*, 2013. 87(20): p. 11031-46.
21. Bochkov, Y.A., et al., Cadherin-related family member 3, a childhood asthma susceptibility gene product, mediates rhinovirus C binding and replication. *Proc Natl Acad Sci U S A*, 2015. 112(17): p. 5485-90.
22. van der Schaar, H.M., et al., Coxsackievirus mutants that can bypass host factor PI4KIIIbeta and the need for high levels of PI4P lipids for replication. *Cell Res*, 2012. 22(11): p. 1576-92.
23. Dorobantu, C.M., et al., Modulation of the Host Lipid Landscape to Promote RNA Virus Replication: The Picornavirus Encephalomyocarditis Virus Converges on the Pathway Used by Hepatitis C Virus. *PLoS Pathog*, 2015. 11(9): p. e1005185.
24. Bekier, M.E., et al., Knockout of the Golgi stacking proteins GRASP55 and GRASP65 impairs Golgi structure and function. *Mol Biol Cell*, 2017. 28(21): p. 2833-2842.
25. Liao, J., et al., ACBD3 is required for FAPP2 transferring glucosylceramide through maintaining the Golgi integrity. *J Mol Cell Biol*, 2018.
26. Wessels, E., et al., A viral protein that blocks Arf1-mediated COP-I assembly by inhibiting the guanine nucleotide exchange factor GBF1. *Dev Cell*, 2006. 11(2): p. 191-201.

27. Wessels, E., et al., Molecular determinants of the interaction between coxsackievirus protein 3A and guanine nucleotide exchange factor GBF1. *J Virol*, 2007. 81(10): p. 5238-45.
28. Bauer, L., et al., Direct-acting antivirals and host-targeting strategies to combat enterovirus infections. *Curr Opin Virol*, 2017. 24: p. 1-8.
29. Fan, J., et al., Acyl-coenzyme A binding domain containing 3 (ACBD3; PAP7; GCP60): an emerging signaling molecule. *Prog Lipid Res*, 2010. 49(3): p. 218-34.
30. Chen, Y., et al., Maturation and activity of sterol regulatory element binding protein 1 is inhibited by acyl-CoA binding domain containing 3. *PLoS One*, 2012. 7(11): p. e49906.
31. Sohda, M., et al., Identification and characterization of a novel Golgi protein, GCP60, that interacts with the integral membrane protein giantin. *J Biol Chem*, 2001. 276(48): p. 45298-306.
32. Lei, X., et al., The Golgi protein ACBD3 facilitates Enterovirus 71 replication by interacting with 3A. *Sci Rep*, 2017. 7: p. 44592.
33. Xiao, X., et al., Enterovirus 3A facilitates viral replication by promoting PI4KB-ACBD3 interaction. *J Virol*, 2017. 91(19): p. e00791-17.
34. Kim, H.S., et al., Arrayed CRISPR screen with image-based assay reliably uncovers host genes required for coxsackievirus infection. *Genome Res*, 2018.
35. Morgens, D.W., et al., Systematic comparison of CRISPR/Cas9 and RNAi screens for essential genes. *Nat Biotechnol*, 2016. 34: p. 634.
36. de Wilde, A.H., et al., Coronaviruses and arteriviruses display striking differences in their cyclophilin A-dependence during replication in cell culture. *Virology*, 2018. 517: p. 148-156.
37. Greninger, A.L., et al., ACBD3 interaction with TBC1 domain 22 protein is differentially affected by enteroviral and kobuviral 3A protein binding. *MBio*, 2013. 4(2): p. e00098-13.
38. Yue, X., et al., ACBD3 functions as a scaffold to organize the Golgi stacking proteins and a Rab33b-GAP. *FEBS Lett*, 2017. 591(18): p. 2793-2802.
39. Langereis, M.A., et al., Knockout of cGAS and STING Rescues Virus Infection of Plasmid DNA-Transfected Cells. *J Virol*, 2015. 89(21): p. 11169-73.
40. Wessels, E., et al., A proline-rich region in the coxsackievirus 3A protein is required for the protein to inhibit endoplasmic reticulum-to-golgi transport. *J Virol*, 2005. 79(8): p. 5163-73.
41. Albulescu, L., et al., Cholesterol shuttling is important for RNA replication of coxsackievirus B3 and encephalomyocarditis virus. *Cell Microbiol*, 2015. 17(8): p. 1144-56.
42. van der Schaar, H.M., et al., A novel, broad-spectrum inhibitor of enterovirus replication that targets host cell factor phosphatidylinositol 4-kinase IIIbeta. *Antimicrob Agents Chemother*, 2013. 57(10): p. 4971-81.

SUPPLEMENTAL MATERIAL

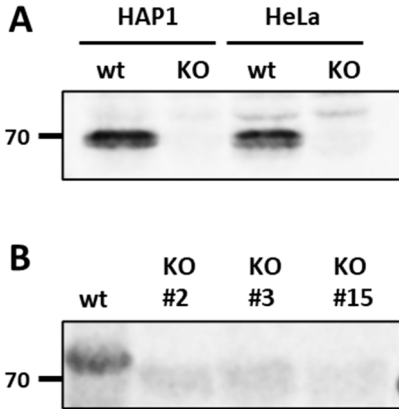


Figure S1. Generation of knockout cells using the CRISPR-Cas9 system. The knockout of ACBD3 in HAP1 and HeLa cells (A) and PI4KB in HeLa cells (three individual clones) (B) was confirmed by Western blot analysis of cell lysates.

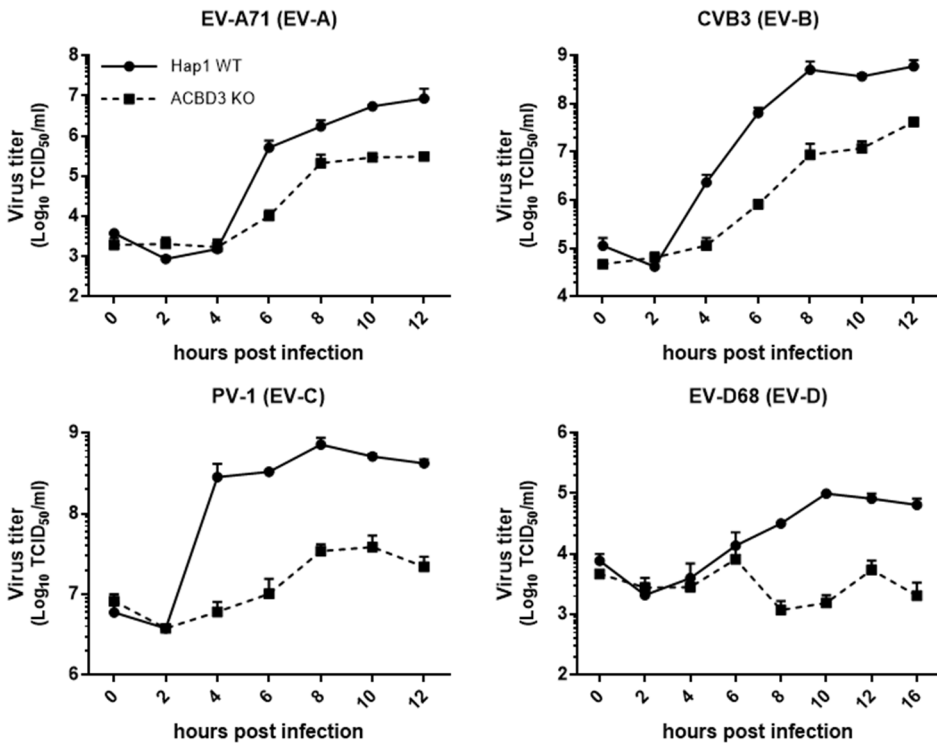


Figure S2. Enterovirus replication is inhibited in HAP1 ACBD3^{KO} cells. Growth curves of enteroviruses in HAP1^{wt} and ACBD3^{KO} cells. After infection at an MOI 3-5 for 30 min, the inoculum was removed and fresh medium was added to the cells. At the indicated time points, cells were freeze-thawed to determine the total virus titers by endpoint dilution.

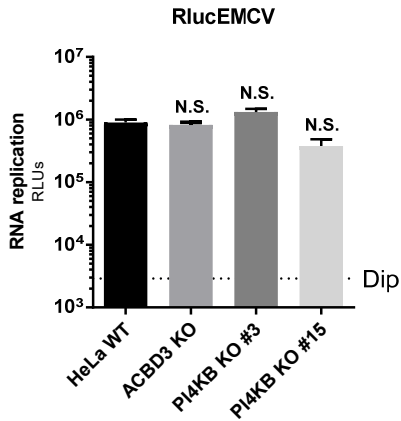


Figure S3. EMCV replication is not sensitive to ACBD3 or PI4KB depletion. HeLa^{wt}, ACBD3^{KO}, and PI4KB^{KO} cells were infected with wt EMCV reporter virus carrying a Renilla luciferase (RlucEMCV) at an MOI 0.1. After 8 h, cells were lysed to determine luciferase activity. Bars represent the mean of triplicate values \pm SEM. Dip: Dipyridamole, an inhibitor of EMCV replication. Values were statistically evaluated compared to the values of HeLa^{wt} cells using a one-way ANOVA. N.S., not significant.

5

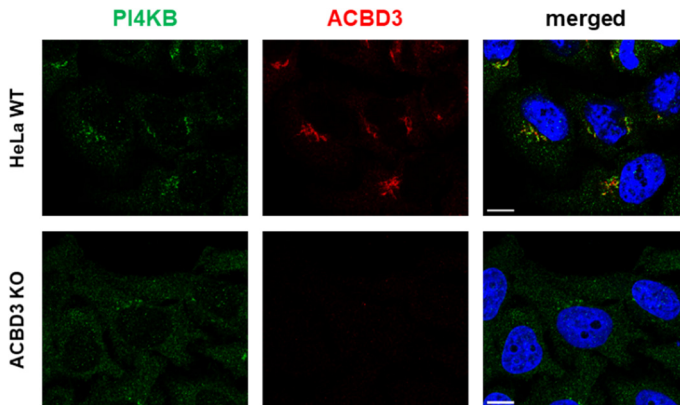


Figure S4. Localization of PI4KB in HeLa^{wt} and ACBD3^{KO} cells. HeLa^{wt} and ACBD3^{KO} cells were fixed and stained with antibodies against PI4KB (green) and ACBD3 (red). Nuclei were stained with DAPI (blue). Scale bars represent 10 μ m.

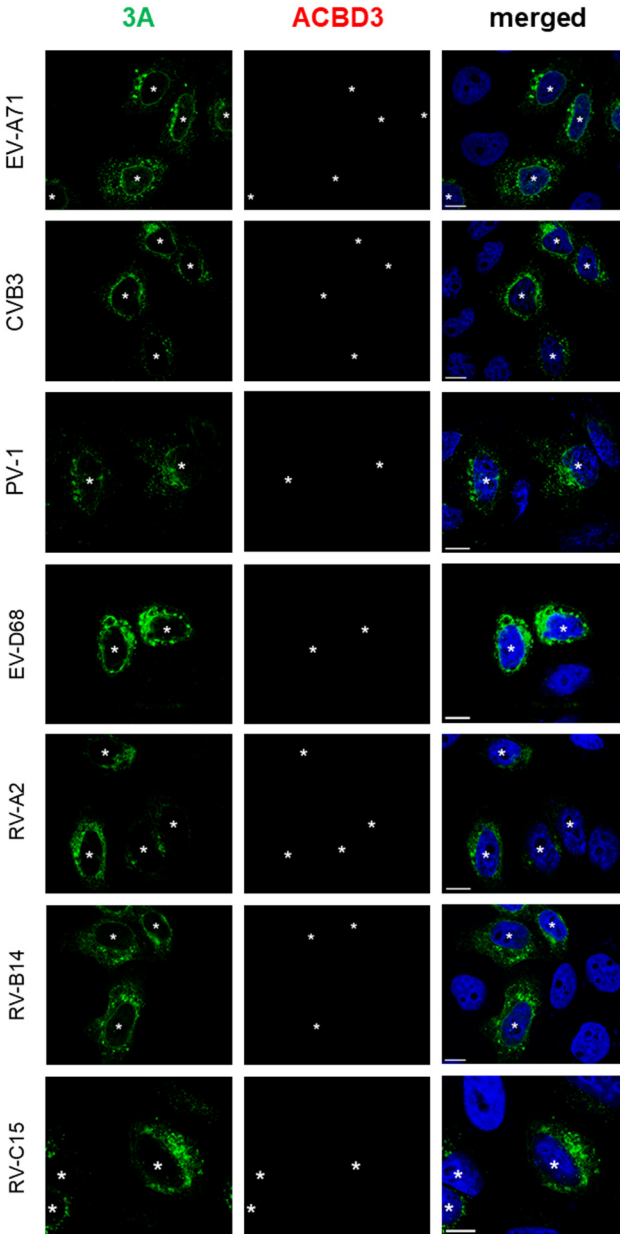


Figure S5. Localization of enterovirus 3A proteins in ACBD3^{KO} cells. HeLa ACBD3^{KO} cells were transfected with plasmids encoding myc-tagged EV-A71 3A, CVB3 3A, PV-1 3A, or EGFP-tagged EV-D68 3A, RV-2 3A, RV-14 3A. The next day, cells were fixed and stained with antibodies against the myc tag to detect 3A (green) and ACBD3 (red). Nuclei were stained with DAPI (blue). Asterisks indicate 3A expressing cells. Scale bars represent 10 μ m.

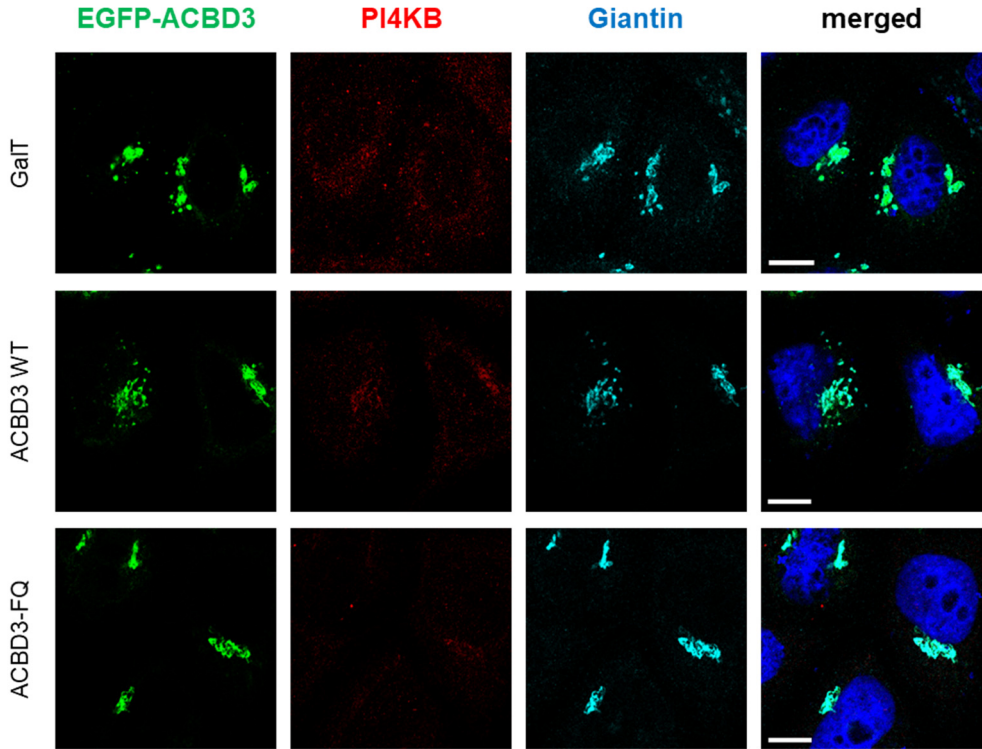


Figure S6. Effects of ACBD3 reconstitution on PI4KB localization in ACBD3^{KO} cells. HeLa ACBD3^{KO} cells were transfected with plasmids encoding EGFP-tagged GalT, ACBD3 wt, or ACBD3-FQ mutant. The next day, cells were fixed and stained with the antibodies against PI4KB (red) and Giantin (light blue). Nuclei were stained with DAPI (blue). Scale bars represent 10 μ m.

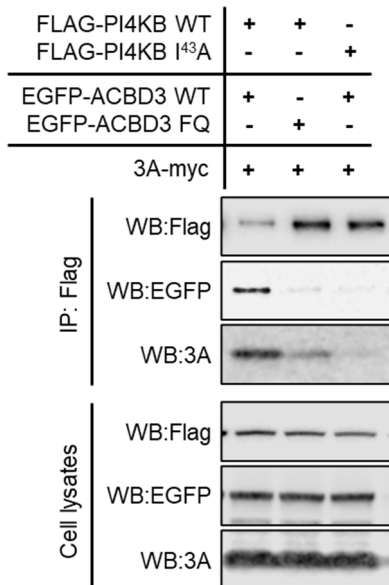


Figure S7. Co-immunoprecipitation of PI4KB with ACBD3 and enterovirus 3A protein. Because enterovirus 3A has been reported to enhance the interaction between ACBD3 and PI4KB (Xiao *et al.*, 2017), we evaluated the ACBD3-PI4KB interaction by co-immunoprecipitation in the presence of CVB3 3A. HEK293T cells were co-transfected with plasmids encoding FLAG-tagged PI4KB wt or I^{43A} mutant, EGFP-tagged ACBD3 wt or FQ mutant, and myc-tagged CVB3 3A. Immunocomplexes were captured by anti-FLAG beads and subjected to Western blot analysis. A PI4KB mutant (I^{43A}) and an ACBD3 mutant (FQ), which have reduced interaction between PI4KB-ACBD3 *in vitro* (Klima *et al.*, 2016; McPhail *et al.*, 2017), clearly disrupted this interaction in cells as well. As CVB3 3A was co-immunoprecipitated with wt PI4KB and ACBD3 but not with the mutants, we confirmed the formation of an enteroviral 3A-ACBD3-PI4KB ternary complex in which ACBD3 links 3A and PI4KB, which is in agreement with previous findings for EV-A71 (Xiao *et al.*, 2017).

CHAPTER 5

SUPPLEMENTAL METHOD

Immunoprecipitation. HEK293T cells were grown on 150 mm dishes. Subconfluent cells were transfected with in total 15 ug of plasmids using Lipofectamine 2000 (Thermo Fisher Scientific/Thermo) according to the manufacturer's protocol. At 24 h post transfection, cells were harvested and lysed by using lysis buffer (50 mM TrisHCl pH 7.4, 150 mM NaCl, 1 mM EDTA, 1 mM DTT, 10% Glycerol, 1% Triton X-100). After 30 min incubation on ice, lysates were centrifuged for 20 min at 10,000 xg. Supernatants were incubated with anti-FLAG M2 magnetic beads (Sigma) at 4°C for 2 h. Beads were washed 3 times with the lysis buffer and then incubated with Laemmli sample buffer for 5 min at 95°C. Eluted proteins were subjected to Western blot analysis.

SUPPLEMENTAL REFERENCES

- Xiao X, Lei X, Zhang Z, Ma Y, Qi J, Wu C, Xiao Y, Li L, He B, Wang J. 2017. Enterovirus 3A facilitates viral replication by promoting PI4KB-ACBD3 interaction. *J Virol.* 91:e00791-17
- Klima M, Toth DJ, Hexnerova R, Baumlova A, Chalupska D, Tykvart J, Rezaczkova L, Sengupta N, Man P, Dubankova A, Humpolickova J, Nencka R, Veverka V, Balla T, Boura E. 2016. Structural insights and in vitro reconstitution of membrane targeting and activation of human PI4KB by the ACBD3 protein. *Sci Rep* 6:23641.
- McPhail JA, Ottosen EH, Jenkins ML, Burke JE. 2017. The Molecular Basis of Aichi Virus 3A Protein Activation of Phosphatidylinositol 4 Kinase IIIbeta, PI4KB, through ACBD3. *Structure* 25:121-131.

CHAPTER 6

CONVERGENT EVOLUTION IN THE MECHANISMS OF ACBD3 RECRUITMENT TO PICORNAVIRUS REPLICATION SITES

Vladimira Horova¹, Heyrhyoung Lyoo², Bartosz Różycki³, Dominika Chalupska¹, Miroslav Smola¹, Jana Humpolickova¹, Jeroen RPM Strating², Frank JM van Kuppeveld^{2,}, Evzen Boura^{1,*}, Martin Klima^{1,*}*

¹Institute of Organic Chemistry and Biochemistry, Czech Academy of Sciences, Prague, Czech Republic

²Faculty of Veterinary Medicine, Utrecht University, Utrecht, The Netherlands

³Institute of Physics, Polish Academy of Sciences, Warsaw, Poland

*Corresponding author

ABSTRACT

Enteroviruses, members of the family of picornaviruses, are the most common viral infectious agents in humans causing a broad spectrum of diseases ranging from mild respiratory illnesses to life-threatening infections. To efficiently replicate within the host cell, enteroviruses hijack several host factors, such as ACBD3. ACBD3 facilitates replication of various enterovirus species, however, structural determinants of ACBD3 recruitment to the viral replication sites are poorly understood. Here, we present a structural characterization of the interaction between ACBD3 and the non-structural 3A proteins of four representative enteroviruses (poliovirus, enterovirus A71, enterovirus D68, and rhinovirus B14). In addition, we describe the details of the 3A-3A interaction causing the assembly of the ACBD3-3A heterotetramers and the interaction between the ACBD3-3A complex and the lipid bilayer. Using structure-guided identification of the point mutations disrupting these interactions, we demonstrate their roles in the intracellular localization of these proteins, recruitment of downstream effectors of ACBD3, and facilitation of enterovirus replication. These structures uncovered a striking convergence in the mechanisms of how enteroviruses and kobuviruses, members of a distinct group of picornaviruses that also rely on ACBD3, recruit ACBD3 and its downstream effectors to the sites of viral replication.

AUTHOR SUMMARY

Enteroviruses are the most common viruses infecting humans. They cause a broad spectrum of diseases ranging from common cold to life-threatening diseases, such as poliomyelitis. To date, no effective antiviral therapy for enteroviruses has been approved yet. To ensure efficient replication, enteroviruses hijack several host factors, recruit them to the sites of virus replication, and use their physiological functions for their own purposes. Here, we characterize the complexes composed of the host protein ACBD3 and the ACBD3-binding viral proteins (called 3A) of four representative enteroviruses. Our study reveals the atomic details of these complexes and identifies the amino acid residues important for the interaction. We found out that the 3A proteins of enteroviruses bind to the same regions of ACBD3 as the 3A proteins of kobuviruses, a distinct group of viruses that also rely on ACBD3, but are oriented in the opposite directions. This observation reveals a striking case of convergent evolutionary pathways that have evolved to allow enteroviruses and kobuviruses (which are two distinct groups of the *Picornaviridae* family) to recruit a common host target, ACBD3, and its downstream effectors to the sites of viral replication.

INTRODUCTION

Enteroviruses are small RNA viruses that belong to the *Enterovirus* genus of the *Picornaviridae* family. They are non-enveloped positive-sense single-stranded RNA viruses with icosahedral capsids, currently consisting of 15 species. Seven enterovirus species (Enterovirus A-D and Rhinovirus A-C) contain human pathogens, such as polioviruses, numbered enteroviruses, echoviruses, coxsackieviruses, and rhinoviruses. They cause a variety of diseases ranging from common cold to acute hemorrhagic conjunctivitis, meningitis, myocarditis, encephalitis, or poliomyelitis [1]. The genome of the enteroviruses encodes the capsid proteins and seven non-structural proteins (named 2A-2C and 3A-3D). The latter carry out many essential processes including genome replication, polyprotein processing, host membrane reorganization, and manipulation of intracellular trafficking. To facilitate these functions, several host factors are recruited to the sites of enterovirus replication through direct or indirect interactions with viral proteins. For instance, the enterovirus non-structural 3A proteins directly bind to the Golgi-specific brefeldin A-resistant guanine nucleotide exchange factor-1 (GBF1) [2] and acyl-CoA-binding domain-containing protein-3 (ACBD3, also known as GCP60) [3].

ACBD3 is a Golgi resident protein involved in the maintenance of the Golgi structure [4] and regulation of intracellular trafficking between the endoplasmic reticulum and the Golgi [5]. ACBD3 is a multidomain protein composed of several domains connected by flexible linkers. Its central glutamine rich domain (Q domain) interacts with the lipid kinase phosphatidylinositol 4-kinase beta (PI4KB) and with the Rab GTPase-activating proteins TBC1D22A and TBC1D22B [6]. The interaction of ACBD3 and PI4KB causes membrane recruitment of PI4KB and enhances its enzymatic activity [7]. The C-terminal Golgi-dynamics domain (GOLD) of ACBD3 has been reported to interact with the Golgi integral protein giantin/golgin B1, which results in the Golgi localization of ACBD3 [5]. However, in enterovirus-infected cells, the ACBD3 GOLD domain interacts preferentially with viral non-structural 3A proteins, which causes re-localization of ACBD3 to the sites of virus replication [8].

The role of ACBD3 in enterovirus replication is not yet fully understood. It has been proposed that recruitment of ACBD3 to the sites of viral replication can lead to the indirect recruitment of its interactors and downstream effectors such as PI4KB, a well-known host factor essential for generation of PI4P-enriched membranes suitable for enterovirus replication [9, 10]. The 3A-ACBD3-PI4KB route represents one of the major described mechanisms of PI4KB recruitment to the sites of enterovirus replication [3, 11], although some other mechanisms employing the viral proteins 2BC [12] or 3CD [13] might be involved as well. Moreover, the formation of the 3A-ACBD3-PI4KB complex represents the major described mechanism of PI4KB recruitment to the replication sites of kobuviruses, members of a distinct group of picornaviruses [3, 14-16]. Previously, it has been suggested that PI4P directly recruits the viral RNA-dependent RNA polymerase ($3D^{pol}$) [9]. Further studies, however, revealed that the affinity of PI4P to $3D^{pol}$ is too weak to attract $3D^{pol}$ to target membranes by itself, suggesting that other factors may be involved [17]. Notably, PI4P gradients between various membranes can be used for the transport of other cellular lipids against their concentration gradient [18, 19]. The PI4P/cholesterol exchange machinery was implicated in replication of several enteroviruses [12, 20], suggesting that PI4P can be used by the viral machinery as a mediator to prepare membranes with a specific lipid composition suitable for viral replication.

ACBD3 is an important host factor of various enterovirus species [21], however, the structural determinants of its recruitment to the viral replication sites are poorly understood. To date, the structural information about any picornavirus 3A proteins is limited to a solution NMR structure of the

uncomplexed poliovirus 3A protein [22] (pdb code 1NG7) and our previously published crystal structure of the aichivirus 3A protein in complex with the ACBD3 GOLD domain [23] (pdb code 5LZ3). Unfortunately, the latter cannot be used for homology modeling of the enterovirus 3A proteins, given the unrelated primary sequences of the enterovirus and kobuvirus 3A proteins, which indicates distinct mechanisms of hijacking ACBD3 by these two groups of viral pathogens.

In this study, we present a structural, biochemical, and biological characterization of the complexes composed of human ACBD3 and the 3A proteins of four representative enteroviruses. The crystal structures revealed the details of the ACBD3-3A interaction, the 3A-3A interaction causing the assembly of the ACBD3-3A heterotetramers, the interaction between the ACBD3-3A complex and the lipid bilayer, and the roles of these interactions in facilitation of enterovirus replication. The comparison of the structures of the ACBD3:enterovirus 3A complexes and the previously known structures of the ACBD3:kobuvirus 3A complexes [23] uncovered a striking convergence in the mechanisms of how the two distinct groups of picornaviruses recruit ACBD3 and its downstream effectors to the sites of virus replication.

RESULTS

Diverse enterovirus species use a conserved mechanism to interact with the host ACBD3 protein.

For the structural characterization of the enterovirus 3A proteins in complex with the host ACBD3 GOLD domain, we selected 3A proteins of six human-infecting enteroviruses each representing different species as follows: enterovirus A71 (EVA71), coxsackievirus B3 (CVB3), poliovirus 1 (PV1), enterovirus D68 (EVD68), rhinovirus A2 (RVA2), and rhinovirus B14 (RVB14) (Fig 1a).

The recombinant cytoplasmic domains of all the 3A proteins were poorly soluble and tended to aggregate and precipitate at the required concentrations. Therefore, we used 3A proteins *N*-terminally fused to a GB1 solubility tag. For the crystallographic analysis of the complexes composed of the ACBD3 GOLD domain and the viral 3A proteins (hereafter referred to as GOLD:3A complexes), the GB1-fused cytoplasmic domains of the 3A proteins were directly co-expressed with the ACBD3 GOLD domain in bacteria. The GOLD:3A complexes were then purified, and the GB1 tag was cleaved off. The GOLD:3A complexes exhibited better protein solubility than the uncomplexed 3A proteins, sufficient for the subsequent crystallographic analysis.

Of the six GOLD:enterovirus 3A complexes, only GOLD:3A/EVD68 and GOLD:3A/RVB14 formed crystals that diffracted to a resolution suitable for subsequent structure determination (i.e. 2.3 Å and 2.9 Å, respectively). Both structures were solved by molecular replacement using a previously published structure of the unliganded ACBD3 GOLD domain (accession number 5LZ1 [23]) as a search model (Fig 1b, Table 1). To improve the crystallization properties of the other four GOLD:3A complexes, we used two different strategies. The first strategy was based on mutagenesis of selected surface-exposed hydrophobic residues of the 3A proteins to improve the solubility of the respective GOLD:3A complexes and their capability to be crystallized at higher protein concentrations. This approach led to a successful crystallization of the GOLD:3A/PV1 complex with an L24A point mutation within the PV1 3A protein. Its structure was then solved at a resolution of 2.8 Å (Fig 1b, Table 1). The second strategy took advantage of the fact that in all three solved GOLD:3A structures the *C* terminus of the ACBD3 GOLD domain was located in the vicinity of the *N* terminus of the ordered part of the 3A protein. This allowed us to design

CONVERGENT EVOLUTION IN THE MECHANISMS OF ACBD3 RECRUITMENT TO PICORNAVIRUS REPLICATION SITES

GOLD-3A fusion proteins with the last residue of ACBD3 (R528^{ACBD3}) fused through a short peptide linker (GSGSG) to the first predicted ordered residues of the respective 3A proteins (e.g. K15^{3A/EVA71}). This approach led to a successful crystallization of the GOLD-3A/EVA71 fusion protein and its structure solution at a resolution of 2.8 Å (Fig 1b, Table 1). The GOLD:3A/CVB3 and GOLD:3A/RVA2 complexes, however, failed to form diffracting crystals even after extensive optimization using both the mutagenesis and fusion-protein strategies.

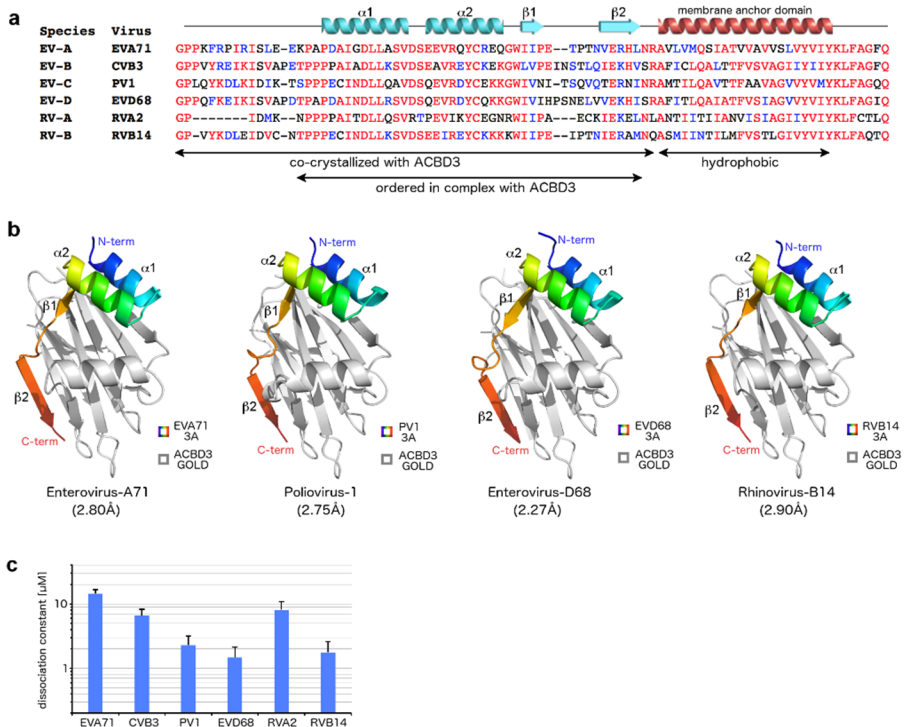


Figure 1. Biochemical and structural characterization of the GOLD:enterovirus 3A complexes. **a**, Multiple alignment of the 3A proteins of selected enteroviruses used in this study. Sequences were aligned using the ClustalX algorithm and colored using the BoxShade utility. Secondary structures present in the crystal structures of the ACBD3:3A complexes (colored in light blue) and the hydrophobic alpha helix anchoring the 3A proteins to the membrane (colored in red) are indicated above the sequences. EV, Enterovirus species; RV, Rhinovirus species; EVA71, enterovirus A71; CVB3, coxsackievirus B3; PV1, poliovirus 1; EVD68, enterovirus D68; RVA2, rhinovirus A2; RVB14, rhinovirus B14. **b**, Overall fold of four different GOLD:enterovirus 3A complexes. The protein backbones are shown in cartoon representation. The ACBD3 GOLD domain is depicted in grey, the viral 3A proteins in rainbow colors ranging from blue (N terminus) to red (C terminus). **c**, Dissociation constants of the complexes composed of the GB1-fused cytoplasmic domains of the enterovirus 3A proteins and the EGFP-fused ACBD3 GOLD domain as obtained by microscale thermophoresis. Data are presented as mean values \pm standard errors of the means (SEMs) from three independent experiments.

The overall structures of all solved GOLD:3A complexes are highly similar to each other. This suggests that neither the L24A mutation in the GOLD:3A/PV1 complex nor the fusion-protein strategy used for the GOLD:3A/EVA71 complex affected the overall fold of the complexes (Fig 1b). No electron density was observed for the N termini of the 3A proteins (approximately the first 15 residues) and we, therefore, assume that this region is intrinsically disordered. This part of the 3A proteins has been previously reported to be involved in the interaction with another host factor GBF1 [2] or it is largely absent (e.g. RVA2) (Fig 1a).

CHAPTER 6

In order to determine the strength of the interaction between the ACBD3 GOLD domain and multiple enterovirus 3A proteins *in vitro*, we used microscale thermophoresis (Fig 1c). The dissociation constants of the GOLD:enterovirus 3A complexes ranged approximately from 1 μM (EVD68 and RVB14) to 15 μM (EVA71).

Table 1. Statistics for data collection and processing, structure solution and refinement of the complexes composed of the ACBD3 GOLD domain and 3A proteins of enterovirus A71, poliovirus 1, enterovirus D68, and rhinovirus B14. Numbers in parentheses refer to the highest resolution shell of the respective dataset. R.m.s.d., root-mean-square deviation.

Crystal	GOLD + EVA71 3A	GOLD + PV1 3A	GOLD + EVD68 3A	GOLD + RVB14 3A
Construct	fusion protein	L24A mutant	wild type	wild type
PDB accession code	6HLW	6HLV	6HLN	6HLT
Data collection and processing				
Space group	P 21 21 21	C 1 2 1	C 1 2 1	P 1 2 1
Cell dimensions - a, b, c (Å)	46.4, 54.9, 208.7	90.7, 53.8, 62.8	96.9, 55.9, 64.5	54.4, 79.0, 70.6
Cell dimensions - α , β , γ (°)	90.0, 90.0, 90.0	90.0, 107.6, 90.0	90.0, 112.1, 90.0	90.0, 112.4, 90.0
Resolution at $I/\sigma(I) = 2$ (Å)	2.80	2.75	2.27	2.90
Resolution range (Å)	48.61 - 2.73 (2.83 - 2.73)	43.20 - 2.50 (2.59 - 2.50)	47.45 - 2.10 (2.18 - 2.10)	42.44 - 2.82 (2.92 - 2.82)
No. of unique reflections	14,873 (1,413)	10,009 (983)	18,521 (1,848)	13,308 (1,286)
Completeness (%)	99.62 (98.95)	98.89 (98.89)	98.34 (99.09)	98.38 (95.33)
Multiplicity	5.0 (5.1)	3.4 (3.5)	3.8 (3.8)	3.8 (3.7)
Mean $I/\sigma(I)$	12.80 (1.62)	7.43 (1.24)	10.78 (1.21)	9.85 (1.61)
Wilson B factor (Å ²)	72.87	55.88	47.36	57.90
R-merge / R-meas (%)	7.76 / 8.67	11.71 / 13.98	7.61 / 8.93	10.97 / 12.78
CC1/2	0.998 (0.730)	0.993 (0.542)	0.997 (0.556)	0.995 (0.665)
CC*	1.000 (0.919)	0.998 (0.838)	0.999 (0.845)	0.999 (0.894)
Structure solution and refinement				
R-work (%)	23.88 (36.97)	21.50 (30.46)	22.07 (36.93)	21.04 (31.80)
R-free (%)	25.68 (44.64)	24.14 (32.46)	25.08 (37.07)	23.94 (37.05)
R.m.s.d. - bonds (Å) / angles (°)	0.003 / 0.73	0.003 / 0.82	0.007 / 1.06	0.008 / 1.02
Average B factors (Å ²)	75.8	52.0	47.7	55.2
Clashscore	0.96	0.74	1.08	0.55
Ramachandran favored/outliers (%)	98 / 0	99 / 0	100 / 0	98 / 0

In summary, our experiments confirmed that the enterovirus 3A proteins interact with the host ACBD3 protein through the GOLD domain of ACBD3 and the cytoplasmic domains of the 3A proteins. These proteins interact directly with dissociation constants within the low micromolar range. Using several approaches, four GOLD:enterovirus 3A complexes were crystallized and their structures were solved. Taken together, these structures document a conserved mechanism how diverse enterovirus species recruit the host ACBD3 protein.

ACBD3:3A interaction promotes recruitment of PI4KB and facilitates enterovirus replication.

We performed an analysis of the GOLD:3A interface to identify amino acid residues important for the ACBD3:3A interaction, co-localization, stimulation of PI4KB recruitment, and facilitation of virus replication in human cells. For this analysis, we chose the GOLD:EVD68 3A complex because we resolved its structure at the highest resolution. Given the high similarity of the various GOLD:enterovirus 3A structures, we assume that the conclusions drawn from the ACBD3:EVD68 3A complex can be applied to the other ACBD3:enterovirus 3A complexes as well.

In the GOLD:EVD68 3A crystal structure, we could trace the polypeptide chain of the 3A protein from T16^{3A} to I58^{3A}. It contains four secondary elements: two alpha helices P19^{3A}-V29^{3A} (α 1^{3A}, Fig 2a) and Q32^{3A}-K41^{3A} (α 2^{3A}, Fig 2b), and two beta strands I44^{3A}-I46^{3A} (β 1^{3A}, Fig 2c) and V53^{3A}-I58^{3A} (β 2^{3A}, Fig 2d). All these segments contribute to the GOLD:3A interaction mediated through multiple hydrophobic interactions and hydrogen bonds (Fig 2a-d). The helices α 1^{3A} and α 2^{3A} bind to a mild cavity of the GOLD domain that is formed by four antiparallel beta strands of ACBD3. The strand β 1^{3A} interacts with the strand K518^{ACBD3}-R528^{ACBD3} of the ACBD3 GOLD domain, while the strand β 2^{3A} binds to the strand V402^{ACBD3}-P408^{ACBD3}, both in the antiparallel orientation. The conformation of all these secondary elements is highly conserved among various GOLD:enterovirus 3A complexes. The lowest homology of the tertiary structures of these complexes within short linkers between the β 1^{3A} and β 2^{3A} strands of the 3A proteins corresponds to the lowest homology of the primary sequences of these proteins within this region (Fig 1a-b).

Calculations [24] of the changes of the interaction energies of various to-alanine mutants of these complexes based on their crystal structures uncovered that multiple amino acid residues of both 3A proteins and ACBD3 are involved in the interaction (Fig S1a-c). To evaluate the relative importance of various segments of the 3A protein on the complex formation, we designed the following EVD68 3A mutants: NLD (N23A/L26A/D30A), QRD (Q32A/R35A/D36A), IVH (I44A/V45A/H47A), and LVK (L52A/V54A/K56A) (Fig 3a, Fig S1a). For all the mutants, the ACBD3:3A interaction was significantly attenuated both in the mammalian-two-hybrid assay (Fig 3b) and in the co-immunoprecipitation assay (Fig 3c), confirming that all four segments of the 3A protein are important for the ACBD3:3A interaction. Nevertheless, some residual affinity of the 3A mutants to ACBD3 was still observed. All the 3A mutants co-localized with endogenous ACBD3 in the Golgi as did the wild-type 3A protein. The lipid kinase PI4KB, however, was recruited to the Golgi significantly more effectively in the cells expressing wild-type 3A compared to the cells expressing the 3A mutants (Fig 3d-e). Under physiological conditions, PI4KB cycles between the cytoplasm and Golgi, where it is recruited by a direct interaction with ACBD3 [7]. In enterovirus-infected cells, the viral 3A protein has been proposed to promote the ACBD3:PI4KB interaction [11]. Thus, considering that no direct interaction between the enterovirus 3A proteins and PI4KB has ever been observed, our data indicate that the stimulation of the ACBD3:PI4KB interaction by the 3A protein and the subsequent increase of the PI4KB recruitment to target membranes in

infected cells depends on the ACBD3:3A interaction. The Golgi-localized PI4P lipid was redistributed in the 3A-expressing cells possibly due to the Golgi disintegration caused by 3A overexpression, nevertheless, no significant change in the PI4P levels was observed in the wild-type 3A-expressing cells compared to the mock-transfected or mutant 3A-expressing cells (Fig S2). Thus, a cooperation with some other viral proteins can be required to increase the PI4KB activity during viral infection.

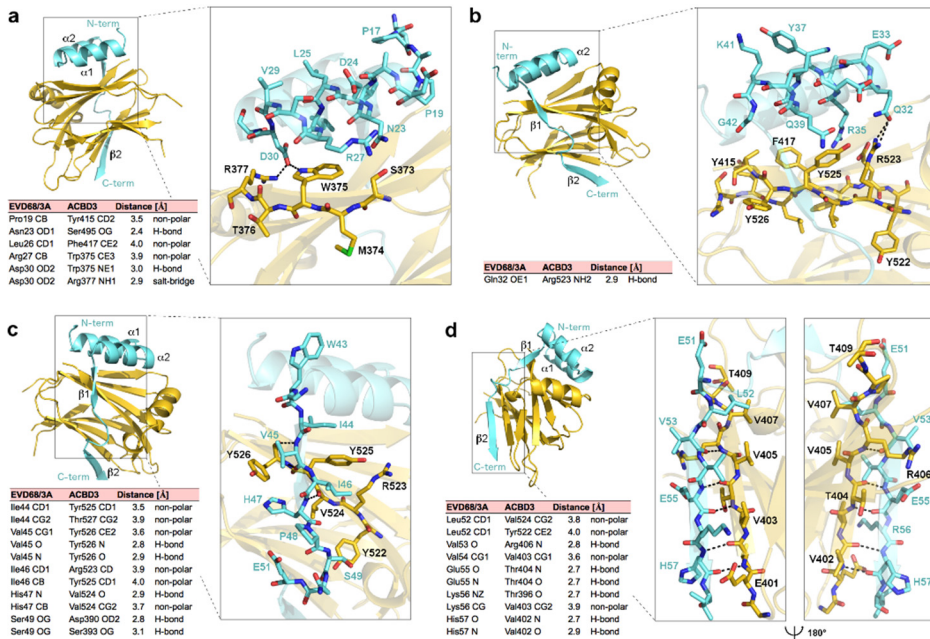


Figure 2. Detailed view of the interface of the GOLD:EVD68 3A complex. a-d, Detailed view of the interface between the GOLD domain and the enterovirus-D68 3A protein residues T16-S31 (a), S31-G42 (b), G42-E51 (c), and E51-I58 (d). In the overall view, the protein backbones are shown in cartoon representation; the ACBD3 GOLD domain is depicted in gold, the EVD68 3A protein in light blue. In the detailed view, the amino acid residues from the indicated segments are highlighted in stick representation and colored according to elements - oxygen atoms are colored in red, nitrogens in blue, sulfurs in green, carbons according to the protein assignment. Hydrogen bonds are shown as dotted black lines; hydrogen atoms are not shown. In the lower left of each panel, hydrogen bonds, non-polar interactions, and salt bridges between the GOLD domain and the EVD68 3A protein are listed. The distance cut-off used for hydrogen bonds is 3.3 Å, and for non-polar interactions and salt bridges 4.0 Å. In the case of non-polar interactions, only the closest atom pair for each pair of residues is listed.

To analyze the impact of these 3A mutations on enterovirus replication, we established a reporter subgenomic replicon assay for EVD68. To determine the background reporter expression directly from the transfected RNA, we used a viral polymerase-lacking mutant ($\Delta 3D^{pol}$). Unexpectedly, no significant replication of the wild-type replicon RNA compared to the $\Delta 3D^{pol}$ mutant was observed in HeLa cells. However, screening of several human cell lines uncovered the U-87 MG glioblastoma cells and HaCaT keratinocytes in which the wild-type replicon RNA significantly replicated. For all analyzed mutants, the viral RNA replication was attenuated in both cell lines (Fig 3f, Fig S3). We observed no replication of the NLD, QRD, and IVH mutants, and a significantly reduced replication of the LVK mutant. Notably, this mutant was the weakest ACBD3 interactor in both co-immunoprecipitation and mammalian-two-hybrid assays, indicating additional unknown important effects distinct from the strength of the ACBD3-3A interaction affecting virus replication. We tested whether this mutant gained resistance to the PI4KB inhibition, nevertheless, we found that this mutant was still sensitive to a highly specific PI4KB inhibitor (compound 10 in *Mejdrova et al.* [10]) (Fig 3g).

CONVERGENT EVOLUTION IN THE MECHANISMS OF ACBD3 RECRUITMENT TO PICORNAVIRUS REPLICATION SITES

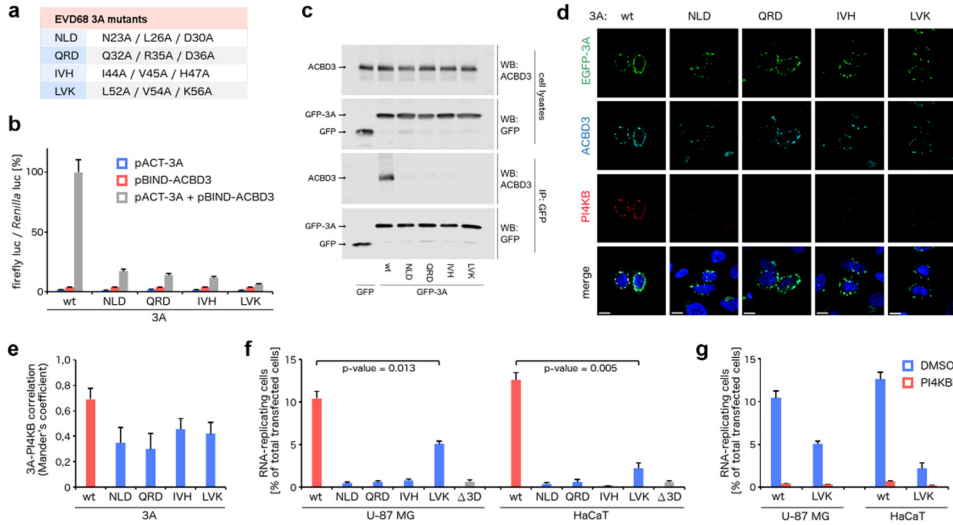


Figure 3. Analysis of the EVD68 3A mutations at the GOLD:EVD68 3A interface. **a**, List of the EVD68 3A mutants designed for further experiments. **b**, Mammalian-two-hybrid assay with the 3A mutants and wild-type ACBD3. HeLa cells were transfected as indicated and the firefly luciferase activity normalized to the *Renilla* luciferase activity was determined using a dual-luciferase reporter assay system. **c**, Co-immunoprecipitation of the 3A mutants and endogenous ACBD3. EGFP-fused wild-type 3A and its mutants were overexpressed in HEK293T cells. The 3A complexes were affinity captured by the GFP-Trap nanobody and resolved by immunoblotting as indicated. **d-e**, Co-localization of the 3A mutants with endogenous ACBD3 and PI4KB. EGFP-fused wild-type 3A and its mutants were overexpressed in HeLa cells. The cells were fixed and immunostained with anti-ACBD3 and anti-PI4KB antibodies. In **(d)**, immunofluorescence images of representative cells are shown; scale bars represent 10 μ m. In **(e)**, the statistical analysis of the 3A-PI4KB co-localization is presented as Mander's correlation coefficients \pm standard deviations (SDs) from at least 12 cells from 2 independent experiments. **f-g**, Viral subgenomic replicon assay. U-87 MG and HaCaT cells were transfected with the T7-amplified EVD68 subgenomic replicon wild-type RNA or its mutants as indicated, and the percentage of cells with the reporter mCherry fluorescence above background was determined by flow cytometry. The viral polymerase-lacking mutant (Δ 3D) was used as a negative control. In **(f)**, cell from the indicated samples were pretreated with a PI4KB-specific inhibitor prior to the transfection of RNA. The data are presented as means \pm SEMs from 2 independent experiments.

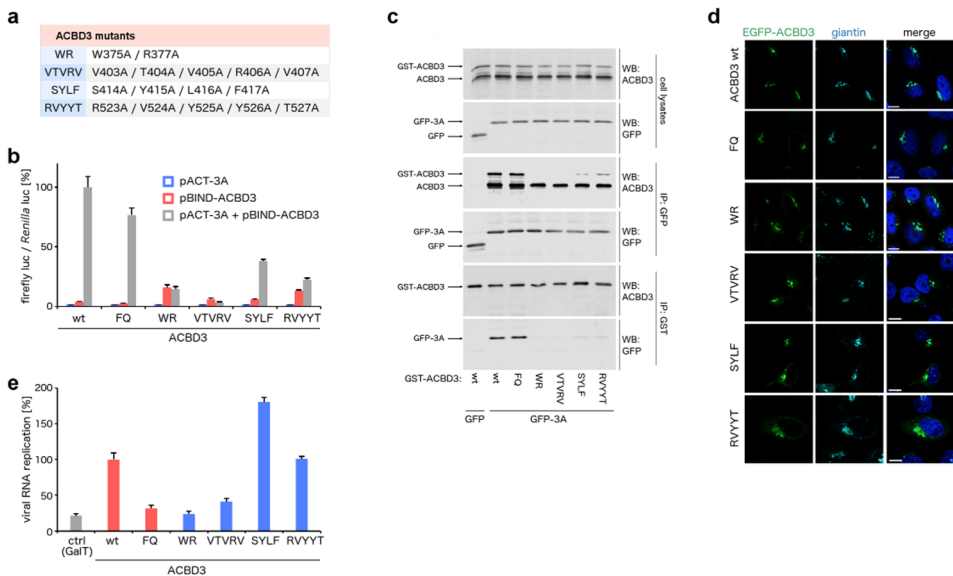


Figure 4. Analysis of the ACBD3 mutations at the GOLD:EVD68 3A interface. (continued on next page)

Figure 4. (continued) **a**, List of the ACBD3 mutants designed for further experiments. **b**, Mammalian-two-hybrid assay with the ACBD3 mutants and wild-type 3A. HeLa cells were transfected as indicated and the firefly luciferase activity normalized to the *Renilla* luciferase activity was determined using a dual-luciferase reporter assay system. **c**, Co-immunoprecipitation of the ACBD3 mutants and wild-type 3A. EGFP-fused wild-type 3A and GST-fused wild-type ACBD3 and its mutants were overexpressed in HEK293T cells. The 3A and ACBD3 complexes were affinity captured by the GFP-Trap nanobody or glutathione sepharose, respectively, and resolved by immunoblotting as indicated. **d**, Localization of the ACBD3 mutants. EGFP-fused wild-type ACBD3 and its mutants were overexpressed in HeLa ACBD3 KO cells. Cells were fixed and immunostained with the anti-giantin antibody. Scale bars represent 10 μ m. **e**, Rescue of enterovirus replication by the ACBD3 mutants. HeLa ACBD3 KO cells were transfected with wild-type ACBD3 or its mutants, and enterovirus replication was determined using the *Renilla* luciferase-expressing CVB3 virus by the *Renilla* luciferase assay system. GalT and ACBD3 F258A/Q259A were used as controls.

To address the effect of mutagenesis of selected residues within ACBD3, we designed the following ACBD3 mutants: WR (W375A/R377A), VTVRV (V403A/T404A/V405A/R406A/V407A), SYLF (S414A/Y415A/L416A/F417A), and RVYYT (R523A/V524A/Y525A/Y526A/T527A) (Fig 4a, Fig S1b-c). In the mammalian-two-hybrid assay (Fig 4b) and in the co-immunoprecipitation assay (Fig 4c), all these ACBD3 mutants displayed a significantly reduced ability to interact with the 3A protein. A weak yet significant effect was observed for the SYLF and RVYYT mutants, while a strong effect resulting in no detectable interaction in both assays was achieved for the WR and VTVRV mutants. Proper intracellular localization of these ACBD3 mutants was verified by their ectopic expression in ACBD3 knock-out cells derived from HeLa cells by CRISPR/Cas9 technology [21]. All these ACBD3 mutants co-localized with giantin, an integral Golgi protein, which has been proposed to directly recruit ACBD3 to the Golgi [5] (Fig 4d).

Finally, we tested the ability of these ACBD3 mutants to rescue enterovirus replication in ACBD3 knock-out cells. The ACBD3 F258A/Q259A mutant, which does not interact with the lipid kinase PI4KB and cannot rescue virus replication [21], was used as a control. The ACBD3 WR and VTVRV mutants failed to rescue virus replication as expected. However, virus replication was still sufficiently restored by the other tested ACBD3 mutants SYLF and RVYYT (Fig 4e). These data document that the remaining affinity of these ACBD3 mutants to the viral 3A protein is still sufficient to fully facilitate enterovirus replication. Surprisingly, the SYLF mutant supports viral replication significantly better than wild-type ACBD3. It is possible that this mutation affects some other ACBD3 properties, such as its ability to interact with some other (known or unknown) proteins involved in enterovirus replication, nevertheless, the exact mechanism of the enhanced enterovirus replication in the ACBD3 SYLF mutant-expressing cells remains unclear. Compared to the ACBD3 WR mutant, the single mutants W375A and R377A still could rescue virus replication (Fig S4a-b), indicating that both mutations at the ACBD3:3A interface are required to sufficiently disrupt the ACBD3:3A interaction to affect virus replication. Several other tested ACBD3 mutants (such as V403A/V405A/ V407A, Y415A/F417A, and R523A/Y525A/Y526A) displayed a reduced affinity to the enterovirus 3A protein and still were able to restore enterovirus replication (Fig S4c-d). Alternatively, virus replication can be inhibited by single mutations interfering with a proper intracellular localization of ACBD3 (through ACBD3 misfolding and/or loss of the interaction with giantin) as documented by the E419A mutant (Fig S4e-f).

In conclusion, our data document that the ACBD3:3A interaction is essential for enterovirus replication. The viral replication, however, can be facilitated by weakly interacting ACBD3 mutants, provided that they are correctly folded and localized in the Golgi in non-infected cells.

ACBD3:enterovirus 3A complexes form heterotetramers with a 2:2 stoichiometry.

The enterovirus 3A proteins have been proposed to form homodimers [22, 25]. Analysis of the crystal structures of the GOLD:3A complexes revealed that the 3A proteins formed either one of the crystal-packing contacts (as in the case of EVD68 and PV1) or contacts with the second 3A molecule when two GOLD:3A complexes per asymmetric unit were present (as in the case of EVA71 and RVB14). This putative dimerization interface is formed by the two central alpha helices of the 3A proteins, which are bent 180° to form a helical hairpin (Fig 5a). These helices are amphipathic with several hydrophobic residues oriented towards the hydrophobic residues of the other 3A monomer. Surprisingly, the C termini of the 3A proteins, which in the cellular environment are anchored to the membranes, are located on the opposite sides of the GOLD:3A heterotetramers. Therefore, we were interested whether the plasticity and flexibility of the 3A dimerization interface together with the plasticity of the lipid bilayer allows to form the GOLD:3A heterotetramers at the intracellular membranes.

To identify amino acid residues of the 3A proteins involved in the dimerization of the GOLD:3A complexes, we calculated [24] the changes of the dimerization energies of various to-alanine mutants of these complexes based on the crystal structures (Fig S5a). The dimerization interface of the GOLD:3A/EVD68 complex consists of the hydrophobic core formed by the residues L25, V29, V34, and Y37, and an additional intermolecular salt bridge between the residues D24 and K41 (Fig 5a). To analyze the dimerization of the GOLD:3A complexes in more detail, we generated a mutant EVD68 3A protein (hereafter referred to as LVVY mutant) with the following four mutations at the putative dimerization interface: L25A, V29A, V34A, and Y37A. As expected, retention volumes of the recombinant wild-type 3A and its LVVY mutant in size exclusion chromatography were significantly shifted corresponding to the dimeric and monomeric state of the wild-type 3A and its LVVY mutant, respectively (Fig 5b).

At the request of a reviewer of our manuscript, we analyzed the dimerization of the L25V, V29Y, L25V/V34L, and V29Y/Y37V mutants (Fig S6). Both L25V and V29Y mutations attenuated the 3A dimerization. The dimerization of the L25V mutant was restored by the V34L mutation, likely due to the compensation of weakening the L25-L25 interaction by strengthening the V34-V34 and V34-V29 interactions. On the other hand, the potential "rescue" Y37V mutation had a negative impact on the 3A dimerization, likely due to the attenuation of the Y37-L25 interaction and a loss of the hydrogen bond between Y37 and D24 (Fig S6).

Next, we investigated the stoichiometry of the GOLD:EVD68 3A complexes. To ensure that the 3A protein is fully complexed with the ACBD3 GOLD domain and to avoid the formation of partial complexes with 1:2 stoichiometry, we designed a GOLD-EVD68 3A fusion protein using a similar approach as for the GOLD-EVA71 3A fusion protein used for the crystallographic analysis as described earlier. Taking advantage of the vicinity of the C terminus of the ACBD3 GOLD domain and the N terminus of the ordered part of the EVD68 3A protein, we connected the last residue of ACBD3 (R528^{ACBD3}) through a short peptide linker (GSGSG) to the first ordered residue of the EVD68 3A protein (T16^{3A/EVD68}) (Fig S5b). Both GOLD-3A wild-type and LVVY mutant fusion proteins formed crystals, which diffracted to a resolution suitable for further structure determination (Fig S5c). The crystal structures of the GOLD:3A complex consisting of two individual proteins, the GOLD-3A fusion protein, and its LVVY mutant were almost identical with low root-mean-square deviations (Fig S5b), confirming that neither the fusion-protein approach nor the LVVY mutation affected the correct folding of these proteins.

Three lines of evidence document the dimeric state of the wild-type GOLD-3A fusion protein and the monomeric state of its LVVY mutant *in vitro*. First, the retention volumes of these proteins in size

exclusion chromatography are significantly shifted (Fig 5c). Secondly, the small-angle X-ray scattering (SAXS) profiles of these proteins correspond to the calculated scattering curves of a dimer of the wild-type GOLD-3A fusion protein (Fig 5d, Fig S7a) and of a monomer of its LVVY mutant (Fig 5e). Thirdly, crystal contacts corresponding to the 3A dimerization interface are not preserved in the crystal structure of the GOLD-3A LVVY mutant (Fig S7b-c), indicating that this mutant cannot dimerize through this interface even at very high protein concentrations (of approximately 20 mM) present within the protein crystal.

Next, we investigated the stoichiometry of the GOLD:3A complexes in cells. For this purpose, we ectopically co-expressed either wild-type GOLD-3A fusion protein or its LVVY mutant *N*-terminally fused to mAmetrine and mPlum fluorescent proteins in HeLa cells and determined the Förster resonance energy transfer (FRET) efficiency by flow cytometry. Owing to the crowding effect, the energy transfer was observed in the case of both proteins. Nevertheless, we observed a significant difference in FRET efficiency between the wild-type GOLD-3A fusion protein and its LVVY mutant (Fig 5f-g). These results confirm that the GOLD:3A complexes are flexible enough to allow the formation of the heterotetramers consisting of two molecules of the viral 3A protein and two molecules of host ACBD3 even in cells at the respective intracellular membranes (Fig 5h).

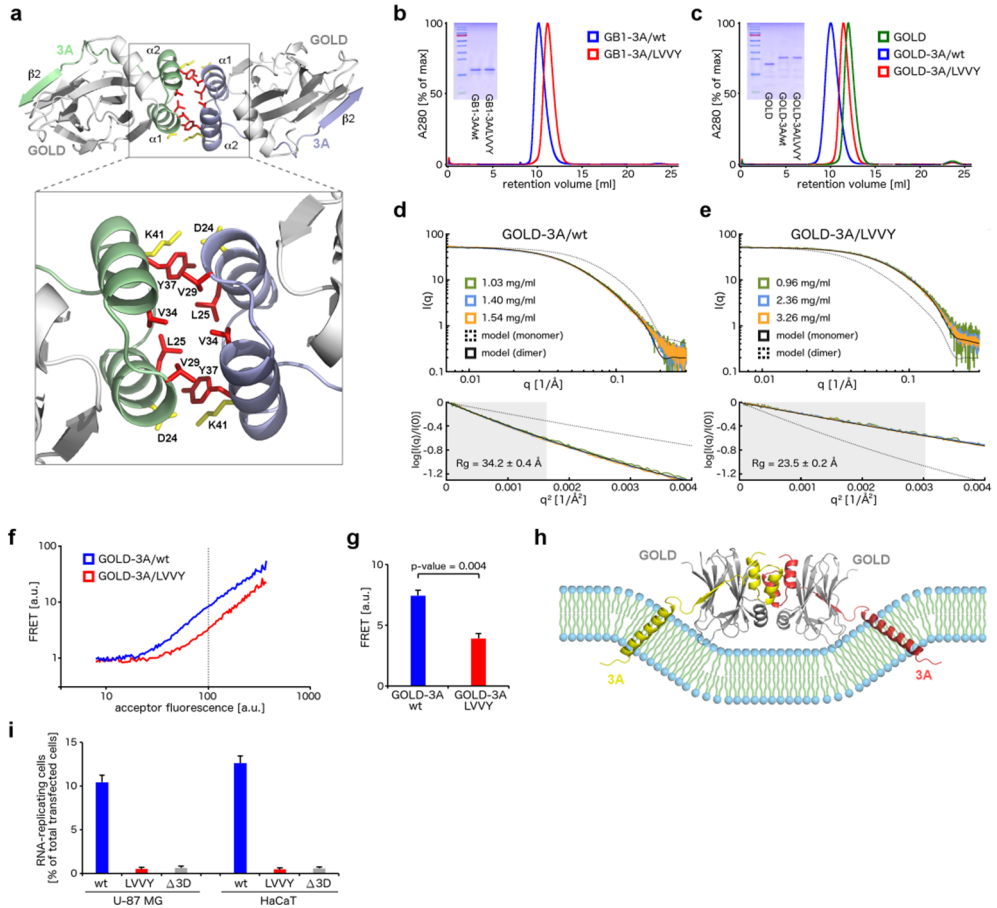
Finally, we analyzed the impact of the LVVY mutation on enterovirus replication. Using a reporter subgenomic replicon assay for EVD68 established earlier, we found replication of this mutant significantly attenuated in both U-87 MG and HaCaT cells (Fig 5i, Fig S3). These findings document that the intact dimerization interface of the viral 3A proteins is required for enterovirus replication.

Proper conformation of the ACBD3:3A complexes at the membrane is essential for enterovirus replication.

In a previous study [23], we identified a novel ACBD3 membrane binding site (MBS) consisting of the residues R399, L514, W515, and R516. The hydrophobic residues L514 and W515 can be inserted directly into the lipid bilayer, while the positively charged residues R399 and R516 can interact with the negatively charged phospholipid head groups (Fig 6a). A vicinity of ACBD3 MBS and the expected position of the transmembrane domain of the enterovirus 3A protein within the ACBD3:3A complexes suggests that ACBD3 MBS may be involved in the stabilization of the ACBD3:3A complexes at the membrane as well.

To experimentally evaluate this hypothesis, we designed the following ACBD3 mutants with several point mutations within MBS: LWR514AAA and, to increase repulsion between ACBD3 MBS and the lipid bilayer, LWR514DDD. Then, we ectopically expressed wild type ACBD3 or its MBS mutants *N*-terminally fused to EGFP in HeLa ACBD3 knock-out cells. We found that wild-type ACBD3 co-localized with the Golgi marker giantin, while both ACBD3 MBS mutants LWR514AAA and LWR514DDD were mostly released to the cytoplasm, although minor yet significant fractions of their pools were still preserved at the Golgi (Fig 6b). Remarkably, when the ACBD3 MBS mutants were co-expressed with the enterovirus 3A protein, they were completely (LWR514AAA mutant) or partially (LWR514DDD mutant) re-localized back to the Golgi (Fig 6c-d). Thus, an intact MBS is required for ACBD3 recruitment to the Golgi by the action of giantin or other cellular factors, however, it is dispensable for ACBD3 stabilization at target membranes through its interaction with enterovirus 3A proteins.

CONVERGENT EVOLUTION IN THE MECHANISMS OF ACBD3 RECRUITMENT TO PICORNAVIRUS REPLICATION SITES



Finally, we tested the capacity of wild-type ACBD3 and its MBS mutants to rescue virus replication in ACBD3 knock-out cells. Both ACBD3 wild type and the LWR514AAA mutant, but not the LWR514DDD and FQ258AA (used as a control [21]) mutants, effectively restored virus replication (Fig 6e). Thus, it seems that not ACBD3 MBS itself but rather the orientation of the ACBD3:3A complex with respect to the membrane plays a role in facilitation of enterovirus replication. To-alanine mutations of ACBD3 MBS still allow the ACBD3:3A complex at the membrane to adopt a conformation suitable for viral replication. On the contrary, to-aspartate mutations of ACBD3 MBS, which repel the negatively charged phospholipids of the lipid bilayer, result in an orientation of the ACBD3:3A complex with respect to the membrane that does not support enterovirus replication.

In summary, ACBD3 MBS is not required for ACBD3 recruitment to target membranes by the action of the enterovirus 3A proteins, however, the proper conformation of the ACBD3:3A complexes at the membrane mediated by ACBD3 MBS is essential for enterovirus replication.

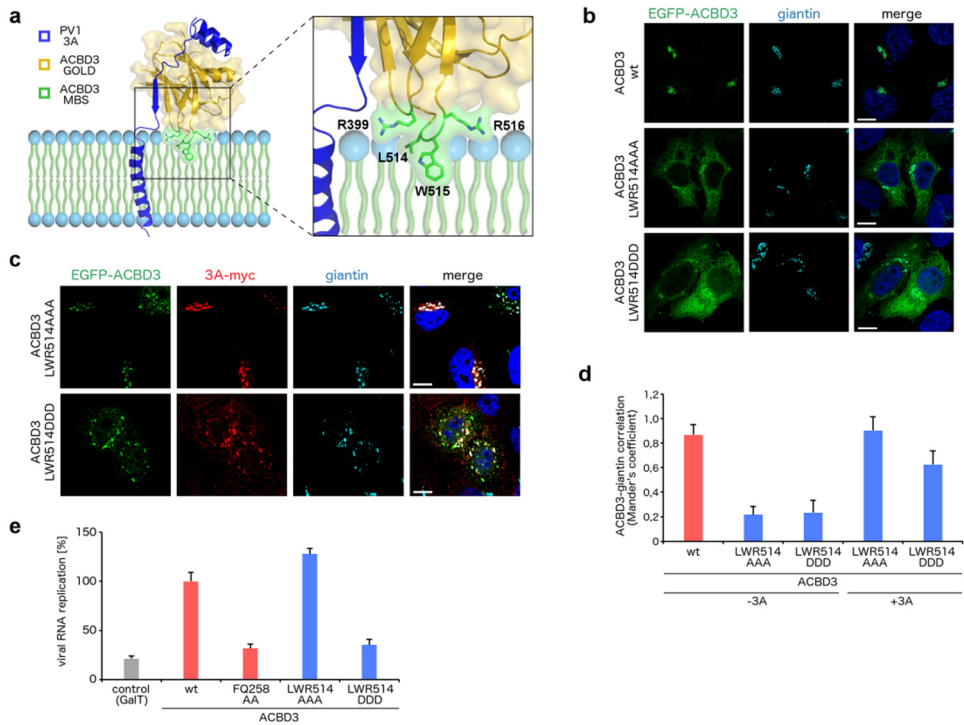


Figure 6. Analysis of the membrane binding site of ACBD3 in complex with the enterovirus 3A protein. **a**, Membrane binding model of the GOLD: poliovirus 3A complex. The ACBD3 GOLD domain is shown in cartoon representation with a semi-transparent surface and colored in gold except for the membrane binding site (MBS) composed of R399, L514, W515, and R516, which is colored in green. The poliovirus 3A protein is depicted in blue. **b**, Localization of the ACBD3 mutants. EGFP-fused wild-type ACBD3 or its mutants were overexpressed in HeLa ACBD3 KO cells. Cells were fixed and immunostained with the anti-giantin antibody (marker of Golgi). Scale bars represent 10 μ m. **c**, Localization of the ACBD3 mutants in 3A-expressing cells. EGFP-fused ACBD3 mutants were co-expressed with myc-tagged CVB3 3A in HeLa ACBD3 KO cells. Cells were fixed and immunostained with the anti-myc and anti-giantin (marker of Golgi) antibodies. Scale bars represent 10 μ m. **d**, Statistical analysis of the ACBD3-giantin co-localization from (b) and (c) is presented as Mander's correlation coefficients \pm SDs from at least 12 cells from 2 independent experiments. **e**, Rescue of enterovirus replication by the ACBD3 mutants. HeLa ACBD3 KO cells were transfected with wild-type ACBD3 or its mutants, and enterovirus replication was determined using the *Renilla* luciferase-expressing CVB3 virus by the *Renilla* luciferase assay system. GalT and ACBD3 FQ258AA were used as controls.

DISCUSSION

Considering the commonness of enterovirus-mediated infections within human population, it is surprising that no antiviral therapy for enteroviruses has been approved yet. Targeting essential host factors instead of rapidly mutating viral enzymes represents a promising strategy. Several host factors essential for enterovirus replication are recruited to the sites of viral replication by a direct protein-protein interaction between the host factor and a viral protein. A detailed knowledge of the structures of such complexes can open up prospects for a structure-guided development of small chemical compounds targeting these interactions, yielding a novel class of antivirals to combat infections caused by these pathogens.

In this study, we present a series of crystal structures of complexes composed of the non-structural 3A proteins of four enterovirus species and the 3A-binding GOLD domain of the host factor ACBD3. Previously, the genetic inhibition of ACBD3 mediated by siRNA has yielded conflicting results on the importance of ACBD3 for virus replication [26, 27]. This conflict in the literature has been recently addressed using CRISPR/Cas9-generated ACBD3 knock-out cells, in which enterovirus replication was severely impeded [8, 21]. This confirmed that ACBD3 is, indeed, an essential host factor for enterovirus replication. However, it seems that a very low concentration of ACBD3 within the cells is still fully capable of facilitating enterovirus replication. This hypothesis is in agreement with our observations that enterovirus replication in ACBD3 knock-out cells can be restored by several ACBD3 mutants with a very low affinity to the viral 3A proteins even at the detection limit of conventional methods assessing the protein-protein interactions, such as protein co-immunoprecipitation.

Among picornaviruses, the interaction between the viral 3A protein and host ACBD3 is not unique for enteroviruses. ACBD3 has been proposed to interact also with the 3A proteins of kobuvirus (e.g. aichivirus), hepatovirus, salivirus (klassevirus), and parechovirus, but not with those of cardiovirus (e.g. Saffold virus) or aphthovirus (foot-and-mouth disease virus, FMDV) [6]. To our best knowledge, all picornaviruses sensitive to PI4KB specific inhibitors (such as enteroviruses and kobuviruses) are able to hijack ACBD3, arguing for ACBD3 as a main mediator of PI4KB recruitment by these viruses. Notably, hepatovirus replicates independently of PI4KB [28], indicating either functionally irrelevant interaction with ACBD3 or another, PI4KB-independent, role of ACBD3 in hepatovirus replication. Picornaviruses that cannot hijack ACBD3 through their 3A proteins are either PI4P-independent (such as FMDV [29]) or their replication depends on another PI4P-producing lipid kinase PI4KA (e.g. cardioviruses [30]).

During the past decades, multiple enterovirus mutants resistant to the inhibitors of PI4KB and the oxysterol binding protein (OSBP), which acts downstream of PI4KB, were isolated and characterized. Most of the resistance-conferring mutations were localized to the 3A-encoding regions of these viruses, e.g. PV1 N45Y, R54W, N57D, A70T, and A71S, CVB3 V45A, I54F, and H57Y, and RVB14 E30D/V/Q, I42V, and M54I (Fig S8a-b) [31-34]. Although many of the PI4KB/OSBP-inhibition resistance-conferring mutations are localized within the ACBD3-interacting regions of the 3A proteins, they seem unlikely to act through modulation of the ACBD3-3A interaction. On the other hand, it is possible that the mutations clustered within the $\beta 2$ strands of the 3A proteins, such as CVB3 H57Y or PV1 R54W, can act through modulation of the interaction of the ACBD3-3A complex (or the uncomplexed 3A protein) with the membrane. The loss of the positive charge of the mutated residues can possibly compensate for the loss of the negative charge of the PI4P head groups upon PI4KB inhibition. Nevertheless, at least the mechanism of action of the mutations located distally with respect to the membrane, mostly clustered within the $\beta 1$ strands of the 3A proteins, remains unclear.

Apart from the crystal structures of the enterovirus 3A: GOLD complexes, to date only the structures of the kobuvirus 3A: GOLD complexes are known [23]. The enterovirus (e.g. poliovirus) and kobuvirus (e.g. aichivirus) 3A proteins share a common overall architecture, i.e. a similar size of approximately 10 kDa, large *N*-terminal soluble cytoplasmic domains followed by hydrophobic membrane-anchoring regions and small *C*-terminal domains (Fig 7a). Despite this common architecture, primary and predicted secondary structures of the enterovirus and kobuvirus 3A proteins are unrelated and cannot be aligned. Furthermore, positions of the ACBD3 binding regions of the enterovirus and kobuvirus 3A proteins are distinct. The ACBD3 binding region of the enterovirus 3A proteins forms the *C*-terminal segments of the cytoplasmic domain (and is preceded by the *N*-terminal GBF1 binding region), while the ACBD3 binding region of the kobuvirus 3A proteins is located at the *N* terminus (and a GBF1 binding region is completely missing). Superposition of the crystal structures of the enterovirus and kobuvirus 3A: GOLD complexes reveals that the enterovirus and kobuvirus 3A proteins bind to the same regions of the ACBD3 GOLD domain, nevertheless, the polypeptide chains of the enterovirus and kobuvirus 3A proteins have opposite polarities (Fig 7b-c). For instance, the poliovirus 3A strand $\beta 2^{3A/PV1}$ binds in the antiparallel orientation to the strand V402^{ACBD3}-P408^{ACBD3} of ACBD3, while the aichivirus 3A strand $\beta 1^{3A/AIV1}$ binds at the same position to the same strand of ACBD3, but in the parallel orientation (Fig 7b-c). The reverse orientation of the enterovirus 3A proteins compared to the kobuvirus 3A proteins may be caused by the specific need of the enterovirus 3A proteins to bind GBF1.

A notable difference between the enterovirus and kobuvirus 3A proteins is represented in the way they are anchored to the membrane. In addition to the *C*-terminal hydrophobic membrane binding regions, kobuvirus 3A proteins are membrane-anchored by the myristoylated *N*-terminal glycines, which is very unusual among picornaviruses [3]. Among enteroviruses, the *N*-terminal myristoylation is not present. To gain more insight into the membrane binding mode of the enterovirus 3A: GOLD protein complex, we performed an all atom molecular dynamics simulation of this complex at the membrane and compared it with our previously published [23] simulation of the kobuvirus 3A: GOLD protein complex at the surface of the lipid bilayer (Fig 7d). These simulations uncovered a similar conformation of the ACBD3 GOLD domain recruited to the membrane by the poliovirus or aichivirus 3A protein, including the insertion of the ACBD3 membrane binding site residues into the lipid bilayer. The position of the *N*-terminal myristoylation of the aichivirus 3A protein functionally substitutes the position of the *C*-terminal transmembrane domain of the poliovirus 3A protein, whereas the *C*-terminal transmembrane domain of the aichivirus 3A protein has no equivalent in the case of the poliovirus 3A protein.

In summary, our findings reveal structural details of how two groups of viral pathogens, enteroviruses and kobuviruses, developed a similar mechanism of hijacking the same host factor (ACBD3) and its downstream effectors (such as PI4KB). These viruses use their 3A proteins with a common architecture yet totally unrelated primary sequences to bind to the same regions of the host ACBD3 protein in the opposite orientations, representing a striking case of convergence in picornavirus evolution. Our results are in agreement with a pioneering work by *Greninger and colleagues* [6, 35], which has forecast such convergent evolutionary strategies of kobuviruses and enteroviruses based on extensive mutagenesis of the ACBD3-3A interface. There are still several other picornavirus genera proposed to recruit ACBD3 through the 3A: GOLD interaction (such as salivirus, hepatovirus, or parechovirus [6]) whose 3A: GOLD complexes remain structurally unexplored. Structural details of their ACBD3 recruitment uncovering whether they utilize the mechanism described for enteroviruses, kobuviruses, or another mechanism distinct from those two, remain to be further elucidated.

CONVERGENT EVOLUTION IN THE MECHANISMS OF ACBD3 RECRUITMENT TO PICORNAVIRUS REPLICATION SITES

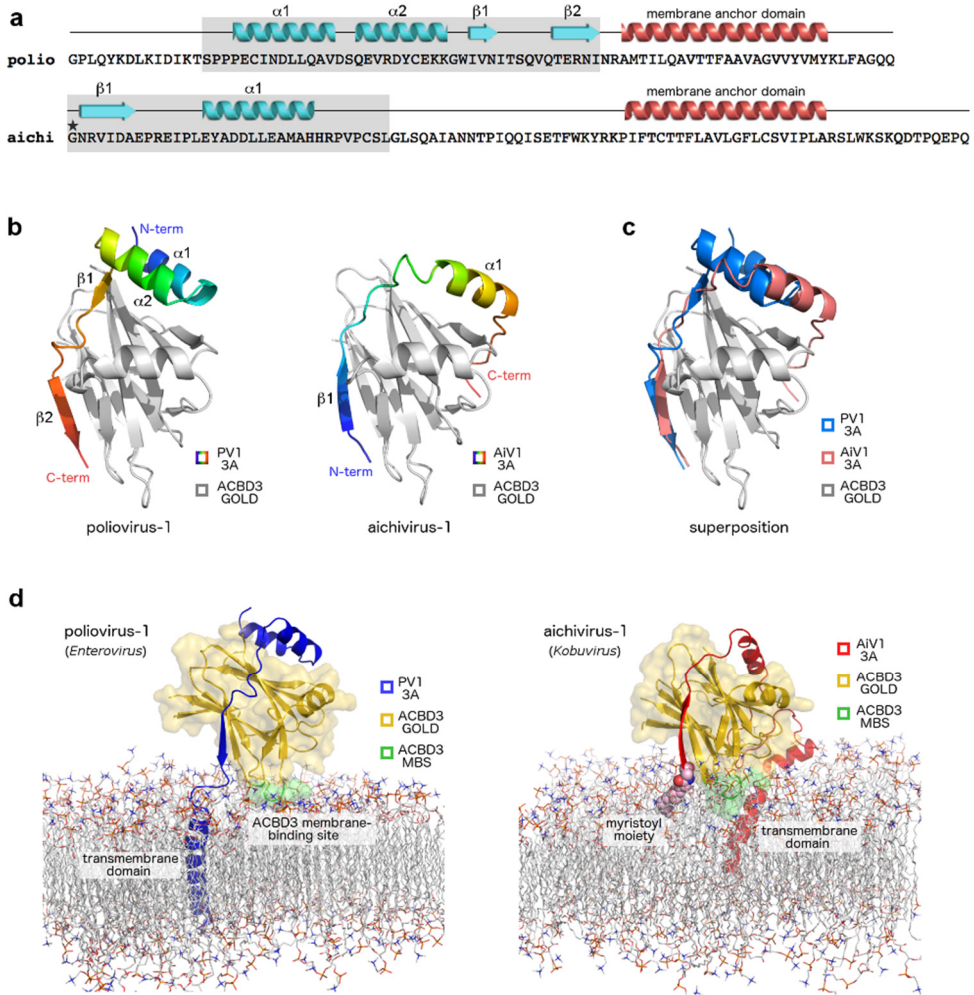


Figure 7. Convergence in the mechanisms of ACBD3 recruitment by enteroviruses and kobuviruses. **a**, Distinct ACBD3-binding regions of enterovirus and kobuvirus 3A proteins. Sequences of the poliovirus-1 (member of enteroviruses) and aichivirus-1 (member of kobuviruses) 3A proteins are shown. Secondary structures present in the crystal structures of the ACBD3: 3A complexes (colored in light blue) and the hydrophobic alpha helices anchoring the 3A proteins to the membrane (colored in red) are indicated above the sequences. ACBD3-binding regions are shaded in grey. Myristoylated Gly1 of the aichivirus-1 3A protein is marked with an asterisk. **b**, Crystal structures of the ACBD3 GOLD domain in complex with the poliovirus (left) and aichivirus (right) 3A proteins. The protein backbones are shown in cartoon representation. The ACBD3 GOLD domain is depicted in grey, the viral 3A proteins in rainbow colors from blue (N terminus) to red (C terminus). **c**, Superposition of the crystal structures from **(b)**. The ACBD3 GOLD domain is depicted in grey, the poliovirus 3A protein in blue, the aichivirus 3A protein in red. **d**, All atom molecular dynamics simulation-based models of the ACBD3 GOLD domain in complex with the poliovirus (left) and aichivirus (right) 3A proteins on the lipid bilayer. The ACBD3 GOLD domain is shown in cartoon representation with a semi-transparent surface and colored in gold except for the membrane binding site, which is colored in green. The poliovirus 3A protein is depicted in blue, the aichivirus 3A protein in red.

MATERIALS AND METHODS

Plasmids – For expression in *E. coli*, full-length human ACBD3 and various enterovirus 3A proteins and their deletion mutants were cloned into pRSFD vector (Novagen) with an *N*-terminal 6xHis tag followed by a GB1 solubility tag and a TEV protease cleavage site using PCR and restriction cloning. For bacterial expression of the EGFP-fusion proteins, the EGFP encoding sequence was inserted between the TEV cleavage site and the target gene encoding regions. For expression of the EGFP-fusion proteins in human cells, target genes encoding regions were recloned into pEGFP-C1 vector (Clontech) with an *N*-terminal EGFP tag. For expression of the GST-, mAmetrine-, and mPlum-fusion proteins in human cells, the EGFP encoding region was replaced by GST or corresponding fluorescent protein encoding sequence by PCR and restriction cloning. The pRib-EVD68/mCherry plasmid for viral subgenomic replicon assays was generated by subcloning of the EVD68 cDNA of a prototypical Fermon strain under T7 promoter and replacing the capsid proteins-encoding region with the mCherry fluorescent protein-encoding gene by Gibson assembly. Mutations were generated using the Q5 Site-Directed Mutagenesis Kit (New England BioLabs). All DNA constructs were verified by sequencing. The pEGFP-ACBD3 and pBIND-ACBD3 plasmids were kindly provided by Carolyn Machamer and Jun Sasaki, respectively. The mAmetrine-C1 and mPlum-C1 plasmids were gifts from Robert Campbell and Michael Davidson (Addgene plasmids #54660 [36] and #54839 [37]). The pEGFP-GalT plasmid was a gift from Jennifer Lippincott-Schwartz (Addgene plasmid #11929 [38]).

Protein expression and purification – All recombinant proteins used in this study were bacterially expressed as fusion proteins with an *N*-terminal 6xhistidine (His₆) tag followed by a GB1 solubility tag and a TEV protease cleavage site. For the crystallographic analysis of the GOLD:3A complexes, the *N*-terminally His₆-GB1-TEV site-fused cytoplasmic domains of the 3A proteins were directly co-expressed with the untagged ACBD3 GOLD domain. The proteins were expressed in *E. coli* BL21 DE3 NiCo cells (New England Biolabs) using the autoinduction ZY medium. Bacterial cells were harvested and lysed in the lysis buffer (50 mM Tris pH 8, 300 mM NaCl, 3 mM β -mercaptoethanol, 30 mM imidazole, 10% glycerol), the lysate was incubated with the HisPur Ni-NTA Superflow agarose (Thermo Fisher Scientific), and the bound proteins were extensively washed with the wash buffer (50 mM Tris pH 8, 300 mM NaCl, 1 mM β -mercaptoethanol, 20 mM imidazole). The protein was eluted with the elution buffer (50 mM Tris pH 8, 200 mM NaCl, 3 mM β -mercaptoethanol, 300 mM imidazole).

For the biochemical analysis of the 3A proteins by microscale thermophoresis or SAXS, the *N*-terminal His₆-GB1 tags were preserved uncleaved to increase protein solubility and to avoid aggregation at required concentrations. For the crystallographic analysis of the GOLD:3A complexes and for the biochemical analysis of the GOLD-3A fusion proteins by SAXS, the *N*-terminal His₆-GB1 tags were removed with home-made TEV protease. Next, the proteins were purified using the size exclusion chromatography at HiLoad 16/60 Superdex 75 or Superdex 200 prep grade columns (GE Healthcare) in the storage buffer (10 mM Tris pH 8, 200 mM NaCl, 3 mM β -mercaptoethanol). In addition, the GOLD:3A complexes used for the crystallographic analysis were further purified by reverse immobilized metal affinity chromatography using the HisTrap HP column (GE Healthcare), while the EGFP-fused ACBD3 GOLD domain used for microscale thermophoresis was further purified using the ion exchange chromatography at a MonoQ 10/100 GL column (GE Healthcare) and then dialyzed back into the storage buffer. The molecular weight and purity of all proteins was verified by SDS-PAGE (Fig S9) and Matrix-Assisted Laser Desorption/Ionisation (MALDI). Purified proteins were concentrated to 1-10 mg/ml, aliquoted, flash frozen in the liquid nitrogen, and stored at -80 °C until needed.

Crystallization and crystallographic analysis – Crystals grew at 291 K in sitting drops by the vapor diffusion method. They were cryoprotected, flash frozen in liquid nitrogen, and analyzed. Measurements were carried out at the MX14.1 beamline of the synchrotron BESSY II at Helmholtz-Zentrum Berlin [39]. The crystallographic datasets were collected from single frozen crystals. Data were integrated and scaled using *XDS* [40] and *XDSAPP* [41]. Structures were solved by molecular replacement using the uncomplexed ACBD3 GOLD domain structure (pdb code 5LZ1) as a search model. The initial models were obtained with *Phaser* [42] from the *Phenix* package [43]. The models were further improved using automatic model building with *Buccaneer* [44] from the *CCP4* suite [45], automatic model refinement with *Phenix.refine* [46] from the *Phenix* package [43], and manual model building with *Coot* [47]. Statistics for data collection and processing, structure solution and refinement are summarized in Table 1. Structural figures were generated with *PyMol* [48]. The atomic coordinates and structural factors were deposited in the Protein Data Bank (www.pdb.org).

Microscale thermophoresis (MST) – MST measurements were carried out using the Monolith NT.115 instrument (NanoTemper Technologies) according to the manufacturer's instructions. The Monolith NT.115 standard treated capillaries were loaded with a mixture of a recombinant EGFP-fused protein at a constant concentration of 150 nM in the MST buffer (30 mM Tris pH 7.4, 150 mM NaCl, 3 mM β -mercaptoethanol) and its binding partner in the

appropriate series of concentrations. The thermophoretic motion of the fluorescent protein and its temperature-dependent changes of fluorescence were analyzed with the Monolith NT Analysis Software.

Tissue cultures and transfections – Human cervical-carcinoma cells HeLa (American Type Culture Collection / ATCC), embryonic kidney cells HEK293T (ATCC), and keratinocytes HaCaT (AddexBio) were maintained in Dulbecco's modified Eagle's medium (Sigma) supplemented with 10% fetal calf serum (Gibco). Human glioblastoma cells U-87 MG (ATCC) were maintained in Minimum Essential Medium Eagle (Sigma) supplemented with 10% fetal calf serum (Gibco), GlutaMAX Supplement (Thermo Fisher Scientific), and non-essential amino acids (Biowest). HeLa cells were transfected using Lipofectamine2000 reagent (Thermo Fisher Scientific) or X-tremeGENE HP DNA Transfection reagent (Sigma/Roche) according to manufacturer's instructions. Transfections of HEK293T cells were performed using polyethylenimine (Sigma) or Fugene6 (Promega).

Co-immunoprecipitation assay – HEK293T cells were transfected with the appropriate mutants of the EGFP-fused EVD68 3A protein and GST-fused ACBD3. The next day, cells were harvested, washed twice with phosphate-buffered saline (PBS) and lysed in the ice-cold lysis buffer (20 mM Tris pH 7.4, 100 mM NaCl, 50 mM NaF, 10 mM EDTA, 10% glycerol, 1% NP-40), supplemented with protease inhibitors (Complete protease inhibitor cocktail, Sigma/Roche). After solubilizing for 15 min on ice, the lysate was pre-cleared by centrifugation at 16,000g for 15 min. The resulting supernatant was incubated with sepharose beads coupled either to GFP nanobody (GFP-Trap, ChromoTek) or glutathione (Protino Glutathione Agarose, Macherey-Nagel) for 1h at 4 °C. After three washes with 10 volumes of the lysis buffer, the bound proteins were directly eluted with the Laemmli sample buffer, subjected to SDS-PAGE, and analyzed by immunoblotting. The whole cell lysates and eluted proteins were stained with mouse monoclonal antibodies to ACBD3 (Santa Cruz Biotechnology, sc-101277) and GFP (Santa Cruz Biotechnology, sc-9996). The images were acquired using the LI-COR Odyssey Infrared Imaging System.

Förster resonance energy transfer (FRET) assay – HeLa cells were co-transfected with plasmids encoding target proteins fused to the FRET pair of fluorescent proteins mAmetrine ("donor") and mPlum ("acceptor"). The next day, cells were harvested, washed twice with PBS, and analyzed by flow cytometry using BD LSR Fortessa (BD Biosciences). The donor and acceptor fluorescence as well as the energy transfer was determined using the optical configurations as follows: mAmetrine - 405 nm laser - 525/50 nm bandpass filter; mPlum - 561 nm laser - 670/30 nm bandpass filter; FRET - 405 nm laser - 655/8 nm bandpass filter. Acquired data were analyzed with the FlowJo software. The acquired fluorescence intensities were compensated and the same gate corresponding to the live transfected cells with the approximately 1:1 donor:acceptor ratio was applied to all samples. The acquired events were binned on the basis of the acceptor fluorescence intensity, and the average FRET fluorescence intensities of each bin were plotted against the respective acceptor fluorescence intensity.

Mammalian two-hybrid assay – HEK293T cells grown in 96-well plates were co-transfected with 50 ng of each pACT, pBIND, and pG5Luc plasmids using Fugene6 (Promega). At 24 hours post transfection, the cells were lysed, and both firefly and *Renilla* luciferase activities were measured using the Dual-Luciferase assay kit (Promega) and Centro LB 960 luminometer (Berthold Technologies) according to the manufacturer's instructions. The firefly luciferase activity was normalized to the *Renilla* luciferase activity (used as an internal control of the transfection efficiency) and then to the activity determined in cells co-expressing wild-type ACBD3 and 3A (which was set to 100 %).

Immunofluorescence assay – HeLa cells grown on coverslips in 24-well plates were transfected with 400 ng of the plasmid DNA using Lipofectamine2000 (Thermo Fisher Scientific). At 16 hours post transfection, the cells were fixed with 4% paraformaldehyde for 15 min at room temperature, permeabilized with 0.1% Triton X-100 in PBS for 5 min, and immunostained with the appropriate primary and secondary antibodies diluted in 2% normal goat serum in PBS. Sources of the antibodies were as follows: anti-ACBD3 (Sigma, WH0064746M1), anti-PI4KB (Merck, 06-578), anti-GM130 (BD Biosciences, 610822), anti-giantin (Enzo Life Science, ALX-804-600-C100), anti-myc (Thermo Fisher Scientific, PA1-981), anti-PI4P (Echelon, Z-P004), and goat-anti-mouse and goat-anti-rabbit secondary antibodies conjugated to AlexaFluor 488, 596, or 647 (Molecular Probes). Nuclei were stained with DAPI. Coverslips were mounted with FluorSave (Calbiochem), and confocal imaging was performed with a Leica Spell confocal microscope.

Virus subgenomic replicon assay – The pRib-EVD68/mCherry wild-type and mutant plasmids were linearized by cleavage with Sall-HF (Thermo Fisher Scientific) and purified using the mini spin columns (Epoch Life Science). Viral subgenomic replicon RNA was generated with TranscriptAid T7 High Yield Transcription Kit (Thermo Fisher Scientific) and purified using the RNeasy mini spin columns (Qiagen). For replicon assays, U-87 MG or HaCaT cells grown in 12-well plates were transfected with T7-amplified RNA using the TransIT mRNA transfection kit (Mirus Bio). At 12 hours post transfection, the reporter mCherry fluorescence was determined by flow cytometry using BD LSR Fortessa (BD Biosciences) and the following optical configuration: 561 nm laser, 670/30 nm bandpass filter. Acquired data were analyzed with the FlowJo software. The level of RNA replication was expressed as a transfection efficiency-

normalized percentage of cells with the mCherry signal above the threshold determined using the viral polymerase-lacking mutant $\Delta 3D^{pol}$.

To test the effect of PI4KB inhibition on virus replication, a PI4KB-specific inhibitor (compound 10 from [10] kindly provided by Radim Nencka) was added to the medium at a final concentration of 1 μ M 30 min prior transfection of the viral subgenomic replicon RNA.

Virus replication rescue assay – Wild-type or ACBD3 knock-out HeLa cells grown in 96-well plates were transfected with plasmids encoding wild-type or mutant ACBD3 or another Golgi-resident protein GalT as a control. At 24 hours post transfection, the cells were infected with the *Renilla* luciferase-expressing CVB3 virus (RLucCVB3) [49]. At 8 hours post infection, the intracellular *Renilla* luciferase activity was determined using the *Renilla* luciferase assay system (Promega) and a Centro LB 960 luminometer (Berthold Technologies). The *Renilla* luciferase activity was normalized to the activity determined in wild-type ACBD3-expressing cells (which was set to 100 %).

Small angle X-ray scattering (SAXS) measurements and data analysis – Proteins were dialyzed against the SAXS buffer (30 mM Tris pH 7.4, 150 mM NaCl, 1 mM TCEP) and concentrated as follows: $c_1 = 1.03$ mg/ml, $c_2 = 1.4$ mg/ml and $c_3 = 1.54$ mg/ml for the wild-type GOLD-3A fusion protein, and $c_1 = 0.96$ mg/ml, $c_2 = 2.36$ mg/ml and $c_3 = 3.26$ mg/ml for the GOLD-3A LVVY mutant. The SAXS data were collected using the beamlines BioSAXS Beamline BM29 (ESRF, Grenoble) and EMBL SAXS beamline P12 (Petra III DESY, Hamburg) that are both equipped with the 2M Pilatus detector (Dectris). The three datasets overlay after rescaling, indicating no protein aggregation in the samples. To structurally interpret the SAXS data, we incorporated the missing loop (D437-K473) into the structures of the wild-type GOLD-3A dimer and GOLD-3A LVVY mutant monomer. Next, we performed the coarse-grained molecular simulations [50] in which only the conformations of the D437-K473 loop were sampled while the crystallized portion of the protein was kept rigid, yielding 10,000 structural models of both proteins. For all structural models, we computed the SAXS intensity profiles using the previously developed algorithms [51], compared them individually to the experimental SAXS data, and selected the models best fitting the SAXS data collected on the samples with the highest protein concentrations. The best models fit the SAXS data with $\chi=1.5$ for the wild-type GOLD-3A dimer and $\chi=1.4$ for the GOLD-3A LVVY mutant monomer.

Molecular modeling and molecular dynamics (MD) simulations – The intrinsically disordered region of the ACBD3 GOLD domain, which was missing in the crystal structure (D437-K473), was modeled as described previously [23]. The C-terminal segment of the poliovirus 3A protein (N57-Q87) was modeled as a loop (N57-M60) followed by a transmembrane alpha helix (T61-F83) and a short C-terminal tail (A84-Q87). This segment was positioned in a planar segment of a lipid bilayer using the PPM server [52].

MD simulations of the ACBD3 GOLD domain in complex with the poliovirus 3A protein in the environment of a lipid bilayer were performed following the procedures recently used to study the ACBD3 GOLD domain in complex with the aichivirus 3A protein [23]. The initial system for MD simulations was prepared using VMD version 1.9.2 [53]. Namely, a POPC bilayer segment with the lateral dimensions of 10 nm by 10 nm was formed using the Membrane Plugin version 1.1 in VMD. The GOLD:3A complex was placed on top of the resulting lipid patch. The lipids overlapping with the transmembrane alpha helix of the 3A protein were removed. The system was solvated using the Solvate Plugin version 1.5 in VMD. Sodium and chloride ions were added to neutralize the simulated system and to reach a physiological concentration of 150 mM. The MD simulations were performed using the NAMD package [54] version 2.9. The CHARMM22 force field [55, 56] with the CMAP correction [57] and the TIP3P water model were used. The simulations were carried out in the NPT ensemble. Temperature was kept at 298K through a Langevin thermostat with a damping coefficient of 1/ps. Pressure was maintained at 1 atm using the Langevin piston Nose-Hoover method with a damping timescale of 50 fs and an oscillation timescale of 100 fs. Short-range non-bonded interactions were cut off smoothly between 1 and 1.2 nm. Long-range electrostatic interactions were computed using the particle-mesh Ewald method with a grid spacing of 0.1 nm. Simulations were performed with an integration time step of 2 fs. After initial energy minimization with a conjugate gradient method, a 10 ns simulation was performed with constraints on the protein backbone atoms in order to equilibrate the lipids, ions and water molecules. Namely, a harmonic potential with the spring constant of 5 kcal/(mol \AA^2) was applied to all backbone atoms of the GOLD:3A complex. After the equilibration, the system was simulated with no constraints for 200 ns. The resulting MD trajectory was visualized and analyzed using VMD.

Statistical analysis – In the graphs, data are presented as mean values \pm standard errors of the means (SEMs) based on three independent experiments, unless stated otherwise. For statistical analyses, two-tailed two-sample Student's t-tests were used. P-values below 0.05 were considered significant.

ACKNOWLEDGEMENTS

We are grateful to Carolyn Machamer and Jun Sasaki for sharing plasmids, and Radim Nencka for providing the PI4KB inhibitor. We thank Helmholtz-Zentrum Berlin (MX beamline 14.1, BESSY II, Berlin, Germany), EMBL Hamburg (SAXS beamline P12 at the Petra III storage ring, DESY, Hamburg, Germany), and ESRF Grenoble (BioSAXS beamline BM29, Grenoble, France) for the allocation of synchrotron radiation beamtime. Imaging was conducted at the Center for Cell Imaging (Faculty of Veterinary Medicine, Utrecht University). We are grateful to Anna Clemens for critical reading of the manuscript.

AUTHOR CONTRIBUTIONS

VH performed DNA cloning, the MST assay, the EVD68 subgenomic replicon assay, protein co-immunoprecipitations, and the FRET assay, HL carried out DNA cloning, the immunofluorescence, mammalian-two-hybrid, and CVB3 virus replication rescue assays, BR performed molecular dynamics simulations and analyzed SAXS data, DC and MS contributed to DNA cloning and protein purifications, JH contributed to the FRET assay, FJMvK, JRPMS, and EB designed the study and revised the manuscript, MK supervised the project, performed the crystallographic analysis, and wrote the manuscript.

ACCESSION CODES

The crystal structures of the ACBD3 GOLD domain in complex with the 3A proteins from EVD68, RVB14, and PV1 (L24A mutant), and the ACBD3 GOLD domain fused to the 3A proteins from EVA71, EVD68 (wild type), and EVD68 (LVVY mutant) from this publication have been submitted to the Protein Data Bank (www.pdb.org) and assigned the identifiers 6HLN, 6HLT, 6HLV, 6HLW, 6HM8, and 6HMV, respectively.

REFERENCES

1. Tapparel C, Siegrist F, Petty TJ, Kaiser L. Picornavirus and enterovirus diversity with associated human diseases. *Infect Genet Evol.* 2013;14:282-93. doi: 10.1016/j.meegid.2012.10.016.
2. Wessels E, Duijsings D, Niu T-K, Neumann S, Oorschot VM, de Lange F, et al. A viral protein that blocks Arf1-mediated COP-I assembly by inhibiting the guanine nucleotide exchange factor GBF1. *Dev Cell.* 2006;11:191-201. doi: 10.1016/j.devcel.2006.06.005.
3. Greninger AL, Knudsen GM, Betegon M, Burlingame AL, DeRisi JL. The 3A protein from multiple picornaviruses utilizes the golgi adaptor protein ACBD3 to recruit PI4KIIIβ. *J Virol.* 2012;86:3605-16. doi: 10.1128/JVI.06778-11.
4. Liao J, Guan Y, Chen W, Shi C, Yao D, Wang F, et al. ACBD3 is required for FAPP2 transferring glucosylceramide through maintaining the Golgi integrity. *J Mol Cell Biol.* 2018. doi: 10.1093/jmcb/mjy030.
5. Sohda M, Misumi Y, Yamamoto A, Yano A, Nakamura N, Ikehara Y. Identification and characterization of a novel Golgi protein, GCP60, that interacts with the integral membrane protein giantin. *J Biol Chem.* 2001;276:45298-306. doi: 10.1074/jbc.M108961200.
6. Greninger AL, Knudsen GM, Betegon M, Burlingame AL, DeRisi JL. ACBD3 interaction with TBC1 domain protein is differentially affected by enteroviral and kobuviral 3A protein binding. *mBio.* 2013;4:e00098-13. doi: 10.1128/mBio.00098-13.
7. Klima M, Tóth DJ, Hexnerova R, Baumlova A, Chalupska D, Tykvar J, et al. Structural insights and in vitro reconstitution of membrane targeting and activation of human PI4KB by the ACBD3 protein. *Sci Rep.* 2016;6:23641. doi: 10.1038/srep23641.
8. Lei X, Xiao X, Zhang Z, Ma Y, Qi J, Wu C, et al. The Golgi protein ACBD3 facilitates Enterovirus 71 replication by interacting with 3A. *Sci Rep.* 2017;7:44592. doi: 10.1038/srep44592.
9. Hsu N-Y, Ilnytska O, Belov G, Santiana M, Chen Y-H, Takvorian PM, et al. Viral reorganization of the secretory pathway generates distinct organelles for RNA replication. *Cell.* 2010;141:799-811. doi: 10.1016/j.cell.2010.03.050.
10. Mejdrova I, Chalupska D, Plackova P, Mueller C, Sala M, Klima M, et al. Rational design of novel highly potent and selective phosphatidylinositol 4-kinase III beta (PI4KB) inhibitors as broad-spectrum antiviral agents and tools for chemical biology. *J Med Chem.* 2017;60(1):100-18. doi: 10.1021/acs.jmedchem.6b01465.
11. Xiao X, Lei X, Zhang Z, Ma Y, Qi J, Wu C, et al. Enterovirus 3A facilitates viral replication by promoting PI4KB-ACBD3 interaction. *J Virol.* 2017. doi: 10.1128/JVI.00791-17.
12. Arita M. Phosphatidylinositol-4 kinase III beta and oxysterol-binding protein accumulate unesterified cholesterol on poliovirus-induced membrane structure. *Microbiol Immunol.* 2014;58:239-56. doi: 10.1111/1348-0421.12144.
13. Banerjee S, Aponte-Diaz D, Yeager C, Sharma SD, Ning G, Oh HS, et al. Hijacking of multiple phospholipid biosynthetic pathways and induction of membrane biogenesis by a picornaviral 3CD protein. *PLoS Pathog.* 2018;14(5):e1007086. doi: 10.1371/journal.ppat.1007086.
14. Sasaki J, Ishikawa K, Arita M, Taniguchi K. ACBD3-mediated recruitment of PI4KB to picornavirus RNA replication sites. *EMBO J.* 2012;31:754-66. doi: 10.1038/emboj.2011.429.
15. Ishikawa-Sasaki K, Sasaki J, Taniguchi K. A complex comprising phosphatidylinositol 4-kinase IIIβ, ACBD3, and Aichi virus proteins enhances phosphatidylinositol 4-phosphate synthesis and is critical for formation of the viral replication complex. *J Virol.* 2014;88:6586-98. doi: 10.1128/JVI.00208-14.
16. McPhail JA, Ottosen EH, Jenkins ML, Burke JE. The molecular basis of Aichi virus 3A protein activation of phosphatidylinositol 4 kinase IIIbeta, PI4KB, through ACBD3. *Structure.* 2017;25(1):121-31. doi: 10.1016/j.str.2016.11.016.
17. Dubankova A, Humpolickova J, Klima M, Boura E. Negative charge and membrane-tethered viral 3B cooperate to recruit viral RNA dependent RNA polymerase 3Dpol. *Sci Rep.* 2017;7(1):17309. doi: 10.1038/s41598-017-17621-6.
18. Mesmin B, Bigay J, Moser von Filseck J, Lacas-Gervais S, Drin G, Antony B. A four-step cycle driven by PI(4)P hydrolysis directs sterol/PI(4)P exchange by the ER-Golgi tether OSBP. *Cell.* 2013;155:830-43. doi: 10.1016/j.cell.2013.09.056.
19. Chung J, Torta F, Masai K, Lucast L, Czapl H, Tanner LB, et al. PI4P/phosphatidylserine countertransport at ORP5- and ORP8-mediated ER-plasma membrane contacts. *Science.* 2015;349:428-32. doi: 10.1126/science.aab1370.
20. Roulin PS, Lötzerich M, Torta F, Tanner LB, van Kuppeveld FJM, Wenk MR, et al. Rhinovirus uses a phosphatidylinositol 4-phosphate/cholesterol counter-current for the formation of replication

- compartments at the ER-Golgi interface. *Cell Host Microbe*. 2014;16:677-90. doi: 10.1016/j.chom.2014.10.003.
21. Lyoo H, van der Schaar HM, Dorobantu CM, Rabouw HH, Strating JRPM, van Kuppeveld FJM. ACBD3 is an essential pan-enterovirus host factor that mediates the interaction between viral 3A protein and cellular protein PI4KB. *mBio*. 2019;10(1):e02742-18. doi: 10.1128/mBio.02742-18.
 22. Strauss DM, Glustrom LW, Wuttke DS. Towards an understanding of the poliovirus replication complex: the solution structure of the soluble domain of the poliovirus 3A protein. *J Mol Biol*. 2003;330:225-34.
 23. Klima M, Chalupska D, Rozycki B, Humpolickova J, Rezakova L, Silhan J, et al. Kobuviral non-structural 3A proteins act as molecular harnesses to hijack the host ACBD3 protein. *Structure*. 2017;25(2):219-30. doi: 10.1016/j.str.2016.11.021.
 24. Schymkowitz J, Borg J, Stricher F, Nys R, Rousseau F, Serrano L. The FoldX web server: an online force field. *Nucleic Acids Res*. 2005;33:W382-8. doi: 10.1093/nar/gki387.
 25. Wessels E, Notebaart RA, Duijsings D, Lanke K, Vergeer B, Melchers WJ, et al. Structure-function analysis of the coxsackievirus protein 3A: identification of residues important for dimerization, viral RNA replication, and transport inhibition. *J Biol Chem*. 2006;281(38):28232-43. doi: 10.1074/jbc.M601122200.
 26. Dorobantu CM, van der Schaar HM, Ford LA, Strating JRPM, Ulferts R, Fang Y, et al. Recruitment of PI4KIIIβ to coxsackievirus B3 replication organelles is independent of ACBD3, GBF1, and Arf1. *J Virol*. 2014;88:2725-36. doi: 10.1128/JVI.03650-13.
 27. Dorobantu CM, Ford-Siltz LA, Sittig SP, Lanke KHW, Belov GA, van Kuppeveld FJM, et al. GBF1- and ACBD3-independent recruitment of PI4KIIIβ to replication sites by rhinovirus 3A proteins. *J Virol*. 2015;89:1913-8. doi: 10.1128/JVI.02830-14.
 28. Esser-Nobis K, Harak C, Schult P, Kusov Y, Lohmann V. Novel perspectives for hepatitis A virus therapy revealed by comparative analysis of hepatitis C virus and hepatitis A virus RNA replication. *Hepatology*. 2015;62(2):397-408. doi: 10.1002/hep.27847.
 29. Berryman S, Moffat K, Harak C, Lohmann V, Jackson T. Foot-and-mouth disease virus replicates independently of phosphatidylinositol 4-phosphate and type III phosphatidylinositol 4-kinases. *J Gen Virol*. 2016;97(8):1841-52. doi: 10.1099/jgv.0.000485.
 30. Dorobantu CM, Albuлесcu L, Harak C, Feng Q, van Kampen M, Strating JRPM, et al. Modulation of the host lipid landscape to promote RNA virus replication: the picornavirus encephalomyocarditis virus converges on the pathway used by hepatitis C virus. *PLoS Pathog*. 2015;11:e1005185. doi: 10.1371/journal.ppat.1005185.
 31. Heinz BA, Vance LM. The antiviral compound enviroxime targets the 3A coding region of rhinovirus and poliovirus. *J Virol*. 1995;69(7):4189-97.
 32. De Palma AM, Thibaut HJ, van der Linden L, Lanke K, Heggmont W, Ireland S, et al. Mutations in the nonstructural protein 3A confer resistance to the novel enterovirus replication inhibitor TTP-8307. *Antimicrob Agents Chemother*. 2009;53(5):1850-7. doi: 10.1128/AAC.00934-08.
 33. Arita M, Wakita T, Shimizu H. Cellular kinase inhibitors that suppress enterovirus replication have a conserved target in viral protein 3A similar to that of enviroxime. *J Gen Virol*. 2009;90(Pt 8):1869-79. doi: 10.1099/vir.0.012096-0.
 34. Arita M, Bigay J. Poliovirus evolution towards independence from the phosphatidylinositol-4 kinase III beta/oxysterol-binding protein family I pathway. *ACS Infect Dis*. 2019. doi: 10.1021/acsinfecdis.9b00038.
 35. Greninger AL. Picornavirus--host interactions to construct viral secretory membranes. *Prog Mol Biol Transl*. 2015;129:189-212. doi: 10.1016/bs.pmbts.2014.10.007.
 36. Ai HW, Hazelwood KL, Davidson MW, Campbell RE. Fluorescent protein FRET pairs for ratiometric imaging of dual biosensors. *Nat Methods*. 2008;5(5):401-3. doi: 10.1038/nmeth.1207.
 37. Kremers GJ, Hazelwood KL, Murphy CS, Davidson MW, Piston DW. Photoconversion in orange and red fluorescent proteins. *Nat Methods*. 2009;6(5):355-8. doi: 10.1038/nmeth.1319.
 38. Cole NB, Smith CL, Sciaky N, Terasaki M, Edidin M, Lippincott-Schwartz J. Diffusional mobility of Golgi proteins in membranes of living cells. *Science*. 1996;273(5276):797-801.
 39. Mueller U, Darowski N, Fuchs MR, Förster R, Hellmig M, Paithankar KS, et al. Facilities for macromolecular crystallography at the Helmholtz-Zentrum Berlin. *J Synchrotron Radiat*. 2012;19:442-9. doi: 10.1107/S0909049512006395.
 40. Kabsch W. XDS. *Acta Crystallogr D*. 2010;66:125-32. doi: 10.1107/S0907444909047337.
 41. Krug M, Weiss MS, Heinemann U, Mueller U. XDSAPP: a graphical user interface for the convenient processing of diffraction data using XDS. *J Appl Crystallogr*. 2012;45:568-72. doi: 10.1107/S0021889812011715.

42. McCoy AJ, Grosse-Kunstleve RW, Adams PD, Winn MD, Storoni LC, Read RJ. Phaser crystallographic software. *J Appl Crystallogr*. 2007;40:658-74. doi: 10.1107/S0021889807021206.
43. Adams PD, Afonine PV, Bunkóczi G, Chen VB, Davis IW, Echols N, et al. PHENIX : a comprehensive Python-based system for macromolecular structure solution. *Acta Crystallogr D*. 2010;66:213-21. doi: 10.1107/S0907444909052925.
44. Cowtan K. The Buccaneer software for automated model building. 1. Tracing protein chains. *Acta Crystallogr D*. 2006;62:1002-11. doi: 10.1107/S0907444906022116.
45. Winn MD, Ballard CC, Cowtan KD, Dodson EJ, Emsley P, Evans PR, et al. Overview of the CCP4 suite and current developments. *Acta Crystallogr D*. 2011;67:235-42. doi: 10.1107/S0907444910045749.
46. Afonine PV, Grosse-Kunstleve RW, Echols N, Headd JJ, Moriarty NW, Mustyakimov M, et al. Towards automated crystallographic structure refinement with phenix.refine. *Acta Crystallogr D*. 2012;68:352-67. doi: 10.1107/S0907444912001308.
47. Emsley P, Cowtan K. Coot : model-building tools for molecular graphics. *Acta Crystallogr D*. 2004;60:2126-32. doi: 10.1107/S0907444904019158.
48. The PyMOL Molecular Graphics System, Version 1.8 Schrödinger, LLC.
49. Lanke KH, van der Schaar HM, Belov GA, Feng Q, Duijsings D, Jackson CL, et al. GBF1, a guanine nucleotide exchange factor for Arf, is crucial for coxsackievirus B3 RNA replication. *J Virol*. 2009;83(22):11940-9. doi: 10.1128/JVI.01244-09.
50. Kim YC, Hummer G. Coarse-grained models for simulations of multiprotein complexes: application to ubiquitin binding. *J Mol Biol*. 2008;375(5):1416-33. doi: 10.1016/j.jmb.2007.11.063.
51. Rozycki B, Kim YC, Hummer G. SAXS ensemble refinement of ESCRT-III CHMP3 conformational transitions. *Structure*. 2011;19(1):109-16. doi: 10.1016/j.str.2010.10.006.
52. Lomize MA, Lomize AL, Pogozheva ID, Mosberg HI. OPM: orientations of proteins in membranes database. *Bioinformatics*. 2006;22(5):623-5. doi: 10.1093/bioinformatics/btk023.
53. Humphrey W, Dalke A, Schulten K. VMD: visual molecular dynamics. *J Mol Graphics*. 1996;14:33-8, 27-8.
54. Phillips JC, Braun R, Wang W, Gumbart J, Tajkhorshid E, Villa E, et al. Scalable molecular dynamics with NAMD. *J Comput Chem*. 2005;26:1781-802. doi: 10.1002/jcc.20289.
55. MacKerell AD, Bashford D, Bellott M, Dunbrack RL, Evanseck JD, Field MJ, et al. All-atom empirical potential for molecular modeling and dynamics studies of proteins. *J Phys Chem B*. 1998;102:3586-616. doi: 10.1021/jp973084f.
56. Klauda JB, Venable RM, Freites JA, O'Connor JW, Tobias DJ, Mondragon-Ramirez C, et al. Update of the CHARMM all-atom additive force field for lipids: validation on six lipid types. *J Phys Chem B*. 2010;114:7830-43. doi: 10.1021/jp101759q.
57. MacKerell AD, Feig M, Brooks CL. Extending the treatment of backbone energetics in protein force fields: limitations of gas-phase quantum mechanics in reproducing protein conformational distributions in molecular dynamics simulations. *J Comput Chem*. 2004;25:1400-15. doi: 10.1002/jcc.20065.

SUPPORTING INFORMATION

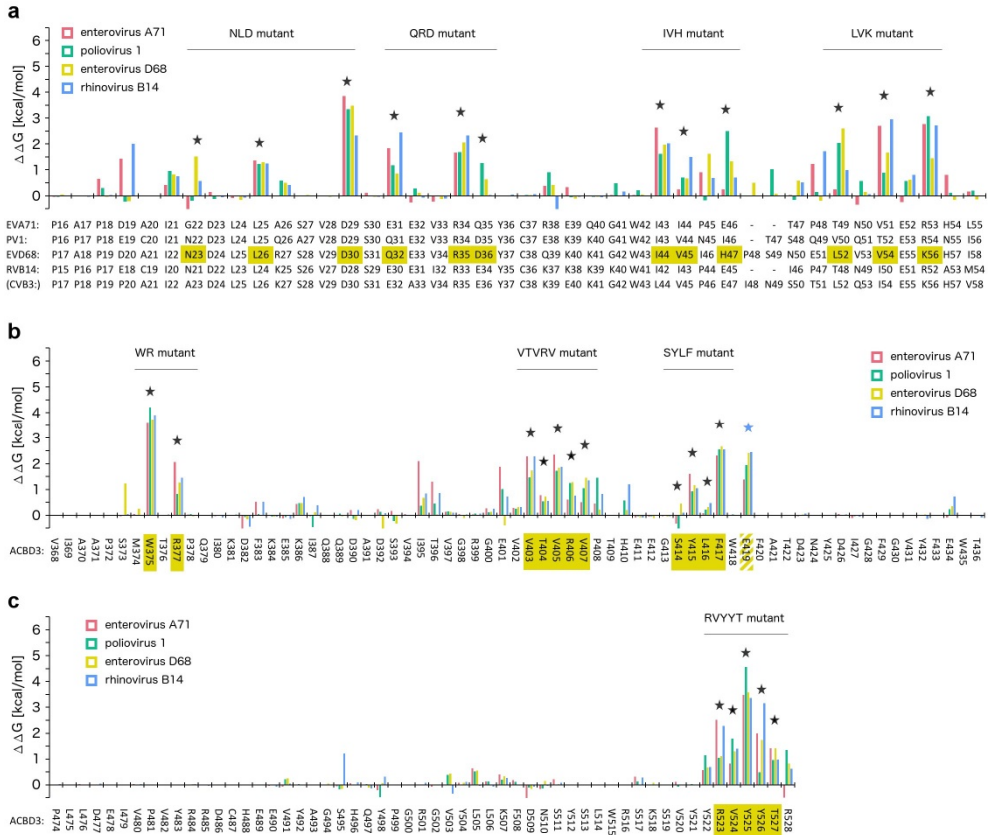


Figure S1. Design of the 3A and ACBD3 mutants used in this study. **a**, Changes of the ACBD3 - 3A interaction energies of to-alanine mutants of 3A as obtained with the *Pssm* tool of the *FoldX* software package [24] using the crystal structures presented in this work. Amino acid residues used for further design of single and multiple 3A mutants are marked by asterisks. **b-c**, Changes of the ACBD3 - 3A interaction energies of to-alanine mutants of ACBD3 within the regions V368-T436 and P474-R528 (c) calculated and visualized as in (a). Data for the intrinsically disordered region D437-K473 are not available. The ACBD3 E419A mutant was released from the Golgi (Fig S4e) and, therefore, excluded from further design of multiple mutants.

6

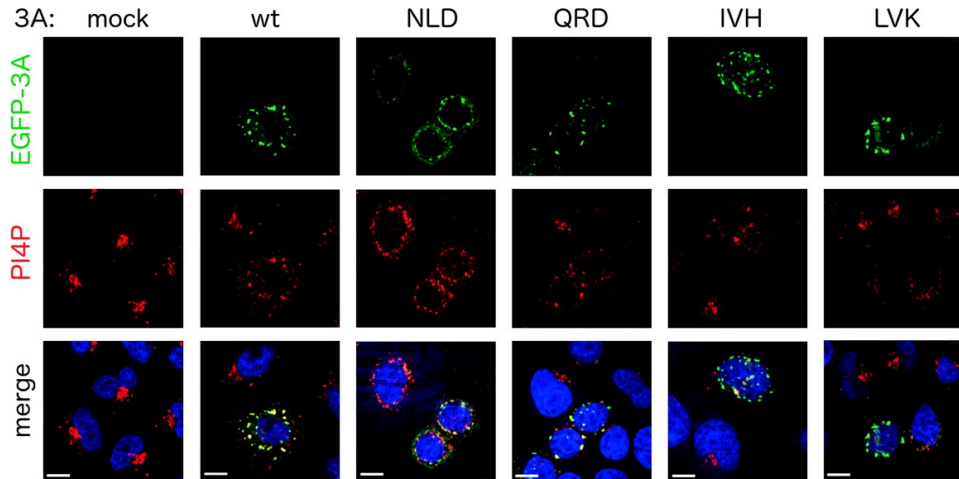


Figure S2. PI4P levels in the wild-type and mutant EVD68 3A-expressing cells. EGFP-fused wild-type EVD68 3A and its mutants were overexpressed in HeLa cells. The cells were fixed and immunostained with the anti-PI4P antibody (Echelon #Z-P004). Scale bars represent 10 μ m.

CONVERGENT EVOLUTION IN THE MECHANISMS OF ACBD3 RECRUITMENT TO PICORNAVIRUS REPLICATION SITES

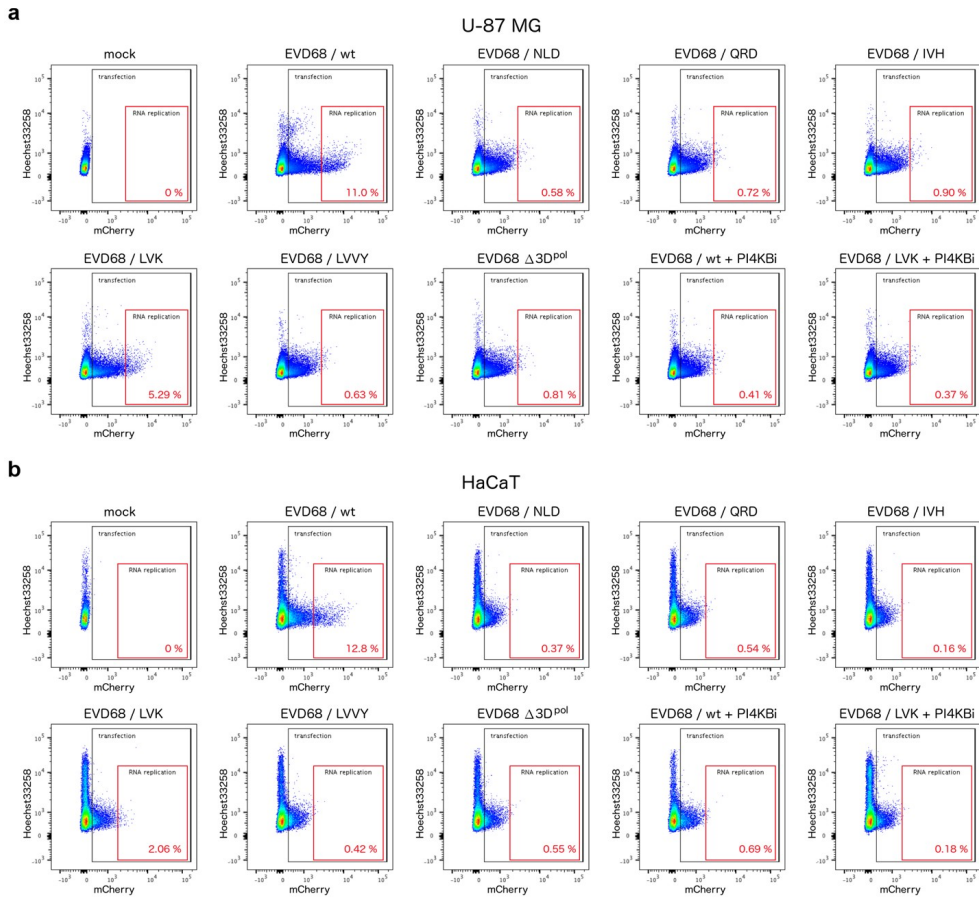


Figure S3. Analysis of the EVD68 mutants by the subgenomic replicon assay (raw data). **a-b**, Human glioblastoma cells U-87 MG (**a**) or keratinocytes HaCaT (**b**) were transfected with the T7-amplified EVD68 Fermon strain subgenomic replicon wild-type RNA or its mutants as indicated, and the reporter mCherry fluorescence was determined by flow cytometry. Staining with the Hoechst33258 dye was added to determine the cell viability. The level of RNA replication was expressed as a percentage of cells with the mCherry signal above the threshold determined using the viral polymerase-lacking mutant $\Delta 3D^{pol}$ (red region), further normalized to the transfection efficiency (black region). Data from one representative experiment are shown; please see Fig 3f-g and Fig 5i for the quantification based on two independent experiments. PI4Kbi, a PI4KB-specific inhibitor (compound 10 in Mejdrova et al. [10]).

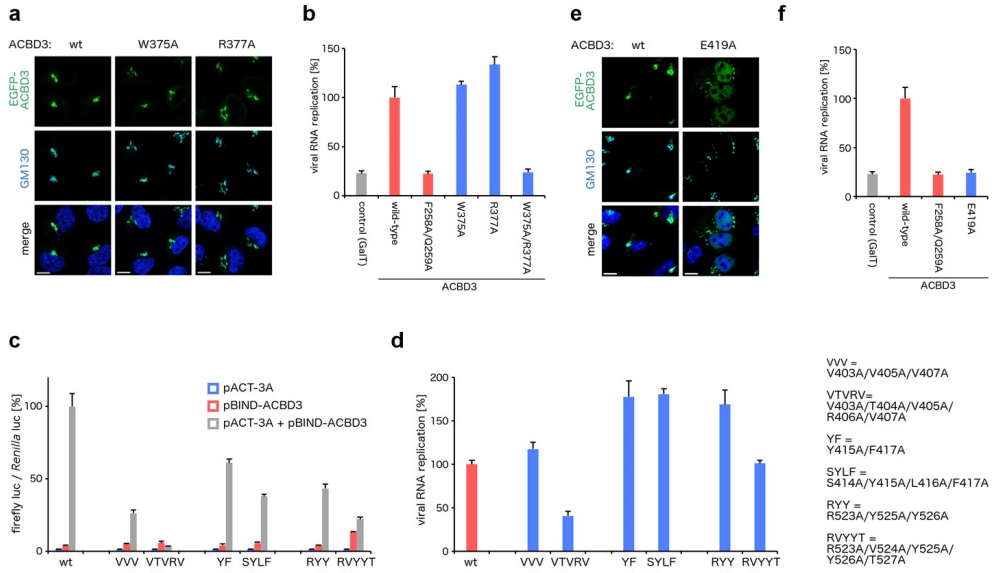


Figure S4. Analysis of the ACBD3-3A interface. **a, e**, Localization of the ACBD3 mutants. EGFP-fused wild-type ACBD3 or its mutants were overexpressed in HeLa ACBD3 knock-out cells. Cells were fixed and immunostained with the anti-GM130 antibody (marker of Golgi). Scale bars represent 10 μ m. **b, d, f**, Rescue of enterovirus replication by the ACBD3 mutants. HeLa ACBD3 knock-out cells were transfected with wild-type ACBD3 or its mutants, and enterovirus replication was determined using the *Renilla* luciferase-expressing CVB3 virus by the *Renilla* luciferase assay system. GalT and ACBD3 F258A/Q259A were used as controls. **c**, Mammalian-two-hybrid assay with the ACBD3 mutants and wild-type 3A. HeLa cells were transfected as indicated and the firefly luciferase activity normalized to the *Renilla* luciferase activity was determined using a dual-luciferase reporter assay system.

CONVERGENT EVOLUTION IN THE MECHANISMS OF ACBD3 RECRUITMENT TO PICORNAVIRUS REPLICATION SITES

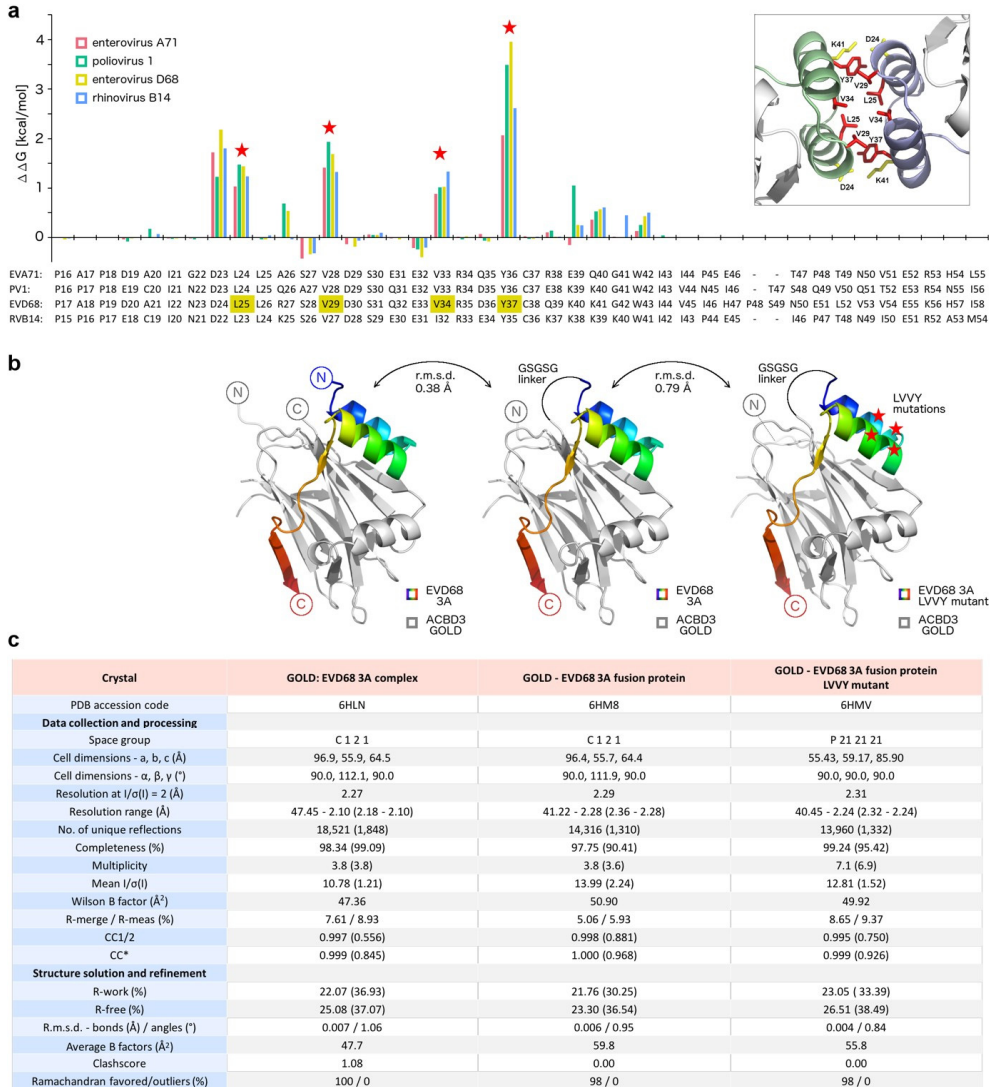


Figure S5. Design and crystallization of the GOLD-3A fusion protein and its LVVY mutant. **a**, Changes of the dimerization energies of to-alanine mutants of the GOLD: 3A complexes as obtained with the *Psm* tool of the *FoldX* software package [24] using the crystal structures presented in this work. Residues forming the hydrophobic core of the dimerization interface are marked by asterisks. In the inset, a detailed view of the EVD68 3A dimerization interface colored as in Fig 5a is shown. **b**, Overall fold of the GOLD: EVD68 3A complex formed by two individual proteins (left), wild-type GOLD - EVD68 3A fusion protein (middle), and its LVVY mutant (right). The ACBD3 GOLD domain is depicted in grey, the EVD68 3A protein in rainbow colors from blue (*N* terminus) to red (*C* terminus). Residues forming the hydrophobic core of the dimerization interface (mutated in the LVVY mutant) are marked by asterisks. **c**, Statistics for data collection and processing, structure solution and refinement of the proteins and protein complexes shown in (b). Numbers in parentheses refer to the highest resolution shell of the respective dataset.

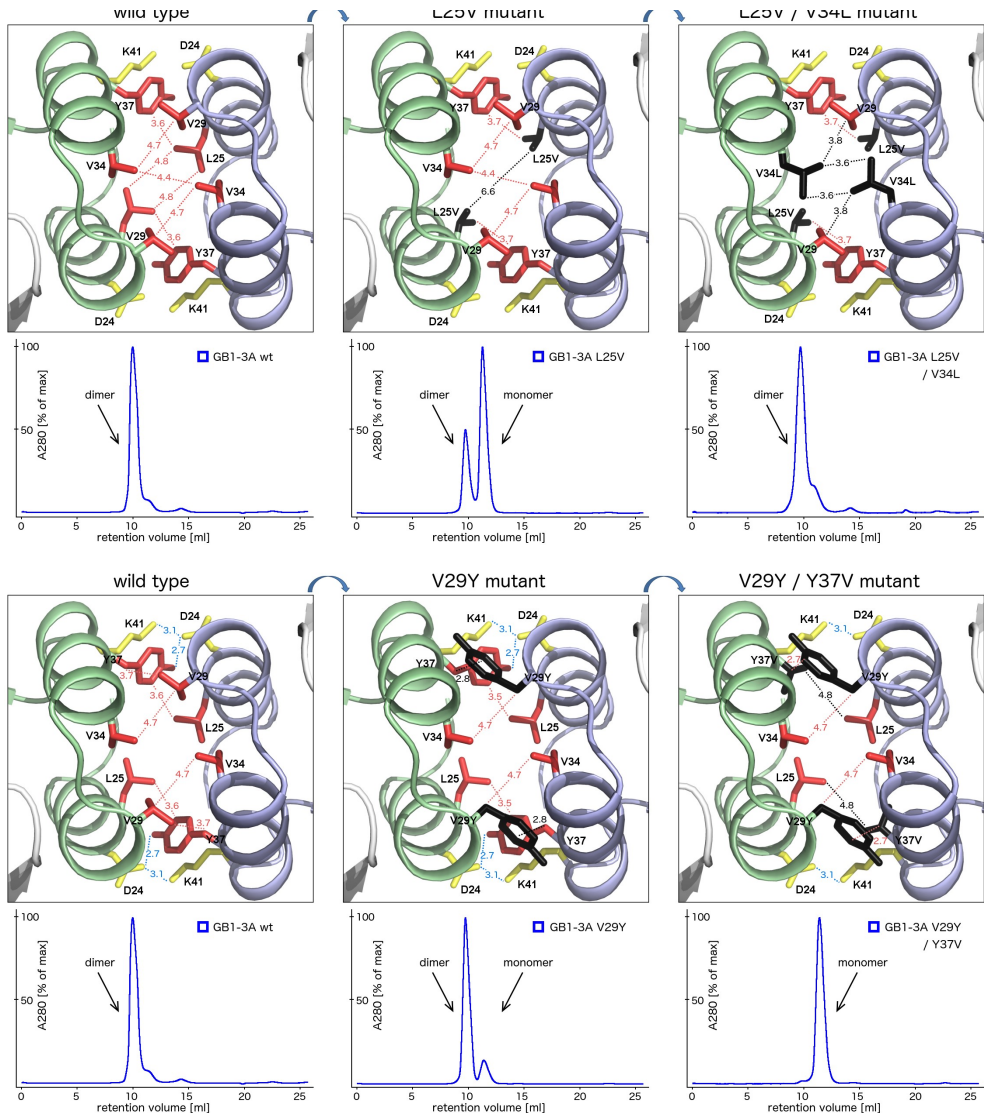


Figure S6. Analysis of the dimerization of selected EVD68 3A mutants. In the upper panels, a detailed view of the EVD68 3A dimerization interface colored as in Fig 5a is shown, except for the mutated residues, which are depicted in black. Distances of the closest atom pairs of selected residues are shown in Angstroms. Homology models of the mutant 3A proteins were generated by mutating the respective residues in Coot followed by the energy minimization in Swiss-PDBViewer. In the lower panels, elution profiles of the GB1-fused wild-type and mutant EVD68 3A proteins are shown. Each protein at a final concentration of 100 μ M was analyzed by size exclusion chromatography using the Superdex 10/300 Increase column (GE Healthcare) and its elution was monitored by the absorbance at 280 nm.

CONVERGENT EVOLUTION IN THE MECHANISMS OF ACBD3 RECRUITMENT TO PICORNAVIRUS REPLICATION SITES

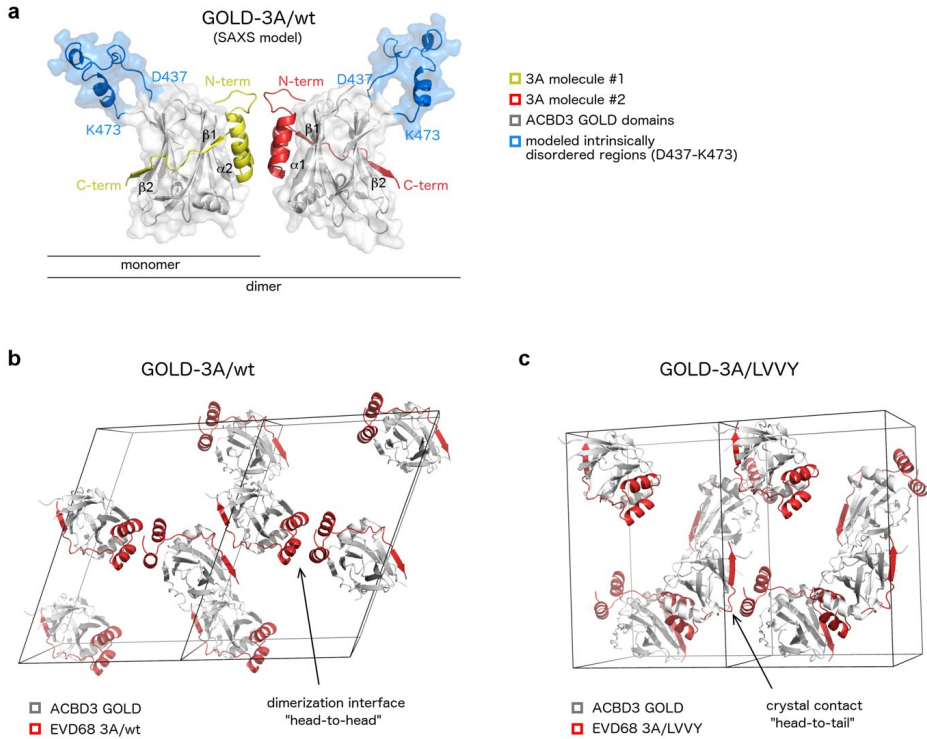


Figure S7. Analysis of the dimerization of selected EVD68 3A mutants. **a**, Structural model of the dimer of the GOLD - EVD68 3A fusion proteins used for the SAXS analysis. The ACBD3 GOLD domains are shown in cartoon representation with a semi-transparent surface and colored in grey except for the modeled intrinsically disordered loops of ACBD3 (D437-K473), which are depicted in blue. The EVD68 3A proteins are colored in yellow and red. **b-c**, Crystal packing of the wild-type GOLD - EVD68 3A fusion protein (**b**) and its LVVY mutant (**c**). The content of two unit cells with protein backbones in cartoon representation is shown. The ACBD3 GOLD domain is depicted in grey, the EVD68 3A protein in red. Wild-type 3A forms a crystal-packing contact through the 3A dimerization interface (**b**), while in the case of the LVVY mutant this contact is not preserved and instead, the *N*-terminal alpha helix of 3A forms a crystal-packing contact with the *C*-terminal beta strand of another 3A molecule (**c**).

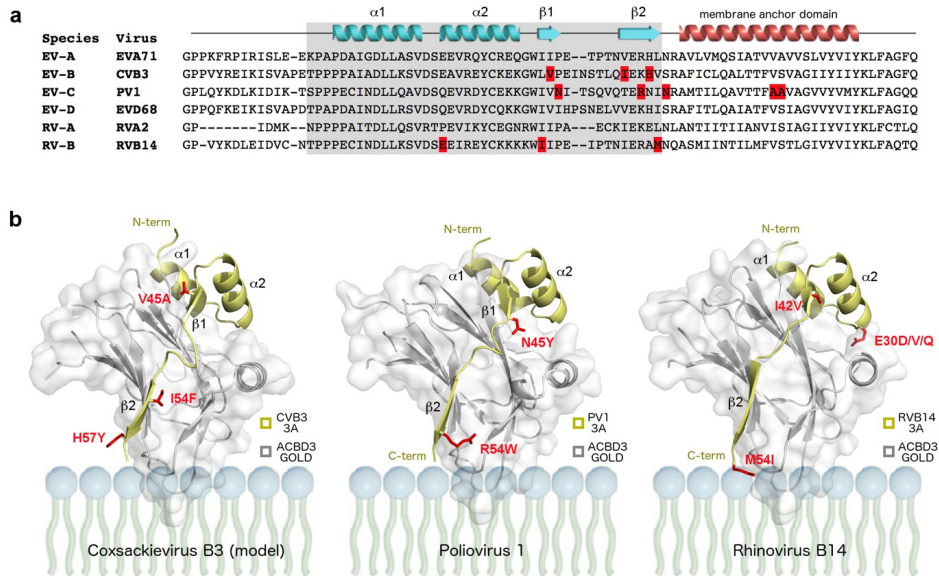


Figure S8. Localization of the PI4KB/OSBP-inhibition resistance-conferring mutations. **a**, Localization of the PI4KB/OSBP-inhibition resistance-conferring mutations within the primary sequences of the enterovirus 3A proteins. Sequences of the 3A proteins of selected enteroviruses used in this study were aligned as in Fig 1a. Secondary structures present in the crystal structures of the ACBD3: 3A complexes (colored in light blue) and the hydrophobic alpha helix anchoring the 3A proteins to the membrane (colored in red) are indicated above the sequences. ACBD3-binding regions are shaded in grey. Residues whose mutations have been reported to confer resistance to the PI4KB/OSBP-specific inhibitors, i.e. PV1 N45Y, R54W, N57D, A70T, and A71S, CVB3 V45A, I54F, and H57Y, and RVB14 E30D/V/Q, I42V, and M54I [31-34], are highlighted in red. **b**, Localization of the PI4KB/OSBP-inhibition resistance-conferring mutations within the structures of the GOLD: 3A complexes. A homology model of the GOLD: CVB3 3A complex was generated by the I-TASSER server [58] using the crystal structure of the GOLD: EVD68 3A complex as a template. The ACBD3 GOLD domain is shown in cartoon representation with a semi-transparent surface and colored in grey; the enterovirus 3A proteins are depicted in yellow. Residues whose mutations have been reported to confer resistance to the PI4KB/OSBP-specific inhibitors are highlighted in red.

CONVERGENT EVOLUTION IN THE MECHANISMS OF ACBD3 RECRUITMENT TO PICORNAVIRUS REPLICATION SITES

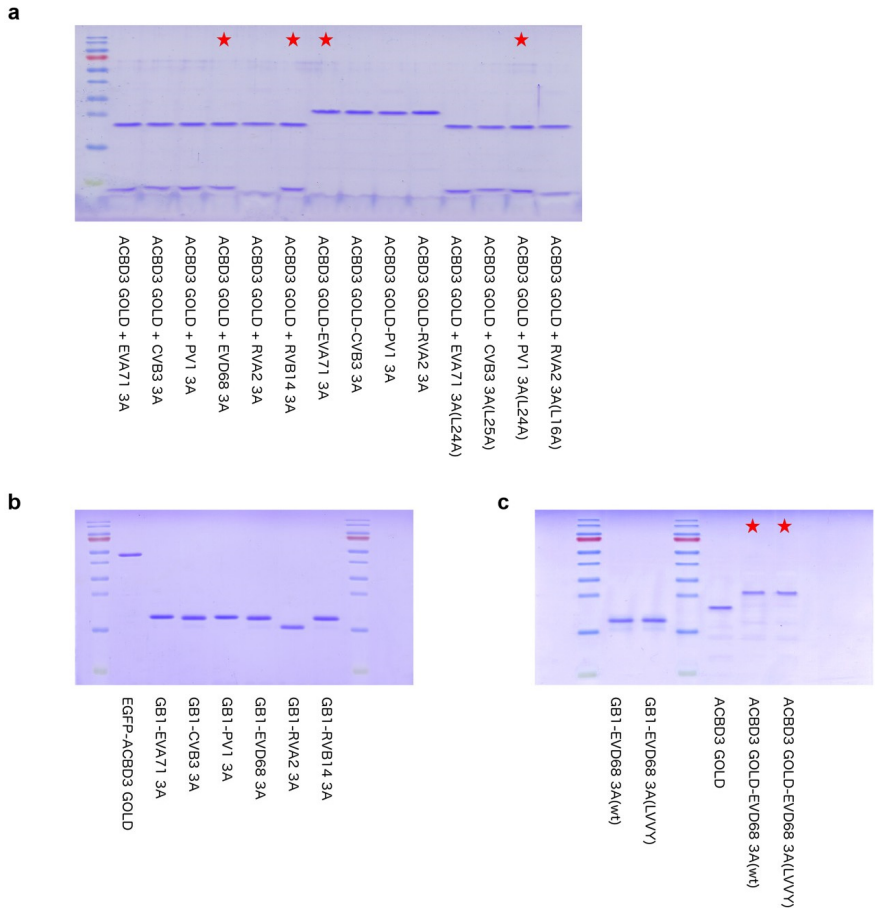


Figure S9. Recombinant proteins used in the study. Recombinant proteins used for the crystallographic analysis (a), microscale thermophoresis (b), and SAXS analysis (c) were resolved by SDS-PAGE using the 15% polyacrylamide gels and stained with Coomassie Blue. The hyphen signs ("-") indicate fusion proteins, while the plus signs ("+") indicate complexes of two individual proteins. The uncomplexed viral proteins used for microscale thermophoresis and SAXS analysis were fused to the B1 domain of streptococcal protein G ("GB1 tag") to improve their solubility and to avoid their non-specific aggregation. Asterisks indicate the successfully crystallized proteins and protein complexes.

SUPPORTING REFERENCE

58. Yang J, Yan R, Roy A, Xu D, Poisson J, Zhang Y. The I-TASSER Suite: protein structure and function prediction. Nat Methods. 2015;12(1):7-8. doi: 10.1038/nmeth.3213.

CHAPTER 7

CHARACTERIZATION OF THE C10ORF76-PI4KB COMPLEX AND ITS NECESSITY FOR GOLGI PI4P LEVELS AND ENTEROVIRUS REPLICATION

Jacob A McPhail¹, Heyrhyoung Lyoo^{2,}, Joshua G Pemberton^{3,*}, Reece M Hoffmann¹, Wendy van Elst², Jeroen RPM Strating², Meredith L Jenkins¹, Jordan TB Stariha¹, Cameron J Powell¹, Martin J Boulanger¹, Tamas Balla^{3,#}, Frank JM van Kuppeveld^{2,#}, John E Burke^{1,#}*

¹Department of Biochemistry and Microbiology, University of Victoria, Victoria, BC, Canada

²Department of Infectious Diseases & Immunology, Virology Division, Faculty of Veterinary Medicine, Utrecht University, Utrecht, The Netherlands.

³Section on Molecular Signal Transduction, Eunice Kennedy Shriver National Institute of Child Health and Human Development, National Institutes of Health, Bethesda, MD, USA

*These authors contributed equally.

#Corresponding author

SUMMARY

The lipid kinase PI4KB, which generates phosphatidylinositol 4-phosphate (PI4P), is a key enzyme in regulating membrane transport and is also hijacked by multiple picornaviruses to mediate viral replication. PI4KB can interact with multiple protein binding partners, which are differentially manipulated by picornaviruses to facilitate replication. The protein c10orf76 is a PI4KB-associated protein that increases PI4P levels at the Golgi, and is essential for the viral replication of specific enteroviruses. We used hydrogen deuterium exchange mass spectrometry to characterize the c10orf76-PI4KB complex and reveal that binding is mediated by the kinase linker of PI4KB, with formation of the heterodimeric complex modulated by PKA-dependent phosphorylation. Complex-disrupting mutations demonstrate that PI4KB is required for membrane recruitment of c10orf76 to the Golgi, and that an intact c10orf76-PI4KB complex is required for the replication of c10orf76-dependent enteroviruses. Intriguingly, c10orf76 was also contributed to proper Arf1 activation at the Golgi, providing a putative mechanism for the c10orf76-dependent increase in PI4P levels at the Golgi.

HIGHLIGHTS

- c10orf76 forms a direct complex with PI4KB, with the interface formed by a disorder-to-order transition in the kinase linker of PI4KB
- The c10orf76 binding site of PI4KB can be phosphorylated by PKA, with phosphorylation leading to decreased affinity for c10orf76
- Complex-disrupting mutants of PI4KB and c10orf76 reveal that PI4KB recruits c10orf76 to the Golgi/TGN
- Depletion of c10orf76 leads to decreases in both active Arf1 and Golgi PI4P levels
- Enteroviruses that rely on c10orf76 for replication depend on formation of the c10orf76-PI4KB complex

KEYWORDS

c10orf76, ARMH3, phosphatidylinositol 4-kinase, PI4KB, PI4KIII β , GBF1, Arf1, phosphoinositide, phosphatidylinositol 4-phosphate, PI4P, PKA, enterovirus, coxsackievirus-A10, viral replication, hydrogen deuterium exchange mass spectrometry, HDX-MS

INTRODUCTION

Phosphoinositides are essential regulatory lipids that play important roles in myriad cellular functions. The phosphoinositide species phosphatidylinositol-4-phosphate (PI4P) is widely distributed and involved in the coordinated regulation of membrane trafficking, cell division, and lipid transport [1,2]. Multiple human pathogens manipulate PI4P levels to mediate their intracellular replication, including *Legionella* [3] and multiple picornaviruses [4,5]. PI4P in humans is generated through the action of four distinct phosphatidylinositol-4-kinases: PI4KII α (PI4K2A), PI4KII β (PI4K2B), PI4KIII α (PI4KA) and PI4KIII β (PI4KB) [6-8]. PI4KB is localized at the Golgi and trans-Golgi-network (TGN), with PI4P pools in the Golgi apparatus generated by both PI4K2A and PI4KB [9]. While the localization and activity of PI4K2A is regulated through its palmitoylation, local membrane composition, and cholesterol levels [10], the activity of PI4KB is regulated by multiple protein-protein interactions and phosphorylation [11-14]. These regulatory protein-protein interactions are in turn manipulated by many pathogenic RNA viruses that have evolved the ability to hijack PI4KB and generate PI4P-enriched replication organelles, which are essential for viral replication [15]. For most picornaviruses, manipulation of PI4P levels is driven by the action of the viral 3A protein and its interactions with PI4KB-binding proteins [13,16-18].

PI4KB plays both important catalytic and non-catalytic functions, with its regulation controlled by interactions with multiple protein binding partners, including acyl CoA Binding Domain 3 (ACBD3), Rab11, 14-3-3, and c10orf76 (chromosome 10, open-reading frame 76, also referred to as Armadillo-like helical domain-containing protein 3 (ARMH3)). PI4KB is a multi-domain lipid kinase containing a disordered N-terminus, a helical domain, and a bi-lobal kinase domain [14,19]. Biophysical and biochemical studies have defined the domains of PI4KB that mediate complex formation with a number of binding partners. The helical domain of PI4KB forms a non-canonical interaction with the small GTPase Rab11a that mediates localization of a pool of Rab11 to the Golgi and TGN [14,20]. PI4KB is primarily localized to the Golgi through the interaction of its N-terminus with ACBD3 [12,13]. PI4KB is activated downstream of ADP-ribosylation factor 1 (Arf1) [21], however, no evidence for a direct Arf1-PI4KB interface has been found, suggesting that this may be an indirect effect. PI4KB contains phosphorylation sites in disordered linkers between domains, including Ser294 in the helical-kinase linker of PI4KB, which is phosphorylated by protein kinase D (PKD). Phosphorylation of Ser294 drives binding of 14-3-3, which stabilizes PI4KB, prevents degradation, and increases Golgi PI4P levels [22-24]. Ser496 in the N-lobe linker of PI4KB is phosphorylated by protein kinase A (PKA) [25], and drives PI4KB localization from the Golgi to nuclear speckles [26]. c10orf76 was identified as a putative PI4KB interacting partner in immunoprecipitation experiments [17,27], with knockout of c10orf76 leading to decreased Golgi PI4P levels [28]. The function of this protein is unknown, however, it contains a domain of unknown function (DUF1741) that is well conserved in many eukaryotes.

Enterovirus proteins do not interact directly with PI4KB – they instead recruit PI4KB-regulatory proteins. A key component of manipulating PI4KB to generate PI4P-enriched replication organelles is the interaction of viral 3A proteins with host PI4KB-binding proteins. The 3A proteins from enteroviruses (i.e. Poliovirus, Rhinovirus, Coxsackievirus, Rhinovirus and Enterovirus 71) and Aichivirus recruit PI4KB to replication organelles through an interaction with ACBD3 [11,13,16-18,29-32]. The viral 3A protein from Aichivirus forms a direct interaction with the GOLD domain of ACBD3, leading to redistribution of PI4KB to replication organelles [11,31]. Enteroviruses also manipulate other lipid signaling pathways, with viral 3A proteins able to recruit the protein Golgi-specific brefeldin A-resistance guanine nucleotide exchange factor 1 (GBF1) that activates Arf1 [4,33-35], and subvert Rab11-positive recycling

endosomes to replication organelles [36]. A new component of the PI4KB hijacking process, c10orf76, was identified as a key host factor in the replication of coxsackievirus A10 (CVA10) replication, but not coxsackievirus B1 (CVB1) [28].

We hypothesized that a direct c10orf76-PI4KB interaction may be critical for the regulation of Golgi PI4P levels and play a role in enterovirus replication. To elucidate the role of c10orf76 in PI4KB-mediated signaling, we utilized a synergy of hydrogen deuterium exchange mass spectrometry (HDX-MS) and biochemical assays to characterize the novel c10orf76-PI4KB complex *in vitro*. This allowed us to engineer complex-disrupting mutations that were subsequently used to define the role of the c10orf76-PI4KB complex in Golgi PI4P-signaling and viral replication *in vivo*. We find that PI4KB and c10orf76 form a high affinity complex mediated by a disorder-to-order transition of the kinase linker of PI4KB, with complex affinity modulated by PKA phosphorylation of the c10orf76 binding site on PI4KB. Knockout of c10orf76 lead to decreased PI4P levels, and disruption of Arf1 activation in cells. Complex-disrupting mutations revealed that c10orf76 is recruited to the Golgi by PI4KB, and that viral replication of enteroviruses that require c10orf76 is mediated by the c10orf76-PI4KB complex.

RESULTS

c10orf76 forms a direct, high affinity complex with PI4KB

c10orf76 was previously identified as a putative PI4KB-binding partner through immunoprecipitation experiments [17,27], however, it was not clear if this was through a direct interaction. To identify a potential direct interaction between PI4KB and c10orf76 *in vitro*, we purified recombinant full-length proteins using a baculovirus and *Spodoptera frugiperda* (Sf9) expression system. Experiments on PI4KB used the slightly smaller isoform 2 variant (1-801, uniprot: Q9UBF8-2), compared to PI4KB isoform 1 (1-816 uniprot: Q9UBF8-1), similar to previous structural studies [14]. His-pulldown assays using NiNTA-agarose beads and purified recombinant proteins showed a direct interaction between PI4KB and His-tagged c10orf76 (Fig. 1A). Pulldown experiments carried out with the PI4KB binding partners Rab11 and ACBD3 revealed that although c10orf76 did not directly bind Rab11 or ACBD3 alone, it could form ternary PI4KB-containing complexes with both (Fig. EV1), indicating a unique c10orf76 binding interface on PI4KB compared to Rab11 and ACBD3. To examine the stoichiometry of the c10orf76-PI4KB complex, we subjected apo c10orf76 and c10orf76 (79 kDa) with PI4KB (89 kDa) to size exclusion chromatography. Apo c10orf76 eluted from the size exclusion column at a volume consistent with a monomer, while the c10orf76-PI4KB complex (158 kDa) eluted at a volume consistent with a 1:1 complex (Fig. 1B). Since cellular knockout of c10orf76 has been shown to reduce PI4P levels *in vivo* [28], we investigated the effect of c10orf76 on PI4KB lipid kinase activity with biochemical membrane reconstitution assays using phosphatidylinositol (PI) vesicles. Intriguingly, c10orf76 was a potent inhibitor of PI4KB, with inhibition being dose-dependent and possessing an IC₅₀ of ~90 nM (Fig. 1C). This inhibitory effect was observed on both pure phosphatidylinositol (PI) vesicles, and vesicles that mimic the composition of the Golgi (20% PI, 10% PS, 45% PE, 25% PC) (Fig. 1D). This paradoxical PI4KB-inhibitory result *in vitro* conflicts with observed Golgi PI4P decreases in c10orf76 deficient cells [28]. This suggests that biochemical assays may not fully recapitulate the environment of the Golgi. To further define the role of this complex we focused on defining the molecular basis of this interface, allowing for generation of binding-deficient mutants for downstream cellular and viral experiments.

HDX-MS reveals that PI4KB and c10orf76 form an extended interface involving a disorder-to-order transition of the PI4KB N-lobe linker

To identify the putative interface between PI4KB and c10orf76, we employed hydrogen-deuterium exchange mass spectrometry (HDX-MS) to map regions protected in both proteins upon complex formation. HDX-MS is an analytical technique that measures the exchange rate of amide hydrogens in proteins. Because one of the main determinants for amide exchange is the presence of secondary structure, their exchange rate is an excellent readout of protein dynamics. HDX-MS is thus a potent tool to determine protein-protein, protein-ligand, and protein-membrane interactions [37-39]. H/D exchange was carried out for three different conditions: apo PI4KB, apo c10orf76, and a 1:1 complex of PI4KB with c10orf76. Deuterium incorporation experiments were carried out at four different timepoints (3, 30 and 300 seconds at 23°C and 3 seconds at 1°C). Deuterium incorporation is determined by quenching the exchange reaction in a solution that dramatically decreases the exchange rate, followed by rapid digestion, peptide separation, and mass analysis. A total of 185 peptides covering 96.9% of the PI4KB sequence, and 108 peptides covering 73.9% of the c10orf76 sequence were generated (Fig. 1E-H-source data 1, Fig. EV2). Significant differences in deuterium exchange between conditions were defined as changes in exchange at any timepoint that met the three following criteria: greater than 7% change in deuterium incorporation, a greater than 0.5 Da difference in peptide mass, and a p-value of less than 0.05 (unpaired student's t-test).

Multiple regions of PI4KB were protected from amide exchange in the presence of c10orf76, revealing an extended binding interface (Fig. 1E, F, H; Fig. EV2). The most prominent difference in exchange was at the C-terminus of the disordered N-lobe linker (residues 486-498), where the presence of c10orf76 led to a significant ordering of this region. This region had no protection from amide exchange in the apo state, revealing it to be disordered, with a very strong stabilization (>80% decrease in exchange) in the presence of c10orf76, indicating a disorder-to-order transition upon c10orf76 binding (Fig. 1H). This N-lobe kinase linker is dispensable for lipid kinase activity, as it can be removed with a minimal effect on PI4KB catalytic activity [19]. In addition to this change there were multiple smaller decreases in exchange in the helical domain (131-138, 149-157, 159-164, and 183-204) and kinase domain (676-688, 725-734, and 738-765). The helical domain of PI4KB mediates binding to Rab11. However, the PI4KB-Rab11 complex was still able to form in the presence of c10orf76 (Fig. EV1). The decreases in exchange with c10orf76 observed in the kinase domain were located in the activation loop (676-688) and the C-lobe (738-765), which may mediate the inhibition observed *in vitro*. The protected surface on PI4KB extensively spans the membrane face of the kinase, which may prevent PI4KB from directly interfacing with the membrane and accessing PI in the presence of c10orf76, at least in the absence of other binding partners *in vitro* (Fig. 1F).

The presence of PI4KB also caused multiple differences in H/D exchange in c10orf76, with increased exchange at the N-terminus (56-62) as well as decreased exchange N-terminal of, and within, the domain of unknown function (DUF1741; 403-408, 534-547, 632-641) (Fig. 1G,H; Fig. EV2). There are no clear structural determinants of c10orf76, with limited homology to any previously solved structure, however, it is predicted to consist of a primarily helical fold arranged into armadillo repeats. The uncharacterized DUF1741 domain of c10orf76 is present throughout many eukaryotes, however, even though the DUF1741 domain is strongly conserved in evolution, c10orf76 is the only protein that contains this domain in humans.

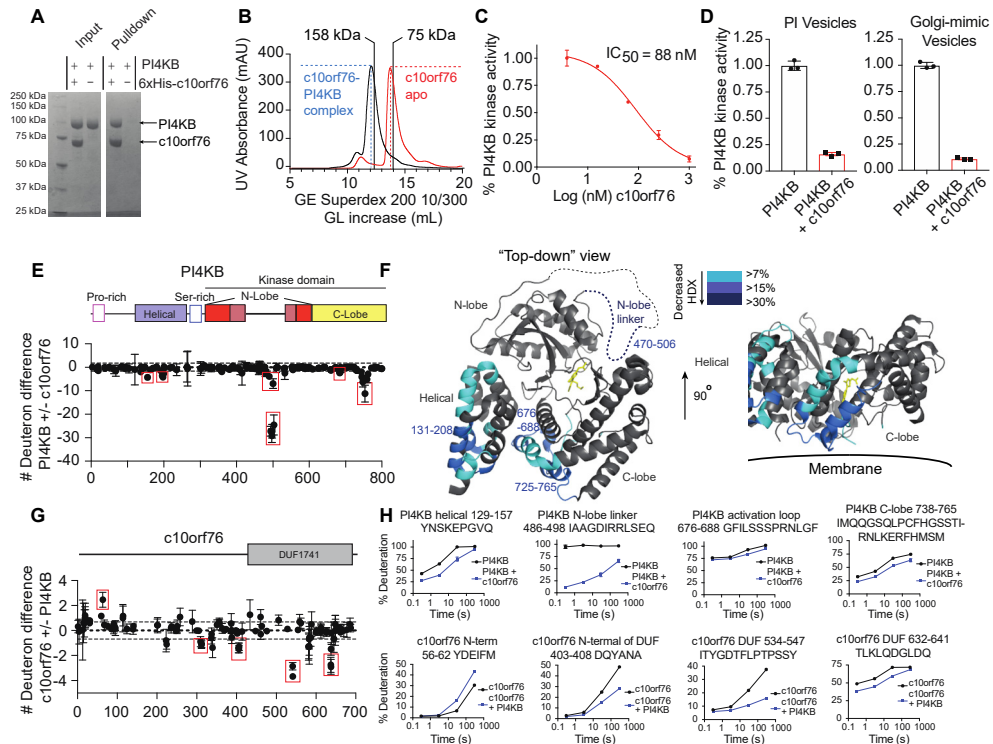


Figure 1. c10orf76 directly binds to PI4KB through an extended interface focused at the N-lobe kinase linker of PI4KB. (A) Recombinant c10orf76 directly binds to PI4KB *in vitro*. His-pull-down assays of baculovirus/*Sf9* produced 6xHis-c10orf76 (3 μ M) were carried out with untagged PI4KB (2.5 μ M). **(B)** PI4KB and c10orf76 form a stable complex. The complex of c10orf76-PI4KB eluted from a S200 superdex 10/300 GL increase gel filtration column (GE) at a volume consistent with a heterodimer (169 kDa), while c10orf76 alone eluted at a volume consistent with a monomer (79 kDa). Lines with MW values indicate elution of MW standards (158 kDa aldolase, 75 kDa conalbumin). **(C)** PI4KB is potently inhibited by c10orf76 in a dose-dependent manner *in vitro*. Kinase assays of PI4KB (20 nM) in the presence of varying concentrations of c10orf76 (1.6 nM-1 μ M) were carried out on pure PI lipid vesicles (0.5 mg/L) in the presence of 100 μ M ATP. The data was normalized to the kinase activity of PI4KB alone. IC_{50} values were determined by one binding site, nonlinear regression (curve fit) using Graphpad. Error bars represent standard deviation ($n=3$). **(D)** PI4KB is potently inhibited by c10orf76 on pure PI vesicles and vesicles mimicking Golgi composition. Kinase assays of PI4KB and c10orf76 were carried out on lipid substrate composed of pure PI vesicles (0.5 mg/ml) with 100 μ M ATP, and Golgi mimic vesicles (0.5 mg/ml, 10% PS, 20% PI, 25% PE, 45% PC) with 10 μ M ATP. PI4KB was present at 20 and 300 nM in the PI and Golgi substrate assays respectively, with c10orf76 present at 500 nM in both experiments. The data is normalized to the kinase activity of PI4KB alone. Error bars represent standard deviation ($n=3$). **(E)** Changes in deuterium incorporation PI4KB in the presence of c10orf76 showed a profound ordering of the kinase domain N-lobe linker and smaller changes in the helical domain and C-lobe of the kinase domain. The sum of the difference mapped as the difference in number of deuterons incorporated for PI4KB (400 nM) in the presence and absence of c10orf76 (400 nM) over all time points (3s at 1 $^{\circ}$ C; 3s, 30s, and 300s at 23 $^{\circ}$ C). Each dot represents a peptide graphed on the x-axis according to the central residue. The red boxes highlight key regions that showed significant changes (>7% decrease in exchange, >0.5 Da difference, and unpaired two-tailed student t-test $p<0.05$). For all panels error bars represent standard deviation ($n=3$). **(F)** c10orf76 binding induces differences in HDX throughout multiple domains of PI4KB. Regions of >7% difference in deuterium exchange in the presence of c10orf76 are colored onto the structure of PI4KB according to the legend (PDB: 4D0L). The N-lobe linker of the kinase domain is disordered in the structure and is represented by a dotted line. **(G)** Changes in the deuterium incorporation of c10orf76 in the presence of PI4KB. H/D exchange reactions displayed as the sum of the difference in HDX in the number of deuterons for c10orf76 (400 nM) in the presence of PI4KB (400 nM) at all time points (3s at 1 $^{\circ}$ C; 3s, 30s, and 300s at 23 $^{\circ}$ C) analyzed. Red boxes highlight regions that showed significant changes (>7% decrease in exchange, >0.5 Da difference, and unpaired two-tailed student t-test $p<0.05$). **(H)** The PI4KB N-lobe linker undergoes a disorder-to-order transition upon binding c10orf76. Selected peptides (including the sequence, domain information, and numbering) of both PI4KB and c10orf76 displayed as the % deuteration incorporation over time.

The largest observed change in deuterium incorporation in either protein was in the PI4KB N-lobe linker (486-496). Interestingly, this region contains a consensus PKA motif (RRxS) that corresponds to Ser496 (Ser511 in PI4KB isoform 1), which is phosphorylated *in vivo* and conserved back to the teleost fishes (Fig. 2A) [26]. Systems level analysis of PKA signaling networks also show that phosphorylation of this site is decreased >90% in PKA knockout cells, indicating that it is likely a direct PKA target [25]. To better understand the regulation of the c10orf76-PI4KB complex, we sought to characterize the effects of Ser496 phosphorylation.

PI4KB is directly phosphorylated at Ser496 by PKA to modulate the affinity of the c10orf76-PI4KB complex

There are three well-validated phosphorylation sites on PI4KB: Ser294, Ser413, Ser496 [40]. To test the role of phosphorylation of PI4KB at Ser496, we generated stoichiometrically phosphorylated PI4KB at only Ser496 using an *in vitro* phosphorylation approach that relied on the production of the purified mouse PKA catalytic subunit in *E. coli*. To minimize complications from any background phosphorylation that occurs in Sf9 cells, we used PI4KB expressed in *E. coli* to ensure the starting protein substrate was non-phosphorylated. Analysis of the Sf9-produced PI4KB revealed significant phosphorylation of Ser294, Ser413, Ser430 and Ser496, while Sf9-produced c10orf76 had evidence of phosphorylation of Ser14, and an additional Ser/Thr phosphorylation in the 325-351 region, although the specific residue is ambiguous from the MS data. No phosphorylation was identified from *E. coli* produced proteins, as expected (Fig. EV3). Dose response assays for the phosphorylation of PI4KB Ser496 using *E. coli*-produced protein were then carried out with increasing concentrations of purified PKA, and the resulting product was analyzed by mass spectrometry for the site-specific incorporation of the phosphate moiety (Fig. 2B). Ser496 in PI4KB was phosphorylated efficiently by PKA, with >99% phosphorylation at Ser496 occurring with a 1:500 ratio of PKA to PI4KB and no detectable phosphorylation at the other major PI4KB phosphorylation sites (Fig. EV3). Lipid kinase assays were then carried out using different concentrations of c10orf76 for both phosphorylated and non-phosphorylated PI4KB. The phosphorylated form had a 3-fold increase in the IC₅₀ value, suggesting that Ser496 phosphorylation decreases c10orf76 binding affinity, with no shift in the IC₅₀ value for the S496A PI4KB mutant (Fig. 2C). Kinase assays carried out on both Ser496 phosphorylated PI4KB and non-phosphorylated PI4KB showed that there is no direct effect of the phosphorylation events on basal lipid kinase activity (Fig. 2D). PKA-mediated phosphorylation-dependent changes in the affinity of protein-protein complexes have been previously described [41,42]. We utilized HDX-MS to test if the altered inhibition profile we saw was due to decreased affinity between c10orf76 and PI4KB, a method previously utilized to quantify the affinity of protein interactions [43]. These experiments were carried out at a single time point of D₂O exposure (5 seconds at 20°C) with differing levels of c10orf76 present. Plotting the difference in deuterium incorporation versus c10orf76 concentration gives a characteristic binding isotherm for both phosphorylated and non-phosphorylated PI4KB; displaying a 2-3-fold decreased affinity for the phosphorylated form of PI4KB (85 nM vs 36 nM, Fig. EV3) Phosphorylated PI4KB Ser496 also displayed a ~2 fold decrease in affinity for c10orf76 when determined by isothermal titration calorimetry (Fig. EV3). Phosphomimic PI4KB mutants S496D and S496E did not mimic the phosphorylation-dependent reduction of c10orf76 affinity, so they could not be utilized to study this effect *in vivo* (Fig. EV3). To better characterize the role of the c10orf76-PI4KB complex *in vivo*, we sought to generate c10orf76-PI4KB complex-disrupting mutations.

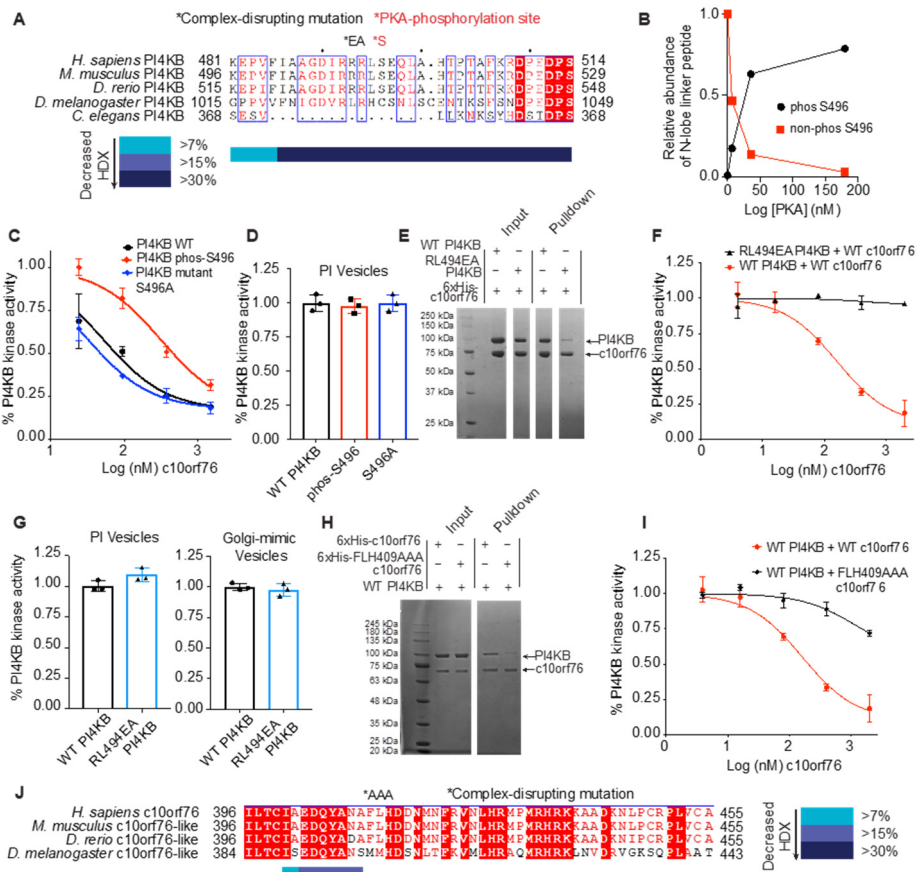


Figure 2. The PI4KB c10orf76 interface is conserved and can be post-translationally modified by PKA, with rationally designed mutations disrupting complex formation. (A) The N-lobe kinase linker region of PI4KB is strongly conserved back to *D. rerio*. The N-lobe linker region of PI4KB sequences of the organisms indicated were analysed using Clustal Omega/ ESpript 3. The consensus PKA motif (RRXS) that is conserved back to *D. rerio* is indicated on the sequence, as well as the RL494EA point mutation. (B) The N-lobe kinase linker of PI4KB can be efficiently phosphorylated by PKA. Recombinant PKA at different concentrations (0, 7, 34, 168, or 840 ng) was incubated with recombinant (*E. coli*) wild-type PI4KB (20 μ g) for 1 hour with 200 μ M ATP and the amount of phosphorylation was followed using mass spectrometry. Relative abundance of Ser496 phosphorylated PI4KB was calculated using the relative intensity (total area) of the phosphorylated vs non-phosphorylated peptide (486-506). (C) PI4KB phosphorylation by PKA alters the affinity for c10orf76. The kinase activity of different variants of PI4KB (15 nM) was measured in the presence of varying amounts of c10orf76 (23 nM-1.5 μ M) with 100% PI lipid substrate (0.5 mg/L) and 100 μ M ATP. The data was normalized to the kinase activity of PI4KB alone. Error bars represent standard deviation (n=3). (D) PI4KB has the same kinase activity when Ser496 is phosphorylated or mutated to alanine. Kinase assay of PI4KB non-phosphorylated, phos-Ser496 or S496A (15 nM) on pure PI lipid vesicles (0.5 mg/L) with 100 μ M ATP. The data was normalized to the kinase activity of WT PI4KB. Error bars represent standard deviation (n=3). (E) Engineered RL494EA PI4KB mutant shows decreased binding to c10orf76. His-pull-down assays of 6xHis-c10orf76 (3 μ M) with wild-type or RL494EA PI4KB (1-2 μ M). (F) RL494EA PI4KB activity is not inhibited by c10orf76. Kinase assays of either wild type or mutant RL494EA PI4KB (40 nM) were carried out with varying concentrations of c10orf76 (3.9 nM-2 μ M) with 100% PI lipid vesicles (0.5 mg/L) and 100 μ M ATP. The data was normalized to the kinase activity of PI4KB alone. Error bars represent standard deviation (n=3). (G) Wild-type PI4KB and RL494EA PI4KB mutant have the same lipid kinase activity. Kinase assays of either wild-type or mutant PI4KB (10 nM) were carried out with 100% PI lipid vesicles (0.5 mg/L), 100 μ M ATP, and PI4KB (300 nM) on Golgi-mimic vesicles (0.5 mg/mL) with 10 μ M ATP. The data was normalized to the kinase activity of WT PI4KB. Error bars represent standard deviation (n=3). (H) FLH409AAA-c10orf76 mutant shows decreased affinity for PI4KB. His-pull-down assays of 6xHis-c10orf76 (1 μ M) with wild-type PI4KB (1 μ M). Samples washed a total of 4 times. (I) Kinase assay shows FLH409AAA c10orf76 inhibition of PI4KB is greatly reduced. Kinase assay of PI4KB (40 nM) and a concentration curve of c10orf76 (3.9 nM-2 μ M) on pure PI lipid vesicles (0.5 mg/L) with 100 μ M ATP. The data was normalized to the kinase activity of PI4KB alone. Error bars represent standard deviation (n=3). (J) The PI4KB-binding region of c10orf76 is strongly conserved back to *D. rerio*. Clustal Omega/ ESpript 3 alignment of the FLH409 region of c10orf76 that binds PI4KB.

Rationally engineered PI4KB and c10orf76 mutants that disrupt complex formation

The c10orf76 binding site within the N-lobe kinase linker of PI4KB identified by HDX-MS is highly conserved in vertebrates, with much of the region also conserved in *D. melanogaster*, but not in *C. elegans* (Fig. 2A). We used a combination of both the sequence conservation and HDX-MS results to design a complex-disrupting mutant. The RL residues at 494-495 were mutated to EA (RL494EA), effectively causing both a charge reversal and decrease in hydrophobicity. The RL494EA mutant disrupted binding to His-tagged c10orf76 bait in a His pulldown assay (Fig. 2E) and prevented inhibition by c10orf76 in kinase assays (Fig. 2F). This mutant had exactly the same basal kinase activity as the WT PI4KB on both PI vesicles and Golgi-mimetic vesicles (Fig. 2G), strongly suggesting that the mutant kinase is properly folded. In an attempt to design rational mutations of c10orf76 that also disrupted binding to PI4KB, multiple mutations were tested in regions 403-408, 534-547 and 632-641 that were identified using HDX-MS. Combining the HDX-MS data and sequence homology, we designed a triple alanine mutant at the end of a putative helix (QYANAFL) that was well conserved in vertebrates (Fig. 2J), close to the HDX-MS protection (FLH residues 409-411 to AAA, referred to as FLH mutant afterwards). The FLH mutant expressed well, significantly reduced binding to PI4KB in a His-pulldown assay (Fig. 2H), and also showed a marked reduction in its ability to inhibit PI4KB activity (Fig. 2I). To confirm the c10orf76 FLH mutant does not affect global protein structure, we compared deuterium incorporation of the c10orf76 wild-type and FLH mutant and observed no changes in deuterium incorporation seen outside of the predicted helix containing the FLH residues (Fig. EV4). The engineering of complex-disrupting mutants that do not alter catalytic activity or protein folding provided an excellent tool to test the importance of the c10orf76-PI4KB complex in cells.

PI4KB recruits c10orf76 to the Golgi

To define the role of the c10orf76-PI4KB interface in cellular localization we utilized fluorescently-tagged variants of the wild-type and complex-disrupting mutants of both PI4KB and c10orf76. Fluorescence microscopy of HEK293 cells expressing GFP-tagged wild-type PI4KB revealed that it primarily localizes to the Golgi (Fig. 3A). GFP-PI4KB RL494EA, which is deficient in c10orf76 binding, also localized mainly to the Golgi, which suggests that c10orf76 plays a minimal role in the Golgi recruitment of PI4KB (Fig. 3A). The wild-type GFP-c10orf76 also localizes to the Golgi. However, the PI4KB binding-deficient FLH mutant is redistributed to the cytosol; revealing an important role for PI4KB in the proper cellular localization of c10orf76 (Fig. 3B). Note that the Golgi localization of GFP-PI4KB or GFP-c10orf76 is only visible with low expression levels as the endogenous binding sites are quickly saturated and the excess cytoplasmic GFP-tagged protein eventually masks the Golgi-bound pools at higher levels of expression. To further analyze the role of PI4KB in the recruitment of c10orf76, we utilized a chemically-inducible protein heterodimerization system that relies on the selective interaction of the FKBP12 (FK506 binding protein 12) and FRB (a 9 kDa fragment of mTOR that binds rapamycin) modules upon treatment with rapamycin [12,44]. Specifically, we fused the FRB domain to residues 34–63 of a CFP-tagged mitochondrial localization signal from mitochondrial A-kinase anchor protein 1 (AKAP1), and fused mRFP-FKBP12 onto the wild-type or mutant variants of human PI4KB (Fig. 3C). These constructs allowed us to examine the localization of the wild-type or mutant GFP-c10orf76 following the acute sequestration of PI4KB to the outer mitochondrial membrane, where other Golgi-associating proteins are not be present. To best demonstrate their co-recruitment upon rapamycin addition, mRFP-FKBP12-PI4KB and eGFP-c10orf76 were expressed at high levels, and thus present as mainly cytosolic due to

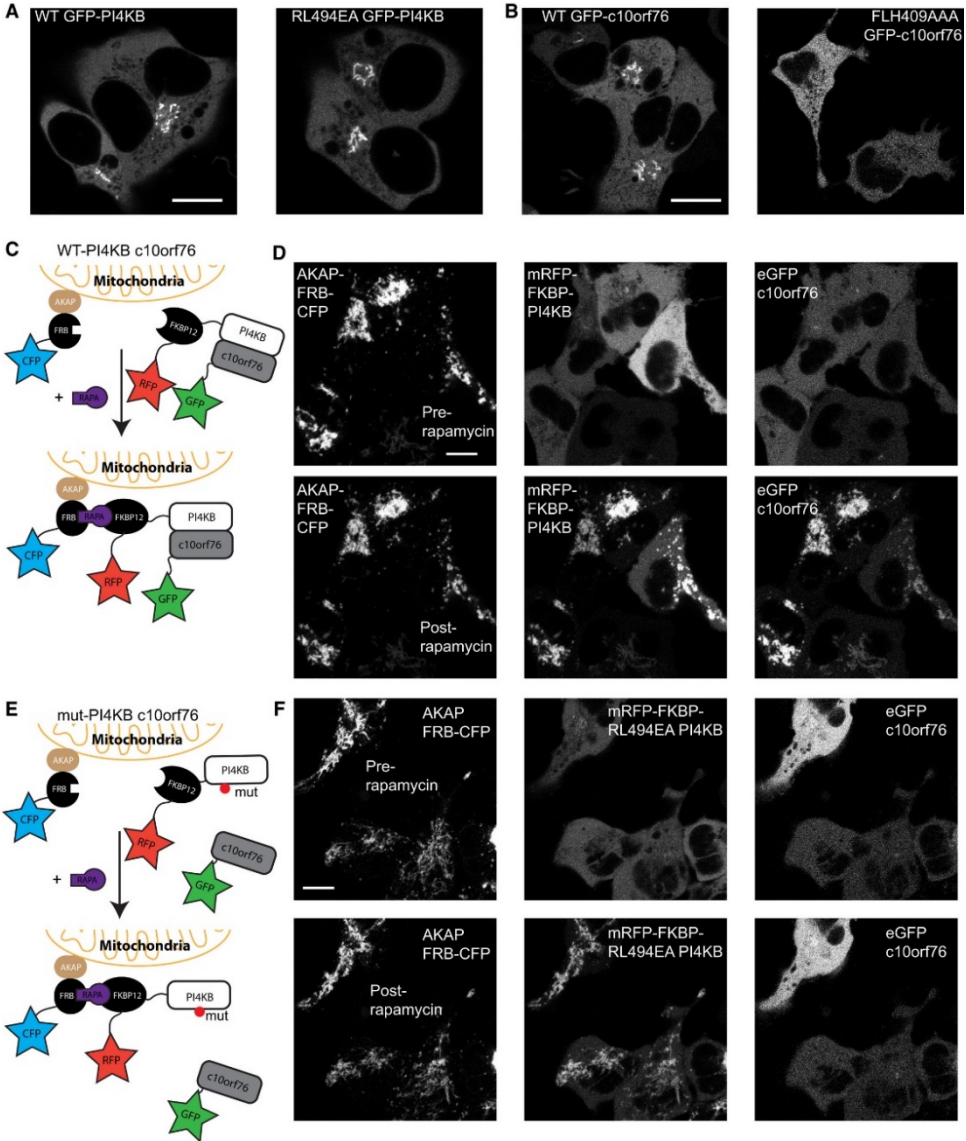


Figure 3. PI4KB recruits c10orf76 to the Golgi in vivo. (A) Transfections of HEK293 cells revealed that both wild-type GFP-PI4KB and RL494EA GFP-PI4KB localize to the Golgi. (B) WT c10orf76 also localized to the Golgi, however, the PI4KB binding deficient mutant of c10orf76 (FLH409AAA) predominantly localized to the cytosol. (C) Cartoon schematic of the rapamycin-inducible mitochondria recruitment. The AKAP1-FRB-CFP construct is localized to the outer mitochondrial membrane, while the RFP-FKBP12-PI4KB and GFP-c10orf76 are localized in the Golgi as well as within the cytoplasm where they can form a complex. Upon addition of rapamycin, the RFP-FKBP12-PI4KB construct is translocated to the mitochondria. (D) Mitochondria recruitment experiment with wild-type PI4KB and c10orf76. Left: AKAP1-FRB-CFP is localized to the mitochondria before (top) and 5 minutes after rapamycin (100 nM) treatment (bottom). Right: GFP-c10orf76 is located in the cytosol before rapamycin (top) and translocates to the mitochondria after rapamycin induction (bottom). (E) Schematic of the rapamycin-inducible mitochondria recruitment experiment with mutant PI4KB and WT c10orf76. (F) Mitochondria recruitment experiment with mutant PI4KB and WT c10orf76. Left: AKAP1-FRB-CFP is localized to the mitochondria before (top) and 5 minutes after (bottom) rapamycin treatment. Middle: RFP-FKBP12-PI4KB(RL494EA) is localized to the cytosol before rapamycin (top) and translocates to the mitochondria after rapamycin induction (bottom). Right: GFP-c10orf76 is located in the cytosol before (top) and after (bottom) rapamycin induction. Bars represent 10 μ m.

saturation of endogenous binding sites (Fig. 3D; Movie EV1). Treatment with rapamycin (100 nM) caused the rapid recruitment of mRFP-FKBP12-PI4KB to the mitochondria, which also caused the rapid co-recruitment of c10orf76 (Fig. 3D; Movie EV1); suggesting that PI4KB is the only component necessary for membrane recruitment of c10orf76. Experiments using mRFP-FKBP12 PI4KB RL494EA showed that although the mutant kinase is relocated to the mitochondria, GFP-c10orf76 does not co-localize (Fig. 3E; Fig. 3F, Movie EV2). To test any effect of the PI4KB S496 phosphorylation site on localization, although the S496E and S496D mutants did not properly mimic phosphorylation (Fig EV3), recruitment experiments were performed with the non-phosphorylatable PI4KB mutant (S496A). At lower expression levels, mRFP-FKBP12 PI4KB S496A and eGFP-c10orf76 maintained normal Golgi localization, and treatment with rapamycin caused recruitment to the mitochondria (Fig. EV5). At higher expression levels, mRFP-FKBP12 PI4KB S496A and eGFP-c10orf76 quickly saturate Golgi sites and flood the cytosol, and treatment with rapamycin caused robustly recruitment to the mitochondria, suggesting phosphorylation of PI4KB S496 is not important in the normal localization of either protein (Fig. EV5). Taken together, these live-cell studies corroborated the protein interaction studies completed *in vitro* and also demonstrate that the newly defined c10orf76-PI4KB interface is required for proper localization of c10orf76 to the Golgi. Compellingly, these findings reveal a novel function of PI4KB in the recruitment of c10orf76.

c10orf76 regulates active Arf1 dynamics and maintains Golgi PI4P levels

The paradoxical finding that the loss of c10orf76 leads to decreased PI4P levels in cells, yet c10orf76 decreased the catalytic activity of PI4KB *in vitro*, suggested that there was an unknown lipid or protein constituent in cells that is not present in our *in vitro* experiments. To determine the role of c10orf76 in cells we examined the distribution of different Golgi-localized signaling components in c10orf76-deficient (knockout) HAP1 cells. In agreement with previous studies [28], we found that there were decreased PI4P levels at the Golgi in c10orf76 knockout cells, as indicated by decreased Golgi staining by an anti-PI4P antibody (Fig. 4A). Intriguingly, there was an apparent increase in Golgi localized PI4KB in the c10orf76 knockout cells (Fig. 4A), similar to what occurs upon treatment with a PI4KB inhibitor [45], clearly indicating that decreased PI4P production was not due to loss of PI4KB recruitment in the absence of c10orf76. We tested the localization of different Golgi markers to verify that decreased PI4P was not due to disruption of Golgi morphology. Giantin, a marker of the cis/medial Golgi, and ACBD3, which binds to Giantin and recruits PI4KB to Golgi membranes [12,13], both showed similar localization in both WT and c10orf76 knockout cells (Fig. 4B). Markers for the cis Golgi (GM130), the trans-Golgi network (TGN46), and the ER-Golgi intermediate compartment (ERGIC53) were also similar, suggesting that Golgi morphology was maintained in the c10orf76 knockout HAP1 cells (Fig. 4B). We confirmed similar expression levels of PI4KB, GBF1 and β -Actin in WT and c10orf76 KO cells to verify any observed differences were not due to protein expression levels (Fig. 4C).

We next tested the localization of the Arf1-GEF GBF1, as active GTP-bound Arf1 is a putative activator of PI4KB [21]. In c10orf76 knockout cells there was a redistribution of GBF1, with GBF1 being more diffuse, with less localized at the Golgi (Fig. 4D). The generation of active GTP-bound Arf1 by Arf-GEFs leads to recruitment of multiple effector proteins, with one of most well characterised being the coatamer proteins, which form COPI coated vesicles that mediate Golgi to ER trafficking. In c10orf76 knockout cells there was more diffuse staining outside of the Golgi for the active Arf1-binding coatamer components COP- β or COP- α/γ (Fig. 4C). Antibody staining with the CM1 antibody, which recognizes

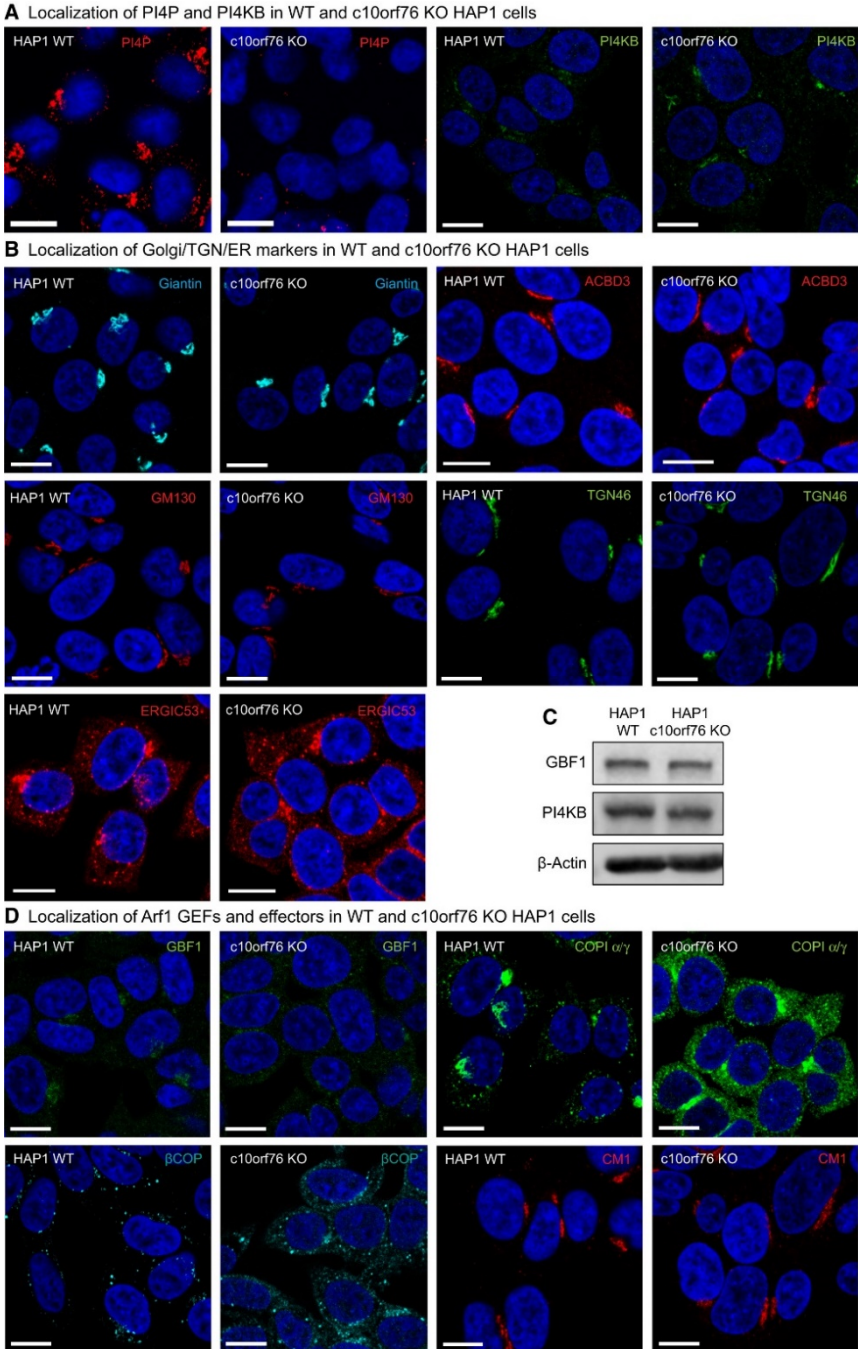


Figure 4. Knockout of c10orf76 in HAP1 cells leads to decreased PI4P levels and disruption of GBF1 / active Arf1 localization despite minimal effects on Golgi morphology. HAP1 cells were fixed and stained with antibodies examining PI4P and PI4KB (A), Golgi morphology markers (B), and markers of Arf1 activation (C). The coatomer proteins COPI α/γ and β COP act as a readout for GTP-bound Arf1, while the native coatomer was detected with the CM1 antibody. Nuclei were stained with DAPI (blue). Bars represent 10 μ m.

the native form of coatamer [46], showed similar distribution for both WT and c10orf76 knockout cells, indicating the formation and distribution of native cytosolic coatamer was not affected (Fig. 4C). This puzzling difference may be caused by an altered recruitment of a subset of coatamer components (COP- β or COP- α/γ), and minor effects on the native coatamer complex. Importantly, the major phenotypic observations in the HAP1 c10orf76 knockout cells (i.e. reduced PI4P and increased PI4KB levels on an intact Golgi, and a more diffuse GBF1 and COP-I staining with less localization at the Golgi), were also observed in HeLa cells in which c10orf76 was knocked out (H.R. Lyoo and F.J.M. van Kuppeveld, personal observation). Overall, these results suggest that c10orf76 plays a role in the regulation of GBF1/Arf1 dynamics at the Golgi.

Replication of c10orf76-dependent enteroviruses requires intact c10orf76-PI4KB interaction

All enteroviruses depend on PI4KB kinase activity for replication. Despite the physical and functional connection between PI4KB and c10orf76, enteroviruses showed different dependencies on c10orf76 [28]. Specifically, while Coxsackievirus A10 (CVA10) replication was impaired in c10orf76 knockout cells, the replication of CVB1 was not. Furthermore, c10orf76 was identified as a pro-viral factor for replication of poliovirus (PV1) [47]. We set out to investigate the importance of the c10orf76-PI4KB interaction for replication of CVA10 and PV1. We first made a side-by-side comparison of virus replication in HAP1 wildtype and c10orf76 knockout cells in a single cycle of replication. The replication of CVA10 was significantly impaired in c10orf76 deficient cells, with partial inhibition of PV1 replication, and no impairment for replication of CVB3 (Fig. 5A).

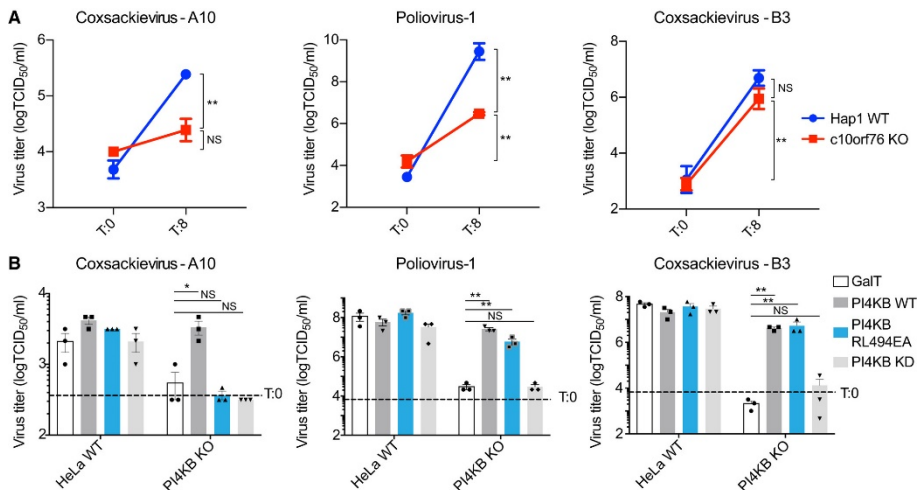


Figure 5. The c10orf76-PI4KB complex is essential for Coxsackievirus A10 replication. (A) Viral infection assays determining viral titers by end-point titration at 0 hours and 8 hours in HAP1 wild-type or c10orf76 knockout cells. Left: Coxsackievirus A10 infection. Middle: Poliovirus-1 infection. Right: Coxsackievirus B3 infection. (B) Viral infection assays determining virus titers by end point titration at 8 hours in HeLa wild-type and PI4KB knockout cells upon transfection of wild-type PI4KB, the complex-disrupting RL494EA PI4KB mutant or the kinase dead D674A PI4KB mutant. Left: Coxsackievirus A10 infection. Middle: Poliovirus-1 infection. Right: Coxsackievirus B3 infection. Values were statistically evaluated compared to the GalT control using a one-way ANOVA. **, P<0.01; *, P<0.05; N.S., P>0.05. For all panels error bars represent standard error (n=3).

Due to the notoriously difficult nature of transfecting HAP1 cells, we determined the importance of the c10orf76-PI4KB interaction for virus replication in HeLa PI4KB knockout cells transfected with different

PI4KB expression plasmids as previously described [29]. Expression of wild type PI4KB efficiently restored the replication of all viruses (Fig. 5B). Expression of the PI4KB RL494EA mutant that is deficient in binding c10orf76 fully rescued replication in CVB3, only partially rescued PV1 replication, and failed to rescue CVA10 replication. These observations suggest that the c10orf76-PI4KB interaction is necessary for CVA10, and to a lesser extent, PV1 replication and thereby implies that functions of c10orf76 are selectively hijacked by specific viruses.

DISCUSSION

Defining the full complement of cellular roles for PI4KB is an important objective in characterizing the integrated control of secretion and membrane trafficking at the Golgi, and also provides a framework for understanding how PI4P can be manipulated by viruses. We have identified the c10orf76-PI4KB interaction as an important Golgi signaling complex and a critical factor in the replication of specific enteroviruses. Multiple mechanisms have been previously described for how PI4KB participates in Golgi signaling and membrane trafficking, including detailed insights into protein binding partners, post-translational modifications, and regulated recruitment to specific membrane compartments. PI4KB was originally identified in yeast (yeast protein PIK1) as an essential gene [48], with its activity playing a key role in secretion from the Golgi [49]. The mammalian isoform was identified soon afterwards through its sensitivity to wortmannin [50-52]. The first identified Golgi activator of PI4KB was the GTPase Arf1 [21]. However, no direct interaction has been established, which indicates a potential indirect mechanism of activation. Phosphorylation of PI4KB by PKD at Ser294 mediates binding to 14-3-3 proteins, with this leading to an increase in PI4KB activity [22,23], that has been suggested to correspond with an increase in PI4KB stability [24]. The most well validated protein binding partner that regulates Golgi recruitment of PI4KB is ACBD3 (previously referred to as GCP60) [13]. ACBD3 forms a direct, high-affinity interface with PI4KB that is mediated by a disorder-to-order transition in the N-terminus of PI4KB upon binding to the Q domain of ACBD3 [11,12]. The recruitment of PI4KB to the Golgi by ACBD3 is controlled through the direct interaction of the GOLD domain of ACBD3 with the Golgi resident transmembrane protein Giantin [53]. In addition to regulatory protein interactions, PI4KB is predicted to contain an amphipathic lipid packing sensor (ALPS) motif at the C-terminus that mediates lipid binding to unsaturated membranes [9]. PI4KB plays key non-catalytic roles through its interaction with the GTPase Rab11, with PI4KB required for localizing a pool of Rab11 to the Golgi and TGN [54]. This interaction is mediated through a non-canonical, nucleotide-independent binding interface with the helical domain of PI4KB [14]. However, there are still many unexplained aspects of PI4KB recruitment and regulation, highlighted by the increased recruitment of PI4KB to the Golgi following treatment with PI4KB inhibitors that is concomitant with a decrease in Golgi PI4P levels [45].

The protein c10orf76 was originally identified as a putative PI4KB interacting partner through co-immunoprecipitation experiments using tagged PI4KB [17,27]. Tests of genetic essentiality identified c10orf76 as a central molecular hub at the Golgi, with it being synthetically lethal in combination with the loss of several different Golgi-signaling proteins, and also showing a genetic link to PI4KB [28]. That study also found that c10orf76 is essential in the KBM7 CML cell line, but not in HAP1 cells, with this relationship also being true for PI4KB. Additional evidence on the essentiality of this protein is highlighted by the homozygous mutant of ARMH3, the mouse homolog of c10orf76, which is lethal at the pre-weaning stage [55]. c10orf76 is highly conserved in vertebrates and we find a strong correlation between the conservation of the kinase linker region of PI4KB and the PI4KB-binding site in c10orf76,

suggesting that a key role of c10orf76 is linked to its ability to form a complex with PI4KB. PI4KB recruitment to the Golgi is not mediated by c10orf76, but instead it appears that PI4KB is responsible for the Golgi-recruitment of c10orf76. *In vitro*, c10orf76 led to decreased lipid kinase activity of PI4KB. However, knockout of c10orf76 in cells led to reduced PI4P levels. This discrepancy could be due to the lack of other PI4KB regulators *in vitro*, such as Arf1/GBF1 or ACBD3, as well as the potential for c10orf76 to alter phosphatidylinositol dynamics. Knockout of c10orf76 led to an increased cytosolic fraction of the Arf GEF GBF1 and active Arf1 effectors (COP- β or COP- α/γ), but not native coatomer, suggesting altered Arf1/GBF1 dynamics in the c10orf76 knockout may be responsible for the disruption of Golgi PI4P levels [21]. This alteration was not due to Golgi disassembly, and despite perturbed Arf1 dynamics the presence of ACBD3 appeared to be sufficient for PI4KB recruitment to Golgi membranes as previously shown [12,13]. The activity of PI4KB is also regulated through the action of phosphatidylinositol transfer proteins (PITPs), which activate PI4KB activity, and c10orf76 may play a role in altering PI dynamics [56]. It is also possible that while PI4KB drives c10orf76 recruitment to the Golgi, endogenous c10orf76 levels *in vivo* engage only a minor fraction of PI4KB, or that c10orf76 itself interacts with other Golgi factors that induce a non-inhibitory confirmation with PI4KB. While further studies will be needed to fully describe the role of the PI4KB/c10orf76 complex, our work reveals c10orf76 as a novel player in regulation of Arf1 dynamics and corresponding Golgi PI4P levels (Fig 6A-B).

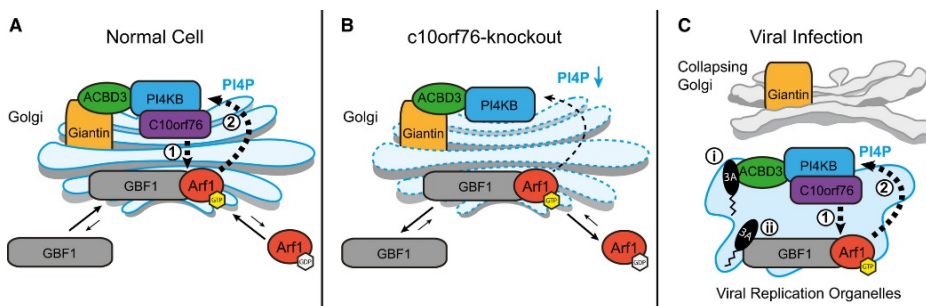


Figure 6. Summary of novel role of c10orf76 in modulating PI4P levels, active Arf1-GTP dynamics and viral replication. (A) At the Golgi, the recruitment of PI4KB can be controlled through the action of ACBD3. PI4KB can recruit c10orf76 to the Golgi, with this playing a role in the dynamics and localization of GBF1 and active Arf1-GTP and their downstream effectors (1). Active, membrane localized Arf1-GTP can activate PI4KB (2). **(B)** In a c10orf76-knockout cell, there is decreased recruitment of GBF1 and active Arf1, with this potentially describing the decreased levels of PI4P. **(C)** In enterovirus infected cells there are multiple mechanisms that can alter PI4P levels and Arf1 activation. The 3A proteins from different viruses can activate PI4KB, primarily through hijacking ACBD3 (i), as well as directly binding to GBF1 (ii). Viruses that require c10orf76 to replicate rely on the PI4KB-c10orf76 and GBF1/Arf1-GTP dynamics to facilitate viral replication.

Enteroviruses hijack numerous lipid signaling processes within infected cells to mediate their replication through the generation of replication organelles, with recruitment of PI4KB [4] and GBF1 [33] playing key roles in this process. Recruitment of these cellular host factors in enteroviruses is primarily mediated through the action of membrane-bound viral 3A proteins, which form either direct or indirect interactions that are important for facilitating replication organelle formation. One of the most well-conserved 3A binding partners in enteroviruses is the Golgi resident protein ACBD3, which interacts with the central part of 3A and recruits as well as activates PI4KB [11,13,18,29,31]. The N-terminal part of the 3A proteins from several enteroviruses (*e.g.*, poliovirus and coxsackie virus B3) directly binds and recruits GBF1, but this interaction is less conserved, severely reduced, or even absent

in the 3A proteins of rhinoviruses due to subtle amino acid differences in their N-terminus [18,33]. Recently, it has been found that there are multiple mechanisms of recruitment of GBF1 downstream of Poliovirus [57], with c10orf76 potentially being involved in this role. We find that c10orf76 is required for replication of coxsackie virus A10, and to a lesser extent poliovirus, and that c10orf76-dependent viruses rely on the c10orf76-PI4KB interface. Poliovirus is the causative agent of poliomyelitis, and coxsackie virus A10 is an important cause of outbreaks of hand-foot-and-mouth disease, but which is also associated with severe, and sometime fatal, clinical symptoms such as aseptic meningitis. Remarkably, replication of coxsackie virus B1 [28] and coxsackie virus B3 (this study) is independent of c10orf76. Why the c10orf76-PI4KB interface is necessary for replication of some enteroviruses, but not others, is unknown. The differential dependence on c10orf76 could possibly be explained by distinct affinity of 3A proteins from different viruses towards GBF1. Alternatively, each virus may require specific threshold PI4P level for efficient formation of its replication complexes or replication organelles. Together, viral 3A, ACBD3, GBF1 and c10orf76 play a role in viral replication organelle formation (Fig. 6C), although more research on the dependence of viral replication on either GBF1 or c10orf76-mediated alteration of PI4P levels is required to better understand how enteroviruses hijack these complex membrane trafficking processes.

Direct inhibition of PI4KB is likely not a useful antiviral strategy due to unexpected deleterious side effects of PI4KB inhibition in animal models [58]. The targeting of other cellular host factors used to manipulate PI4KB signaling or feedback is a potential avenue for development of novel antiviral therapeutics. Identification of a direct high-affinity c10orf76-PI4KB complex that regulates the cellular localization of c10orf76 represents key insight into the multifaceted regulation of PI4KB signaling. The important role of the c10orf76-PI4KB complex in the replication of select enteroviruses represents a novel molecular platform which is targeted by viruses that hijack lipid signaling. The involvement of c10orf76 in Arf1 dynamics, as well as the dependence on PI4KB for Golgi localization of c10orf76, reveals a potential role of the c10orf76-PI4KB complex in Arf1 activation and subsequent PI4P production.

MATERIALS AND METHODS

Protein expression and purification

c10orf76 and PI4KB

The human *C10orf76* gene (Uniprot Q5T2E6) was synthesized by GeneArt (ThermoFisher). c10orf76 and PI4KB (Uniprot Q9UBF8-2) were each expressed with an N-terminal 6xHis-tag followed by a TEV protease site. The c10orf76 and PI4KB proteins purified for HDX-MS were expressed in *Spodoptera frugiperda* (*Sf9*) cells by infecting 1-4 L of cells at a density of 1.5×10^6 cells/mL with baculovirus encoding the kinase. After 60-72 hours infection at 27°C, *Sf9* cells were harvested and washed in phosphate-buffered saline (PBS). The c10orf76 and PI4KB proteins utilized for assays, mutational analysis and studying PKA phosphorylation were expressed in Rosetta (DE3) *E. coli* (c10orf76) or BL21 C-41(DE3) *E. coli* (PI4KB) induced overnight at 16 °C with 0.1 mM IPTG at an OD_{600} of 0.6. Cell pellets containing c10orf76 or PI4KB were sonicated in NiNTA Buffer (20 mM Tris-HCl pH 8.0, 100 mM NaCl, 20 mM imidazole, 5% (v/v) glycerol, 2 mM β -mercaptoethanol) containing protease inhibitors (Millipore Protease Inhibitor Cocktail Set III, Animal-Free) for 5 minutes on ice. Triton X-100 (0.1% v/v) was added to the cell lysate and the lysed cell solution was centrifuged for 45 minutes at 20,000 x g at 2°C. Supernatant was filtered through a 5 μ m filter and loaded onto a 5 mL HisTrap™ FF crude (GE) column in NiNTA buffer. The column was washed with 1.0 M NaCl and 20 mM imidazole in NiNTA buffer and protein was eluted with 200-250 mM imidazole in NiNTA buffer. Eluted c10orf76 or PI4KB was pooled and concentrated onto a 5 mL HiTrap™ Q column (GE) equilibrated with Q buffer (20 mM Tris-HCl pH 8.0, 100 mM NaCl, 5% glycerol v/v, 2 mM β -mercaptoethanol) and eluted with an increasing concentration of NaCl. Protein was pooled and concentrated using an Amicon 30K concentrator and incubated

overnight on ice with the addition of TEV protease. Size exclusion chromatography (SEC) was performed using a Superdex™ 200 10/300 GL increase (GE) column equilibrated in SEC buffer (20 mM HEPES pH 7.5, 150 mM NaCl and 0.5 mM TCEP). Fractions containing the protein of interest were pooled, concentrated, spun down to remove potential aggregate and flash frozen in liquid nitrogen for storage at -80 °C. c10orf76-PI4KB complex SEC trace was generated by mixing c10orf76 and PI4KB in a 1:1 ratio after individual anion exchange runs and then injecting onto the Superdex™ 200 10/300 GL increase (GE) column. Elution volumes of protein standards were obtained from the GE Instruction 29027271 AH Size exclusion chromatography columns document. See *Protein Kinase A (PKA) treatment of PI4KB* for details on producing the phosphorylated variant of PI4KB.

ACBD3, Rab11a and PKA

ACBD3 and Rab11a were expressed with N-terminal GST tags, with Protein kinase A (*M. musculus* PKA catalytic subunit alpha; Addgene 14921) expressed with an N-terminal His tag. ACBD3, Rab11a, and PKA were expressed in BL21 C-41(DE3) *E. coli* cells, with ACBD3 and Rab11 expression carried out overnight at 16 °C with 0.1 mM IPTG, and PKA expression was carried out for 4 hours at 28 °C with 1 mM IPTG. ACBD3, Rab11, and PKA were purified as previously published [11,14,59]. In brief, cell pellets containing expressed ACBD3 or Rab11a were sonicated in Q Buffer (20 mM Tris-HCl pH 8.0, 100 mM NaCl, 5% (v/v) glycerol, 2 mM β-mercaptoethanol) containing protease inhibitors (Millipore Protease Inhibitor Cocktail Set III, Animal-Free) for 5 minutes on ice. Triton X-100 (0.1% v/v) was added to the cell lysate and the lysed cell solution was centrifuged for 45 minutes at 20,000 x g at 2 °C. Supernatant was filtered through a 5 μm filter and incubated with 1-4mL of Glutathione Sepharose™ 4B beads (GE) for 1-2 hours at 4 °C. Beads were then washed with Q buffer, and GST-tagged proteins were eluted with 20 mM glutathione in Q buffer. Protein was further purified using anion exchange and size-exclusion chromatography as described above and final protein was spun down to remove potential aggregate and flash frozen in liquid nitrogen for storage at -80 °C. Nickel purification of PKA proceeded as described for PI4KB, and nickel elute was concentrated, spun down to remove potential aggregate and flash frozen in liquid nitrogen for storage at -80 °C.

Nickel and GST Pulldown Assays. For His pulldowns, NINTA agarose beads (Qiagen) (20 μL) were washed three times by centrifugation and resuspension in NINTA buffer. His-tagged bait protein was then added to a concentration of 1-3 μM and incubated with the beads on ice for 10 minutes in a total volume of 50 μL. Beads were washed three times with 150 μL NINTA buffer at 4 °C. Non-His-tagged prey protein was then added to a final concentration of 1-2 μM in a total volume of 50 μL, at which point 10 μL was taken for SDS-PAGE analysis. The mixture was incubated on ice for an additional 30 minutes and then washed four times with 120 μL NiNTA buffer at 4 °C at which time an aliquot was taken as the output for SDS-PAGE analysis. For GST pulldowns, Glutathione Sepharose™ 4B beads (GE healthcare) were washed three times by centrifugation and resuspension in Q buffer. GST-tagged bait protein (or control GST) was then added to a concentration of 3-6 μM in 50 μL and incubated with the beads on ice for 10 minutes in a total volume of 50 μL. Beads were washed three times with 150 μL Q buffer at 4 °C. Non-GST-tagged prey protein were then added to a final concentration of 2-4 μM in a total volume of 50 μL, at which point the input was taken for SDS-PAGE analysis. The mixture was incubated on ice for an additional 30 minutes and then washed four times with 120 μL Q buffer at 4 °C, at which time an aliquot was taken as the output for SDS-PAGE analysis.

Vesicle Preparation and Lipid Kinase Assays. Lipid kinase assays were carried out using the Transcreener® ADP² FI Assay (BellBrook Labs) following the published protocol as previously described [11]. In brief, substrate stocks were made up containing 1.0 mg/mL PI vesicles or 4.0 mg/mL Golgi-mimetic vesicles (10% PS, 20% PI, 25% PE, 45% PC) and were extruded through a 100 nm Nanosizer Extruder (T&T Scientific) and then combined with in a buffer containing 20 mM Hepes pH 7.5, 100 mM KCl and 0.5 mM EDTA (200 μM ATP with 1.0 mg/mL PI vesicles, 20 μM ATP with 1.0 mg/mL Golgi-mimetic vesicles). Kinase reactions were started by adding 2 μL of this substrate stock in a 384-well black low volume plates (Corning 4514). Proteins were thawed on ice and spun down to remove precipitate. Proteins were diluted individually to 4X the desired concentration in Kinase Buffer (40 mM Hepes pH 7.5, 200 mM NaCl, 20 mM MgCl₂, 0.8% Triton-X, and 0.2 mM TCEP) on ice. Proteins were then mixed together or with additional Kinase buffer resulting in 2X desired concentrations of each protein. To start the reaction, 2 μL of 2X protein stock was added to 2 μL of 2X substrate stock in plates. After mixing, the 4 μL reactions consisted of 30 mM HEPES pH 7.5 (RT), 100 mM NaCl, 50 mM KCl, 10mM MgCl₂, 0.25 mM EDTA, 0.4% (v/v) Triton-X, 0.1 mM TCEP, 10 μM ATP and 0.5 mg/mL vesicles. PI4KB was run at a final concentration of 15 nM, 20 nM or 40 nM and c10orf76 was run in 4-fold curves from 1 μM – 3.9 nM, or 1.5 μM – 23 nM, or 5-fold curves from 2 μM – 1.6 nM. Reactions proceeded at 23 °C for 20-30 minutes. Reactions were stopped using 4 μL of the transcreener stop buffer (1X Stop & Detect Buffer B, 8 nM ADP Alexa594 Tracer, 97 μg/ml ADP2 Antibody-IRDye® QC-1). Fluorescence intensity was measured using a Spectramax M5 plate reader with λ_{exc}=590 nm and λ_{em}=620 nm (20nm bandwidth). Data was plotted using Graphpad Prism software, with IC₅₀ values determined by nonlinear regression (curve fit). No

detectable nonspecific ATPase activity was detected in reactions containing 250 nM wild-type PI4KB without vesicle substrate.

Mapping the c10orf76-PI4KB binding interface using HDX-MS. HDX reactions were conducted in 50 μ L reactions with a final concentration of 400 nM of protein per sample (c10orf76-PI4KB, 400 nM each). Reactions were initiated by the addition of 45 μ L of D₂O Buffer Solution (10 mM HEPES pH 7.5, 50 mM NaCl, 97% D₂O) to 5 μ L of protein solution, to give a final concentration of 87% D₂O. Exchange was carried out for four timepoints, (3s at 1°C and 3s, 30s, and 300s at 23 °C). Exchange was terminated by the addition of acidic quench buffer giving a final concentration 0.6 M guanidine-HCl and 0.8% formic acid. All experiments were carried out in triplicate. Samples were immediately frozen in liquid nitrogen and stored at -80°C until mass analysis.

Comparison of FLH409AAA and WT c10orf76 secondary structure. HDX-MS reactions were performed with 40 μ L final volume with a protein concentration of 0.25 μ M in each sample. Reactions were started by the addition of 39 μ L D₂O buffer (100mM NaCl, 35 mM Hepes, 91.7% D₂O) to 1 μ L of protein (Final: 89.4% D₂O). Reactions were quenched by the addition of 30 μ L of acidic quench buffer (3% formic acid, 2M Guanidine) resulting in final 1.28% Formic acid and 0.85M guanidine-HCl. Proteins were allowed to undergo exchange reactions for either 3s or 300s at 23°C prior to addition of quench buffer and flash freezing in liquid N₂. All samples were set and run in triplicate. Samples were stored at -80°C until injection onto the UPLC for MS analysis.

HDX-MS data analysis. Protein samples were rapidly thawed and injected onto a UPLC system kept in a cold box at 2°C. The protein was run over two immobilized pepsin columns (Applied Biosystems; porosyme, 2-3131-00) stored at 10°C and 2°C at 200 μ L/min for 3 min and the peptides were collected onto a VanGuard precolumn trap (Waters). The trap was subsequently eluted in line with an Acquity 1.7 μ m particle, 100 \times 1 mm² C18 UPLC column (Waters), using a gradient of 5-36% B (buffer A 0.1% formic acid, buffer B 100% acetonitrile) over 16 minutes. MS experiments were performed on an Impact QTOF (Bruker) and peptide identification was done by running tandem MS (MS/MS) experiments run in data-dependent acquisition mode. The resulting MS/MS datasets were analyzed using PEAKS7 (PEAKS) and a false discovery rate was set at 1% using a database of purified proteins and known contaminants. HD-Examiner Software (Sierra Analytics) was used to automatically calculate the level of deuterium incorporation into each peptide. All peptides were manually inspected for correct charge state and presence of overlapping peptides. Deuteration levels were calculated using the centroid of the experimental isotope clusters. Attempts at generating fully deuterated protein samples to allow for the control of peptide back exchange levels during digestion and separation were made for all proteins. Protein was incubated with 3M guanidine for 30 minutes prior to the addition of D₂O, where they were further incubated for an hour on ice. The reactions were then quenched as before. Generation of a fully deuterated sample was successful for PI4K using this method, however generation of fully deuterated c10orf76 failed. Results for c10orf76 are therefore presented as relative levels of deuterium incorporation and the only control for back exchange was the level of deuterium present in the buffer (87%). The average error of all time points and conditions for each HDX project was less than 0.2 Da. Therefore, changes in any peptide at any time point greater than both 7% and 0.5 Da between conditions with an unpaired t-test value of p<0.05 was considered significant. The full details of H/D exchange for all peptides are shown in Source data, with statistics described in Extended View Table 1.

Protein Kinase A (PKA) Treatment of PI4KB. PKA (mouse catalytic subunit) was serially diluted and different concentrations were incubated with PI4KB in 20 μ L reactions on ice for 1 hour (20 μ g PI4KB, 20 mM MgCl₂, 200 μ M ATP and either 840 ng, 168 ng, 34 ng, 7 ng or 0 ng PKA). Reactions were terminated by the addition of acidic quench buffer giving a final concentration 0.6 M guanidine-HCl and 0.8% formic acid and then flash frozen in liquid N₂ prior to MS phosphorylation analysis. To generate *E. coli* expressed, PKA phosphorylated PI4KB for use in kinase assays and HDX-MS, phosphorylation of Ser496 was carried out using 1.0 mg PI4KB, 20 mM MgCl₂, 200 μ M ATP and 4.2 μ g PKA in NiNTA buffer, with the reaction allowed to proceed for 1 hour on ice. The reaction was quenched with 20 mM EDTA, and immediately loaded onto a GE 1 mL HisTap FF crude to remove His-tagged PKA. Phosphorylated PI4KB was concentrated followed by size exclusion chromatography as described for PI4KB above. In tandem, a non-phosphorylated PI4KB control was purified in the same manner except MgCl₂, ATP, and PKA were not added. Protein was flash frozen in liquid N₂ for storage at -80 °C.

HDX-MS dose response of c10orf76 of phosphorylated PI4KB. Phosphorylated and non-phosphorylated PI4KB were generated and purified as described above. HDX reactions were conducted in 130 μ L reaction volumes with a final concentration of 20nM PI4KB (phosphorylated or non-phosphorylated) per sample, with 0 nM, 5 nM, 10 nM, 20 nM, 40 nM, 80 nM, 160 nM and 320 nM c10orf76. Exchange was carried out for 5 seconds, in triplicate for each concentration of c10orf76. Hydrogen deuterium exchange was initiated by the addition of 80 μ L of D₂O buffer solution (10mM HEPES (pH 7.5), 50mM NaCl, 97% D₂O) to the protein solution, to give a final concentration of 60% D₂O. Exchange was terminated by the addition of 20 μ L ice cold acidic quench buffer at a final concentration 0.6M

guanidine-HCl and 0.9% formic acid. Samples were immediately frozen in liquid nitrogen at -80°C . Data analyzed as described above in HDX-MS data analysis.

Phosphorylation Analysis. LC-MS/MS analysis of phosphorylated variants of PI4KB was carried out as described in the HDX-MS data analysis section. MS/MS datasets were analyzed using PEAKS7 to identify phosphorylated peptides in PI4KB and c10orf76. A false discovery rate was set at 0.1% using a database of purified proteins and known contaminants. To measure PI4KB phosphorylation levels using Bruker Data analysis, the phosphorylated and non-phosphorylated peptides of interest were extracted, and the total area of each peptide was manually integrated to determine the amount of phosphorylated vs non-phosphorylated species under given experimental conditions. No phosphorylation was detected in *E. coli* derived PI4KB. For *Sf9* derived PI4KB Ser294 phosphorylation, the peptides KRTAS*NPKVENEDE (290-303) and KRTAS*NPKVENEDEPVLADERE (290-312) were averaged, for Ser413 phosphorylation DTTSVPARIPENRIRSTRS*VENLPECGITHE (395-425) was used, for Ser430 phosphorylation GITHEQRAGS*F (430-441) was used, and for Ser496 phosphorylation IAAGDIRRRRLS*EQLAHTPTA (486-505) and IAAGDIRRRRLS*EQ-LAHTPTAF (486-506) were averaged. No phosphorylation was detected in *E. coli* derived c10orf76. For *Sf9* derived c10orf76 Ser14 phosphorylation, LRKSS*ASKKPLKE (10-22) was used, and for the 325-351 phosphorylation (exact location of phosphorylation ambiguous) VTTVPSPAPTTPTVPLGTTTPSSD (326-348), VTTVPSPAPTTPTVPLGTTTPSSDVISS (325-351) and VTTVPSPAPTTPTVPLGTTTPSS (325-347) were averaged.

Isothermal Titration Calorimetry. Purified c10orf76, non-phosphorylated PI4KB, and Ser496-phosphorylated PI4KB were dialyzed separately into buffer containing 20 mM Hepes pH 7.5, 150 mM NaCl and 0.5 mM TCEP. All ITC experiments were carried out at 20°C on a MicroCal iTC200 instrument (GE Healthcare). The sample cell contained non-phosphorylated PI4KB or Ser496-phosphorylated PI4KB (5 μM), and c10orf76 (50 μM) was added in 19 injections of 2 μL each. Data was processed using Origin software (MicroCal) and the dissociation constants (Kd) were determined using a one-site model. Figures are of a single experiment, but are representative of three independent experiments using protein from two different protein preparations.

Alignments. Protein sequences from the Uniprot database were aligned using Clustal Omega [60] and figures were generated using ESPrnt [61]. Uniprot PI4KB entries used: *H. sapiens* (Q9UBF8-2), *M. musculus* (Q8BK8C), *D. rerio* (Q49GP3), *D. melanogaster* (Q9BKJ2), *C. elegans* (Q20077). Uniprot c10orf76 entries used: *H. sapiens* (Q5T2E6), *M. musculus* (Q6PD19), *D. rerio* (Q6PGW3), *D. melanogaster* (Q7KSU3).

DNA Constructs and Antibodies. The following antibodies were used to examine protein localization in WT and c10orf76 knockout HAP1 cells. Mouse monoclonal antibodies included anti-GBF1 (BD Biosciences), anti-CM1 (a gift from Felix Wieland, Heidelberg University, Germany), anti-GM130 (BD Biosciences), anti-Giantin (Enzo Life Science), anti-ERGIC53 (Enzo Life Science), anti- βCOP (Sigma), anti-PI4P (Echelon), anti-ACBD3 (Sigma). Rabbit polyclonal antibodies included anti-PI4KB (Millipore), anti-COPI α/γ (a gift from Felix Wieland), anti-TGN46 (Novus Biologicals). Conjugated goat anti-rabbit and goat anti-mouse Alexa Fluor 488, 596, or 647 (Molecular Probes) were used as secondary antibodies. The following antibodies were used for Western blot analysis to examine protein expression level in WT and c10orf76 knockout HAP1 cells. Mouse monoclonal antibodies included anti-GBF1 (BD Biosciences), anti- β -actin (Sigma), and Rabbit polyclonal antibodies included anti-PI4KB (Millipore). IRDye conjugated goat anti-mouse or anti-rabbit (LI-COR) were used as secondary antibodies. GFP-PI4KB, GFP-PI4KB RL494EA, GFP-c10orf76, and GFP-c10orf76 FLH409AAA were cloned using Gibson assembly [62] into the pEGFP-C1 vector (Clontech). mRFP-FKBP12-PI4KB and mRFP-FKBP12-PI4KB RL494EA were generated by amplifying the mRFP-FKBP12 insert from mRFP-FKBP12-5ptase domain [63] and replacing the N-terminal GFP in either GFP-PI4KB or GFP-PI4KB RL494EA using a single digest with NdeI. AKAP-FRB-CFP, which is used to selectively recruit FKBP12-tagged proteins to the outer mitochondrial membrane, has been described previously [64].

Cell Culture, Transfection, and Live-Cell Confocal Microscopy of Rapamycin Recruitment. HEK293-AT1 cells, which stably express the AT1a rat Angiotensin II receptor [65], were cultured in Dulbecco's Modified Eagle Medium (DMEM-high glucose) containing 10% (vol/vol) FBS and supplemented with a 1% solution of penicillin/streptomycin. This cell line is regularly tested for *Mycoplasma* contamination using a commercially-available detection kit (InvivoGen) and, after thawing, the cells are treated with plasmocin prophylactic (InvivoGen) at 500 $\mu\text{g}/\text{ml}$ for the initial three passages (6-9 days) as well as supplemented with 5 $\mu\text{g}/\text{ml}$ of plasmocin prophylactic for all subsequent passages. For confocal microscopy, HEK293-AT1 cells (3×10^5 cells/well) were plated on 29 mm circular glass-bottom culture dishes (#1.5; Cellvis) pre-coated with 0.01% poly-L-lysine solution (Sigma). The cells were allowed to attach overnight prior to transfection of plasmid DNAs (0.1-0.2 $\mu\text{g}/\text{well}$) using Lipofectamine 2000 (Invitrogen) and Opti-MEM (Invitrogen) according to the manufacturer's instructions. Please note that studies using the rapamycin-inducible protein hetero-dimerization system used a 1:2:1 ratio of plasmid DNA for transfection of the FKBP12-tagged PI4KB enzyme, AKAP-FRB-CFP recruiter, and GFP-c10orf76 variant (total DNA: 0.4 $\mu\text{g}/\text{well}$). After 18-20 hr of transfection, cells were incubated in 1 mL of modified Krebs-Ringer solution (containing 120 mM NaCl, 4.7 mM KCl,

CHAPTER 7

2 mM CaCl₂, 0.7 mM MgSO₄, 10 mM glucose, 10 mM HEPES, and adjusted to pH 7.4) and images were acquired at room temperature using a Zeiss LSM 710 laser-scanning confocal microscope (Carl Zeiss Microscopy). Rapamycin treatment of cells was carried out at a final concentration of 100 nM. Image acquisition was performed using the ZEN software system (Carl Zeiss Microscopy), while the image preparation was done using the open-source FIJI platform [66].

Cell Culture, Transfection, and Live-Cell Confocal Microscopy of HAP1 WT and c10orf76 Knockout Cells

Cells and viruses

HAP1 WT cells and HAP1 c10orf76 knockout cells were obtained from T. Brummelkamp, and are now carried by Horizon Discovery. The generation and validation of the Hap1 c10orf76 KO cell clone was described previously [28]. HeLa R19 cells were obtained from G. Belov (University of Maryland and Virginia-Maryland College of Veterinary Medicine, US). HeLa PI4KB knockout cells were described previously [29]. HAP1 cells were cultured in IMDM (Thermo Fisher Scientific) supplemented with 10% fetal calf serum (FCS) and penicillin–streptomycin. HeLa cells were cultured in DMEM (Lonza) supplemented with 10% FCS and penicillin–streptomycin. All cells were grown at 37°C in 5% CO₂. The following enteroviruses were used: CVA10 (strain Kowalik, obtained from the National Institute for Public Health and Environment; RIVM, The Netherlands), CVB3 (strain Nancy, obtained by transfection of the infectious clone p53CB3/T7 as described previously [67], PV1 (strain Sabin, ATCC). Virus titers were determined by end-point titration analysis and expressed as 50% tissue culture infectious dose (TCID₅₀).

Replication rescue assay

HeLa cells were transfected with plasmids carrying WT or mutant PI4KB (RL494EA), Golgi-targeting EGFP (pEGFP-GalT) or kinase-dead PI4KB (PI4KB-KD) as a negative control. At 24 h post-transfection, the cells were infected with CVA10, CVB3, and PV1. At 8 h p.i., the infected cells were frozen, and virus titers were determined by end-point titration analysis and expressed as 50% tissue culture infectious dose (TCID₅₀).

Immunofluorescence microscopy of WT and c10orf76 knockout HAP1 cells

HAP1 cells were grown on ibiTreat slides μ-slide 18-wells (Ibidi) one day prior to infection. Cells were fixed by submersion in a 4% paraformaldehyde solution for 15 minutes. Nuclei were stained with DAPI. Confocal imaging was performed with a Leica Spell confocal microscope.

7

AUTHOR CONTRIBUTIONS

JAM, RMH, MLJ, and JTBS expressed and purified proteins. JAM and JEB designed complex-disrupting mutations. JAM carried out pulldown and kinase assays. JAM, MLJ, RMH and JEB carried out HDX-MS and analysis. CJP, JAM and MJB performed ITC. HRL and WvE performed viral infection assays, and HRL characterized c10orf76 knockout cells. JGP and TB performed cellular c10orf76 recruitment experiments. JAM, JRPMS, TB, FJMK, and JEB designed the research. JAM and JEB wrote the manuscript with input from all authors.

ACKNOWLEDGEMENTS

J.E.B. wishes to thank CIHR (CIHR new investigator grant and CIHR open operating grant FRN 142393) and MSFHR (scholar award 17646) for support. JAM and MLJ were supported by graduate scholarships from Natural Sciences and Engineering Research Council of Canada (NSERC). J.G.P. and T.B. are supported by the National Institutes of Health (NIH) Intramural Research Program (IRP), with additional support to J.G.P. from an NICHD Visiting Fellowship and Natural Sciences and Engineering Research Council of Canada (NSERC) Banting Postdoctoral Fellowship. Work in the lab of FJMvK is supported by research grants from the Netherlands Organization for Scientific Research (NWO-VICI-91812628, NWO-ECHO-711.017.002) and from the European Union (Horizon 2020 Marie Skłodowska-Curie ETN ‘ANTIVIRALS’, grant agreement number 642434). JRPMS is supported by a research grant from the Netherlands Organization for Scientific Research (NOW-VENI-722.012.066). The plasmid for ACBD3 and mCherry-GBF1 was a gift from Jun Sasaki and Catherine Jackson respectively. We appreciate the feedback on the manuscript pre-submission by Dr Julie Brill.

CONFLICT OF INTEREST

The authors declare that they have no conflict of interest.

REFERENCES

1. Tan J, Brill JA (2014) Cinderella story: PI4P goes from precursor to key signaling molecule. *Crit Rev Biochem Mol Biol* 49: 33–58.
2. Balla T (2013) Phosphoinositides: tiny lipids with giant impact on cell regulation. *Physiol Rev* 93: 1019–1137.
3. Weber SS, Ragaz C, Reus K, Nyfeler Y, Hilbi H (2006) Legionella pneumophila exploits PI(4)P to anchor secreted effector proteins to the replicative vacuole. *PLoS Pathog* 2: e46.
4. Hsu N-Y, Ilnytska O, Belov G, Santiana M, Chen Y-H, Takvorian PM, Pau C, van der Schaar H, Kaushik-Basu N, Balla T, et al. (2010) Viral reorganization of the secretory pathway generates distinct organelles for RNA replication. *Cell* 141: 799–811.
5. van der Schaar HM, Dorobantu CM, Albuлесcu L, Strating JRPM, van Kuppeveld FJM (2016) Fat(al) attraction: Picornaviruses Usurp Lipid Transfer at Membrane Contact Sites to Create Replication Organelles. *Trends Microbiol* 24: 535–546.
6. Burke JE (2018) Structural Basis for Regulation of Phosphoinositide Kinases and Their Involvement in Human Disease. *Mol Cell* 71: 653–673.
7. Dornan GL, McPhail JA, Burke JE (2016) Type III phosphatidylinositol 4 kinases: structure, function, regulation, signalling and involvement in disease. *Biochemical Society Transactions* 44: 260–266.
8. Boura E, Nencka R (2015) Phosphatidylinositol 4-kinases: Function, structure, and inhibition. *Exp Cell Res*.
9. Mesmin B, Bigay J, Polidori J, Jamecna D, Lacas-Gervais S, Antonny B (2017) Sterol transfer, PI4P consumption, and control of membrane lipid order by endogenous OSBP. *EMBO J* 36: 3156–3174.
10. Lu D, Sun H-Q, Wang H, Barylko B, Fukata Y, Fukata M, Albanesi JP, Yin HL (2012) Phosphatidylinositol 4-kinase II α is palmitoylated by Golgi-localized palmitoyltransferases in cholesterol-dependent manner. *J Biol Chem* 287: 21856–21865.
11. McPhail JA, Ottosen EH, Jenkins ML, Burke JE (2017) The Molecular Basis of Aichi Virus 3A Protein Activation of Phosphatidylinositol 4 Kinase III β , PI4KB, through ACBD3. *Structure* 25: 121–131.
12. Klima M, Tóth DJ, Hexnerova R, Baumlová A, Chalupská D, Tykvar J, Rezaczkova L, Sengupta N, Man P, Dubankova A, et al. (2016) Structural insights and in vitro reconstitution of membrane targeting and activation of human PI4KB by the ACBD3 protein. *Sci Rep* 6: 23641.
13. Sasaki J, Ishikawa K, Arita M, Taniguchi K (2012) ACBD3-mediated recruitment of PI4KB to picornavirus RNA replication sites. *EMBO J* 31: 754–766.
14. Burke JE, Inglis AJ, Perisic O, Masson GR, McLaughlin SH, Rutaganira F, Shokat KM, Williams RL (2014) Structures of PI4KIII β complexes show simultaneous recruitment of Rab11 and its effectors. *Science* 344: 1035–1038.
15. Altan-Bonnet N, Balla T (2012) Phosphatidylinositol 4-kinases: hostages harnessed to build panviral replication platforms. *Trends in Biochemical Sciences* 37: 293–302.
16. Téoulé F, Brisac C, Pelletier I, Vidalain P-O, Jégouic S, Mirabelli C, Bessaud M, Combelas N, Autret A, Tangy F, et al. (2013) The Golgi protein ACBD3, an interactor for poliovirus protein 3A, modulates poliovirus replication. *PLoS Pathog* 8: 11031–11046.
17. Greninger AL, Knudsen GM, Betegon M, Burlingame AL, DeRisi JL (2013) ACBD3 interaction with TBC1 domain 22 protein is differentially affected by enteroviral and kobuviral 3A protein binding. *MBio* 4: e00098–13.
18. Greninger AL, Knudsen GM, Betegon M, Burlingame AL, DeRisi JL (2012) The 3A protein from multiple picornaviruses utilizes the golgi adaptor protein ACBD3 to recruit PI4KIII β . *J Virol* 86: 3605–3616.
19. Fowler ML, McPhail JA, Jenkins ML, Masson GR, Rutaganira FU, Shokat KM, Williams RL, Burke JE (2016) Using hydrogen deuterium exchange mass spectrometry to engineer optimized constructs for crystallization of protein complexes: Case study of PI4KIII β with Rab11. *Protein Sci* 25: 826–839.
20. de Graaf P, Zwart WT, van Dijken RAJ, Deneka M, Schulz TKF, Geijsen N, Coffey PJ, Gadella BM, Verkleij AJ, van der Sluijs P, et al. (2004) Phosphatidylinositol 4-kinasebeta is critical for functional association of rab11 with the Golgi complex. *Mol Biol Cell* 15: 2038–2047.
21. Godi A, Pertile P, Meyers R, Marra P, Di Tullio G, Iurisci C, Luini A, Corda D, De Matteis MA (1999) ARF mediates recruitment of PtdIns-4-OH kinase-beta and stimulates synthesis of PtdIns(4,5)P2 on the Golgi complex. *Nat Cell Biol* 1: 280–287.
22. Hausser A, Storz P, Märtens S, Link G, Toker A, Pfizenmaier K (2005) Protein kinase D regulates vesicular transport by phosphorylating and activating phosphatidylinositol-4 kinase IIIbeta at the Golgi complex. *Nat Cell Biol* 7: 880–886.

23. Hausser A, Link G, Hoene M, Russo C, Selchow O, Pfizenmaier K (2006) Phospho-specific binding of 14-3-3 proteins to phosphatidylinositol 4-kinase III beta protects from dephosphorylation and stabilizes lipid kinase activity. *J Cell Sci* 119: 3613–3621.
24. Chalupská D, Eisenreichova A, Rózycki B, Rezaczkova L, Humpolickova J, Klima M, Boura E (2017) Structural analysis of phosphatidylinositol 4-kinase III β (PI4KB) - 14-3-3 protein complex reveals internal flexibility and explains 14-3-3 mediated protection from degradation in vitro. *J Struct Biol*.
25. Isobe K, Jung HJ, Yang C-R, Claxton J, Sandoval P, Burg MB, Raghuram V, Knepper MA (2017) Systems-level identification of PKA-dependent signaling in epithelial cells. *Proc Natl Acad Sci USA* 114: E8875–E8884.
26. Szivak I, Lamb N, Heilmeyer LMG (2006) Subcellular localization and structural function of endogenous phosphorylated phosphatidylinositol 4-kinase (PI4K92). *J Biol Chem* 281: 16740–16749.
27. Jovic M, Kean MJ, Szentpetery Z, Polevoy G, Gingras A-C, Brill JA, Balla T (2012) Two phosphatidylinositol 4-kinases control lysosomal delivery of the Gaucher disease enzyme, β -glucocerebrosidase. *Mol Biol Cell* 23: 1533–1545.
28. Blomen VA, Májek P, Jae LT, Bigenzahn JW, Nieuwenhuis J, Staring J, Sacco R, van Diemen FR, Olk N, Stukalov A, et al. (2015) Gene essentiality and synthetic lethality in haploid human cells. *Science* 350: 1092–1096.
29. Lyoo H, van der Schaar HM, Dorobantu CM, Rabouw HH, Strating JRPM, van Kuppeveld FJM (2019) ACBD3 Is an Essential Pan-enterovirus Host Factor That Mediates the Interaction between Viral 3A Protein and Cellular Protein PI4KB. *MBio* 10: 282.
30. Xiao X, Lei X, Zhang Z, Ma Y, Qi J, Wu C, Xiao Y, Li L, He B, Wang J (2017) Enterovirus 3A facilitates viral replication by promoting PI4KB-ACBD3 interaction. *J Virol* 91: 799.
31. Klima M, Chalupská D, Rózycki B, Humpolickova J, Rezaczkova L, Silhan J, Baumlová A, Dubankova A, Boura E (2017) Kobuviral Non-structural 3A Proteins Act as Molecular Harnesses to Hijack the Host ACBD3 Protein. *Structure* 25: 219–230.
32. Ishikawa-Sasaki K, Sasaki J, Taniguchi K (2014) A complex comprising phosphatidylinositol 4-kinase III β , ACBD3, and Aichi virus proteins enhances phosphatidylinositol 4-phosphate synthesis and is critical for formation of the viral replication complex. *J Virol* 88: 6586–6598.
33. Wessels E, Duijsings D, Niu T-K, Neumann S, Oorschot VM, de Lange F, Lanke KHW, Klumperman J, Henke A, Jackson CL, et al. (2006) A viral protein that blocks Arf1-mediated COP-I assembly by inhibiting the guanine nucleotide exchange factor GBF1. *Developmental Cell* 11: 191–201.
34. Lanke KHW, van der Schaar HM, Belov GA, Feng Q, Duijsings D, Jackson CL, Ehrenfeld E, van Kuppeveld FJM (2009) GBF1, a guanine nucleotide exchange factor for Arf, is crucial for coxsackievirus B3 RNA replication. *J Virol* 83: 11940–11949.
35. Wessels E, Duijsings D, Lanke KHW, van Dooren SHJ, Jackson CL, Melchers WJG, van Kuppeveld FJM (2006) Effects of picornavirus 3A Proteins on Protein Transport and GBF1-dependent COP-I recruitment. *J Virol* 80: 11852–11860.
36. Ilnytska O, Santiana M, Hsu N-Y, Du W-L, Chen Y-H, Viktorova EG, Belov G, Brinker A, Storch J, Moore C, et al. (2013) Enteroviruses harness the cellular endocytic machinery to remodel the host cell cholesterol landscape for effective viral replication. *Cell Host Microbe* 14: 281–293.
37. Masson GR, Jenkins ML, Burke JE (2017) An overview of hydrogen deuterium exchange mass spectrometry (HDX-MS) in drug discovery. *Expert Opin Drug Discov* 12: 981–994.
38. Vadas O, Jenkins ML, Dornan GL, Burke JE (2017) Using Hydrogen-Deuterium Exchange Mass Spectrometry to Examine Protein-Membrane Interactions. *Meth Enzymol* 583: 143–172.
39. Vadas O, Burke JE (2015) Probing the dynamic regulation of peripheral membrane proteins using hydrogen deuterium exchange-MS (HDX-MS). *Biochem Soc Trans* 43: 773–786.
40. Hornbeck PV, Zhang B, Murray B, Kornhauser JM, Latham V, Skrzypek E (2015) PhosphoSitePlus, 2014: mutations, PTMs and recalibrations. *Nucleic Acids Res* 43: D512–D520.
41. Ward DG, Ashton PR, Trayer HR, Trayer IP (2001) Additional PKA phosphorylation sites in human cardiac troponin I. *Eur J Biochem* 268: 179–185.
42. Marx SO, Reiken S, Hisamatsu Y, Jayaraman T, Burkhoff D, Rosemblyt N, Marks AR (2000) PKA phosphorylation dissociates FKBP12.6 from the calcium release channel (ryanodine receptor): defective regulation in failing hearts. *Cell* 101: 365–376.
43. Zhu MM, Rempel DL, Du Z, Gross ML (2003) Quantification of protein-ligand interactions by mass spectrometry, titration, and H/D exchange: PLIMSTEX. *J Am Chem Soc* 125: 5252–5253.
44. Hammond GRV, Fischer MJ, Anderson KE, Holdich J, Koteci A, Balla T, Irvine RF (2012) PI4P and PI(4,5)P2 are essential but independent lipid determinants of membrane identity. *Science* 337: 727–730.

45. van der Schaar HM, van der Linden L, Lanke KHW, Strating JRP, Pürstinger G, de Vries E, de Haan CAM, Neyts J, van Kuppeveld FJM (2012) Coxsackievirus mutants that can bypass host factor PI4KIII β and the need for high levels of PI4P lipids for replication. *Cell Res* 22: 1576–1592.
46. Palmer DJ, Helms JB, Beckers CJ, Orci L, Rothman JE (1993) Binding of coatamer to Golgi membranes requires ADP-ribosylation factor. *J Biol Chem* 268: 12083–12089.
47. Staring J, Castelmur von E, Blomen VA, van den Hengel LG, Brockmann M, Baggen J, Thibaut HJ, Nieuwenhuis J, Janssen H, van Kuppeveld FJM, et al. (2017) PLA2G16 represents a switch between entry and clearance of Picornaviridae. *Nature* 541: 412–416.
48. Flanagan CA, Schnieders EA, Emerick AW, Kunisawa R, Admon A, Thorner J (1993) Phosphatidylinositol 4-Kinase - Gene Structure and Requirement For Yeast-Cell Viability. *Science* 262: 1444–1448.
49. Walch-Solimena C, Novick P (1999) The yeast phosphatidylinositol-4-OH kinase pik1 regulates secretion at the Golgi. *Nat Cell Biol* 1: 523–525.
50. Nakanishi S, Catt KJ, Balla T (1995) A wortmannin-sensitive phosphatidylinositol 4-kinase that regulates hormone-sensitive pools of inositolphospholipids. *Proc Natl Acad Sci USA* 92: 5317–5321.
51. Balla T, Downing GJ, Jaffe H, Kim S, Zolyomi A, Catt KJ (1997) Isolation and molecular cloning of wortmannin-sensitive bovine type III phosphatidylinositol 4-kinases. *J Biol Chem* 272: 18358–18366.
52. Meyers R, Cantley LC (1997) Cloning and characterization of a wortmannin-sensitive human phosphatidylinositol 4-kinase. *J Biol Chem* 272: 4384–4390.
53. Sohda M, Misumi Y, Yamamoto A, Yano A, Nakamura N, Ikehara Y (2001) Identification and characterization of a novel Golgi protein, GCP60, that interacts with the integral membrane protein giantin. *J Biol Chem* 276: 45298–45306.
54. Polevoy G, Wei H-C, Wong R, Szentpetery Z, Kim YJ, Goldbach P, Steinbach SK, Balla T, Brill JA (2009) Dual roles for the *Drosophila* PI 4-kinase four wheel drive in localizing Rab11 during cytokinesis. *J Cell Biol* 187: 847–858.
55. Dickinson ME, Flenniken AM, Ji X, Teboul L, Wong MD, White JK, Meehan TF, Weninger WJ, Westerberg H, Adissu H, et al. (2016) High-throughput discovery of novel developmental phenotypes. *Nature* 537: 508–514.
56. Wang Y, Mousley CJ, Lete MG, Bankaitis VA (2019) An equal opportunity collaboration between lipid metabolism and proteins in the control of membrane trafficking in the trans-Golgi and endosomal systems. *Curr Opin Cell Biol* 59: 58–72.
57. Viktorova EG, Gabaglio S, Meissner JM, Lee E, Moghimi S, Sztul E, Belov GA (2019) A redundant mechanism of recruitment underlies the remarkable plasticity of the requirement of poliovirus replication for the cellular ArfGEF GBF1. *J Virol* JVI.00856–19.
58. Spickler C, Lippens J, Laberge M-K, Desmeules S, Bellavance É, Garneau M, Guo T, Hucke O, Leyssen P, Neyts J, et al. (2013) Phosphatidylinositol 4-kinase III beta is essential for replication of human rhinovirus and its inhibition causes a lethal phenotype in vivo. *Antimicrob Agents Chemother* 57: 3358–3368.
59. Slice LW, Taylor SS (1989) Expression of the catalytic subunit of cAMP-dependent protein kinase in *Escherichia coli*. *J Biol Chem* 264: 20940–20946.
60. Sievers F, Wilm A, Dineen D, Gibson TJ, Karplus K, Li W, Lopez R, McWilliam H, Remmert M, Söding J, et al. (2011) Fast, scalable generation of high-quality protein multiple sequence alignments using Clustal Omega. *Mol Syst Biol* 7: 539–539.
61. Robert X, Gouet P (2014) Deciphering key features in protein structures with the new ENDscript server. *Nucleic Acids Research* 42: W320–W324.
62. Gibson DG, Young L, Chuang R-Y, Venter JC, Hutchison CA, Smith HO (2009) Enzymatic assembly of DNA molecules up to several hundred kilobases. *Nat Methods* 6: 343–345.
63. Várnai P, Thyagarajan B, Rohacs T, Balla T (2006) Rapidly inducible changes in phosphatidylinositol 4,5-bisphosphate levels influence multiple regulatory functions of the lipid in intact living cells. *J Cell Biol* 175: 377–382.
64. Csordás G, Várnai P, Golenár T, Roy S, Purkins G, Schneider TG, Balla T, Hajnóczky G (2010) Imaging interorganelle contacts and local calcium dynamics at the ER-mitochondrial interface. *Mol Cell* 39: 121–132.
65. Hunyady L, Baukal AJ, Gaborik Z, Olivares-Reyes JA, Bor M, Szaszak M, Lodge R, Catt KJ, Balla T (2002) Differential PI 3-kinase dependence of early and late phases of recycling of the internalized AT1 angiotensin receptor. *J Cell Biol* 157: 1211–1222.
66. Schindelin J, Arganda-Carreras I, Frise E, Kaynig V, Longair M, Pietzsch T, Preibisch S, Rueden C, Saalfeld S, Schmid B, et al. (2012) Fiji: an open-source platform for biological-image analysis. *Nat Methods* 9: 676–682.

CHAPTER 7

67. Wessels E, Duijsings D, Notebaart RA, Melchers WJG, van Kuppeveld FJM (2005) A proline-rich region in the coxsackievirus 3A protein is required for the protein to inhibit endoplasmic reticulum-to-golgi transport. *J Virol* 79: 5163–5173.
68. Masson GR, Burke JE, Ahn NG, Anand GS, Borchers C, Brier S, Bou-Assaf GM, Engen JR, Englander SW, Faber J, et al. (2019) Recommendations for performing, interpreting and reporting hydrogen deuterium exchange mass spectrometry (HDX-MS) experiments. *Nat Methods* 16: 595–602.

EXPANDED VIEW FIGURES

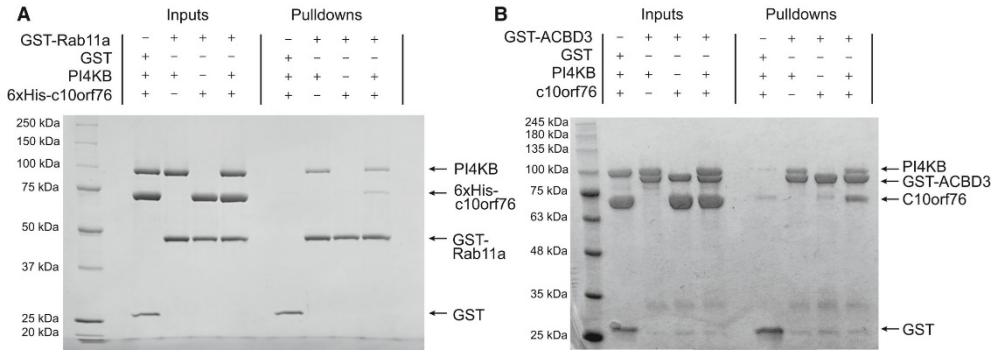
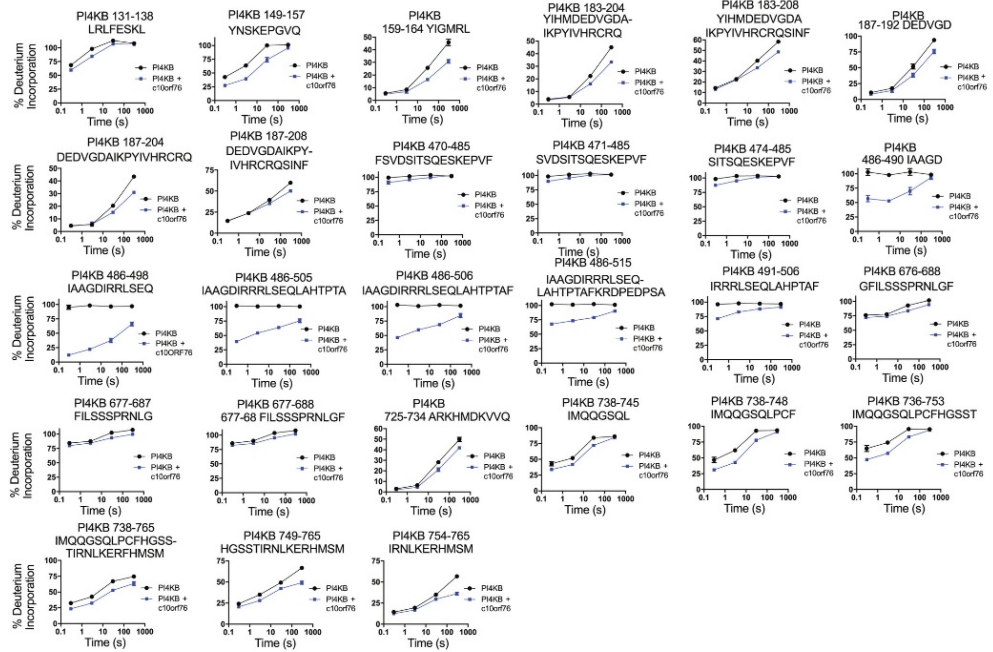


Figure EV1. PI4KB forms ternary complexes with c10orf76, Rab11a and ACBD3 (refers to Fig. 1). (A) PI4KB can form ternary complexes with Rab11a and c10orf76 *in vitro*. GST-pulldown assays were carried out using GST-Rab11a(Q70L) (6 μ M) or GST alone (3 μ M) as the bait, using 6xHis-c10orf76 (4 μ M), PI4KB (2 μ M) as the prey. (B) PI4KB can form ternary complexes with ACBD3 and c10orf76 *in vitro*. GST-pulldown assays were carried out using GST-ACBD3 (4 μ M) or GST alone (4 μ M) as the bait, and 6xHis-c10orf76 (3 μ M) and PI4KB (2 μ M) as the prey. Samples were washed a total of 4 times in all experiments.

A PI4KB peptides showing HDX differences in presence of c10orf76 (significant difference >7 %D and 0.5 #D, unpaired student T-test <0.05)



B c10orf76 peptides showing HDX differences in presence of PI4KB (significant difference >7 %D and 0.5 #D, unpaired student T-test <0.05)

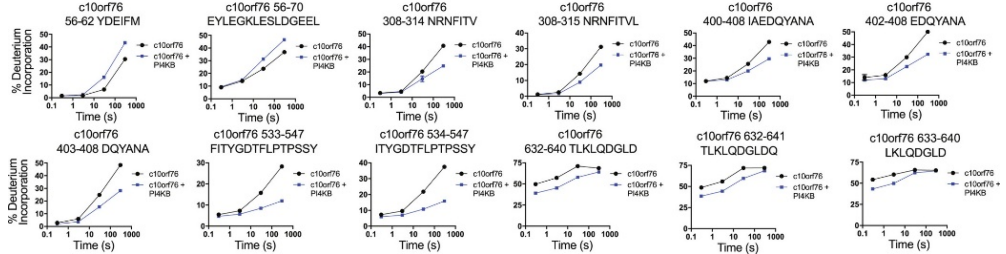


Figure EV2. PI4KB and c10orf76 form an extended interface with spanning multiple regions (refers to Fig. 1). All peptides of both PI4KB (A) and c10orf76 (B) with a significant difference in H/D exchange with >7% decrease in exchange, >0.5 Da difference, and unpaired two-tailed student t-test <0.05 at any time point (3s at 1°C; 3s, 30s, and 300s at 23°C).

THE C10ORF76-PI4KB COMPLEX AND ITS NECESSITY FOR GOLGI PI4P LEVELS & ENTEROVIRUS REPLICATION

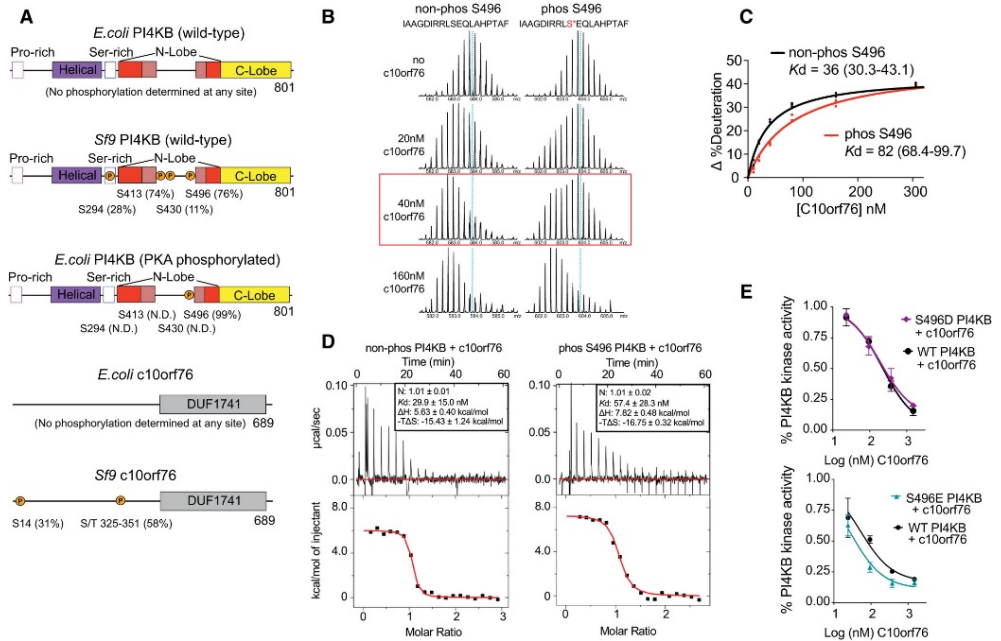


Figure EV3. PKA phosphorylation of PI4KB Ser496 reduces affinity for c10orf76 (refers to Fig. 2). (A) PKA phosphorylates the Ser496 site in PI4KB. Relative abundance of phosphorylated PI4KB at Ser294, Ser413 and Ser496 sites and c10orf76 at S14 and S/T from 325-351 expressed in *Sf9*, *E. coli*, or expressed in *E. coli* and treated with PKA (PI4KB) were calculated using the relative intensity (total area) of the phosphorylated vs non-phosphorylated peptides (290-303, 290-312, 395-425, 430-441, 486-505 and 486-506) for PI4KB and (10-22 and 325-351) for c10orf76. For 325-351 the definitive phosphorylated Ser/Thr residue could not be determined. N.D. indicates no phosphorylation was identified. (B) Raw deuterium incorporation data for PI4KB peptide 488-508 used to generate panel C. The deuterium incorporation for the phosphorylated and non-phosphorylated variants of PI4KB are shown in the presence of different concentrations of c10orf76. Dotted blue line indicates mass centroid of PI4KB peptide in absence of c10orf76, red box highlights the clear difference in deuterium incorporation at 40 nM c10orf76 between non-phosphorylated and phosphorylated Ser496 PI4KB. (C) Phosphorylation of Ser496 reduces PI4KB affinity for c10orf76. Deuterium incorporation of the PI4KB kinase linker region peptide 488-508 (20 nM) at a single time point (5 seconds of D₂O exposure at 23°C) was monitored in the presence of increasing concentrations of c10orf76 (0-320 nM c10orf76). K_d values were generated using a one binding site, nonlinear regression (curve fit), and are shown with 95% confidence intervals. Error bars represent standard deviation ($n=3$), most are smaller than the size of the point. (D) Representative ITC binding isotherms following the titration of c10orf76 into a solution of non-phosphorylated PI4KB (left) or Ser496 phosphorylated PI4KB (right). Parameter values are an average with standard deviation ($N=3$). (E) PI4KB S496D/E mutants do not mimic Ser496 phosphorylation modulation of c10orf76 binding. The kinase activity of S496D/E variants of PI4KB (15 nM) was measured in the presence of varying amounts of c10orf76 (23 nM-1.5 μ M) with 100% PI lipid substrate (0.5 mg/L) and 100 μ M ATP. The data was normalized to the kinase activity of PI4KB alone. Error bars represent standard deviation ($n=3$).

7

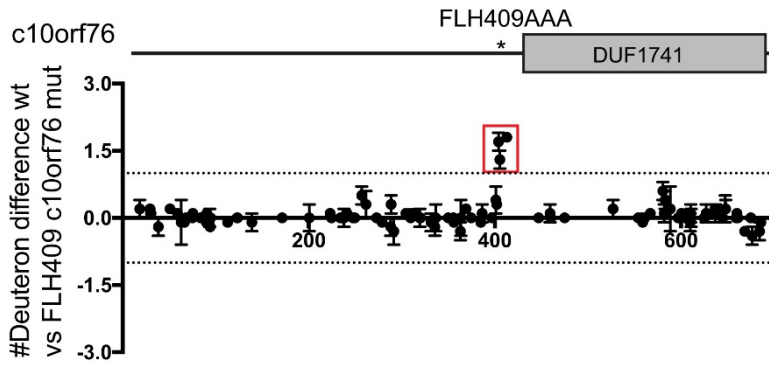


Figure EV4. The FLH409AAA c10orf76 mutant maintains similar overall secondary structure to wild-type with a destabilization at the mutation site (refers to Fig. 2) Differences in the changes in the deuterium incorporation of wild type and FLH409AAA mutant c10orf76. H/D exchange reactions of c10orf76 (400 nM) were carried out for 3s and 300s, and the average difference in number of deuterons incorporated between wild-type and FLH409AAA c10orf76 (400 nM) was graphed. Error bars represent standard deviation (n=3).

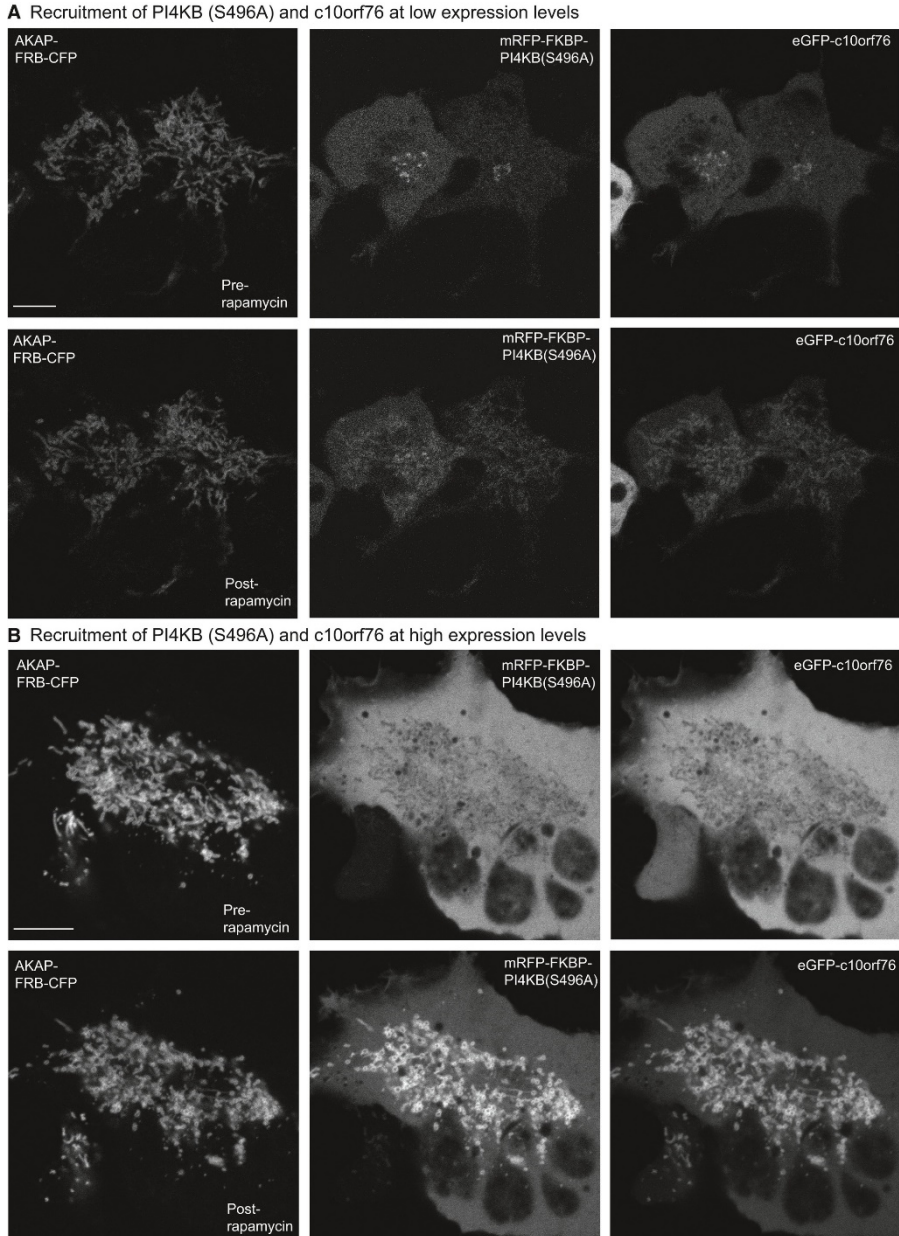


Figure EV5. PI4KB (S496A) does not affect PI4KB or c10orf76 recruitment to the Golgi *in vivo* (refers to Fig. 3). (A) Mitochondria recruitment experiment with PI4KB(S496A) and c10orf76 at low expression levels. Left: AKAP1-FRB-CFP is localized to the mitochondria before (top) and 5 minutes after rapamycin (100 nM) treatment (bottom). Middle: mRFP-FKBP12-PI4KB(S496A) at a low expression level is located at the Golgi before rapamycin (top) and translocates to the mitochondria after rapamycin induction (bottom). Right: eGFP-c10orf76 at a low expression level is located at the Golgi before rapamycin (top) and translocates to the mitochondria after rapamycin induction (bottom). (B) Mitochondria recruitment experiment with PI4KB(S496A) and c10orf76 at high expression levels (single cell zoom-in). Left: AKAP1-FRB-CFP is localized to the mitochondria before (top) and 5 minutes after rapamycin (100 nM) treatment (bottom). Middle: mRFP-FKBP12-PI4KB(S496A) at a high expression level saturates the Golgi and cytosol before rapamycin (top) and robustly translocates to the mitochondria after rapamycin induction (bottom). Right: eGFP-c10orf76 at a high expression level saturates the Golgi and cytosol before rapamycin (top) and robustly translocates to the mitochondria after rapamycin induction (bottom). Bars represent 10 μ m.

Table EV1. Full statistics on all hydrogen deuterium exchange experiments according to the guidelines from the International Conference on HDX-MS [68] (refers to Fig. 1).

Data Set	PI4KB	c10orf76	FLH409AAA c10orf76 mutant
HDX reaction details	%D ₂ O=87.4% pH _(read) = 7.5 Temp= 23°C	%D ₂ O=87.4% pH _(read) = 7.5 Temp= 23°C	%D ₂ O=90.5% pH _(read) = 7.5 Temp= 23°
HDX time course	3s at 1°C 3s, 30s, 300s at 23°C	3s at 1°C 3s, 30s, 300s at 23°C	3s, 300s at 23°C
HDX controls	N/A	N/A	N/A
Back-exchange	Corrected using a fully deuterated (FD) sample	Corrected based on %D ₂ O	Corrected based on %D ₂ O
Number of peptides	185	108	111
Sequence coverage	96.9%	73.9%	72.8%
Average peptide length/ redundancy	Length = 13.8 Redundancy = 3.2	Length = 12.1 Redundancy = 1.9	Length = 10.7 Redundancy = 1.7
Replicates	3	3	3
Repeatability	Average StDev = 1.2%	Average StDev = 0.6%	Average StDev = 1%
Significant differences in HDX	>7% and >0.5 Da and unpaired t-test <0.05	>7% and >0.5 Da and unpaired t-test <0.05	>7% and >0.5 Da and unpaired t-test <0.05

Movie EV1. Rapamycin recruitment of PI4KB to the Golgi, and subsequent recruitment of c10orf76 (refers to Figure 3).

Movie EV2. Rapamycin recruitment of mutant RL494EA PI4KB to the Golgi, with no recruitment of c10orf76 (refers to Figure 3).

CHAPTER 8

SUMMARY AND GENERAL DISCUSSION

SUMMARY

Enteroviruses include poliovirus (PV), rhinoviruses (RVs), coxsackieviruses (CVs), and numbered enteroviruses (EVs) that are causative agents of diverse diseases. Besides PV, which causes poliomyelitis, there are more than 280 serotypes of non-polio enteroviruses that can cause various mild and more severe diseases, especially in young children and immunocompromised individuals. Currently, approved antiviral drugs are only available against a few viruses [1]. Despite being one of the largest genera, there are no approved antivirals for treating infections caused by enteroviruses. To target the large variety of enteroviruses as well as to minimize the risk of PV circulation in the post-eradication era, there is a great need for (broad-acting) antivirals against enteroviruses.

Several direct-acting inhibitors have been developed, including capsid binders, which block virus entry, and inhibitors of viral enzymes required for genome replication. Capsid binders and protease inhibitors have been clinically evaluated but failed due to limited efficacy or toxicity issues. As an alternative approach, a function of essential host factors can be a promising target to treat a broad range of enteroviruses. Drug repurposing screens can be useful to uncover promising new inhibitors with disparate viral and host targets. In **chapter 2**, a detailed summary of antiviral drug development strategies against enterovirus infection as well as the drug development status as of 2016 is described.

The formation of replication organelles (ROs) is a universal feature that can be found in infected cells by any positive-strand RNA viruses including enteroviruses. ROs have a unique structure composed of different membrane lipids, and both viral proteins and host factors are required for the formation of ROs. For enteroviruses, viral protein 3A and the cellular lipid kinase phosphatidylinositol 4-kinase type III β (PI4KB), among other viral and cellular factors, have been suggested to be the key factors that drive this process. In the experimental chapters of this thesis, we provide mechanistic insights on the role of PI4KB and its interactors in enterovirus replication and RO formation.

Single amino acid substitutions in enterovirus 3A proteins were previously demonstrated to confer resistance to inhibitors of PI4KB and oxysterol binding protein (OSBP), which is a lipid transfer protein that controls cholesterol/PI4P exchange and that is essential for enterovirus replication. The exact escape mechanism, however, is not clearly understood.

Although enterovirus replication depends on PI4KB, its role, and that of its product PI4P, is only partially understood. In **chapter 3**, we employed a mutant coxsackievirus resistant to PI4KB inhibition (i.e., CVB3 3A-H57Y), and uncover that PI4KB activity has distinct functions in RO biogenesis and in proteolytic processing of viral polyprotein. Remarkably, under PI4KB inhibition the mutant virus could replicate its genome in the absence of ROs, using instead the intact Golgi apparatus. This impaired RO biogenesis provided an opportunity to investigate the proposed role of ROs in shielding enteroviral RNA from cellular sensors. Neither accelerated sensing of viral RNA nor enhanced innate immune responses were observed under these conditions. Altogether, these findings point out that enterovirus ROs are not absolutely required for genome replication and question their role as a physical barrier against innate immune sensors.

Growing evidence suggests that alterations in lipid homeostasis affect the proteolytic processing of the enterovirus polyprotein. In **chapters 3 and 4**, we studied the effect of PI4KB or OSBP inhibition on proteolytic processing of the CVB3 polyprotein during infection as well as in a replication-independent system. The escape mutation (3A-H57Y) rectified a proteolytic processing defect imposed by PI4KB or OSBP inhibition, pointing to a possible escape mechanism. Besides the 3A substitutions in CVB3,

another mutation was identified in each of the PI4KB inhibitor-resistant CVB3 pools, namely substitution N2D in 2C. In **chapter 4**, we show that 2C-N2D by itself did not confer any resistance to inhibitors of PI4KB and OSBP. However, the double mutant (i.e., 2C-N2D/3A-H57Y) showed better replication than the 3A-H57Y single mutant in the presence of inhibitors. We show that both PI4KB and OSBP inhibitors specifically affected the cleavage at the 3A-3B junction, and that mutation 3A-H57Y recovered impaired proteolytic processing at this junction. Although 2C-N2D enhanced replication of the 3A-H57Y single mutant, we did not detect additional effects of this substitution on polyprotein processing, which leaves the mechanism of how 2C-N2D contributes to the resistance to be revealed.

The enteroviral 3A protein recruits PI4KB to ROs, but the exact mechanism remained elusive. **Chapters 5 and 6** describe how viral 3A protein recruits PI4KB via another host factor, Acyl-coenzyme A binding domain containing 3 (ACBD3). In **chapter 5**, we investigated the role of ACBD3 in PI4KB recruitment to ROs during enterovirus infection using ACBD3 knockout cells. Replication of representative enteroviruses and rhinoviruses was all impaired in ACBD3 knockout cells and PI4KB recruitment by different enterovirus 3A proteins was not observed as well. In the absence of ACBD3, individually expressed 3A was found in the ER instead of the Golgi, indicating that ACBD3 is required for proper localization of 3A. Reconstitution of wild-type ACBD3 restored both PI4KB recruitment and 3A localization, while an ACBD3 mutant that cannot bind to PI4KB restored only 3A localization, but not virus replication. Consistently, reconstitution of a PI4KB mutant that cannot bind ACBD3 failed to restore virus replication in PI4KB knockout cells. By utilizing ACBD3 mutants lacking specific domains, we show that Acyl-coenzyme A binding (ACB) and charged amino acids region (CAR) domains are dispensable for 3A-mediated PI4KB recruitment and efficient enterovirus replication. Both the glutamine-rich region (Q) and the Golgi dynamics domain (GOLD) that are mediating interaction with PI4KB and 3A, respectively, are required for PI4KB recruitment and efficient enterovirus replication. Altogether, our data provide new insight into the central role of ACBD3 in recruiting PI4KB by enterovirus 3A and reveal the minimal domains of ACBD3 involved in recruiting PI4KB and supporting enterovirus replication.

In **chapter 6**, we determined the crystal structure of the ACBD3 GOLD domain together with 3A proteins from several enteroviruses (PV, EV-A71, EV-D68, and RV-B14) to gain a better understanding of structural determinants of ACBD3 recruitment to the viral replication sites. In addition to the characterization of multiple 3A:ACBD3 GOLD complex, we also provide evidence supporting the presence of ACBD3-3A heterotetramers, which is induced by 3A-3A interaction. A model of ACBD3 GOLD:3A complex on the lipid bilayer was generated to understand how the complex and membranes would interact. By utilizing mutants of 3A or ACBD3 that are generated based on structural information, we identified the critical binding interface mediating 3A-ACBD3 interaction as well as 3A-3A dimerization and ACBD3-membrane interaction. Superposition of the crystal structures of the enterovirus 3A:GOLD complexes and previously identified kobuvirus 3A:GOLD complexes revealed that the enterovirus and kobuvirus 3A proteins bind to the same regions of the ACBD3 GOLD domain. In a nutshell, we uncovered a striking convergence in the mechanisms of how distinct picornaviruses recruit ACBD3 and its downstream effectors to the replication sites.

Protein c10orf76, a PI4KB-interacting protein that is poorly characterized, has been identified as a host factor required for coxsackievirus A10 (CVA10). In **chapter 7**, we aimed to identify the function of c10orf76 in uninfected cells as well as its possible role in enterovirus replication. We used hydrogen-deuterium exchange mass spectrometry to characterize the c10orf76-PI4KB complex and revealed that

CHAPTER 8

binding is mediated by the kinase linker of PI4KB. Complex-disrupting mutations demonstrated that PI4KB is required for the recruitment of c10orf76 to the Golgi, while c10orf76 did not affect the localization of PI4KB. An intact c10orf76-PI4KB complex is required for the replication of c10orf76-dependent enteroviruses, CVA10 and poliovirus. Intriguingly, c10orf76 also contributed to the localization of GBF1 to the Golgi and subsequent activation of Arf1 at the Golgi. These findings provide a putative mechanism for the c10orf76-dependent increase in PI4P levels at the Golgi and at the virus replication sites.

DISCUSSION

Phosphatidylinositol 4-phosphate (PI4P)-enriched replication organelles (ROs) have been observed in cells infected with several (+)RNA viruses including enteroviruses, cardioviruses, kobuviruses (*Picornaviridae*), and hepatitis C viruses (HCV; *Flaviviridae*) [2-4]. Enteroviruses and kobuviruses depend on the Golgi-resident phosphatidylinositol 4-kinase type III β (PI4KB) to induce PI4P production at ROs, while cardioviruses and HCV require the ER-resident PI4KA. Subsequently, the importance of PI4KB in virus replication and its potential as an antiviral target have been studied over the past 10 years (summarized in **chapter 2**). This discussion consists of 3 parts. First, we will focus on the mechanism behind the recruitment and the activation of PI4KB at enterovirus replication sites. The second part will cover the roles of cellular lipids including PI4P in enterovirus replication and RO formation. Different functions of enterovirus ROs are addressed in the last part.

I. Mechanism of PI4KB recruitment and its activation at enterovirus replication sites

Conserved role of ACBD3 in the recruitment of PI4KB to picornavirus replication sites

Several lines of evidence supported the importance of PI4KB in the formation of replication organelles (ROs) of at least two different picornavirus genera. Kobuviruses recruit PI4KB to the replication sites through acyl-CoA binding domain containing 3 (ACBD3) which directly interacts with viral protein 3A [3, 5]. ACBD3 is a Golgi-resident, multifunctional protein that is also well-known to recruit PI4KB to the Golgi [3, 6, 7]. Upon kobuvirus infection, viral protein 3A recruits PI4KB via 3A-ACBD3-PI4KB interaction which could promote PI4P synthesis and eventually the formation of ROs [3, 5, 7-9]. A recently solved crystal structure of the kobuvirus 3A:ACBD3 GOLD complex substantiated how this interaction occurs [8, 9].

Several enterovirus 3A proteins have been shown to directly bind to ACBD3 [7, 10]. Despite the direct interaction between ACBD3 and enterovirus 3A proteins [7, 10], there had not yet been a consensus about the importance of ACBD3 for enterovirus replication and PI4KB recruitment. Several studies have investigated whether enteroviruses depend on ACBD3 to recruit PI4KB. While silencing of ACBD3 inhibited PV replication in one study [7], another reported no inhibition of PV replication upon ACBD3-knockdown [11]. Similar to this, neither inhibition of CVB3 or RV replication nor effects on PI4KB recruitment were observed in ACBD3-silenced cells [10, 12]. The discrepancy in the role of ACBD3 from one study to others likely resulted from insufficient suppression of ACBD3 function by RNA interference. When ACBD3 was completely depleted by gene knockout, we (**chapter 5 and 6**) and others [13-15] eventually could demonstrate the functional significance of ACBD3 in enterovirus replication. In **chapter 5**, we demonstrated that ACBD3 is an essential host factor for enteroviruses and the mediator of PI4KB recruitment. Replication of different human enterovirus species (EV-A/B/C/D) and rhinovirus species (RV-A/B) was dependent on ACBD3 as it was severely impaired in ACBD3 knockout cells. Neither virus infection nor the expression of enterovirus 3A alone elicited PI4KB recruitment in the absence of ACBD3.

Four domains are recognized in ACBD3: the acyl-CoA binding (ACB) domain, the charged amino acids region (CAR), the glutamine-rich region (Q), and the Golgi dynamics domain (GOLD) (Figure 1A). The ACB domain, which is relatively conserved among all known ACBD proteins (ACBD1-7), is suggested to have a similar electrostatic surface potential which can mediate binding to long-chain acyl-CoA such as palmitoyl-CoA [16]. ACB domain of ACBD3 is also shown to directly bind to sterol regulatory element

binding protein 1 (SREBP1), and this interaction is important for regulating *de novo* palmitate synthesis [17]. The CAR domain contains a nuclear localization signal [18], yet the function of the CAR domain is unknown. The Q domain interacts with the N-terminal helix of PI4KB [6]. The GOLD domain interacts with Giantin, and by doing so, tethers ACBD3 to the Golgi membrane [18]. Enterovirus and Kobuvirus 3A proteins bind to the GOLD domain, most probably at the same site as Giantin [3, 10]. ACBD3 mutants containing only Q and GOLD domains were sufficient to support enterovirus replication (**chapter 5**) indicating that the interaction between ACBD3 and PI4KB is crucial for enterovirus replication. ACB and CAR domains seem to be nonessential for enterovirus replication suggesting that the functions of the ACB and CAR domains, as well as the cellular proteins and/or lipids that interact with these domains, are unlikely required for enterovirus replication. One thing to be noted is that all these findings were made in HeLa cells, therefore, the importance of the ACB domain in regulating lipids could only be observed in cells exhibiting many lipid droplets and more active lipid metabolism, such as hepatocytes [19].

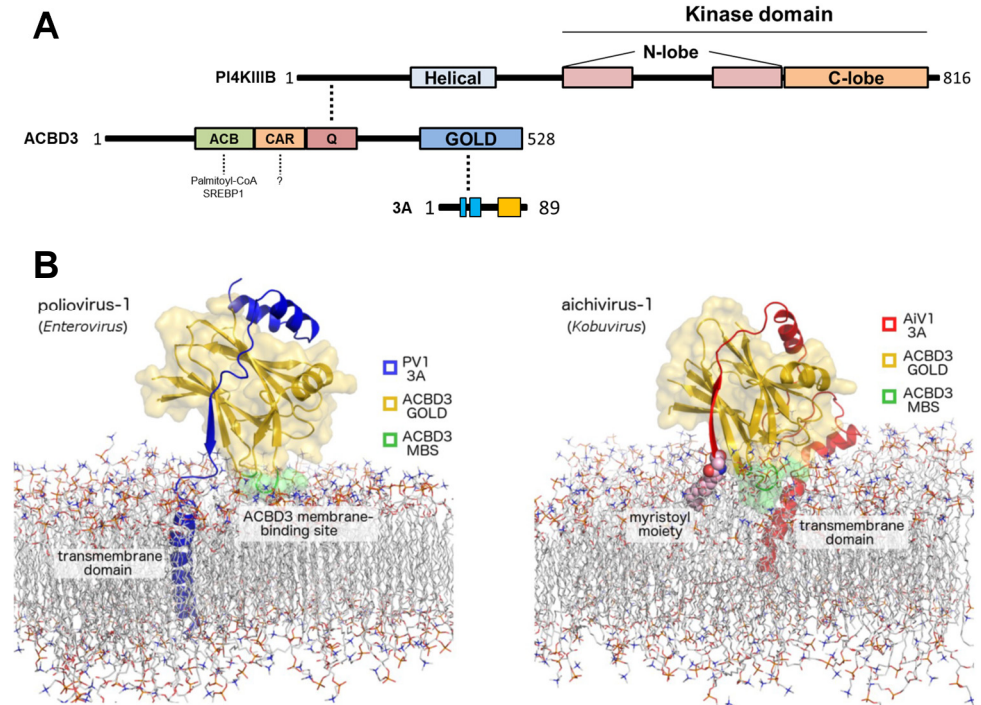


Figure 1. Schematic representation of enterovirus 3A – ACBD3 – PI4KB interaction domains and models of ACBD3 GOLD domain together with viral 3A proteins. (A) Domains of PI4KB, ACBD3, and enterovirus 3A with their known interactors. ACB, acyl-CoA binding; CAR, charged amino acids region; Q, glutamine-rich region; GOLD, Golgi dynamics domain. **(B)** Molecular dynamics simulation-based models of the ACBD3 GOLD domain in complex with the poliovirus (left) and aichivirus (right) 3A proteins on the lipid bilayer (adapted from chapter 6). MBS, membrane binding sites.

Besides its role as a mediator of PI4KB recruitment, we also discovered that ACBD3 has a profound effect on enterovirus 3A protein localization. When it is solely expressed, 3A was found almost exclusively at the ER in ACBD3 knockout cells, whereas in wild-type cells it showed a punctate localization mostly on Golgi-derived membranes (**chapter 5**). This phenotype was restored when 3A

and wild-type ACBD3 were co-expressed in the knockout cells. This suggests that ACBD3 possibly plays a role as a scaffold positioning 3A near other ACBD3-interacting proteins such as PI4KB. This role of ACBD3 still needs to be validated in the infection condition. Since the replication of wild-type CVB3 is significantly inhibited in ACBD3 knockout cells, a replication-independent system, where viral proteins are expressed independently from viral RNA (vRNA) replication, can be a valuable tool to investigate this further. Another useful tool will be the CVB3 3A-H57Y mutant virus, which is resistant to PI4KB inhibition and thereby less dependent on ACBD3 (**chapter 5**).

ACBD3 could play a role in exploiting Golgi membranes by assisting 3A targeting of Golgi. The Golgi apparatus, where ACBD3 intrinsically resides, has been suggested as one of the key membrane donors to ROs [2, 20-22], and the disintegration of Golgi and RO formation were often found to take place sequentially [23, 24]. In **chapter 3**, by utilizing CVB3 3A-H57Y mutant virus upon PI4KB inhibition, we demonstrated that virus replication can instead occur at the intact Golgi in the absence of ROs. With recently developed whole-cell electron microscopy, enterovirus RO formation was revealed to originate from the ER followed by exploiting Golgi membranes [25]. Based on collected evidence, RO formation could be directed to Golgi via 3A-ACBD3 interaction. Whether RO biogenesis absolutely requires ER membranes in the absence of ACBD3 or whether enteroviruses could flexibly utilize different cellular organelles needs further investigation.

The interaction between the viral 3A protein and ACBD3 is also found in other picornaviruses belonging to other genera such as *Kobuvirus*, *Hepatovirus*, *Salivirus*, and *Parechovirus*, but not *Cardiovirus* and *Aphthovirus* [26]. The crystal structure of kobuvirus 3A in complex with the ACBD3 GOLD domain was revealed recently [8, 9]. Kobuvirus 3A wraps around ACBD3 and stabilizes ACBD3 on membranes through its membrane-binding features at the myristoylated N-terminal and hydrophobic C-terminal ends. However, enterovirus 3A differs greatly in sequence from kobuvirus 3A, and also does not have the myristoylated N-terminal end. Enterovirus 3A can only bind to membranes via its hydrophobic C-terminal end, which suggested that enterovirus 3A interacts with ACBD3 differently.

To better understand how exactly enterovirus 3A protein interacts with ACBD3, we sought to reveal the crystal structure of the enterovirus 3A:ACBD3 GOLD complex (**chapter 6**; Figure 1B). Structures of ACBD3 GOLD together with 3A proteins from four representative enteroviruses were successfully solved. Superposition of the crystal structures of the enterovirus 3A:ACBD3 complexes and the previously known structures of kobuvirus 3A:ACBD3 GOLD complexes [6] revealed that the enterovirus and kobuvirus 3A proteins bind to the same regions of the ACBD3 GOLD domain but in the opposite orientation. The different orientation of enterovirus 3A may be required for proper interaction with other 3A interactors, such as GBF1. Altogether, we uncovered a striking convergence in the mechanisms of how the two distinct groups of picornaviruses recruit ACBD3 and its downstream effectors (i.e., PI4KB) to replication sites.

ACBD3 itself does not contain a membrane-anchoring domain but it inheres membrane binding sites (MBS) consisting of several hydrophobic residues that ensure stable connection to membranes. Disrupting the MBS led to delocalization of ACBD3 from the Golgi, but it was stabilized back to membranes when 3A was co-expressed. This finding seems to contradict the suggested role of ACBD3 as a scaffold directing proper localization of 3A which has been discussed above. However, the interaction with ACBD3 might induce the conformational change of 3A in a way that aids membrane targeting of 3A thereby bringing 3A and 3A-ACBD3 complex to membranes. Whether Golgi membranes

are still targeted by 3A during infection in the presence of an MBS disrupted-ACBD3 mutant requires further investigation.

Its property as a pan-enterovirus host factor makes ACBD3 as a potential target for antiviral drug development. As recently shown in a CVB3 animal model, the lack of ACBD3 in the pancreas effectively suppressed virus replication [27]. This study not only demonstrates the importance of ACBD3 in enterovirus infection *in vivo* but also indicates that targeting ACBD3 or ACBD3-3A interaction can be an effective way to treat enterovirus and kobuvirus infection.

Mechanism of PI4KB activation at ROs

We have shown that picornaviruses that are dependent on PI4KB adopt a shared mechanism to recruit this kinase to the replication sites, namely via 3A-ACBD3-PI4KB interaction. Whether this interaction also suffices for the activation of PI4KB is questionable. PI4KB is a cytosolic lipid kinase that must be recruited to membranes to exert its function and to generate a PI4P-enriched environment. In an *in vitro* setting, PI4KB recruitment by ACBD3 to membranes enhanced its enzymatic activity [6]. However, it is likely that more factors are involved in the activation of PI4KB in enterovirus-infected cells as the expression of 3A alone could not lead to the enrichment of PI4P (**chapter 6** and [28]).

The small GTPase Arf1 is suggested to be involved in PI4KB recruitment to Golgi membranes and its consequent activation in non-infected cells [29], yet no direct interaction between Arf1 and PI4KB has been established. Arf1 belongs to the Arf (ADP-ribosylation factor) family of G proteins, which includes six Arfs and more than 20 Arf-like proteins that regulate vesicle trafficking, organelle structure, and cellular signaling (reviewed in [30, 31]). The activity of Arfs is regulated through a cycle of GTP binding and GTP hydrolysis mediated by Arf guanine exchange factors (GEFs) (e.g., GBF1, BIG1, BIG2) and GTPase-activating proteins (GAPs), respectively. In Figure 2A, the subcellular localization of Arfs and their GEFs that are relevant to this chapter are depicted.

Whether Arf1 is also responsible for the activation of PI4KB at enterovirus ROs is not clearly understood and the mechanism of how Arf1 itself is recruited to the RO membranes also remains to be clarified. Recruitment of Arfs to membranes was previously shown to be induced by enterovirus 3A as well as 3CD [32]. When RNAs coding 3A or 3CD were translated in HeLa cell extracts, it was found that more Arfs are associated with membranes. Translocation of Arfs to membranes was prevented by the large ArfGEF inhibitor, Brefeldin A (BFA) which indicates that this is mediated by Arf GEFs. As 3A directly interacts with one Arf GEF, GBF1 [33-38], initially it was believed that 3A-GBF1-Arf1 pathway is responsible for PI4KB activation. However, we (**chapter 6**) and others [28] showed that the expression of 3A alone is not sufficient for the activation of PI4KB, which rebuts the role of 3A-GBF1-Arf1 pathway in PI4KB activation at least in the setting where 3A is expressed alone.

Accumulating evidence is supporting the role of 3CD in the activation of PI4KB and subsequent PI4P production upon enterovirus replication. 3CD and 3A exploit different mechanisms to induce targeting of Arfs to membranes. As mentioned above, 3A induces this via GBF1, while 3CD-dependent Arf activation appears to rely on two other GEFs, BIG1 and BIG2 [32, 39]. It is unknown if 3CD can directly interact with BIG1/2. Unlike 3A, which contains a membrane-binding domain at its C-terminus, 3CD does not have any intrinsic membrane-binding property. Therefore, how 3CD mediates Arf1 activation on membranes is still obscure. Nevertheless, the importance of a 3CD-dependent PI4KB activation pathway was confirmed in cells expressing 3CD alone, where Arf1 activation and consequent accumulation of PI4P were observed [28].

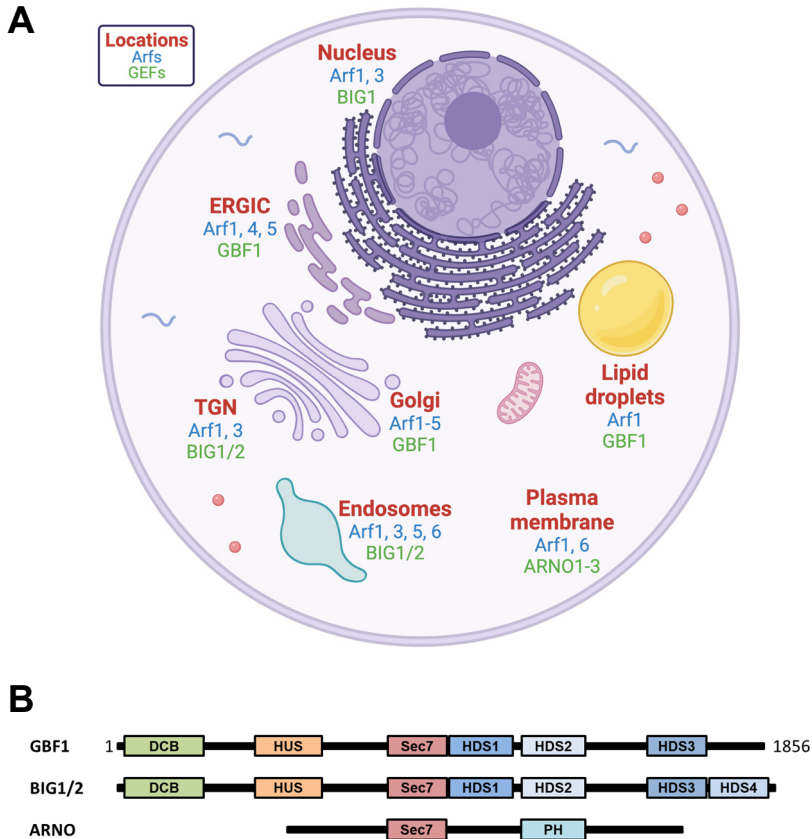


Figure 2. Subcellular localization of Arf GTPases and Arf GEFs that are relevant to this chapter and domain organization of Arf GEFs. (A) More detailed information for these localizations is provided in [30, 31]. ERGIC, ER-Golgi intermediate compartment; GEFs, guanine nucleotide exchange factors; TGN, *trans*-Golgi network. Created with BioRender.com. (B) A schematic representation of Arf GEFs. Protein length are not drawn to scale. DCB, dimerization and cyclophilin binding; HDS(1-4), homology downstream of Sec7; HUS, homology upstream of Sec7; PH, pleckstrin homology.

One issue with this mechanism is that it contradicts previous findings where BIG1 and BIG2 were shown to be not required by enteroviruses when GBF1 remained functional [40]. In Madin-Darby canine kidney (MDCK) cells, GBF1 contains a naturally occurring mutation in its catalytic Sec7 domain (i.e., M832L) which confers resistance to BFA. Therefore, BFA inhibits the function of BIG1 and BIG2 in MDCK cells, while GBF1 remains unaffected. RNA replication of CVB3 was insensitive to BFA in MDCK cells, and a similar observation was made for PV in a Vero-derived cell line (BER-40) expressing another BFA-resistant GBF1 mutant (i.e., A795E) [33]. These findings question the importance of BIG1 and BIG2 in enterovirus replication as well as the importance of the 3CD-dependent PI4KB activation pathway which is presumably mediated by BIG1 and BIG2.

One possible scenario is that another GEF might be able to substitute the other and mediate Arf activation. For instance, GBF1 constructs containing the Sec7 domain of another ArfGEF, ARNO, which is responsible for the activation of Arf on the plasma membrane, were fully functional in poliovirus replication [41]. This suggests that Arf activation at the ROs may be mediated by other ArfGEFs rather than exclusively by one specific GEF. Although 3CD preferentially targets BIG1 and BIG2 under normal

conditions, it might be that a BFA-resistant GBF1 replaces their functions in the presence of BFA. One way to confirm this will be expressing 3CD alone in the presence of BFA in either MDCK or BER-40 cell lines and looking for GBF1 and Arf recruitment to membranes as well as subsequent PI4P accumulation.

Importance of the 3A-GBF1 interaction?

Whether the 3A-GBF1 interaction is crucial for PI4KB activation and enterovirus replication remains ambiguous. Mutations in 3A that abolish the interaction with GBF1 have relatively small effects on genome replication of PV and CVB3 [33, 36, 38, 40]. Furthermore, rhinoviruses which also rely on high levels of PI4P produced by PI4KB [42], recruit GBF1 to their ROs, despite that their 3A proteins have little or no interaction with GBF1 [12, 37]. These studies suggested the existence of a redundant mechanism in GBF1 recruitment by enterovirus. This possibility was recently further investigated in more details in poliovirus replication by utilizing the large ArfGEF inhibitor, Brefeldin A (BFA) [41]. Replication of a virus with a mutation in 3A that disrupts its interaction with GBF1 was (partially) rescued by a full-length BFA-resistant GBF1 but not by a version lacking its C-terminal part (i.e., GBF1/1-1060) against BFA. Similarly, the full-length BFA-resistant GBF1, but not C-terminus deleted GBF1, restored replication of RV-A2 and RV-B14 in the presence of BFA [12]. Altogether, this indicates that the C-terminal part of GBF1 can partially compensate for the defects in 3A-GBF1 interaction and may also be able to mediate the recruitment of GBF1 to ROs as well as subsequent Arf1 activation in 3A-independent manner. Recently, c10orf76, an interactor of PI4KB, was found to directly bind to the C-terminal part of GBF1 [43], and the potential role of c10orf76 in PI4KB activation and enterovirus replication is discussed in the following section.

What is the role of c10orf76?

The recent identification of protein c10orf76 as a host factor for some enteroviruses adds another layer of complexity in understanding the mechanism of PI4KB activation. c10orf76 was identified as a putative PI4KB-interacting partner [17,27], but still not much is known about this protein including its function, structure, and localization. The knockout of c10orf76 led to decreased Golgi PI4P levels (**chapter 7** and [28]), indicating a role in regulating PI4P level at the Golgi. In **chapter 7**, we showed that c10orf76 is recruited to the Golgi by interacting with PI4KB, while the localization of PI4KB at the Golgi was not dependent on c10orf76. We also observed a more diffuse GBF1 pattern with reduced localization at the Golgi in c10orf76 knockout cells. As a result of mislocalization of GBF1 in c10orf76 knockout cells, there was more diffuse staining outside of the Golgi for the coatomer components COP- β or COP- α/γ , whose membrane interaction relies on active Arf1, indicating that the activation of Arf1 was affected in the knockout cells. In accordance with that, c10orf76 was recently found to have a direct interaction with the C-terminal part of GBF1 and to regulate GBF1 recruitment to the Golgi [43]. Clearly, whether and how c10orf76 plays a role in the recruitment of GBF1 to ROs and the subsequent activation of PI4KB needs further investigation.

It is important to emphasize that the c10orf76-dependent pathway is unlikely to be the sole mechanism of PI4KB activation, as not all enteroviruses are dependent on c10orf76 for their replication. For example, the replication of CVB1 [44] and CVB3 (**chapter 7**) was not impaired in c10orf76 knockout cells. However, the replication of CVA10 was significantly impaired in c10orf76 knockout cells, and the replication could be rescued by expression of wild-type PI4KB in PI4KB knockout cells, but not by expression of the PI4KB RL494EA mutant that is deficient in binding c10orf76, implying that the

c10orf76-PI4KB interaction is necessary for CVA10 replication. In another study, c10orf76 was identified as a pro-viral factor for poliovirus replication [45] and poliovirus replication was inhibited in c10orf76 KO cells, albeit to a lesser extent than CVA10 (**chapter 7**). Poliovirus replication was partially rescued in PI4KB knockout cells when PI4KB RL494EA mutant was expressed which suggests that c10orf76-PI4KB interaction is required for poliovirus replication at least to a certain extent.

Why the c10orf76-PI4KB interaction is required for replication of some enteroviruses, but not others, is a puzzling question. Whether c10orf76 is involved in the recruitment of GBF1 when there is a defect in 3A-GBF1 interaction needs to be determined. However, this is unlikely to be the case since replication of rhinoviruses in c10orf76 knockout cells was not hindered (Lyoo et al., unpublished data). Moreover, we did not observe impaired interaction of CVA10 3A with GBF1 in a mammalian two-hybrid system (Lyoo et al., unpublished data). Taken together, the role of c10orf76 in enterovirus replication remains uncertain and would need to be further evaluated.

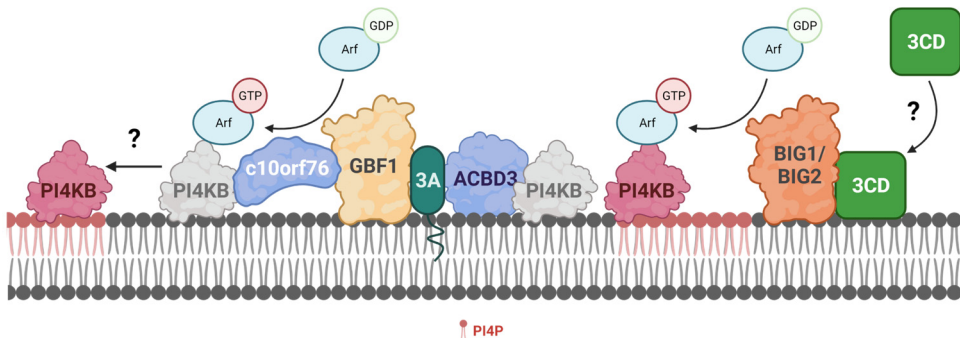


Figure 3. A model of PI4KB activation in enterovirus-infected cells. Created with BioRender.com.

Involvement of Arf isoforms

Among the six Arf isoforms (Arf1-6), Arf2 is lost in primates. Arfs are divided into three classes based on their structures: Arf1 and 3 (class 1); Arf4 and 5 (class 2); Arf6 (class 3) [46]. As indicated in Figure 2A, Arf1-5 and GBF1 localize predominantly at the ERGIC and the Golgi, while Arf6 is mainly found at the plasma membrane. Previously, the depletion of one or more Arfs by knockdown or knockout was shown not to significantly affect enterovirus replication [10, 40, 47] which questioned the importance of Arfs in supporting enterovirus replication.

However, by utilizing cell lines stably expressing individual Arfs fused to fluorescent proteins, a recent study revived the potential significance of Arfs for enterovirus replication [48]. Arf1 was the first one to be recruited to the replication sites early in infection (i.e., 3 hpi), followed by sequential recruitment of all other Arfs including Arf6. The translocation of Arf6 in infected cells was rather surprising considering that it localizes almost exclusively at plasma membrane and is not activated by GBF1 in noninfected cells. Whether this is driven by its known GEF, ARNO or by other GEFs (GBF1 or BIG/2) is unclear.

While viral protein 2B strongly colocalized with Arfs, other viral proteins such as 2C, 3A, and 3D showed less colocalization with Arfs especially at the early stages of infection. Double-stranded RNA was separated from Arf-enriched membranes suggesting that these Arf-enriched ROs might not be the sites

for active genome replication. Altogether, these observations support a complex mechanism of Arf activation in enterovirus-infected cells involving multiple viral proteins, Arfs and ArfGEFs. Dissecting the detailed molecular mechanisms of PI4KB activation by different Arfs will be a challenging task but monitoring the increase of PI4P together with the recruitment of specific Arfs throughout the course of infection can be a good starting point. In addition, by following Arfs translocation and PI4P induction after individual expression of either 3A or 3CD, we might be able to understand the detailed mechanism of PI4KB activation during enterovirus replication.

II. Role of lipids in enterovirus replication

The lipid composition of cellular membranes is tightly regulated to maintain the homeostasis and the integrity of organelles. (+)RNA viruses rely heavily on membranes throughout their replication cycle from entry to progeny virus production. Naturally, many viruses have evolved to hijack cellular proteins that are involved in lipid metabolism such as lipid kinases (reviewed in [49]). Among diverse lipid species, several phospholipids and sterols have been identified to be crucial for efficient virus replication.

PI4P and cholesterol: two key players

Phosphatidylinositol 4-phosphate (PI4P)-enriched replication organelles (ROs) are induced by diverse viruses including enteroviruses, cardioviruses, and kobuviruses (*Picornaviridae*), hepatitis C viruses (HCV; *Flaviviridae*) [2-4], and tomato bushy stunt virus (*Tombusviridae*) [50, 51]. These viruses recruit phosphatidylinositol 4-kinases (PI4Ks) to replication sites to increase local PI4P levels [2-4, 52]. Remarkably, recently also some (-)RNA viruses, i.e., human parainfluenza virus and human respiratory syncytial virus (*Paramyxoviridae*), were found to induce PI4P-enriched inclusion bodies to promote virus replication [53].

PI4P has diverse functions in cells. One of them is to mediate cholesterol exchange at the ER-Golgi interface. PI4P recruits oxysterol binding protein (OSBP) to facilitate local cholesterol exchange [4, 54, 55] via newly created membrane contact sites (MCSs) between ER and Golgi [56]. This function of PI4P is often exploited by several viruses that utilize PI4P-enriched membranes [4, 42, 56-59] to create a novel MCS between ER and ROs, resulting in increased cholesterol levels in RO membranes [60]. As a negatively charged lipid, PI4P has been suggested to play a role in recruiting other viral proteins such as the viral polymerase 3D [2, 61] to promote efficient RNA replication on RO membranes, but firm evidence for this is lacking. In this thesis, we propose two other functions of PI4P and cholesterol during enterovirus replication, which are described in the following paragraphs.

Role in viral polyprotein processing

Previously, alterations in lipid homeostasis were shown to affect the proteolytic processing of the poliovirus (PV) polyprotein [60, 62, 63]. Upon PI4KB inhibition, accumulation of P2P3 and 3D, as well as a decrease of 2C and 3CD were observed [63]. In another study, 3AB accumulation was found in PV-infected cells in the presence of a PI4KB inhibitor, while other proteins were unaffected [57]. In **chapters 3 and 4**, we argue a role for PI4P and cholesterol as regulators of viral polyprotein processing in coxsackievirus infection. The production of 3A protein from its precursor 3AB was prominently perturbed by both PI4KB inhibition and OSBP inhibition independently, indicating a defect in proteolytic processing at the 3A-3B junction. This could be rectified by a single point amino acid substitution in 3A

which conferred resistance to both PI4KB and OSBP inhibitors. It is not clear how the single amino acid substitutions in 3A protein can rescue the inefficient cleavage at the 3A-3B junction, but one possible explanation could be that this substitution alters the orientation of viral protein 3A in PI4P/cholesterol depleted membranes, resulting in a better exposure and accessibility of the 3A-3B cleavage site to 3C(D) protease, which cleaves 3AB (Figure 4). Indeed, PI4KB resistant mutations in both poliovirus (A70T) and CVB3 (H57Y) lie within or proximal to the hydrophobic domain of the 3A protein [64, 65].

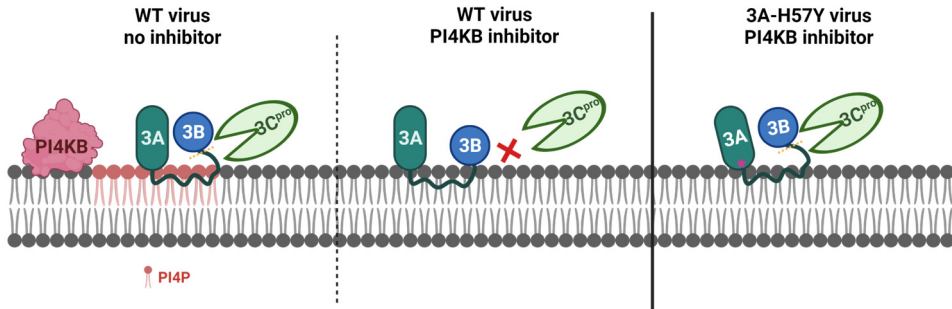


Figure 4. A schematic model for a role of PI4P in viral polyprotein processing. Created with BioRender.com.

Yet, it is unclear that whether PI4P and cholesterol together or either one alone is required for a proper cleavage event at the 3A-3B. PI4KB inhibitors limit PI4P accumulation and thus limit OSBP-mediated cholesterol transfer. OSBP inhibitors do not directly affect PI4P synthesis but influence its distribution [66, 67] and thereby may alter the level of PI4P at the membranes. Low cholesterol levels in membranes caused directly by OSW-1 and indirectly by PI4KB inhibitors could affect proteolytic processing of the viral polyprotein. Previously, depletion of free cholesterol or chemical disruption of cholesterol organization within membranes stimulated processing at the 3C-3D junction in PV-infected cells [60]. This was not observed upon OSBP inhibition by OSW-1 (**chapter 4**) either in CVB3-infected cells or in CVB3 replication-independent system. This suggests that the role of cholesterol in polyprotein processing can differ depending on which stage of the regulatory pathway of cholesterol homeostasis is affected.

It was speculated that 3AB is processed to 3A and 3B (VPg) only after a tyrosine residue in the 3B region of 3AB or its other precursors has been uridylylated [68] by 3C(D) (uridylylation process of VPg is reviewed in [69]). It is unlikely that PI4P or cholesterol (in fact any cellular lipids) would be directly required for VPg uridylylation as *in vitro* uridylylation has been successfully demonstrated in the presence of 3C(D) and VPg substrates alone [70, 71]. Still, PI4P- and cholesterol-enriched membranes might contribute to this process for example by recruiting 3C(D) or by contributing to a conformational shift in viral polyprotein resulting in efficient uridylylation of VPg and following proteolytic cleavage at the 3A-3B junction.

Role in the expansion of ROs

In **chapter 3**, we made number of observations with the CVB3 3A-H57Y mutant, which is resistant to PI4KB inhibition, that argue for a role of PI4P in the expansion of ROs rather than in the initiation of RO formation. Under PI4KB inhibition, RO formation was not abolished but delayed to beyond the

exponential RNA synthesis phase. RO structures lacking PI4P-enriched membranes were still morphologically akin to ROs in the absence of PI4KB inhibitors. This suggests that PI4P may not have an intrinsic structural role for RO formation and high PI4P levels are not strictly required for the formation of ROs but may accelerate the process. The dispensable role of PI4P in the formation of ROs is supported by the findings from another PI4P-dependent virus, encephalomyocarditis virus (EMCV; *Cardiovirus* genus), which usurps another PI4 kinase (PI4KA) to accumulate PI4P lipids at its ROs [72]. The ROs of PI4KA inhibitor-resistant mutant (EMCV 3A-A32V) were formed at a similar time point as the uninhibited wild-type virus, even in the presence of a PI4KA inhibitor.

It is plausible that the cholesterol that is recruited via the PI4P-OSBP-cholesterol pathway directs the development of ROs, as cholesterol in uninfected cells can induce morphological changes in cellular membranes [73-75]. Cholesterol can be supplied to replication sites also via other routes, for instance via endosomal transfer [57, 60] or from lipid droplets (LDs) [42]. Whether the cholesterol supply via these alternative routes is involved in the formation of ROs when PI4P levels are suppressed, requires further investigation.

Lipid droplets as the source of lipid supply and an emerging role of phosphatidylcholine

The origin of enterovirus ROs remains unclear. Both ER and Golgi, where the early vRNA synthesis was observed, have been suggested to serve as donors of membranes and membrane-regulating host factors for enteroviral ROs [76]. In **chapter 3**, enterovirus RNA synthesis was shown to occur at a morphologically intact Golgi in the absence of ROs also supporting the idea of Golgi membranes contributing to RO biogenesis. RO formation often coincided with the Golgi disassembly in infected cells, which have pointed transformation of Golgi membranes into ROs [2, 3, 7, 11, 12, 35-37, 40, 42, 77-80]. Growing evidence also suggests inputs from ER membranes and the hijacked autophagic pathway [81-92].

Clearly a tremendous amount of lipids is needed as building blocks. Lipid droplets (LDs) are one of the most lipid-rich cellular organelles. LDs serve as a reservoir for esterified, nonpolar lipids such as triacylglycerols (TAGs) and sterol ester (e.g., cholesterol). Besides its role as lipid storage, LDs also play diverse roles in cells by interacting with other cellular organelles via membrane contact sites (MCSs) (reviewed in [93]). Upon infection, the induction of new MCSs between LDs and ROs was observed in HCV-infected [94, 95] and Dengue-infected cells [96-98]. LDs were also found near enterovirus replication sites [25, 42, 99] supporting the notion of LDs as the supplier of lipid building blocks to ROs. Yet, how these new MCSs are formed remains a question. Recent findings advocate the involvement of viral proteins 2B, 2C, 2BC, and 3A in the process [99]. Both 2B and 2C, as well as their precursor 2BC, can target LDs via their amphipathic helix domains, and the self-oligomerization property of 2C may be able to induce clustering of LDs. Direct interactions and functional linkages between 3A and 2C were previously shown [100, 101], implying that interaction between RO-localizing 3A and LD-localizing 2C (or 2BC) could drive the formation of MCSs between LDs and ROs. Furthermore, 3A was shown to directly interact with LD-associated lipases, ATGL and HSL *in vitro* [99], which hints that 3A could maintain the close contacts between ROs and LDs. GBF1, a direct interactor of 3A, also directly interacts with ATGL, and the GBF1-Arf1-COPI machinery is shown to be involved in recruiting ATGL and adipophilin (ADRP) to LDs [102, 103]. Whether 3A directly or via GBF1 drives the interaction between ROs and LDs or that 2B, 2C, or 2BC are involved in the formation of this new MCS requires further investigation.

While the mechanism that underlies the role of PI4P and cholesterol in RO formation remains unclear, there is growing evidence for the involvement of other lipids such as phosphatidylcholine (PC) [104]. A significantly increased level of PC was found as a conserved feature among several (+)RNA viruses, namely brome mosaic virus, HCV, and poliovirus [105]. Various picornaviruses including poliovirus induce fatty acid uptake and PC synthesis [106-109]. Poliovirus 2A^{pro} protein was previously shown to mediate PC synthesis via activating long-chain acyl-CoA synthetase 3 (Acsl3), independently of its protease activity [110]. More recently, another enzyme called CCT α was identified as a key modulator of PC synthesis for the expansion of poliovirus ROs [111]. CCT α is a rate-limiting enzyme for PC production in mammalian cells [112]. CCT α contains nuclear localization signals but traffics to the cytosol through nuclear pore complex (NPC) to exert its enzymatic function. Massive translocation of CCT α to replication sites was observed upon poliovirus infection and this process required protease activity of 2A^{pro} [111].

Amongst known targets of 2A^{pro}, several NPC proteins are known to be cleaved resulting in a nucleocytoplasmic trafficking disorder (NCTD) (reviewed in [113, 114]). Viral subversion of nucleocytoplasmic trafficking is not limited to enteroviruses but is triggered by several viruses, including cardiovirus, coronavirus, and flavivirus [115-123]. The benefits of nucleocytoplasmic trafficking disorder to virus replication are not evident, but it is mainly suggested as a part of the innate immunity evasion mechanism. For instance, degradation of nucleoporins by poliovirus and rhinovirus 2A blocks nuclear import of proteins with nuclear localization signal (NLS) via Kap α / β 1 and Kap β 2 pathway [124] and may interfere with nuclear import of cellular proteins such as phosphorylated STAT1, which can activate the transcription of interferon-stimulated genes (ISGs). Inhibition of nuclear import also may result in the accumulation of many RNA-binding and RNA-chaperone proteins (e.g., PCBP2, La protein, PTBP1) in the cytoplasm, which otherwise mainly reside in the nucleus, that are required for facilitating translation of viral RNA. Together with the abovementioned nuclear-resident RNA-binding proteins, CCT α may also be relocated to the cytosol in a similar manner to promote RO formation and efficient virus replication.

III. Understanding the functional role of enterovirus ROs

As discussed above, the formation process of ROs is quite dynamic and complex involving miscellaneous hijacked host factors. Although the structure and the composition of ROs can differ among viruses, the morphology of ROs can be divided into two types: invagination type and protrusion type [125, 126]. In the invagination-type ROs that are induced by flaviviruses and tombusviruses (reviewed in [127]), vRNA replication takes place inside spherules (formed by invagination of membranes) which also serve as a physical barrier protecting vRNAs. The inner part of the spherules is connected to the cytosol through a narrow pore that allows the exchange of small molecules such as nucleotides or newly synthesized RNAs, but not the passage of cellular RNA sensors [128, 129] (see below for more details).

Double-membrane vesicles (DMVs) are the hallmark structures found in many protrusion-type ROs, but DMV biogenesis can occur through different pathways. For enteroviruses as well as norovirus and hepatitis C virus (HCV), DMVs are gradually derived from single membrane vesicles or tubules and eventually transformed to multilamellar structures [22, 23, 130-133]. In coronavirus (CoV)-infected cells, however, DMVs are developed through bending and fission of paired ER membranes [134-136]. Despite the morphological differences, two functions of ROs are generally accepted as common features; as a genome replication facility and as a fortress to hide vRNA replication intermediates from

cellular sensors [126]. In the following section, these functions of ROs in enterovirus-infected cells will be discussed together with additional potential functions of ROs.

Role of ROs in enteroviral RNA synthesis?

DMVs are the most abundant component of CoV ROs and double-stranded RNA (dsRNA) is found inside DMVs [137-140]. As CoV-induced DMVs appeared as completely closed compartments, it remained a mystery that if DMVs serve as the vRNA replication sites how synthesized RNAs would be transported out of DMVs. A recent discovery finally revealed the presence of a molecular pore complex spanning membranes of DMVs in CoV-infected cells which allows RNA to be exported to the cytosol [139].

Unlike DMVs in CoV-infected cells, viral RNA synthesis of enteroviruses is not anticipated to occur within the DMVs. DMVs in enterovirus-infected cells are often found as a closed compartment without any sign of pores [23]. More importantly, the majority of vRNA synthesis in enterovirus-infected cells precedes the formation of DMVs and is associated with the cytosolic side of single membrane structures (**chapter 3** and [22, 23, 141, 142]). DMVs appear in large numbers after the exponential phase of vRNA replication indicating that DMVs may contribute to other steps of the viral life cycle, such as virus assembly.

In **chapter 3**, we show CVB3 3A-H57Y mutant virus upon PI4KB inhibition can replicate at the ER and an intact Golgi by utilizing, albeit less efficiently than when ROs are formed. ROs are formed at the later stage of the replication cycle, but again the formation was beyond the exponential phase of vRNA synthesis. A similar observation was made in poliovirus-infected cells devoid of ROs [111]. When the synthesis of phosphatidylcholine (PC) was inhibited, ROs were not generated while PV replication remained unaffected during single-cycle replication. Altogether, these findings suggest that RO formation is not an absolute prerequisite for enterovirus RNA synthesis.

Yet, specific membrane conditions and/or structures of ROs could facilitate the formation of membrane-associated RNA replication complexes consisting of viral and cellular proteins and viral RNA template for more efficient RNA synthesis. Under low PI4P conditions, viral RNA synthesis at the Golgi was less efficient (**chapter 3**), whereas inhibition of PC synthesis did not affect RNA synthesis [111]. Further investigation into where the RNA replication occurs under low PC conditions will help to understand if specific lipids (such as PI4P) play a more important than others (e.g., PC) to sustain RNA replication.

Seclusion of vRNA replication complexes from cellular antiviral mechanisms

Pattern-recognition receptors (PRRs) provide the host with the ability to counteract infection by pathogens including viruses. These sensors recognize pathogen-associated molecular patterns (PAMPs) such as virus-derived nucleic acids, leading to the induction of inflammatory responses and the production of type I interferons (IFNs). Released IFNs upregulate the expression of IFN-stimulated genes (ISGs), triggering an antiviral state in cells that restricting the further spread of virus infection [143, 144]. Among diverse PRRs, Toll-like receptors (TLRs) and retinoic acid-inducible gene-I (RIG-I)-like receptors (RLRs) can detect non-self RNA, and three mammalian RLRs (RIG-I, MDA5, LGP2) have been identified as RNA sensors to trigger antiviral responses [145].

One of the proposed benefits of building ROs by (+)RNA viruses is that ROs can be a physical barrier to hide vRNA replication intermediates from innate immune sensors [126, 146]. Yet this concept has

hardly been investigated. The invagination-type ROs that are induced by flaviviruses and tombusviruses evidence this shielding intuitively. The narrow openings connecting the spherule interior to the cytosol only allow the exchange of small molecules such as nucleotides or newly synthesized RNAs but are likely not sufficiently large for cellular RNA sensors to pass through [128, 129]. The DMVs generated by nidoviruses serve as the main stage for RNA synthesis [137, 147], and a molecular pore spanning the membranes of DMVs is also likely just wide enough to allow RNA to be exported to the cytosol [139].

However, the morphology of enterovirus ROs provides less clear-cut explanations to the role of ROs as a shield, and vRNA synthesis of enteroviruses is not occurring inside of ROs [22, 23, 142]. Notably, neither the IFN- β response nor the premature activation of MAVS and PKR was found in the absence of ROs upon PI4KB inhibition in cells infected with CVB3 3A-H57Y, despite the presence of abundant vRNAs (**chapter 3**). In PV-infected cells, the level of RNA replication and virus production were sustained during a single round of replication cycle even when ROs were not formed due to PC depletion [111]. In contrast to our finding in **chapter 3**, the phosphorylation of IRF3 was increased, indicating the activation of RLR pathway possibly due to exposed dsRNA intermediates. Consistently, the virus yield after multiple rounds of replication cycles was much lower in cells devoid of ROs indicating that if the viral RNA replication complexes are not protected by the membranes, the infection becomes more sensitive to the cellular defense mechanisms since neighboring cells could mount a stronger antiviral state. In agreement with this, RNA replication was severely impaired in the absence of ROs upon IFN pretreatment [111]. One thing to be noted is that the effects of PI4P depletion and PC depletion on RO biogenesis can differ and also endomembrane system in cells could have been altered differently which could have an (indirect) influence on RLRs pathways. To be able to establish the role of ROs as a shield, the impact of IFN pretreatment in combination with PI4KB inhibition on virus replication needs to be further looked into. Also, whether the absence of ROs upon PI4KB inhibition would result in the reduction in virus production after multiple rounds of infection needs to be investigated.

ROs as platforms for virion assembly

Enteroviruses do not rely on a specific RNA packaging signal but rather govern the specificity of encapsidation by interactions between viral proteins (i.e., between capsid VP3 and the RNA-binding 2C protein) [148, 149]. Only newly replicated RNAs are able to be encapsidated [150, 151] indicating that the encapsidation step is tightly coupled to vRNA synthesis (reviewed in [152]). The full-length, positive-sense genomic RNA can serve three functions during the picornavirus life cycle, i.e., as mRNA for translation, as a template for (-)RNA synthesis, and as a genome for encapsidation). The direct coupling of genome replication and encapsidation is therefore an intrinsic mechanism ensuring the successful translation, replication, and packaging of the viral genome, sequentially [150, 153]. This tight connection between steps might also reduce the risk of vRNAs being detected by innate immunity sensors by limiting the exposure of “naked” vRNAs in the cytoplasm.

Still, relatively little is known about the necessity of membranes for the encapsidation process. Membrane-associated replication complexes of PV were found to contain capsid 5S protomers and 14S pentamers [154], and 14S pentamers association with vRNA is suggested as a first step in the encapsidation [155]. In accordance with this, EMCV particles were observed in near proximity to ROs [72], which could indicate a similar association between RNA synthesis and virion assembly in EMCV-infected cells.

The formation or the expansion of ROs indeed may be coupled with the transition from genome replication to virion assembly. In enterovirus-infected cells, structures of ROs gradually evolve from single membrane tubules/vesicles to DMVs, which appears after the exponential phase of RNA replication that coincides with the onset of the exponential phase of viral particle production [22, 141]. Previously, a poliovirus mutant (GG PV) that is unable to cleave at the 3B-3C junction, was shown to exhibit a more drastic reduction in virus production than in genome replication. RNA replication was reduced to within one log of wild type, while a near 5-log reduction was shown in the amount of infectious virus produced [156] indicating a more severe defect in the assembly than in genome replication of this mutant. This assembly-defective poliovirus mutant was unable to induce the structural conversion of RO tubules to vesicular clusters [141]. Similarly, when RO formation was delayed upon PI4KB inhibition, infectious virus production by CVB3 3A-H57Y was more affected than genome replication (**chapter 3**). However, the absence of ROs as a consequence of choline depletion still resulted in successful virus production [111], indicating that specific lipids might be held accountable for the coupling of assembly steps and membranes. Overall, it remains a question whether virus particles assemble at (designated) ROs and whether a specific membrane composition is required to coordinate the assembly.

Enveloping naked virus particles in DMVs: non-lytic release via extracellular vesicles

Although host cell lysis has been accepted as a canonical exit strategy for naked viruses, mounting evidence is suggesting that the en bloc transmission of virions via infectious extracellular vesicles (ExVs) is playing a prominent role in the transmission of various picornaviruses (reviewed in [157, 158]). ExVs harboring large numbers of virions were found to be released from poliovirus- and CVB3-infected HeLa cells [159, 160]. Similarly, the shedding of exosomes containing infectious particles from enterovirus A71-infected RD cells was observed [161]. The exact mechanism of this en bloc virus transmission is yet to be determined, though the non-degradative secretory autophagy seems to be exploited by viruses.

Autophagy is a process that mediates the clearance and recycling of cellular components, such as lipids, proteins, and damaged organelles to maintain cellular homeostasis. While traditionally autophagy is considered as an auto-digestive process, the secretory autophagy pathway has been identified as one form of unconventional secretion [162]. In contrast to degradative autophagy, the autophagosomes fuse with the membrane and release single membrane vesicles carrying cellular contents.

The structures of enterovirus ROs gradually evolve from single membrane tubules/vesicles to DMVs, and the formation of DMVs and the subsequent enwrapping process are reminiscent of autophagosome formation. During enterovirus infection, multiple infectious viral particles are shown to be incorporated in DMVs containing autophagy marker LC3 and enriched in phosphatidylserine [159, 163-165]. In accordance with this, many enteroviruses facilitate the production of autophagosomes, and inhibition of autophagy impeded virus infection [81-92]. DMVs that are found in enterovirus-infected cells have been suggested to serve as vehicles for this [163, 166, 167]. As enterovirus capsid proteins have been shown to bind to LC3 [168], LC3 on these vesicles may be in charge of engulfing progeny virions.

Enteroviruses must prevent the fusion of these autophagosome-like vesicles with lysosomes to avoid the degradation of newly formed virions. It is thought that this is achieved by disrupting the interaction between the SNARE complex proteins SNAP29, STX17, and VAMP8, which mediate the fusion between autophagosomes and lysosomes [82, 163, 164]. For instance, by cleaving SNAP29, EV-D68 3C^{pro} can

prevent the degradation of progeny viruses. EV-A71 2BC protein was shown to directly interact with STX17 and SNAP29 [169] indicating that 2BC could also contribute to the avoidance of the fusion event. Infection through infectious ExVs carries several advantages such as efficient infection by delivering multiple viral genomes and evasion of neutralizing antibodies [161, 170]. Phosphatidylserine (PS) on vesicle membranes increases the uptake by neighboring cells, allowing the efficient spread of multiple virions into a new host cell [163]. It has to be noted that the infection of new cells by these secreted vesicles is still dependent on the specific enterovirus receptor, while PS aids this entry step as a co-factor [163]. A recent study found that ExVs secreted during PV infection also carry viral non-encapsidated RNAs (both positive- and negative-strand RNA), viral non-structural proteins, and host proteins [160] that could facilitate the entry step and the onset of a new infection. All these studies suggest a possible link between autophagy and viral release, yet there is no direct evidence showing ROs as the origin of DMV containing virions. When RO formation was delayed upon PI4KB inhibition, infectious virus production by CVB3 3A-H57Y was more affected than genome replication (**chapter 3**), although it is not clear whether the release of infectious ExVs was reduced in this condition. An absence of ROs resulted from choline depletion did not affect overall virus production [111], but the implications for ExVs production need further investigation.

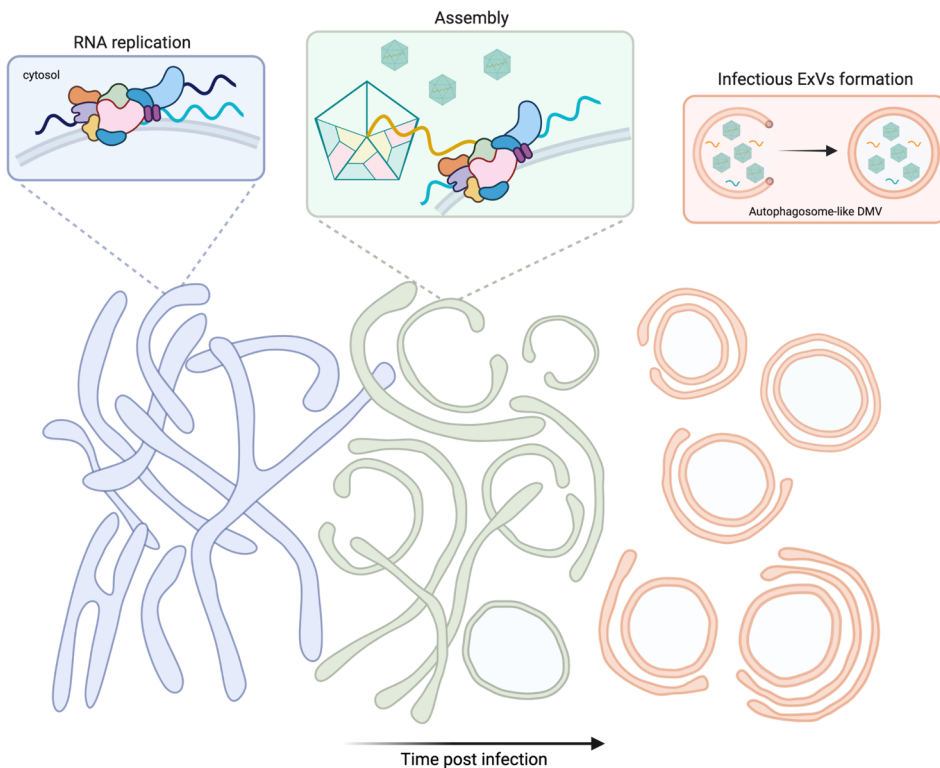


Figure 5. A transition model for CVB3-induced ROs and suggested roles of ROs. The transition model is inspired from [23]. ExVs, extracellular vesicles. Created with BioRender.com.

CONCLUDING REMARKS

In this thesis, we investigated the role of host factors that regulating cellular membranes in enterovirus replication. Membrane reorganization induced by enterovirus is a dynamic process that involves several different viral proteins as well as diverse host factors. Findings described in the experimental chapters provide a deeper understanding of the functions of specific lipids and the underlying mechanisms regulating the levels of lipids during enterovirus replication. Yet we could be overlooking other important factors or the interaction among factors since much research has been often focused on a fixed moment of the replication cycle and/or it has been biased toward certain viral/host factors. Evolving membrane structures of ROs over the course of virus replication likely serve distinct functions throughout the viral life cycle, although we cannot offer a clear answer to that yet. Therefore, a more comprehensive understanding of the changing of RO membranes is required. Multi-omics approaches such as lipidomic or proteomic analysis of the isolated RO membranes for the duration of replication cycle can be one way to look into the dynamics of these changes in an unbiased manner. A recently developed single-molecule imaging assay called virus infection real-time imaging (VIRIM) [171], which was co-developed in our lab, opens up unprecedented opportunities to study translation/replication of the incoming viral RNAs. Advanced microscopy techniques such as expansion microscopy can further aid in characterizing the membrane contact sites that occurs during the development of ROs and understanding the progress of structural changes. By understanding the changes in the components of RO membranes as well as viral/host factors involved in the process we will be able to grasp the implications of specific RO structures in virus replication. Further research into this membrane reorganization process will not only allow us to better understand how enteroviruses benefit from cellular membranes but also may reveal potential antiviral drug targets with a broad-spectrum activity.

REFERENCES

1. De Clercq, E. and G. Li, Approved Antiviral Drugs over the Past 50 Years. *Clin Microbiol Rev*, 2016. 29(3): p. 695-747.
2. Hsu, N.Y., et al., Viral reorganization of the secretory pathway generates distinct organelles for RNA replication. *Cell*, 2010. 141(5): p. 799-811.
3. Sasaki, J., et al., ACBD3-mediated recruitment of PI4KB to picornavirus RNA replication sites. *EMBO J*, 2012. 31(3): p. 754-66.
4. Dorobantu, C.M., et al., Modulation of the Host Lipid Landscape to Promote RNA Virus Replication: The Picornavirus Encephalomyocarditis Virus Converges on the Pathway Used by Hepatitis C Virus. *PLoS Pathog*, 2015. 11(9): p. e1005185.
5. Ishikawa-Sasaki, K., J. Sasaki, and K. Taniguchi, A Complex Comprising Phosphatidylinositol 4-Kinase III β , ACBD3, and Aichi Virus Proteins Enhances Phosphatidylinositol 4-Phosphate Synthesis and Is Critical for Formation of the Viral Replication Complex. *J Virol*, 2014. 88(12): p. 6586-6598.
6. Klima, M., et al., Structural insights and in vitro reconstitution of membrane targeting and activation of human PI4KB by the ACBD3 protein. *Sci Rep*, 2016. 6: p. 23641.
7. Greninger, A.L., et al., The 3A protein from multiple picornaviruses utilizes the golgi adaptor protein ACBD3 to recruit PI4KIII β . *J Virol*, 2012. 86(7): p. 3605-16.
8. Klima, M., et al., Kobuviral Non-structural 3A Proteins Act as Molecular Harnesses to Hijack the Host ACBD3 Protein. *Structure*, 2017. 25(2): p. 219-230.
9. McPhail, J.A., et al., The Molecular Basis of Aichi Virus 3A Protein Activation of Phosphatidylinositol 4 Kinase III β , PI4KB, through ACBD3. *Structure*, 2017. 25(1): p. 121-131.
10. Dorobantu, C.M., et al., Recruitment of PI4KIII β to coxsackievirus B3 replication organelles is independent of ACBD3, GBF1, and Arf1. *J Virol*, 2014. 88(5): p. 2725-36.
11. Teoule, F., et al., The Golgi protein ACBD3, an interactor for poliovirus protein 3A, modulates poliovirus replication. *J Virol*, 2013. 87(20): p. 11031-46.
12. Dorobantu, C.M., et al., GBF1- and ACBD3-independent recruitment of PI4KIII β to replication sites by rhinovirus 3A proteins. *J Virol*, 2015. 89(3): p. 1913-8.
13. Lei, X., et al., The Golgi protein ACBD3 facilitates Enterovirus 71 replication by interacting with 3A. *Sci Rep*, 2017. 7: p. 44592.
14. Xiao, X., et al., Enterovirus 3A facilitates viral replication by promoting PI4KB-ACBD3 interaction. *J Virol*, 2017. 91(19): p. e00791-17.
15. Kim, H.S., et al., Arrayed CRISPR screen with image-based assay reliably uncovers host genes required for coxsackievirus infection. *Genome Res*, 2018.
16. Fan, J., et al., Acyl-coenzyme A binding domain containing 3 (ACBD3; PAP7; GCP60): an emerging signaling molecule. *Prog Lipid Res*, 2010. 49(3): p. 218-34.
17. Chen, Y., et al., Maturation and activity of sterol regulatory element binding protein 1 is inhibited by acyl-CoA binding domain containing 3. *PLoS One*, 2012. 7(11): p. e49906.
18. Sohda, M., et al., Identification and characterization of a novel Golgi protein, GCP60, that interacts with the integral membrane protein giantin. *J Biol Chem*, 2001. 276(48): p. 45298-306.
19. Walther, T.C. and R.V. Farese, Jr., Lipid droplets and cellular lipid metabolism. *Annu Rev Biochem*, 2012. 81: p. 687-714.
20. Schlegel, A., et al., Cellular origin and ultrastructure of membranes induced during poliovirus infection. *J Virol*, 1996. 70(10): p. 6576-88.
21. Richards, A.L., et al., Generation of unique poliovirus RNA replication organelles. *mBio*, 2014. 5(2): p. e00833-13.
22. Belov, G.A., et al., Complex dynamic development of poliovirus membranous replication complexes. *Journal of virology*, 2012. 86(1): p. 302-312.
23. Limpens, R.W.A.L., et al., The transformation of enterovirus replication structures: a three-dimensional study of single- and double-membrane compartments. *mBio*, 2011. 2(5): p. e00166-11.
24. van der Schaar, H.M., et al., Illuminating the Sites of Enterovirus Replication in Living Cells by Using a Split-GFP-Tagged Viral Protein. *mSphere*, 2016. 1(4).
25. Melia, C.E., et al., Origins of Enterovirus Replication Organelles Established by Whole-Cell Electron Microscopy. *mBio*, 2019. 10(3).
26. Greninger, A.L., et al., ACBD3 interaction with TBC1 domain 22 protein is differentially affected by enteroviral and kobuviral 3A protein binding. *MBio*, 2013. 4(2): p. e00098-13.

27. Shin, H.J., et al., A Crucial Role of ACBD3 Required for Coxsackievirus Infection in Animal Model Developed by AAV-Mediated CRISPR Genome Editing Technique. *Viruses*, 2021. 13(2).
28. Banerjee, S., et al., Hijacking of multiple phospholipid biosynthetic pathways and induction of membrane biogenesis by a picornaviral 3CD protein. *PLoS Pathog*, 2018. 14(5): p. e1007086.
29. Godi, A., et al., ARF mediates recruitment of PtdIns-4-OH kinase-beta and stimulates synthesis of PtdIns(4,5)P2 on the Golgi complex. *Nat Cell Biol*, 1999. 1(5): p. 280-7.
30. Sztul, E., et al., ARF GTPases and their GEFs and GAPs: concepts and challenges. *Mol Biol Cell*, 2019. 30(11): p. 1249-1271.
31. Donaldson, J.G. and C.L. Jackson, ARF family G proteins and their regulators: roles in membrane transport, development and disease. *Nature Reviews Molecular Cell Biology*, 2011. 12(6): p. 362-375.
32. Belov, G.A., M.H. Fogg, and E. Ehrenfeld, Poliovirus proteins induce membrane association of GTPase ADP-ribosylation factor. *J Virol*, 2005. 79(11): p. 7207-16.
33. Belov, G.A., et al., A critical role of a cellular membrane traffic protein in poliovirus RNA replication. *PLoS Pathog*, 2008. 4(11): p. e1000216.
34. Belov, G.A., et al., Poliovirus replication requires the N-terminus but not the catalytic Sec7 domain of ArfGEF GBF1. *Cell Microbiol*, 2010. 12(10): p. 1463-79.
35. Wessels, E., et al., A proline-rich region in the coxsackievirus 3A protein is required for the protein to inhibit endoplasmic reticulum-to-golgi transport. *J Virol*, 2005. 79(8): p. 5163-73.
36. Wessels, E., et al., A viral protein that blocks Arf1-mediated COP-I assembly by inhibiting the guanine nucleotide exchange factor GBF1. *Dev Cell*, 2006. 11(2): p. 191-201.
37. Wessels, E., et al., Effects of picornavirus 3A Proteins on Protein Transport and GBF1-dependent COP-I recruitment. *J Virol*, 2006. 80(23): p. 11852-60.
38. Wessels, E., et al., Molecular determinants of the interaction between coxsackievirus protein 3A and guanine nucleotide exchange factor GBF1. *J Virol*, 2007. 81(10): p. 5238-45.
39. Belov, G.A., et al., Activation of cellular Arf GTPases by poliovirus protein 3CD correlates with virus replication. *J Virol*, 2007. 81(17): p. 9259-67.
40. Lanke, K.H., et al., GBF1, a guanine nucleotide exchange factor for Arf, is crucial for coxsackievirus B3 RNA replication. *J Virol*, 2009. 83(22): p. 11940-9.
41. Viktorova, E.G., et al., A Redundant Mechanism of Recruitment Underlies the Remarkable Plasticity of the Requirement of Poliovirus Replication for the Cellular ArfGEF GBF1. *J Virol*, 2019. 93(21).
42. Roulin, P.S., et al., Rhinovirus uses a phosphatidylinositol 4-phosphate/cholesterol counter-current for the formation of replication compartments at the ER-Golgi interface. *Cell Host Microbe*, 2014. 16(5): p. 677-90.
43. Chan, C.J., et al., BioID Performed on Golgi Enriched Fractions Identify C10orf76 as a GBF1 Binding Protein Essential for Golgi Maintenance and Secretion. *Mol Cell Proteomics*, 2019. 18(11): p. 2285-2297.
44. Blomen, V.A., et al., Gene essentiality and synthetic lethality in haploid human cells. *Science*, 2015. 350(6264): p. 1092-6.
45. Staring, J., et al., PLA2G16 represents a switch between entry and clearance of Picornaviridae. *Nature*, 2017. 541(7637): p. 412-416.
46. Moss, J. and M. Vaughan, Structure and function of ARF proteins: activators of cholera toxin and critical components of intracellular vesicular transport processes. *J Biol Chem*, 1995. 270(21): p. 12327-30.
47. Ferlin, J., et al., Investigation of the role of GBF1 in the replication of positive-sense single-stranded RNA viruses. *J Gen Virol*, 2018. 99(8): p. 1086-1096.
48. Moghimi, S., et al., Enterovirus Infection Induces Massive Recruitment of All Isoforms of Small Cellular Arf GTPases to the Replication Organelles. *J Virol*, 2020. 95(2).
49. Zhang, Z., et al., Host Lipids in Positive-Strand RNA Virus Genome Replication. *Frontiers in Microbiology*, 2019. 10(286).
50. Feng, Z., J.I. Inaba, and P.D. Nagy, The retromer is co-opted to deliver lipid enzymes for the biogenesis of lipid-enriched tombusviral replication organelles. *Proc Natl Acad Sci U S A*, 2021. 118(1).
51. Sasvari, Z., et al., Co-opted Cellular Sac1 Lipid Phosphatase and PI(4)P Phosphoinositide Are Key Host Factors during the Biogenesis of the Tombusvirus Replication Compartment. *J Virol*, 2020. 94(12).
52. Reiss, S., et al., Recruitment and activation of a lipid kinase by hepatitis C virus NSSA is essential for integrity of the membranous replication compartment. *Cell Host Microbe*, 2011. 9(1): p. 32-45.
53. Li, Z., et al., PI4KB on Inclusion Bodies Formed by ER Membrane Remodeling Facilitates Replication of Human Parainfluenza Virus Type 3. *Cell Rep*, 2019. 29(8): p. 2229-2242 e4.
54. Wang, P.Y., J. Weng, and R.G. Anderson, OSBP is a cholesterol-regulated scaffolding protein in control of ERK 1/2 activation. *Science*, 2005. 307(5714): p. 1472-6.

55. Arita, M., et al., Oxysterol-binding protein family I is the target of minor enviroxime-like compounds. *J Virol*, 2013. 87(8): p. 4252-60.
56. Strating, J.R., et al., Itraconazole inhibits enterovirus replication by targeting the oxysterol-binding protein. *Cell Rep*, 2015. 10(4): p. 600-15.
57. Arita, M., Phosphatidylinositol-4 kinase III beta and oxysterol-binding protein accumulate unesterified cholesterol on poliovirus-induced membrane structure. *Microbiol Immunol*, 2014. 58(4): p. 239-56.
58. Albulescu, L., et al., Cholesterol shuttling is important for RNA replication of coxsackievirus B3 and encephalomyocarditis virus. *Cellular Microbiology*, 2015. 17(8): p. 1144-1156.
59. Ishikawa-Sasaki, K., et al., Model of OSBP-Mediated Cholesterol Supply to Aichi Virus RNA Replication Sites Involving Protein-Protein Interactions among Viral Proteins, ACBD3, OSBP, VAP-A/B, and SAC1. *J Virol*, 2018. 92(8).
60. Illytska, O., et al., Enteroviruses harness the cellular endocytic machinery to remodel the host cell cholesterol landscape for effective viral replication. *Cell Host Microbe*, 2013. 14(3): p. 281-93.
61. Dubankova, A., et al., Negative charge and membrane-tethered viral 3B cooperate to recruit viral RNA dependent RNA polymerase 3D. *Sci Rep*, 2017. 7(1): p. 17309.
62. Arita, M., Mechanism of Poliovirus Resistance to Host Phosphatidylinositol-4 Kinase III β Inhibitor. *ACS Infectious Diseases*, 2016. 2(2): p. 140-148.
63. Ford Siltz, L.A., et al., New small-molecule inhibitors effectively blocking picornavirus replication. *J Virol*, 2014. 88(19): p. 11091-107.
64. Towner, J.S., T.V. Ho, and B.L. Semler, Determinants of membrane association for poliovirus protein 3AB. *J Biol Chem*, 1996. 271(43): p. 26810-8.
65. Wessels, E., et al., Structure-function analysis of the coxsackievirus protein 3A: identification of residues important for dimerization, viral rna replication, and transport inhibition. *J Biol Chem*, 2006. 281(38): p. 28232-43.
66. Albulescu, L., et al., Broad-range inhibition of enterovirus replication by OSW-1, a natural compound targeting OSBP. *Antiviral Res*, 2015. 117: p. 110-4.
67. Mesmin, B., et al., A four-step cycle driven by PI(4)P hydrolysis directs sterol/PI(4)P exchange by the ER-Golgi tether OSBP. *Cell*, 2013. 155(4): p. 830-43.
68. Kräusslich, H.G., et al., Polyprotein processing in picornavirus replication. *Biochimie*, 1988. 70(1): p. 119-30.
69. Sun, Y., Y. Guo, and Z. Lou, Formation and working mechanism of the picornavirus VPg uridylylation complex. *Curr Opin Virol*, 2014. 9: p. 24-30.
70. Paul, A.V., et al., Biochemical and genetic studies of the VPg uridylylation reaction catalyzed by the RNA polymerase of poliovirus. *J Virol*, 2003. 77(2): p. 891-904.
71. Strauss, D.M. and D.S. Wuttke, Characterization of protein-protein interactions critical for poliovirus replication: analysis of 3AB and VPg binding to the RNA-dependent RNA polymerase. *J Virol*, 2007. 81(12): p. 6369-78.
72. Melia, C.E., et al., The Origin, Dynamic Morphology, and PI4P-Independent Formation of Encephalomyocarditis Virus Replication Organelles. *mBio*, 2018. 9(2).
73. Lippincott-Schwartz, J. and R.D. Phair, Lipids and cholesterol as regulators of traffic in the endomembrane system. *Annu Rev Biophys*, 2010. 39: p. 559-78.
74. Yesylevskyy, S.O., et al., Cholesterol induces uneven curvature of asymmetric lipid bilayers. *ScientificWorldJournal*, 2013. 2013: p. 965230.
75. Kawakami, L.M., et al., Understanding How Sterols Regulate Membrane Remodeling in Supported Lipid Bilayers. *Langmuir*, 2017. 33(51): p. 14756-14765.
76. Suh, D.A., T.H. Giddings, Jr., and K. Kirkegaard, Remodeling the endoplasmic reticulum by poliovirus infection and by individual viral proteins: an autophagy-like origin for virus-induced vesicles. *J Virol*, 2000. 74(19): p. 8953-65.
77. Doedens, J.R. and K. Kirkegaard, Inhibition of cellular protein secretion by poliovirus proteins 2B and 3A. *The EMBO journal*, 1995. 14(5): p. 894-907.
78. Sandoval, I.V. and L. Carrasco, Poliovirus infection and expression of the poliovirus protein 2B provoke the disassembly of the Golgi complex, the organelle target for the antipoliovirus drug Ro-090179. *Journal of Virology*, 1997. 71(6): p. 4679-4693.
79. Gazina, E.V., et al., Differential requirements for COPI coats in formation of replication complexes among three genera of Picornaviridae. *J Virol*, 2002. 76(21): p. 11113-22.
80. Wang, J., Z. Wu, and Q. Jin, COPI is required for enterovirus 71 replication. *PLoS One*, 2012. 7(5): p. e38035.
81. Alirezaei, M., et al., Pancreatic acinar cell-specific autophagy disruption reduces coxsackievirus replication and pathogenesis in vivo. *Cell Host Microbe*, 2012. 11(3): p. 298-305.

82. Corona, A.K., et al., Enteroviruses Remodel Autophagic Trafficking through Regulation of Host SNARE Proteins to Promote Virus Replication and Cell Exit. *Cell Rep*, 2018. 22(12): p. 3304-3314.
83. Delorme-Axford, E., et al., BPIFB3 regulates autophagy and coxsackievirus B replication through a noncanonical pathway independent of the core initiation machinery. *mBio*, 2014. 5(6): p. e02147.
84. Fu, Y., et al., Enterovirus 71 induces autophagy by regulating has-miR-30a expression to promote viral replication. *Antiviral Res*, 2015. 124: p. 43-53.
85. Huang, S.C., et al., Enterovirus 71-induced autophagy detected in vitro and in vivo promotes viral replication. *J Med Virol*, 2009. 81(7): p. 1241-52.
86. Jackson, W.T., et al., Subversion of cellular autophagosomal machinery by RNA viruses. *PLoS Biol*, 2005. 3(5): p. e156.
87. Kemball, C.C., et al., Coxsackievirus infection induces autophagy-like vesicles and megaphagosomes in pancreatic acinar cells in vivo. *J Virol*, 2010. 84(23): p. 12110-24.
88. Klein, K.A. and W.T. Jackson, Human rhinovirus 2 induces the autophagic pathway and replicates more efficiently in autophagic cells. *J Virol*, 2011. 85(18): p. 9651-4.
89. Shi, Y., et al., Coxsackievirus A16 elicits incomplete autophagy involving the mTOR and ERK pathways. *PLoS One*, 2015. 10(4): p. e0122109.
90. Tabor-Godwin, J.M., et al., The role of autophagy during coxsackievirus infection of neural progenitor and stem cells. *Autophagy*, 2012. 8(6): p. 938-53.
91. Wong, J., et al., Autophagosome supports coxsackievirus B3 replication in host cells. *J Virol*, 2008. 82(18): p. 9143-53.
92. Yoon, S.Y., et al., Coxsackievirus B4 uses autophagy for replication after calpain activation in rat primary neurons. *J Virol*, 2008. 82(23): p. 11976-8.
93. Herker, E., et al., Lipid Droplet Contact Sites in Health and Disease. *Trends Cell Biol*, 2021. 31(5): p. 345-358.
94. Salloum, S., et al., Rab18 binds to hepatitis C virus NS5A and promotes interaction between sites of viral replication and lipid droplets. *PLoS Pathog*, 2013. 9(8): p. e1003513.
95. Lee, J.Y., et al., Spatiotemporal Coupling of the Hepatitis C Virus Replication Cycle by Creating a Lipid Droplet- Proximal Membranous Replication Compartment. *Cell Rep*, 2019. 27(12): p. 3602-3617.e5.
96. Heaton, N.S. and G. Randall, Dengue virus-induced autophagy regulates lipid metabolism. *Cell Host Microbe*, 2010. 8(5): p. 422-32.
97. Tang, W.C., et al., Rab18 facilitates dengue virus infection by targeting fatty acid synthase to sites of viral replication. *J Virol*, 2014. 88(12): p. 6793-804.
98. Zhang, J., et al., Flaviviruses Exploit the Lipid Droplet Protein AUP1 to Trigger Lipophagy and Drive Virus Production. *Cell Host Microbe*, 2018. 23(6): p. 819-831.e5.
99. Laufman, O., J. Perrino, and R. Andino, Viral Generated Inter-Organelle Contacts Redirect Lipid Flux for Genome Replication. *Cell*, 2019. 178(2): p. 275-289.e16.
100. Teterina, N.L., et al., Evidence for functional protein interactions required for poliovirus RNA replication. *J Virol*, 2006. 80(11): p. 5327-37.
101. Xiang, W., et al., Complete protein linkage map of poliovirus P3 proteins: interaction of polymerase 3DPol with VPg and with genetic variants of 3AB. *J Virol*, 1998. 72(8): p. 6732-41.
102. Ellong, E.N., et al., Interaction between the triglyceride lipase ATGL and the Arf1 activator GBF1. *PLoS One*, 2011. 6(7): p. e21889.
103. Soni, K.G., et al., Coatomer-dependent protein delivery to lipid droplets. *J Cell Sci*, 2009. 122(Pt 11): p. 1834-41.
104. Belov, G.A. and F.J.M. van Kuppeveld, Lipid Droplets Grease Enterovirus Replication. *Cell Host Microbe*, 2019. 26(2): p. 149-151.
105. Zhang, J., et al., Positive-strand RNA viruses stimulate host phosphatidylcholine synthesis at viral replication sites. *Proc Natl Acad Sci U S A*, 2016. 113(8): p. E1064-73.
106. Vance, D.E., E.M. Trip, and H.B. Paddon, Poliovirus increases phosphatidylcholine biosynthesis in HeLa cells by stimulation of the rate-limiting reaction catalyzed by CTP: phosphocholine cytidyltransferase. *J Biol Chem*, 1980. 255(3): p. 1064-9.
107. PENMAN, S., STIMULATION OF THE INCORPORATION OF CHOLINE IN POLIOVIRUS-INFECTED CELLS. *Virology*, 1965. 25: p. 149-52.
108. Caligiuri, L.A. and I. Tamm, The role of cytoplasmic membranes in poliovirus biosynthesis. *Virology*, 1970. 42(1): p. 100-11.
109. Schimmel, H. and P. Traub, The effect of mengovirus infection on lipid synthesis in cultured Ehrlich ascites tumor cells. *Lipids*, 1987. 22(2): p. 95-103.

110. Nchoutmboube, J.A., et al., Increased long chain acyl-Coa synthetase activity and fatty acid import is linked to membrane synthesis for development of picornavirus replication organelles. *PLoS Pathog*, 2013. 9(6): p. e1003401.
111. Viktorova, E.G., et al., Phospholipid synthesis fueled by lipid droplets drives the structural development of poliovirus replication organelles. *PLoS Pathog*, 2018. 14(8): p. e1007280.
112. Jacquemyn, J., A. Cascalho, and R.E. Goodchild, The ins and outs of endoplasmic reticulum-controlled lipid biosynthesis. *EMBO Rep*, 2017. 18(11): p. 1905-1921.
113. Wubben, J.M., S.C. Atkinson, and N.A. Borg, The Role of Protein Disorder in Nuclear Transport and in Its Subversion by Viruses. *Cells*, 2020. 9(12).
114. Flather, D. and B.L. Semler, Picornaviruses and nuclear functions: targeting a cellular compartment distinct from the replication site of a positive-strand RNA virus. *Front Microbiol*, 2015. 6: p. 594.
115. Watters, K., et al., Differential Disruption of Nucleocytoplasmic Trafficking Pathways by Rhinovirus 2A Proteases. *J Virol*, 2017. 91(8).
116. Belov, G.A., et al., Bidirectional increase in permeability of nuclear envelope upon poliovirus infection and accompanying alterations of nuclear pores. *J Virol*, 2004. 78(18): p. 10166-77.
117. Castello, A., et al., RNA nuclear export is blocked by poliovirus 2A protease and is concomitant with nucleoporin cleavage. *J Cell Sci*, 2009. 122(Pt 20): p. 3799-809.
118. Gustin, K.E. and P. Sarnow, Effects of poliovirus infection on nucleo-cytoplasmic trafficking and nuclear pore complex composition. *EMBO J*, 2001. 20(1-2): p. 240-9.
119. Park, N., et al., Differential targeting of nuclear pore complex proteins in poliovirus-infected cells. *J Virol*, 2008. 82(4): p. 1647-55.
120. Gustin, K.E. and P. Sarnow, Inhibition of nuclear import and alteration of nuclear pore complex composition by rhinovirus. *J Virol*, 2002. 76(17): p. 8787-96.
121. Jans, D.A. and A.J. Martin, Nucleocytoplasmic Trafficking of Dengue Non-structural Protein 5 as a Target for Antivirals. *Adv Exp Med Biol*, 2018. 1062: p. 199-213.
122. Kato, K., et al., Overexpression of SARS-CoV-2 protein ORF6 dislocates RAE1 and NUP98 from the nuclear pore complex. *Biochem Biophys Res Commun*, 2021. 536: p. 59-66.
123. Lidsky, P.V., et al., Nucleocytoplasmic traffic disorder induced by cardiomyoviruses. *J Virol*, 2006. 80(6): p. 2705-17.
124. Yarbrough, M.L., et al., Viral subversion of nucleocytoplasmic trafficking. *Traffic*, 2014. 15(2): p. 127-40.
125. Harak, C. and V. Lohmann, Ultrastructure of the replication sites of positive-strand RNA viruses. *Virology*, 2015. 479-480: p. 418-33.
126. Romero-Brey, I. and R. Bartschlagler, Membranous replication factories induced by plus-strand RNA viruses. *Viruses*, 2014. 6(7): p. 2826-2857.
127. Nagy, P.D., J.R. Strating, and F.J. van Kuppeveld, Building Viral Replication Organelles: Close Encounters of the Membrane Types. *PLoS Pathog*, 2016. 12(10): p. e1005912.
128. Welsch, S., et al., Composition and three-dimensional architecture of the dengue virus replication and assembly sites. *Cell host & microbe*, 2009. 5(4): p. 365-375.
129. Gillespie, L.K., et al., The endoplasmic reticulum provides the membrane platform for biogenesis of the flavivirus replication complex. *Journal of virology*, 2010. 84(20): p. 10438-10447.
130. Romero-Brey, I., et al., Three-dimensional architecture and biogenesis of membrane structures associated with hepatitis C virus replication. *PLoS Pathog*, 2012. 8(12): p. e1003056.
131. Doerflinger, S.Y., et al., Membrane alterations induced by nonstructural proteins of human norovirus. *PLOS Pathogens*, 2017. 13(10): p. e1006705.
132. Ferraris, P., et al., Sequential biogenesis of host cell membrane rearrangements induced by hepatitis C virus infection. *Cellular and Molecular Life Sciences*, 2013. 70(7): p. 1297-1306.
133. Paul, D., et al., Glycine Zipper Motifs in Hepatitis C Virus Nonstructural Protein 4B Are Required for the Establishment of Viral Replication Organelles. *Journal of Virology*, 2018. 92(4): p. e01890-17.
134. Oudshoorn, D., et al., Expression and Cleavage of Middle East Respiratory Syndrome Coronavirus nsp3-4 Polyprotein Induce the Formation of Double-Membrane Vesicles That Mimic Those Associated with Coronavirus RNA Replication. *mBio*, 2017. 8(6).
135. Oudshoorn, D., et al., Antiviral Innate Immune Response Interferes with the Formation of Replication-Associated Membrane Structures Induced by a Positive-Strand RNA Virus. *mBio*, 2016. 7(6).
136. van der Hoeven, B., et al., Biogenesis and architecture of arterivirus replication organelles. *Virus Res*, 2016. 220: p. 70-90.
137. Knoops, K., et al., SARS-coronavirus replication is supported by a reticulovesicular network of modified endoplasmic reticulum. *PLoS Biol*, 2008. 6(9): p. e226.

138. Knoops, K., et al., Ultrastructural characterization of arterivirus replication structures: reshaping the endoplasmic reticulum to accommodate viral RNA synthesis. *J Virol*, 2012. 86(5): p. 2474-87.
139. Wolff, G., et al., A molecular pore spans the double membrane of the coronavirus replication organelle. *Science*, 2020. 369(6509): p. 1395-1398.
140. Snijder, E.J., et al., A unifying structural and functional model of the coronavirus replication organelle: Tracking down RNA synthesis. *PLoS Biol*, 2020. 18(6): p. e3000715.
141. Oh, H.S., et al., Multiple poliovirus-induced organelles suggested by comparison of spatiotemporal dynamics of membranous structures and phosphoinositides. *PLoS Pathog*, 2018. 14(4): p. e1007036.
142. Bienz, K., D. Egger, and L. Pasamontes, Association of polioviral proteins of the P2 genomic region with the viral replication complex and virus-induced membrane synthesis as visualized by electron microscopic immunocytochemistry and autoradiography. *Virology*, 1987. 160(1): p. 220-6.
143. Bowie, A.G. and L. Unterholzner, Viral evasion and subversion of pattern-recognition receptor signalling. *Nat Rev Immunol*, 2008. 8(12): p. 911-22.
144. Gürtler, C. and A.G. Bowie, Innate immune detection of microbial nucleic acids. *Trends Microbiol*, 2013. 21(8): p. 413-20.
145. Yoneyama, M., et al., The RNA helicase RIG-I has an essential function in double-stranded RNA-induced innate antiviral responses. *Nat Immunol*, 2004. 5(7): p. 730-7.
146. Scutigliani, E.M. and M. Kikkert, Interaction of the innate immune system with positive-strand RNA virus replication organelles. *Cytokine Growth Factor Rev*, 2017. 37: p. 17-27.
147. Snijder, E.J., et al., A unifying structural and functional model of the coronavirus replication organelle: Tracking down RNA synthesis. *PLoS Biol*, 2020. 18(6): p. e3000715.
148. Liu, Y., et al., Direct interaction between two viral proteins, the nonstructural protein 2C and the capsid protein VP3, is required for enterovirus morphogenesis. *PLoS Pathog*, 2010. 6(8): p. e1001066.
149. Liu, Y., et al., Direct Interaction between Two Viral Proteins, the Nonstructural Protein 2CATPase and the Capsid Protein VP3, Is Required for Enterovirus Morphogenesis. *PLOS Pathogens*, 2010. 6(8): p. e1001066.
150. Nugent, C.I., et al., Functional coupling between replication and packaging of poliovirus replicon RNA. *J Virol*, 1999. 73(1): p. 427-35.
151. Molla, A., A.V. Paul, and E. Wimmer, Cell-free, de novo synthesis of poliovirus. *Science*, 1991. 254(5038): p. 1647-51.
152. Jiang, P., et al., Picornavirus morphogenesis. *Microbiol Mol Biol Rev*, 2014. 78(3): p. 418-37.
153. Wimmer, E. and A.V. Paul, The Making of a Picornavirus Genome, in *The Picornaviruses*. 2010. p. 33-55.
154. Pfister, T., et al., Immunocytochemical localization of capsid-related particles in subcellular fractions of poliovirus-infected cells. *Virology*, 1992. 188(2): p. 676-84.
155. Pfister, T., D. Egger, and K. Bienz, Poliovirus subviral particles associated with progeny RNA in the replication complex. *J Gen Virol*, 1995. 76 (Pt 1): p. 63-71.
156. Pathak, H.B., et al., Picornavirus genome replication: roles of precursor proteins and rate-limiting steps in oril-dependent VPg uridylylation. *J Biol Chem*, 2008. 283(45): p. 30677-88.
157. Altan-Bonnet, N. and Y.H. Chen, Intercellular Transmission of Viral Populations with Vesicles. *J Virol*, 2015. 89(24): p. 12242-4.
158. Mutsafi, Y. and N. Altan-Bonnet, Enterovirus Transmission by Secretory Autophagy. *Viruses*, 2018. 10(3).
159. Robinson, S.M., et al., Coxsackievirus B exits the host cell in shed microvesicles displaying autophagosomal markers. *PLoS Pathog*, 2014. 10(4): p. e1004045.
160. Yang, J.E., et al., Complexity and ultrastructure of infectious extracellular vesicles from cells infected by non-enveloped virus. *Sci Rep*, 2020. 10(1): p. 7939.
161. Mao, L., et al., Enterovirus 71 transmission by exosomes establishes a productive infection in human neuroblastoma cells. *Virus Genes*, 2016. 52(2): p. 189-94.
162. Ponpuak, M., et al., Secretory autophagy. *Curr Opin Cell Biol*, 2015. 35: p. 106-16.
163. Chen, Y.H., et al., Phosphatidylserine vesicles enable efficient en bloc transmission of enteroviruses. *Cell*, 2015. 160(4): p. 619-630.
164. Mohamud, Y., et al., Enteroviral Infection Inhibits Autophagic Flux via Disruption of the SNARE Complex to Enhance Viral Replication. *Cell Rep*, 2018. 22(12): p. 3292-3303.
165. Too, I.H., et al., Enterovirus 71 infection of motor neuron-like NSC-34 cells undergoes a non-lytic exit pathway. *Sci Rep*, 2016. 6: p. 36983.
166. Bird, S.W., et al., Nonlytic viral spread enhanced by autophagy components. *Proc Natl Acad Sci U S A*, 2014. 111(36): p. 13081-6.
167. Taylor, M.P., et al., Role of microtubules in extracellular release of poliovirus. *J Virol*, 2009. 83(13): p. 6599-609.

168. Abernathy, E., et al., Differential and convergent utilization of autophagy components by positive-strand RNA viruses. *PLoS Biol*, 2019. 17(1): p. e2006926.
169. Lai, J.K.F., et al., 2BC Non-Structural Protein of Enterovirus A71 Interacts with SNARE Proteins to Trigger Autolysosome Formation. *Viruses*, 2017. 9(7).
170. Feng, Z., et al., A pathogenic picornavirus acquires an envelope by hijacking cellular membranes. *Nature*, 2013. 496(7445): p. 367-71.
171. Boersma, S., et al., Translation and Replication Dynamics of Single RNA Viruses. *Cell*, 2020. 183(7): p. 1930-1945 e23.

APPENDICES

- I. NEDERLANDSE SAMENVATTING
- II. 한글 요약
- III. ACKNOWLEDGEMENTS
- IV. CURRICULUM VITAE
- V. LIST OF PUBLICATION

NEDERLANDSE SAMENVATTING

De rol van gastheerfactoren die membraanhomeostase reguleren tijdens enterovirus replicatie

De enterovirussen, behorend tot de familie van picornavirussen, zijn een grote groep ziekteverwekkers, waartoe het poliovirus, rhinovirussen, coxsackievirussen (CV), en de zogenaamde genummerde enterovirussen (EV, zoals EV-D68 en EV-A71) behoren. Naast het poliovirus, bekend als de verwekker van poliomyelitis, bestaan er meer dan 280 verschillende soorten (ofwel serotypen) enterovirussen, die een breed scala aan milde tot ernstige ziektebeelden kunnen veroorzaken. De ernstige ziektebeelden komen voornamelijk voor bij jonge kinderen en mensen met een verminderde afweer. Tot op heden zijn er maar weinig antivirale medicijnen beschikbaar, die werkzaam zijn tegen een klein aantal virussen. Ondanks het feit dat de enterovirussen een van de grootste virusgroepen is, zijn er helaas nog geen antivirale medicijnen op de markt tegen enterovirussen, terwijl deze hard nodig zijn om infecties te bestrijden en mogelijk ook gebruikt kunnen worden in de strijd om het poliovirus uit te roeien.

In de strijd tegen enterovirussen zijn er verschillende remmers in ontwikkeling geweest die direct aangrijpen op het virus. De “capside binders” zijn remmers die aan de buitenkant van het virusdeeltje binden en daardoor verhinderen dat het virus de gastheercel kan binnen dringen. Daarnaast zijn er remmers getest die aangrijpen op de virale enzymen, zoals de virale proteases, die essentieel zijn voor de vermenigvuldiging (“replicatie”) van het virus. Zowel de capsid binders alsmede de protease remmers bleken helaas niet succesvol te zijn in klinische studies door toxiciteit of beperkte werkzaamheid. Virus replicatie kan ook geblokkeerd worden door het gebruik van een remmer die aangrijpt op een cellulaire component (factor) die essentieel is voor het virus. Een mogelijk voordeel van deze benadering is dat het virus minder makkelijk resistent zou kunnen worden tegen een dergelijke remmer door middel van mutatie. Een ander mogelijk voordeel is dat de meeste enterovirussen afhankelijk zijn van dezelfde cellulaire factoren voor virus replicatie; hierdoor zou met één remmer infecties door de grote groep enterovirussen aangepakt kunnen worden. Een elegante en snelle strategie voor het vinden van nieuwe antivirale middelen is de “drug repurposing screen”, waarin medicijnen die al goedgekeurd zijn voor een ander doeleinde getest worden op antivirale activiteit. In Hoofdstuk 2 wordt een gedetailleerde samenvatting gegeven over strategieën die worden gebruikt in de ontwikkeling van antivirale middelen tegen enterovirussen.

De vorming van “replicatie organellen” (RO’s) in cellen is een universeel kenmerk van infectie met positief-strengs RNA virussen, waartoe ook de enterovirussen behoren. RO’s hebben een unieke structuur en zijn opgebouwd uit verschillende membraan lipides. Zowel virale eiwitten als cellulaire factoren zijn benodigd voor de vorming van RO’s. Het virale eiwit 3A en het cellulaire enzym phosphatidylinositol 4-kinase type IIIβ (PI4KB) hebben een essentiële rol in de vorming van enterovirus RO’s. In de hoofdstukken van dit proefschrift die experimenteel werk beslaan worden er mechanistische inzichten gegeven in de rol van PI4KB in het proces van enterovirus RO vorming.

Hoewel PI4KB onmisbaar is, is de precieze rol van PI4KB tijdens enterovirus replicatie nog niet geheel duidelijk. In Hoofdstuk 3 is er gebruik gemaakt van een coxsackievirus (serotype B3) mutant die door

een enkele aminozuur verandering, te weten H57Y in het 3A eiwit, resistent is geworden tegen remming van PI4KB. Door het gebruik van deze mutant (CVB3 3A-H57Y) is ontdekt dat P4KB activiteit verschillende functies heeft in RO vorming en in proteolytische digestie van het polyproteïne. Een bijzondere observatie was dat de CVB3 3A-H57Y mutant zijn virale genoom kon vermenigvuldigen in de afwezigheid van RO's, maar in plaats daarvan een schijnbaar intact Golgi apparaat gebruikte voor genoom replicatie. Deze bevinding bood de mogelijkheid om de rol van RO's te onderzoeken in het afschermen van enteroviraal RNA voor cellulaire afweersensoren. In cellen gedepleteerd van verschillende afweer sensoren werd er geen versterkte activatie van de afweer waargenomen tijdens virus replicatie in afwezigheid van RO's. Tezamen tonen deze resultaten aan dat enterovirus RO's niet noodzakelijk zijn voor virus replicatie en zet vraagtekens bij hun rol als fysieke barrière tegen cellulaire afweersensoren.

Er zijn sterke aanwijzingen dat veranderingen in lipide huishouding van de cel invloed heeft op de proteolytische digestie van het enterovirus polyproteïne. In Hoofdstuk 3 en 4 is het effect van remming van PI4KB en oxysterol-binding protein (OSBP) op de digestie van het enterovirus polyproteïne onderzocht. Remming van PI4KB of OSBP bleek de digestie van het polyproteïne te beïnvloeden, met name de digestie tussen het 3A en 3B eiwit is verminderd, terwijl dit effect niet werd waargenomen voor de mutant CVB3 3A-H57Y. Naast de CVB3 3A-H57Y mutant is ook een andere mutant onderzocht, te weten de N2D substitutie in het 2C eiwit welke in een eerdere studie naar de resistentie tegen PI4KB remmers werd gedetecteerd. In Hoofdstuk 4 is aangetoond dat de 2C-N2D alleen geen resistentie biedt tegen remming van PI4KB of OSBP. Echter, de combinatie van 2C-N2D met 3A-H57Y bleek de resistentie tegen PI4KB of OSBP remming te vergroten, want de dubbel mutant CVB3 2C-N2D, 3A-H57Y repliceerde beter dan CVB3 3A-H57Y tijdens remming van PI4KB of OSBP. De 2C-N2D bleek geen detecteerbaar effect te hebben op digestie van het enterovirus polyproteïne, waardoor het mechanisme van versterkte resistentie in combinatie met 3A-H57Y onopgehelderd blijft.

Het enterovirale 3A eiwit is verantwoordelijk voor de aanwezigheid van PI4KB op de RO's, maar het onderliggende mechanisme is onbekend. Hoofdstuk 5 en 6 beschrijven hoe het 3A eiwit PI4KB aantrekt via een andere cellulaire factor genaamd Acyl-coenzyme A binding domain containing 3 (ACBD3). In Hoofdstuk 5 wordt de rol van ACBD3 in het aantrekken van PI4KB naar enterovirus RO's onderzocht door gebruik te maken van cellen waar het ACBD3 gen uit is gehaald (ACBD3 "knock-out" cellen). De replicatie van verscheidene enterovirussen en rhinovirussen was sterk geremd in ACBD3 knock-out cellen, terwijl de remming in deze cellen werd opgeheven door transiënte expressie van ACBD3. Ook was de interactie tussen het 3A eiwit en PI4KB verstoord in deze cellen en het 3A eiwit bevond zich op een andere cellulaire locatie, namelijk op endoplasmatisch reticulum (ER) in plaats van op het Golgi apparaat. Door transiënte expressie van een ACBD3 mutant die geen interactie meer aan kan gaan met PI4KB werd wel de localisatie van 3A naar het Golgi apparaat hersteld, terwijl virus replicatie werd niet hersteld door deze mutant. In lijn hiermee kon een PI4KB mutant die niet meer aan ACBD3 kon binden ook de virus replicatie niet herstellen in ACBD3 knock-out cellen. Door gebruik te maken van ACBD3 mutanten waar verschillende domeinen zijn uitgehaald is onderzocht welke domeinen belangrijk zijn voor de interactie met het 3A eiwit en PI4KB. Het CAR domein ("charged amino acids region") bleek essentieel voor de aantrekking van PI4KB en voor efficiënte virus replicatie. Het glutamine-rijke (Q) domein en het "Golgi dynamics domain" (GOLD) waren respectievelijk verantwoordelijk voor de ACBD3-PI4KB interactie en de ACBD3-3A interactie. Tezamen leveren deze resultaten nieuwe inzichten in de centrale rol van ACBD3 in de 3A-PI4KB interactie.

APPENDIX I

In Hoofdstuk 6 is de kristalstructuur van het ACBD3 GOLD domein samen met het 3A eiwit van verschillende enterovirussen (poliovirus, EV-A71, EV-D68 en RV-B14) opgehelderd om zo een beter inzicht te krijgen in de structurele vereisten voor deze interactie. Naast deze karakterisatie wordt er ook bewijs geleverd voor de aanwezigheid van ACBD3-3A heterotetrameren, die tot stand komen door de 3A-3A interactie. Er is een model gemaakt van het 3A-ACBD3 complex op een lipide dubbellaag om inzichtelijk te krijgen hoe het 3A-ACBD3 complex gesitueerd zou kunnen zijn op het membraan van een RO. Door gebruik te maken van verschillende 3A en ACBD3 mutanten die gemaakt zijn op basis van structurele informatie, zijn de raakvlakken die kritisch zijn voor de 3A-ACBD3, 3A-3A, en ACBD3-membraan interacties opgehelderd. Hierdoor is een opmerkelijke gelijkenis gevonden in de mechanismen die verschillende picornavirussen gebruiken om ACBD3 en bijbehorende factoren aan te trekken naar RO's.

Het eiwit c10orf76, dat een interactie aangaat met PI4KB maar waar verder weinig over bekend is, is in een eerdere studie geïdentificeerd als een belangrijke cellulaire factor benodigd voor coxsackievirus A10 (CVA10) replicatie. Hoofdstuk 7 beschrijft de studie die uitgevoerd is om de functie van c10orf76 op te helderen. "Hydrogen-deuterium exchange" massa spectrometrie is gebruikt om het c10orf76-PI4KB complex te karakteriseren, waaruit bleek dat de binding gemedieerd werd door de kinase linker van PI4KB. Met behulp van mutaten is aangetoond dat PI4KB nodig is voor de aantrekking van c10orf76 naar het Golgi apparaat, terwijl c10orf76 zelf geen invloed had op de localisatie van PI4KB. Een intact c10orf76-PI4KB complex was nodig voor replicatie van enterovirussen die afhankelijk zijn van c10orf76, zoals CVA10 en poliovirus. Een opmerkelijke bevinding was dat c10orf76 ook bijdroeg aan de localisatie van GBF1 op het Golgi apparaat en activatie van Arf1. Deze resultaten hebben geleid tot een vermoedelijk mechanisme van een c10orf76-afhankelijk stijging van de PI4P lipide concentratie op het Golgi apparaat en de locatie van virus replicatie.

한글 요약

엔테로바이러스 복제 과정에 세포막 항상성을 조절하는 숙주 인자들의 역할

엔테로바이러스(enterovirus; EV)는 폴리오바이러스(poliiovirus; PV), 리노바이러스(rhinovirus; RV), 콕사키바이러스(coxsackievirus; CV), 그리고 숫자와 함께 표시한 엔테로바이러스 등 다양한 질병을 일으키는 병원체를 포괄적으로 가리킨다. 소아마비로 잘 알려진 폴리오바이러스 외에도 280 종이 넘는 혈청형의 엔테로바이러스들이 있으며, 이들은 특히 유아와 면역이 저하된 사람에게서 경·중증 질병을 일으킬 수 있다. 현재까지 사용이 허가된 항바이러스제는 그 수가 매우 적다. 더욱이 엔테로바이러스는 가장 큰 바이러스 속(屬)임에도, 이 바이러스들에 의한 질병 치료용으로 검증된 항바이러스제는 아직 없다. 지금은 폴리오바이러스 종식 이후의 재유행 위험에 대비하는 한편, 다양한 엔테로바이러스들을 저지하려면 (넓은 적용 범위를 가진) 항엔테로바이러스제가 필요한 시점이다.

바이러스를 직접 억제하는 몇 종류의 직접형 억제제들이 개발되었는데, 이 중에는 바이러스의 세포 침입을 막는 캡시드 바인더(capsid binders)와 바이러스 복제 과정에 필수적인 바이러스 효소에 대한 저해제가 있다. 몇 종류의 캡시드 바인더와 프로테아제(protease) 저해제들이 임상 시험을 통해 평가받았지만 제한된 효능 또는 독성 등의 이유로 허가를 받지 못했다. 그 대안으로, 바이러스 복제에 필수적인 숙주 인자의 기능을 억제하는 방향으로 접근한다면 더 넓은 범위의 엔테로바이러스성 질병을 치료할 수도 있을 것이다. 약물 재창출[drug repurposing]은 여러 종류의 바이러스와 숙주세포 인자를 억제할 가능성이 높은 새로운 억제제를 발견할 수 있는 유용한 방법이다. 제 2 장에서는 2016 년을 기준으로 엔테로바이러스 감염에 대처하는 항바이러스제의 개발 현황과 여러 개발 전략에 대하여 비교적 자세한 요약을 제시한다.

양성(+) 단일가닥 RNA 바이러스들이 감염한 세포 내에는 복제 소기관[replication organelles; ROs]이라는 구조가 공통으로 발견된다. 복제 소기관은 다양한 막 지질로 구성된 독특한 구조를 가지는데, 그 생성과정에는 바이러스 단백질과 숙주세포 단백질이 모두 필요하다. 엔테로바이러스의 경우, 바이러스 단백질 3A 와 세포의 지질인산화 효소 PI4KB(phosphatidylinositol 4-kinase beta)가 이 과정에 중요한 역할을 한다고 알려졌다. 이 학위논문에서는 PI4KB, 그리고 이 효소와 상호작용을 하는 여러 인자가 엔테로바이러스의 복제과정과 복제 소기관 형성에 어떠한 역할을 하는지에 대한 동역학적인 이해를 높이고자 하였다.

PI4KB 와 더불어 지질 수송 단백질인 OSBP(oxysterol binding protein)가 엔테로바이러스 복제에 중요한 역할을 한다. 이 두 인자의 저해제는 바이러스의 복제를 효과적으로 억제할 수 있지만, 엔테로바이러스는 3A 단백질의 단일 아미노산 치환을 통해 이 억제에서 벗어날 수 있음이 알려졌다. 그러나 이 회피 기제는 아직 자세히 밝혀져 있지 않다.

엔테로바이러스가 복제를 위해 PI4KB 에 의존한다는 것이 알려졌지만, PI4KB 와 그 생성물인 PI4P(phosphatidylinositol 4-phosphate)의 정확한 역할은 다 밝혀지지 않았다. 제 3 장에서는 PI4KB 억제에 저항성을 지닌 돌연변이 콕사키바이러스를 이용하여, PI4KB 가 복제 소기관의 형성과 바이러스

다단백질체[polyprotein] 처리 과정에 관여한다는 사실을 밝혔다. 놀랍게도 이 변이 바이러스는 PI4KB 기능이 저해된 상황에서, 복제 소기관이 없음에도 손상되지 않은 골지체에서 유전체를 복제할 수 있었다. 이 복제 소기관 생성 장애를 기회로 삼아 복제 소기관이 엔테로바이러스 RNA 를 세포 내 감지 인자들로부터 보호하는 역할을 한다는 기존의 제안을 점검해본 결과, 바이러스 RNA 의 감지 증가나 선천성 면역 반응 증가는 보이지 않았다. 요컨대 엔테로바이러스 복제 소기관은 유전체 복제에 반드시 필요하지는 않으며, 선천성 면역 인자에 대한 물리적 보호막의 역할은 재고의 여지가 있다.

지질 항상성의 변화가 엔테로바이러스 다단백질체 처리 과정에 영향을 끼친다는 실험적 증거들이 늘어나고 있다. **제 3 장과 제 4 장**은 PI4KB 또는 OSBP 기능의 저해가 콕사키바이러스 B3 형의 다단백질체 처리 과정에 미치는 영향에 관한 연구결과를 담고 있다. PI4KB 또는 OSBP 기능 저해에 따른 다단백질체 처리 과정 장애는 바이러스 3A 단백질의 회피 변이[escape mutant](H57Y; 57 번째 아미노산이 히스티딘에서 타이로신으로 치환)로 해결되었다. 3A 단백질의 아미노산 치환 이외에도 2C 단백질의 N2D(2 번째 아미노산이 아스파라긴에서 아스파라긴산으로 치환)가 PI4KB 저해제에 저항성을 가진 콕사키바이러스 B3 풀(pool)에서 확인되었다. **제 4 장**에서는 이 2C-N2D 변이가 그 자체로는 PI4KB 또는 OSBP 저해제에 대한 저항성을 부여하지 못하지만 이중변이(2C-N2D/3A-H57Y) 바이러스가 단일변이(3A-H57Y) 바이러스보다 향상된 복제율을 나타낸다는 결과를 기술했다. PI4KB 저해제와 OSBP 저해제 모두 특이적으로 3A 와 3B 단백질 절단에 영향을 끼쳐 전구체인 3AB 단백질의 과도한 축적 원인이 되었는데, 이 현상은 3A-H57Y 변이로 해소되었다. 2C-N2D 변이가 복제를 향상에는 도움이 되었지만 다단백질체 처리 과정에서는 추가적인 이점이 확인되지 않아, 이 변이가 복제율 향상에 어떻게 이바지하는지를 밝히기 위한 추가 연구가 필요하다.

엔테로바이러스 3A 단백질이 PI4KB 를 복제 소기관으로 이끄는 것은 잘 알려졌지만, 그 정확한 메커니즘은 아직 분명하지 않다. **제 5 장과 제 6 장**에서는 3A 단백질이 어떤 방식으로 또 다른 숙주 인자인 ACBD3(Acyl-coenzyme A binding domain containing 3)을 동원해 PI4KB 를 복제 소기관으로 불러 모으는지 제시하였다. **제 5 장**에서는 ACBD3 유전자-제거 세포를 이용하여 ACBD3 가 PI4KB 기용 과정에 중요한 역할을 한다는 것을 밝혔다. 실험에 포함된 대표적 엔테로바이러스와 리노바이러스 모두가 ACBD3 유전자-제거 세포에서 복제 장애를 보였으며, 복제 소기관을 향한 PI4KB 의 이동도 관찰되지 않았다. 이때 엔테로바이러스 3A 단백질도 골지체가 아닌 소포체에 자리했으며 이는 3A 가 세포 내에서 적절한 자리를 찾는 데 ACBD3 이 필요하다는 것을 의미한다. PI4KB 이동과 3A 배치에서 확인된 장애는 야생형 ACBD3 의 발현에 따라 해소되었으나 PI4KB 와 결합하지 못하는 돌연변이 ACBD3 의 발현은 3A 의 자리만 회복시켰을 뿐, 바이러스의 복제를 정상으로 회복시키지는 못하였다. 마찬가지로, ACBD3 과 결합하지 못하는 돌연변이 PI4KB 의 발현은 PI4KB 유전자-제거 세포에서 바이러스의 복제를 지원하지 못했다. 일부 도메인이 결실된 돌연변이 ACBD3 을 활용한 결과, ACB (Acyl-coenzyme A binding; 아실-조효소 A 결합) 도메인과 CAR (charged amino acids region; 전하를 띤 아미노산 구역) 도메인은 3A 에 의한 PI4KB 모집과 엔테로바이러스 복제 과정에 중요하지 않다는 것을 확인하였다. PI4KB 와 직접 결합하는 Q (glutamine-rich region; 글루타민-풍부 구역) 도메인과 3A 와 직접 결합하는 GOLD (Golgi dynamics domain; 골지체 동역학) 도메인은 둘 다 PI4KB 의 모집과 효율적인 바이러스 복제에

필수적이었다. 요컨대 **제 5 장**에서는 ACBD3 이 엔테로바이러스의 PI4KB 활용 메커니즘에 핵심 역할을 한다는 것, 그리고 이 메커니즘과 엔테로바이러스의 복제를 지원하는 ACBD3 의 필수 도메인을 밝혔다.

제 6 장에서는 ACBD3 의 GOLD 도메인과 몇몇 엔테로바이러스(PV, EV-A71, EV-D68, RV-B14)의 3A 단백질의 결정 구조를 밝힘으로써 ACBD3 이 복제 소포체로 이동하는데 필요한 구조적 요건을 탐구하는 과정을 기술하였다. 먼저 여러 3A:ACBD3 GOLD 복합체 구조의 특징을 밝혔으며, ACBD3-3A 이형 사합체[heterotetramer]가 3A-3A 상호 작용을 통해 형성될 수 있다는 것도 함께 제시하였다. 또한, ACBD3-3A 복합체가 지질 이중층에 자리하는 모델을 제시하여 이 복합체가 세포 내막과 어떻게 상호작용하는지 이해하고자 하였다. 이렇게 얻어진 복합체 구조에 대한 정보를 바탕으로 돌연변이 3A 와 ACBD3 을 만들어 3A 사이, 3A 와 ACBD3 사이, 그리고 ACBD3 과 세포 내막 사이의 상호작용에 핵심적인 결합면을 확인하였다. 이 연구를 통해 확인된 엔테로바이러스 3A:ACBD3 GOLD 도메인 복합체의 결정 구조와 기존에 밝혀진 코부 바이러스(kobuvirus) 3A:ACBD3 GOLD 도메인 복합체의 결정 구조를 겹쳐서 비교함으로써 두 바이러스의 3A 단백질이 ACBD3 GOLD 도메인의 같은 부위에 결합한다는 사실을 확인하였다. 이는 피코르나바이러스과(*Picornaviridae*)의 전혀 다른 두 바이러스가 ACBD3 과 그 하위 인자들을 복제 장소로 이끌어 이용하기 위해 수렴 진화했음을 보여주는 놀라운 사례이다.

또 다른 세포 단백질인 c10orf76 은 PI4KB 와 상호작용하는 인자 중 하나이지만 최근 콕사키바이러스 A10 형의 복제에 필요한 숙주 인자라고 밝혀진 것 이외는 그 특성이 잘 알려지지 않았다. **제 7 장**에서는 c10orf76 이 감염되지 않은 세포에서 어떤 기능을 하는지, 그리고 엔테로바이러스 복제에는 또 어떤 역할을 할 수 있는지 확인하였다. 수소-중수소 교환 질량 분석법(hydrogen-deuterium exchange mass spectrometry)을 이용하여 c10orf76-PI4KB 복합체의 특징을 검토하고 더불어 두 인자의 결합이 PI4KB 의 키나아제 연결부위에 의존한다는 것을 밝혔다. 이 복합체의 형성을 막는 돌연변이를 활용하여, c10orf76 이 골지체에 자리잡으려면 PI4KB 의 매개자 역할이 필요하지만, 그 역은 적용되지 않는다는 것도 확인하였다. c10orf76-의존적 엔테로바이러스인 콕사키바이러스 A10 형과 폴리오바이러스의 복제에는 온전한 c10orf76-PI4KB 복합체가 필요했다. c10orf76 은 놀랍게도 다른 숙주 인자인 GBF1 가 골지체로 배치되는 현상과 그 뒤에 이어지는 Arf1 활성화에 이바지하였다. 이러한 결과들은 숙주세포의 c10orf76 이 골지체 및 바이러스 복제 장소에서 어떻게 PI4P 수치를 높이는지에 관한 잠정적인 메커니즘을 제공한다.

ACKNOWLEDGEMENTS

Hello! Hallo! 안녕하세요!

My journey as a PhD student has finally & officially come to an end! It was definitely not like driving on a German highway, but luckily I was not walking this path alone. I would like to express my gratitude for all of you who have led me, accompanied me, or crossed paths with me throughout this journey. I have become the person I am today thanks to you.

Frank, we started off as professor van Kuppeveld and Ms. Lyoo back in 2015. It took me 2-3 emails till I finally accepted that it is okay to call you just Frank without any titles. That was probably the moment that I already started picturing myself being in this flat country. The first interview with you went quite unconventional. You gave me the whole overview of the research lines in the lab until my company VPN suddenly decided to shut off the skype connection. On one hand, I was relieved that you did not give me the chance to show how nervous I am, but mostly I was amazed by your enthusiasm for science which also got me excited. Since then, you only got busier and busier but somehow you always made time for discussion and feedback as you promised that you will do so. I have to admit that in the beginning, I was stumbling along with “Nederlandse directheid”. But now, I have to be more cautious when I speak Korean, so I guess I adapted fairly successfully. There are many things that I learned from you, but if I have to mention only one thing, it will be that you encouraged me to expand my comfort zone greatly. Even when I got frustrated, you showed trust in me and gave me the chance to push the limits of my own and eventually stretch them. And that is probably the most valuable asset that I will carry on.

I had the privilege to have two daily supervisors one after another during the progress of PhD years, at the right time at the right moment. Hilde, you were my ACBD3! You were the mediator between knowledge gaps, lab skill gaps, and also between cultural gaps that I was going through especially at the beginning. I could ask you literally anything either work-related or life-related, which I am still doing occasionally. You have a keen eye for finding something positive like a silver lining. That is how I knew something went really wrong when you could not find any words, but luckily that happened very rarely (right?). Thanks to you, writing became much less of a burden on me over time. Thank you for giving me detailed feedback and encouraging me to be more confident to speak out. Also thanks a lot for your help in writing the Dutch summary. Jeroen, thanks for all the support you gave so I can be mature and more independent. I really appreciated your honesty and perspectives which allowed me to accept things as it is whether it is good or bad without being too dramatic. With your guidance, I could take the lead in communicating with collaborators and I learned a lot during that period. Thanks for making time for discussion and providing quick feedback on my writings, despite all the students and duties that were on your shoulders.

I would like to take this opportunity to thank the assessment committee, prof. Bernd Helms, prof. Emmanuel Wiertz, prof. Eric Snijder, prof. Thijn Brummelkamp, and dr. Ginny Farias, for their time and effort in reading and evaluating my thesis.

This thesis would not have become this good without all the collaborators. Thank you, Charlotte, Montse, Martin, Jacob, Joshua, Tamas, and John. I truly enjoyed the collaboration with you, and it was an eye-opening experience broadening my understanding of completely different fields, the world of electron microscopy and structural biology. I would also like to thank Richard and Esther from CCI who helped me with microscopy.

To my awesome paranympths, Ieva and Maryam. With a bit of exaggeration, I can probably write a whole book (did not say in what font size :P) for you two, but let's keep it short here. Ieva, my sudoku twin! I was so happy when you joined the lab, especially the nearly being deserted Team Replication. You brought a fresh spirit and new insight which I appreciated a lot. It was also nice to have someone to share ideas and frustrations. I really enjoyed all our discussions, occasionally and spontaneously over beer. Thank you for patiently answering all my English grammar questions and feeding me delicious homemade cakes. I was secretly hoping that you have overripe bananas more often. Maryam, my nonbiological sister! People say that every lab should have Maryam but not everyone is lucky to be chosen by you (lucky me and Shakeeb). You spoiled me so much over the years, so I almost completely withered when you left. But I grew back strong with your support. Thanks for letting me be just as I am but at the same time also encouraging me to challenge myself. I think I have been receiving more compliments from you than any other person. You can definitely write down "a professional self-esteem booster" on your CV.

Cristina, I still vividly remember the day that I found an unexpected birthday gift in my office from you. That really gave me the energy to keep going. Thanks for listening to my rather unstructured thoughts and concerns and giving me sincere advice when it is needed. It is such a delight to visit your house and to spend time together with Marius, Tesla, and now also with baby Alma which gives me so much warmth.

Two men in Lopertjes, Jim and Hendrik. I can confirm that I laughed the most when you two were here. Thanks for initiating the running group in the middle of winter. Since then running became a good hobby for me although it is not that fun. I also appreciated your interest in my projects and all the scientific/non-scientific discussions that we had. Although sometimes it was not clear if that is us or the beer talking, I enjoyed as much as all the beer bottles that we collected on the shelf. Hartstikke bedankt! Sepha, thank you for all the thoughtful and unique gifts, but above all, for your kind spirit. I believe Sien also got that from her mama. I am looking forward to the day when I can travel to Leuven again and meet you all (also Claudia and Svea). Jim, Huib, and Linda thank you for your attempt to learn Korean. I did regret teaching you some words but overall I had so much fun and it soothed homesickness a little bit. 고마워!

Ivy, thank you for introducing me to your lovely family. It is always a great pleasure to spend time with you, Vincent, Jonathan, and Anna over the food that we love. Wentao, the lab is never the same without you! Even though we never worked on the same project, you were always there to help. I really admired your motivation and dedication. Thanks for all your suggestions, and also for all the delicious home-cooked meals that you were generously sharing. You are truly the living example of "sharing is caring". Hongbo, Wenjuan, and Chunyan thank you for listening to my questions and complaints. You were always willing to help despite your crazy busy work which I benefited quite often.

Arno, becoming your roommate is one of the few nice things that happened during this pandemic. Thanks for thinking along with me whenever I am having issues with cloning. You will remain the coolest person in the lab until you retire. Dus, appeltje? Nancy, thank you very much for all the things that you do behind the scenes, so the lab can be functional. It was a relief that we could often talk(=complain) about the same things. Hope I can go diving with you someday! Marleen, thanks to your enormous help with lab work, I could finish writing this thesis at the right time. I also learned a lot by supervising five master students: Wendy, Henrike, Alex, Raquel, and Kyra K. Thank you for your efforts and contributions.

I would like to extend my gratitude to all the other present & former members of the lab for their help and advice, and also for making a more positive work environment: Anja, Berend-Jan, Brenda, Chunhua, Erhard, Erik, Fiona, Floor, Herman, Irina, Lisa, Lisbeth, Louisa, Lucian, Maidina, Malte, Marianthi, Martijn G., Martijn L., Mengying, Mirte, Peter F., Peter R., Raoul, Ruben, Rui, Sander, Shan, Susanne, Tabitha, Tim, Tony, Vera, Xander, Xuesheng, Yifei, Yongle, and Yongtao. My special best wishes to current part-time/full-time members of the Picorna group: Chiara, Dan, Esther, Itziar, Jelle, Judith, Justyna, Katrien, Kyra D., Lonneke, Mayra, Rutger, Xiaoyao, and Xinyi.

Doing a PhD as a part of ANTIVIRALS-ITN was challenging but also provided me a unique chance to meet a lot of people from different sectors and to gain diverse experiences. Clasiën, thank you for your efforts in organizing the network meeting/program and for listening to our feedback to make our experience better each time. Robert, thank you for making time to listen to my concerns and sharing your thoughts and experiences. It was really helpful to receive mentoring from you. Thierry and Clara, thanks a lot for your hospitality during my secondment in Vienna. It was a valuable experience that helped me to be more acquainted with structure-based drug design, and I also enjoyed exploring the beauty of Vienna. Angelica, I feel very lucky to meet one kindred spirit! Thanks for your support over the years and for a shared enthusiasm for K-food and drama. Looking forward to meeting you again very soon.

Living in Utrecht has presented opportunities to meet many amazing people. Bora and Jeseung, thanks for sharing tips and tricks on PhD life and for living in the Netherlands. The best landlord/neighbor I can ask for: Sander, Lex, and Margot, thank you for all your help which made me feel at home very easily and quickly. I will never forget your kind heart, Margot. Dear my Korean bbq crew, Younjung and Yujin. My life here has become much more interesting with your company. Good luck with your next upcoming adventure! Ans, who is much more than my Dutch teacher. You and Lex are teaching so many things beyond language. I will forever cherish this special bond that brought us together. Thanks for being such a powerful supporter.

Not to forget to mention prof. Yong-Seok Jeong and other members of the molecular virology lab at Kyung Hee University who led me to the world of viruses. What I learned there has been the solid ground for learning new knowledge and techniques. Also, I would like to thank dr. Hyun-Joo Kim who supervised me at Animal and Plant Quarantine Agency, for supporting me in pursuing a PhD abroad. I wish you the very best of luck in your new job!

I want to thank all my friends for their supports from a distance. Jihye and Sinae who are bearing with me all these years, thank you for making a personal visit all the way to the Netherlands. I promise I will be a better host next time!

Last but not the least, a big thank you to my family for their unconditional love and support. It would have been impossible for me to come this far without you. My loving sister Heyrhea, thank you for being my best friend and advisor from the beginning and thank you for your advice on the cover design as well. Hyeonjoon, thank you for being such a nice brother-in-law. Jeyne, I am so proud of how far you have come to be where you are at now. Good luck with finishing up your PhD. My dearest mom and dad, for as long as I remember, you two never stopped learning. No matter how busy you are, how difficult the situation is, you put the effort in and you did not make excuses. Your attitude towards life has been my biggest inspiration and also made me not afraid of trying out new things. Thank you for all your hard work and sacrifices, also for your unending support. 사랑합니다.

CURRICULUM VITAE



Heyrhyoung Lyoo was born on February 28, 1988, in Seoul, South Korea. After graduating from high school in 2006, she started her study in Biology at Kyung Hee University. She joined the laboratory of molecular virology as an undergraduate research assistant in 2008, where she continued her master's study under the supervision of prof. dr. Yong-Seok Jeong. Her master's thesis described the role of host factors in the establishment of Japanese encephalitis virus persistent infection. From 2013 to 2015, she worked as a researcher in the new emerging diseases laboratory at Animal and plant quarantine agency under the supervision of dr. dvm. Hyun-Joo Kim and contributed to the development of molecular diagnostic tools for foreign viral infections including Rift valley fever and MERS.

In 2015, Heyrhyoung moved to the Netherlands and started working as a Ph.D. student in the virology division at Utrecht University under the supervision of prof. dr. Frank van Kuppeveld. As a Marie-Curie fellow of the European Training Network ANTIVIRALS, she worked on the identification of important host factor(s) for enteroviruses, which can be further developed as a target of a broad-spectrum antiviral drug.

Since 2020, upon the COVID-19 outbreak, she has been engaged in several coronavirus-related works including two main projects, SCORE and PanCoroNed, where she is contributing to the discovery of antivirals against SARS-CoV2 and other coronavirus infections.

LIST OF PUBLICATIONS

In this thesis

J. A. McPhail, H. Lyoo*, J. G. Pemberton*, R. M. Hoffmann, W. van Elst, J. R. P. M. Strating, M. L. Jenkins, J. T. B. Stariha, C. J. Powell, M. J. Boulanger, T. Balla, F. J. M. van Kuppeveld, J. E. Burke. Characterization of the c10orf76-PI4KB Complex and Its Necessity for Golgi PI4P Levels and Enterovirus Replication. 2020. EMBO Rep. (*equal contribution)

V. Horova, H. Lyoo, B. Różycki, D. Chalupska, M. Smola, J. Humpolickova, J. R. P. M. Strating, F. J. M. van Kuppeveld, Evzen Boura, Martin Klima. Convergent Evolution in the Mechanisms of ACBD3 Recruitment to Picornavirus Replication Sites. 2019. PLoS Path.

H. Lyoo, H. M. van der Schaar, C. M. Dorobantu, H. H. Rabouw, J. R. P. M. Strating, and F. J. M. van Kuppeveld. ACBD3 is an essential pan-enterovirus host factor that mediates the interaction between viral 3A protein and cellular protein PI4KB. 2019. mBio.

H. Lyoo, C. M. Dorobantu, H. M. van der Schaar, and F. J. M. van Kuppeveld. Modulation of proteolytic polyprotein processing as a resistance mechanism of coxsackievirus mutants to inhibitors targeting phosphatidylinositol-4-kinase III β and oxysterol binding protein. 2017. Antiviral Research.

C. E. Melia*, H.M. van der Schaar*, H. Lyoo, R. W. A. L. Limpens, Q. Feng, M. Wahedi, G. J. Overheul, R. P. van Rij, E. J. Snijder, A. J. Koster, M. Bárcena, and F. J.M. van Kuppeveld. Escaping host factor PI4KB inhibition: enterovirus genomic RNA replication in the absence of replication organelles. 2017. Cell Reports. (*equal contribution)

L. Bauer*, H. Lyoo*, H. van der Schaar, J. R. P. M. Strating, and F. J. M. van Kuppeveld. Direct-acting antivirals and host-targeting strategies to combat enterovirus infection. 2016. Current Opinion in Virology. (*equal contribution)

Additional publications

J. Baggen*, Y. Liu*, H. Lyoo, A. L. W. van Vliet, M. Wahedi, J. W de Bruin, R. W Roberts, P. Overduin, A. Meijer, M. G Rossmann, H. Jan Thibaut, F. J. M. van Kuppeveld. Bypassing Pan-Enterovirus Host Factor PLA2G16. 2019. Nat. Comm. (*equal contribution)

H. Kim, H. Lyoo, J. Choi, Y. Lee, B. Kim, and H. Yoo. Development of a Quantitative RT-PCR Assay to Differentiate Rift Valley Fever Virus Smithburn Vaccine Strain from Clone 13 Vaccine Strain. 2019. Vector-Borne and Zoonotic Diseases.

C. E. Melia, H. M. van der Schaar, A. W. M. de Jong, H. Lyoo, E. J. Snijder, A. J. Koster, F. J. M. van Kuppeveld, M. Bárcena. The Origin, Dynamic Morphology, and PI4P-Independent Formation of Encephalomyocarditis Virus Replication Organelles. 2018. mBio.

C. M. Dorobantu, L. Albuлесcu, H. Lyoo, M. van Kampen, R. De Francesco, V. Lohmann, C. Harak, H. M. van der Schaar, J. R. P. M. Strating, A. E. Gorbalenya, and F. J. M. van Kuppeveld. Mutations in Encephalomyocarditis Virus 3A Protein Uncouple the Dependency of Genome Replication on Host Factors Phosphatidylinositol 4-Kinase III α and Oxysterol-Binding Protein. 2016. mSphere.

R. Ulferts, S. M. de Boer, L. van der Linden, L. Bauer, H. Lyoo, M. J. Maté, J. Lichière, B. Canard, D. Lelieveld, W. Omta, D. Egan, B. Coutard, and F. J. M. van Kuppeveld. Screening of a Library of FDA-Approved Drugs Identifies Several Enterovirus Replication Inhibitors That Target Viral Protein 2C. 2016. Antimicrob Agents Chemother.

H. Kim, H. Lyoo, J. Park, J. Choi, J. Lee, H. Jeoung, Y. Cho, and I. Cho. Surveillance of Rift Valley Fever Virus in Mosquito Vectors of the Republic of Korea. 2016. Vector-Borne and Zoonotic Diseases.

H. Lyoo, S. Y. Park, J. Y. Kim, and Y. S. Jeong. Constant Up-regulation of BiP/GRP78 Expression Prevents Virus-Induced Apoptosis in BHK-21 Cells with Japanese Encephalitis Virus Persistent Infection. 2015. Virology Journal.

J. Y. Kim, S. Y. Park, H. Lyoo, E. S. Koo, M. S. Kim, and Y. S. Joeng. Extended Stability of Cyclin D1 Contributes to the Limited Cell Cycle Arrest at G1-phase in the BHK-21 Cells with Japanese Encephalitis Virus Persistent Infection. 2015. The Journal of Microbiology.

E. S. Koo, C. H. Yoo, Y. Na, S. Y. Park, H. Lyoo, and Y. S. Jeong. Reliability of Non-culturable Virus Monitoring by PCR-based Detection Methods in Environmental Waters Containing Various Concentrations of Target RNA. 2012. The Journal of Microbiology.

